



UNIVERSITAT DE  
BARCELONA

# Replication stress: mechanisms and molecules involved in DNA replication progression and reinitiation

Sònia Feu i Coll



Aquesta tesi doctoral està subjecta a la llicència **Reconeixement- NoComercial – Compartir Igual 4.0. Espanya de Creative Commons.**

Esta tesis doctoral está sujeta a la licencia **Reconocimiento - NoComercial – Compartir Igual 4.0. España de Creative Commons.**

This doctoral thesis is licensed under the **Creative Commons Attribution-NonCommercial-ShareAlike 4.0. Spain License.**

DOCTORAL PROGRAMME IN BIOMEDICINE

SCHOOL OF MEDICINE AND HEALTH SCIENCES, UNIVERSITY OF BARCELONA

**Replication stress:  
mechanisms and molecules involved in  
DNA replication progression and reinitiation**

Thesis presented by

**Sònia Feu i Coll**

to qualify for the degree of Doctor in Biomedicine

by the University of Barcelona



UNIVERSITAT DE  
BARCELONA

This thesis has been performed in the Department of Biomedicine of the  
School of Medicine and Health Science of University of Barcelona,  
under the supervision of Prof. Neus Agell i Jané, Ph.D.

Barcelona, March 2019



**“A journey of a thousand miles begins with one step”**

Benjamin Franklin



# **ACKNOWLEDGEMENTS**



Quan arribo a aquestes línies, toca una visualització breu (o això espero) dels anys que deixo enrere. Ara ja farà gairebé 6 anys que vaig entrar per primera vegada al laboratori de Senyalització i *Checkpoints* del Cicle Cel·lular. En aquell moment encara no sabia on em portaria la vida, ni la ciència!

L'estiu abans de començar el Màster de Biomedicina estava fent entrevistes per tal d'escollir el grup on fer el Treball Final i em vaig topar amb tu, Neus. Per què em vaig decidir fer el màster al teu grup? Bàsicament per tu, pel que em vas transmetre i inspirar. Perquè sincerament, en aquell moment els conceptes d'estrès de replicació, de l'APC/C i de la forqueta de replicació em quedaven molt llunyans. I evidentment, no em vaig equivocar. Sempre he pensat que he sigut molt afortunada per tenir-te com a "jefa". Gràcies a la teva manera de ser, al teu optimisme i a la teva implicació he pogut recórrer aquest camí, que de vegades no ha estat fàcil. Gràcies per ensenyar-me que no hi ha resultats incorrectes, sinó que ens plantegen diferents camins per respondre a les nostres preguntes. Gràcies per cuidar-me, per sentir-me recolzada i per tot el suport, també en aquesta última etapa. Si vaig continuar aquesta aventura en la recerca va ser principalment per tu. No puc continuar sinó parlant de la Montse també. Sempre he tingut la teva ajuda i suport infinit en el dia a dia al laboratori. Només puc donar-vos les gràcies a les dues per crear aquesta "petita família" de la qual formem part, i ens sentim molt orgullosos. Moltes gràcies!

Un altre reconeixement que haig de fer és a la meva "mini-jefa", Amaia. Contigo compartí mis primeros años de esta aventura, que fueron indispensables para mí y mi formación. En parte, tú también eres responsable de que continuara con el doctorado después del máster. Además de aguantarme, me transmitiste tu implicación y dedicación por la ciencia, tus ganas y también tu entusiasmo. ¡Ojalá me lleve un poco de esto conmigo! Gracias por tu confianza eterna, y porque siempre has estado pendiente de mí, ¡aunque estés lejos! ¡¡Mil gracias!!

Si aquestes pàgines serveixen per sincerar-se una mica i fer una mica de reflexió haig de dir que també he deixat molts moments de frustració enrere. Diuen que la ciència és paciència, i no sé si l'he aconseguit, però intentar-ho, us asseguro que ho he intentat! També sento alegria i tristesa quan penso en aquesta etapa, i aquests dos sentiments van de la mà, per haver recorregut aquest camí i per la gent que m'hi ha acompanyat. I en aquest punt, vull fer una menció especial al meu #churricore. Com bé deies Edu, no podeu anar un sense l'altra. Edu i

Débora, els meus dos mosqueters. Com pot ser que ja us trobi tant a faltar? De veritat, que sóc una afortunada d'haver-vos trobat i haver pogut compartir aquesta etapa amb vosaltres. Si penso en moments en el laboratori, sempre hi sortiu vosaltres dos. No hauria estat el mateix si no fos pel meu "duo dinàmic", d'això n'estic segura. Mil gràcies per tot, els ànims i l'ajuda infinita, les mil converses acompanyades de berenar o cerveses, els riures, els *scaperooms*, les sortides a Cabotro's, les escapades a Camprodon,... Però això no s'acaba aquí, perquè encara queda #churricore per estona! Potser no us ho dic suficient, però us feu estimar!

I com no, una menció a la resta del grup Neus (#churrilab), del passat i del present. Alba Villaret, la meva primera alumna. Gràcies per la teva alegria i la teva manera de fer, m'ho vas posar molt fàcil! Ara et desitjo tota la sort i la felicitat del món, perquè t'ho mereixes! Triana, tú nos trajiste tu energía y entusiasmo en el lab. Gracias por tu apoyo siempre y tu manera de ser. ¡No lo pierdas nunca! Núria, tu no pots faltar tampoc amb aquests agraiments. Si una cosa destaco de tu és la teva constància i perseverança. Les teves ganes per la ciència i per aprendre. El teu esforç. Estic segura que seràs una gran científica i arribaràs on vulguis! Molts ànims en aquesta etapa! Juanito, ¿qué puedo decir de ti? Que nos trajiste mucha alegría en el lab, sobre todo cuando Edu no estaba, porque si no eso era un caos... ¡Es broma! Gracias porque nos alegraste mucho la vida a todos durante el tiempo que estuviste en el lab. I en aquest punt no podies faltar tu, Fer. Amb tu he compartit aquesta última etapa, potser la més estressant per mi. Gràcies per l'ajuda que m'has brindat aquest últim temps, i ara que ja ets el nou "mini-jefe" del *checkpoint* et desitjo tota la sort del món. L'estrès de replicació no és un món fàcil però espero que el balanç final sigui molt positiu. *Baraa, we have not shared much time together but I hope that you have good luck in the future and that your time in the laboratory brings only good things to you.* I tampoc puc deixar d'esmentar-te, Sònia Brun. Gràcies per compartir tot aquest temps, ets la constant en el nostre laboratori. De veritat que moltes gràcies per ajudar-me amb la biologia molecular, sobretot les PCRs, i per estar sempre pendent que les coses del lab funcionin! Guardo records molt apreciats de tots i cadascun de vosaltres.

Moltes gràcies als companys del CELLEX: Albert Chavero, Elsa, Patri, Frede, Alba F., Marta B., Carles R., Siscu, Albert P., Carles E. Moltes gràcies per l'ajuda, per les idees i comentaris aportats als seminaris, per la quantitat de reactius que ens heu deixat,... I també alguna

quedada al bar de davant per fer cerveses! Gràcies especialment a tu, Albert, que vas començar el teu doctorat en el nostre laboratori, i tot i que vas tornar aviat al CELLEX, sempre et consideraré una mica del grup Neus! Molta sort en la teva última etapa! Gràcies també a les noies de Microscopia Confocal: Maria M., Anna B. i Elisenda. A vosaltres també us dec molt del que hi ha aquesta tesis. Moltes gràcies per la paciència amb el nostre estimat *fiber*, i per la vostra predisposició a ajudar-me sempre! Us ho agraeixo molt! I ara un agraïment conjunt als membres del CELLEX i del Confo per tots els moments compartits en els seminaris, els sopars de Nadal, les calçotades, les paellades! No perdeu mai aquestes tradicions que són vida!

I en quant a la burocràcia, sempre agrairé l'ajuda de les secretàries, especialment a la Núria. Sort n'he tingut de tu. Moltes gràcies!

Finalment també em toca agrair a aquelles persones que potser no estan tan relacionades amb la tesis, però que sense elles el camí hauria sigut molt diferent.

Primer, els meus amics "Biotec" que potser han sigut els que més han entès quan els explicava el que feia. Anna S., moltes gràcies per tot. Amb tu vaig començar al laboratori, costat a costat, a Girona. Ens vam traslladar plegades a fer el màster a Barcelona, on també treballàvem costat a costat. Gràcies per haver-me acollit a casa teva aquest últim temps, per haver estat sempre al meu costat, i per entendre'm sempre. A tu i a l'Oscar, gràcies per tots els moments i les cerveses compartides aquests anys. M'ha encantat viure aquesta experiència al vostre costat, "mano a mano". Judit, Marta i Jose gràcies per no deixar que la distància ens canviï. Sempre és un plaer tornar a retrobar-nos, i veure que malgrat que els anys passen, l'amistat perdura.

També gràcies als Pirat's, per alegrar-me i distreure'm els caps de setmana a parts iguals. Especialment, a l'Anna Vergés, la meva meitat. Sempre intentant entendre el que estava fent al laboratori (tot i que no sé si ho he aconseguit). Moltes gràcies per les trucades infinites, les visites exprés,... El teu suport incansable m'ha ajudat molt!

Gràcies a la família també. Després d'anys fora de casa, m'heu rebut amb els braços oberts i m'heu facilitat i ajudat molt en aquesta última etapa. Moltes gràcies, perquè sou l'energia i el suport, potser no tan obvi, però que sempre hi és! Especialment, a les meves tres petites guerrerres, pel vostre amor i gentilesa. La vostra tieta està molt orgullosa de cadascuna de vosaltres, i sé que arribareu a on us proposeu!

I, per últim, gràcies a tu, amor. Per empassar-te els meus mals moments, per cuidar-me i no deixar mai d'animar-me. Per fer-me veure més enllà del laboratori. Per ser-hi sempre, sense condicions. Per regalar-me tants bons moments. I per il·lusionar-me amb un nou projecte que realitzarem junts. Només puc dir-te dues paraules: gràcies i t'estimo!

# INDEX



<b>ABBREVIATIONS.....</b>	<b>17</b>
<b>INTRODUCTION.....</b>	<b>23</b>
<b>1. CELL CYCLE.....</b>	<b>25</b>
1.1. CELL CYCLE REGULATION BY CYCLIN-CDKS .....	26
1.1.1. REGULATION OF CYCLIN-CDKS.....	28
1.2. CELL CYCLE REGULATION BY UBIQUITIN PROTEASOME SYSTEM.....	31
1.2.1. SCF COMPLEX .....	32
1.2.2. APC/C COMPLEX.....	34
<b>2. DNA REPLICATION.....</b>	<b>40</b>
2.1. DNA REPLICATION INITIATION .....	41
2.2. DNA REPLICATION ELONGATION .....	44
2.3. DNA REPLICATION TERMINATION.....	46
2.4. DNA REPLICATION ORGANIZATION.....	47
<b>3. REPLICATION STRESS.....</b>	<b>49</b>
3.1. DNA REPLICATION STRESS CAUSES .....	49
3.2. CELL-CYCLE CHECKPOINTS .....	52
3.2.1. DNA REPLICATION CHECKPOINT .....	54
3.2.2. DNA DAMAGE CHECKPOINT .....	60
3.3. REPLICATION RESTART OR REPAIR PATHWAYS.....	64
<b>4. REPLICATION STRESS AND CANCER .....</b>	<b>72</b>
<b>OBJECTIVES.....</b>	<b>77</b>
<b>RESULTS.....</b>	<b>81</b>
<b>CHAPTER 1: LACK OF APC/C<sup>Cdh1</sup> ACTIVATION IN S PHASE AFTER A SEVERE REPLICATION STRESS ALLOWS RESUMPTION OF DNA SYNTHESIS IN TUMOUR CELLS .....</b>	<b>83</b>
PREVIOUS DATA.....	85
RESULTS.....	90
1.1. Tumour cell lines are predominantly deficient in APC/C <sup>Cdh1</sup> activation in S phase and are able to resume replication in response to a prolonged HU treatment .....	90
1.2. New origin firing contributes to replication recovery in HCT116 cells after a prolonged HU treatment.....	92

1.3. HCT116 cells acquire genomic instability after a prolonged HU treatment .....	94
1.4. Emi1 depletion-induced APC/C <sup>Cdh1</sup> activation compromises replication resumption and genomic instability acquisition in HCT116 cells .....	97
<b>CHAPTER 2: FORK REMODELLING AFTER AN ACUTE HU-INDUCED REPLICATION STRESS .....</b>	<b>101</b>
PREVIOUS DATA.....	103
RESULTS.....	109
2.1. CMG helicase maintains its integrity and association with chromatin after an acute replication stress in hTERT-RPE cells.....	109
2.2. CMG helicase is disengaged from nascent DNA after an acute replication stress indifferently of CDK activity in hTERT-RPE cells.....	110
2.3. FBH1 depletion reduces the amount of single-stranded nascent DNA, but does not impair replication fork restart in hTERT-RPE cells .....	111
2.4. Replisome disengagement from nascent DNA correlates with large amounts of single- stranded parental DNA and RPA accumulation .....	115
2.5. Nascent DNA is not degraded by Mre11 after an acute replication stress in hTERT-RPE cells.....	117
2.6. Replication resumption occurs without long stretches of single-stranded parental DNA in hTERT-RPE cells.....	120
<b>CHAPTER 3: ROLE OF RAD51 IN REPLICATION FORKS IN RESPONSE TO REPLICATION STRESS...</b>	<b>123</b>
RESULTS.....	125
3.1. RAD51 depletion does not affect the number of restarted forks, but impairs fork progression after an acute replication stress in hTERT-RPE cells .....	125
3.2. RAD51 depletion does not cause fork degradation after an acute replication stress in hTERT-RPE cells.....	128
3.3. RAD51 depletion does not impair replication recovery after an acute replication stress in hTERT-RPE cells.....	129
3.4. RAD51 depletion increases genomic instability in hTERT-RPE cells .....	131
3.5. RAD51 inhibition does not affect fork progression in hTERT-RPE cells .....	132
3.6. RAD51 inhibition does not affect the number of restarted forks, but impairs fork progression after an acute replication stress in hTERT-RPE cells .....	133
3.7. RAD51 inhibition does not cause fork degradation after an acute replication stress in hTERT-RPE cells.....	135

3.8. RAD51 is necessary for an efficient fork restart and progression after an acute replication stress in hTERT-RPE cells.....	135
3.9. RAD51 inhibition affects cell cycle progression in hTERT-RPE cells .....	137
3.10. RAD51 inhibition increases genomic instability after an acute replication stress in hTERT-RPE cells.....	140
3.11. RAD51 inhibition affects fork progression during a mild replication stress in hTERT-RPE cells.....	142
3.12. RAD51 inhibition affects fork progression in colorectal cancer cells .....	145
<b>CHAPTER 4: OZF IS ESSENTIAL TO MAINTAIN FORK PROGRESSION RATE UNDER REPLICATION STRESS CONDITIONS .....</b>	<b>149</b>
PREVIOUS DATA.....	151
RESULTS.....	154
4.1. OZF interacts with Cdc45 and MCM.....	154
4.2. OZF is not essential for replication in hTERT-RPE cells.....	154
4.3. OZF depletion reduces fork progression under mild replication stress conditions in hTERT-RPE cells.....	156
4.4. OZF depletion does not increase genomic instability in hTERT-RPE cells .....	160
4.5. OZF depletion reduces fork progression in colorectal cancer cells.....	163
<b>DISCUSSION .....</b>	<b>167</b>
I. LACK OF APC/C <sup>CDH1</sup> ACTIVATION IN S PHASE AFTER A SEVERE REPLICATION STRESS ALLOWS RESUMPTION OF DNA SYNTHESIS IN TUMOUR CELLS.....	170
II. FORK REMODELLING AFTER AN ACUTE HU-INDUCED REPLICATION STRESS .....	173
III. ROLE OF RAD51 IN REPLICATION FORKS IN RESPONSE TO REPLICATION STRESS.....	178
IV. OZF IS ESSENTIAL TO MAINTAIN FORK PROGRESSION RATE UNDER REPLICATION STRESS CONDITIONS .....	182
<b>CONCLUSIONS.....</b>	<b>187</b>
<b>MATERIALS AND METHODS.....</b>	<b>193</b>
1. CELL CULTURE .....	195
1.1. CELL LINES AND CULTURE CONDITIONS .....	195
1.2. MAINTENANCE OF CULTURED CELLS.....	196

1.3. CRYOPRESERVATION .....	196
1.4. AGENTS USED .....	197
1.5. THYMIDINE SYNCHRONIZATION .....	198
1.6. DNA TRANSFECTION METHODS .....	198
1.7. siRNA TRANSFECTION METHODS .....	199
<b>2. CELL PROLIFERATION AND SURVIVAL ASSAYS .....</b>	<b>202</b>
2.1. COLONY FORMATION ASSAY .....	202
<b>3. ELECTROPHORESIS AND WESTERN BLOT (WB).....</b>	<b>203</b>
3.1. PREPARATION OF SAMPLES .....	203
3.2. PROTEIN QUANTIFICATION .....	205
3.3. SAMPLE PREPARATION .....	208
3.4. ELECTROPHORESIS AND WB .....	208
<b>4. IPOND: ISOLATION OF PROTEINS ON NASCENT DNA .....</b>	<b>215</b>
4.1. PREPARATION OF SAMPLES .....	215
4.2. DNA PURIFICATION AND VALIDATION OF SONICATION.....	217
4.3. DOT-BLOT .....	217
4.4. IPOND.....	218
<b>5. IMMUNOPRECIPITATION.....</b>	<b>219</b>
5.1. IMMUNOPRECIPITATION OF HA-OZF .....	219
5.2. IMMUNOPRECIPITATION OF MCM3 .....	220
<b>6. FLOW CYTOMETRY .....</b>	<b>222</b>
<b>7. IMMUNOFLUORESCENCE.....</b>	<b>223</b>
7.1. 53BP1/CycD1, 53BP1/γH2AX AND 53BP1 IMMUNOFLUORESCENCE .....	223
7.2. ssDNA ANALYSIS BY BRDU IMMUNOFLUORESCENCE UNDER NATIVE CONDITIONS.....	224
<b>8. QUANTITATIVE IMAGE-BASED CYTOMETRY (QIBC) .....</b>	<b>225</b>
<b>9. DNA FIBER ANALYSIS.....</b>	<b>226</b>
<b>10. STATISTICAL ANALYSIS.....</b>	<b>228</b>
<b>BIBLIOGRAPHY .....</b>	<b>229</b>

## **ABBREVIATIONS**



**APS:** ammonium persulfate  
**APC:** anaphase-promoting complex/cyclosome  
**ATM:** ataxia-telangiectasia mutated  
**ATR:** ATM and Rad3-related  
**ATRIP:** ATR-interacting protein  
**BER:** base excision repair  
**BIR:** break-induced replication  
**bp:** base pairs  
**BRCA1/BRCA2:** breast cancer type 1/ breast cancer type 2  
**BSA:** bovine serum albumin  
**CAK:** CDK-activating kinase  
**Cdc45:** cell cycle division 45  
**Cdc6:** cell division cycle 6  
**CDK:** cyclin-dependent kinase  
**Cdt1:** Cdc10-dependent transcript 1  
**Chk1/Chk2:** checkpoint kinase 1/ checkpoint kinase 2  
**CKI:** CDK inhibitory subunit  
**CFS:** common fragile site  
**CRL:** cullin RING ligase  
**CtIP:** CtBP-interacting protein  
**Co-IP:** co-immunoprecipitation  
**DDK:** Dbf4-dependent kinase  
**DDR:** DNA damage response  
**D-loop:** displacement loop  
**DNA-PK:** DNA-dependent protein kinase  
**DMEM:** Dulbecco's modified Eagle's medium  
**DNA:** deoxyribonucleic acid  
**dNTP:** deoxyribonucleotide triphosphate  
**DSB:** double-strand break  
**dsDNA:** double-stranded DNA  
**DTT:** dithiothreitol

*ABBREVIATIONS*

**DUB:** deubiquitylating enzyme  
**DUE-B:** DNA unwinding element  
**ETAA1:** Ewing tumour-associated antigen 1  
**FBS:** foetal bovine serum  
**FEN1:** flap endonuclease 1  
**G1/G2:** gap 1/gap2  
**GEMC1:** geminin coiled-coil containing protein 1  
**GINS:** go ichi ni san  
**h:** hours  
**HECT:** homologous to E6-AP carboxyl terminus  
**HR:** homologous recombination  
**HU:** hydroxyurea  
**ICL:** interstrand crosslink  
**iPOND:** isolation of proteins on nascent DNA  
**Kb:** kilobase  
**KDa:** kilodaltons  
**Mb:** megabase  
**Min:** minutes  
**MMR:** mismatch repair  
**MRN:** Mre11-Rad50-Nbs1  
**MS:** mass spectrometry  
**NER:** nucleotide excision repair  
**NHEJ:** non-homologous end-joining  
**OIS:** oncogene-induced senescence  
**ORC:** origin-recognition complex  
**OZF:** only zinc-finger  
**PARP1:** poly(ADP-ribose) polymerase 1  
**PBS:** phosphate buffered saline  
**PBS-T:** phosphate buffered saline Tween 20  
**PCNA:** proliferating cell nuclear antigen  
**PI:** propidium iodide

**PIC:** protease inhibitor cocktail  
**PLK1:** polo-like kinase 1  
**PMSF:** phenylmethylsulfonyl fluoride  
**pre-IC:** pre-initiation complex  
**pre-RC:** pre-replication complex  
**QIBC:** quantitative image-based cytometry  
**RFB:** replication fork barrier  
**RHINO:** Rad9-Hus1-Rad1-interacting nuclear orphan  
**RING:** really interesting new gene  
**RFC:** replication factor C  
**RPA:** replication protein A  
**RS:** replication stress  
**RT:** room temperature  
**SAC:** spindle assembly checkpoint  
**SCF:** Skp1/Cul1/F-box-protein  
**SDS:** sodium dodecil sulphate  
**SMC:** structural maintenance chromosomes protein  
**SSB:** single-strand break  
**ssDNA:** single-stranded DNA  
**TBS:** tris buffered saline  
**TBS-T:** tris buffered saline Tween 20  
**TEMED:** tetrametyletilendiamine  
**TLS:** translesion synthesis  
**TopBP1:** topoisomerase-binding protein 1  
**UPS:** ubiquitin proteasome system  
**UBC:** ubiquitin conjugating enzyme  
**WB:** Western blot  
**53BP1:** p53-binding protein 1



# **INTRODUCTION**



## 1. CELL CYCLE

The cell cycle is the cellular life cycle which is essential for all the organisms. On the one hand, unicellular organisms generate a new organism through this process. On the other hand, pluricellular organisms require thousands of consecutive cell divisions to develop and maintain their *status quo*<sup>1</sup>.

The cell cycle is defined as the series of events that take place in a cell leading to DNA replication and segregation of replicated chromosomes into two separate cells<sup>2</sup>. This process occurs in four consecutive cell cycle phases. The duplication of genetic material takes place in **S phase** or synthesis phase, a process known as **DNA replication**<sup>3</sup>. It is a fundamental stage that has to be properly and accurately completed once per cell cycle to avoid loss of information and the acquisition of genomic instability, a hallmark of cancer<sup>4,5</sup>. Once duplicated, the genetic material must be divided into two identical daughter cells, each bearing a diploid complement of chromosomes. This division occurs in **M phase** or **mitosis**, which includes different stages. During **prophase**, the chromosomes condense, nuclear envelope breaks down and mitotic spindle starts to form. Then, the mitotic spindle begins to capture and organize the chromosomes in a process known as **prometaphase**. During **metaphase**, microtubules are attached to kinetochore and the chromosomes are aligned in the midline of the cell. The separation of duplicated chromosomes indicates the beginning of **anaphase**, in which each sister chromatid is moved towards one of the spindle poles. Finally, the DNA is decondensed and the new nuclear envelope is formed around daughter chromosomes in a phase named **telophase**. Then, cell is divided by a process known as **cytokinesis**, forming two daughter cells genetically identical between themselves and ending the M phase of cell cycle<sup>1</sup>.

For proper DNA duplication and cell division, two additional phases are required to provide an additional time for growth and control cell cycle: **G1** (gap 1) and **G2** (gap 2) phases. G1 phase precedes S phase and is necessary for the cell to supervise the environment and its own size, and when cells receive extracellular signals that determine cell cycle entry, they bypass the restriction point, making the decisive step towards DNA replication. G2 phase precedes M

phase and is necessary for cell to ensure that DNA replication has occurred accurately, and that DNA damage is repaired prior to mitotic entry<sup>1,3</sup>.

Cell cycle is a proliferative state and the switching between proliferative state and quiescent state is often reversible to achieve tissue homeostasis. The quiescent state, termed **G0 phase**, represents a resting state where cells are not preparing to divide. Reduced levels of mitogens, contact inhibition and various stress conditions are known to promote quiescence before cells pass through the restriction point in G1 phase, but the transitions between these states are still poorly understood<sup>1,6</sup>. Recently, it has been postulated that the irreversible APC/C<sup>Cdh1</sup> activation (explained in section 1.2.2) marks the point of no return for cell-cycle entry<sup>7</sup>.

Each cell cycle is a complex process that requires the ordered and correct progression through different phases, which is tightly regulated by **cyclin-CDK** (cyclin-dependent kinases) complexes, different and specific for each phase<sup>3</sup>, and **E3 ubiquitin ligases**, which mediate the timely and precise ubiquitin-proteasome-dependent degradation of cyclins<sup>2,8</sup>.

Proper cell cycle is also controlled by several **checkpoints**, defined as quality-control pathways that sense defects in the process and induce cell-cycle arrest till the previous phase is completed<sup>2,9</sup>.

### 1.1. CELL CYCLE REGULATION BY CYCLIN- CDKS

The transition from one cell phase to another occurs in an ordered manner and is controlled by cyclin-CDK complexes<sup>3</sup>. CDKs are a family of serine/threonine protein kinases that are activated at specific points of the cell cycle by the association with cyclins, the regulatory subunits which control kinase activity and substrate specificity<sup>3,10</sup>. The number of CDKs and cyclins has increased during evolution, with 20 CDK and 29 cyclin proteins existing in mammals<sup>11,12</sup>. CDK and cyclin families function in a variety of cellular processes apart from cell cycle regulation, such as transcription, RNA processing, translation, metabolism and neurogenesis, among others<sup>10,11,13</sup>.

In the classical model for mammalian cell cycle, just some specific CDK-cyclin complexes are responsible for cell cycle progression, in an orderly and sequentially manner<sup>14</sup>. Four CDKs

(CDK1, CDK2, CDK4 and CDK6) and four classes of cyclins (A- B- D- and E-type cyclins) are responsible for driving cell cycle progression<sup>3,14</sup>. When mitogenic signals are sensed by D-type cyclins (D1, D2 and D3 isoforms), they bind to CDK4 or CDK6 and form complexes that are essential for the entry in G1 phase, a stage where cells are preparing to initiate DNA synthesis in the next cell cycle phase. To do so, the expression of E-type cyclin is allowed, by a partial inactivation of pocket proteins (pRB, p107 and p130), and it binds and activates CDK2 to regulate progression from G1 into S phase. The availability of E-type cyclins (E1 and E2 isoforms) is tightly controlled and limited to early stages of DNA replication; during late states of DNA duplication, CDK2 is activated by A-type cyclins (A1 and A2 isoforms) to drive the transition from S phase to G2. Finally, CDK1 is activated by A-type cyclins at the end of G2 to facilitate the mitotic onset. After prophase, A-type cyclins are degraded, and CDK1 is activated by B-type cyclins (B1, B2 and B3 isoforms), responsible for triggering mitosis (**Figure 1**)<sup>3,14–16</sup>.

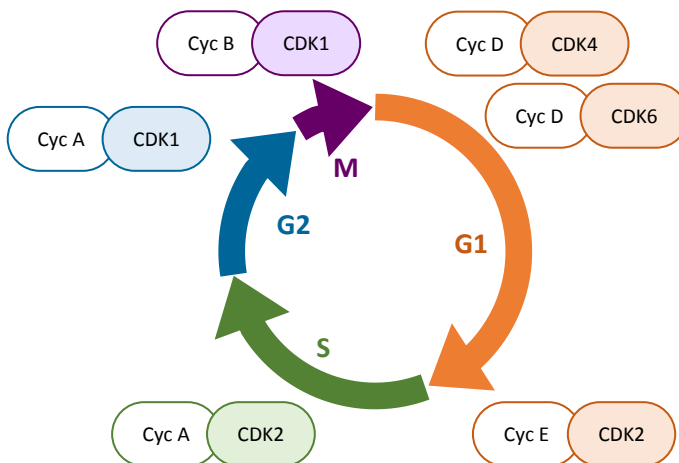


**Figure 1. Cell cycle regulation by cyclin-CDKs.** The classical model of cyclin-CDK complexes responsible for cell cycle progression. Adapted from “The cell cycle: a review of regulation, deregulation and therapeutic targets in cancer”<sup>3</sup>. Cyc: cyclins.

This “classical” model, in which each cell cycle phase is driven by specific CDKs, has been recently challenged by the generation of knockout mice for several CDKs<sup>10,14,16,17</sup>. Those studies revealed that CDK2, CDK4 and CDK6 are not essential for cell cycle of most cell types, except in highly specialized cell types: for instance, CDK2 is essential for meiotic division of germ cells<sup>18,19</sup>, CDK4 is essential for proliferation pancreatic  $\beta$ -cells and pituitary lactotrophs

<sup>20,21</sup> and CDK6 is essential for haematopoietic cells <sup>22</sup>. Only CDK1 is essential, since its elimination causes cell cycle arrest, preventing the development beyond the two-cell stage <sup>23</sup>. Thus, under certain conditions, CDK1 can be used as a substitute for the other CDKs.

### 1.1.1. REGULATION OF CYCLIN-CDKS

Due to the importance of cyclin-CDK complexes for correct and ordered cell cycle progression, these complexes are tightly regulated by several mechanisms explained below.

#### Regulation of cyclin protein levels

First, as previously mentioned, CDKs need to bind with cyclins, their activating proteins, in order to become functional. The interaction of CDKs with cyclins promotes a conformational change in the CDK subunit necessary to expose the catalytic site and the substrate binding interface <sup>10,12</sup>. Each of the cell cycle phases are characterized by the expression of a distinct type of cyclin, while CDK protein levels remain stable during cell cycle. Oscillations in cyclin protein level during cell cycle represent the primary mechanism by which CDK activity is regulated, through the synthesis and degradation of cyclins <sup>24</sup>.

**E2F** transcription factors are downstream effectors of the pRb pathway and allow the expression of many genes required for the entry into S phase and cell cycle progression. In the last decades, eight members of the E2F family have been identified, and they have been classified into “activators” (E2F1-3) and “repressors” (E2F4-8), although these opposite roles are context-dependent <sup>25–27</sup>. These transcription factors are important regulators that control S-phase entry and mitotic entry, and are also involved in processes such DNA replication, DNA repair, apoptosis, differentiation and development <sup>28</sup>.

E2F family is regulated by their association with **pocket family proteins** (pRb, p107 and p130), which interact and repress the function of E2F proteins in absence of appropriate extracellular signals. Therefore, growth factor stimulation induces pRb phosphorylation, allowing E2F release and activating their transcriptional activity <sup>24,28</sup>.

In this sense, during G1 and in response to mitogenic signals, the activation of D-type cyclin-CDK4/6 induces the phosphorylation and inactivation of the pocket proteins (pRb, p107 and

p130). These proteins form complexes with E2F transcription factors. Thus, phosphorylation of pocket proteins by D-type cyclin-CDK4/CDK6 allows the release and activation of E2F1-3 to their promoters, inducing the transcription of some substrates required for entry and progression into S phase, such as E-type cyclin, A-type cyclin, Emi1 (early mitotic inhibitor 1), nucleotide synthesis and replication enzymes<sup>24,26,28</sup>. Importantly, A-type cyclin expression is delayed relative to E-type cyclin, due to partial (in the case of E-type cyclin) or complete (in the case of A-type cyclin) inactivation of the pocket proteins.

Once in S phase, the activity of E2F decreases by A-type cyclin-CDK2-mediated phosphorylation and inactivation of E2F proteins, due to E2F7-8-mediated repression of E2F1-3-induced genes till the end of mitosis<sup>26,29</sup>.

Apart from their synthesis, cyclin levels are also controlled by the ubiquitin-proteasome system. Two different E3 ubiquitin ligase complexes target cyclins and other cell cycle regulators: the SCF (Skp1/Cul1/F-box-protein) complex and the APC/C (anaphase-promoting complex/cyclosome) complex<sup>24,29-31</sup>. D-type and E-type cyclins are degraded by SCF complex, while A-type and B-type cyclins are degraded by APC/C complex. These complexes and their mediated-degradation of cell cycle components are explained in section 1.2<sup>31</sup>.

#### Regulation by phosphorylation and dephosphorylation

In addition to cyclin availability, CDK activity is also regulated by phosphorylation/dephosphorylation on conserved threonine and tyrosine residues<sup>3</sup>.

On the one hand, CDK1, CDK2 and CDK4 require a phosphorylation of threonine 161, 160 and 172, respectively, to stabilize the activated form of the kinase. Cyclin binding to CDKs changes the T-loop from a closed conformation to an open conformation where threonine becomes accessible for phosphorylation<sup>3,12,32</sup>. These sites are phosphorylated by a cyclin-CDK complex, the **CAK** (CDK-activating kinase). The kinase is composed of three subunits: CDK7, cyclin H and MAT1. The phosphorylation made by CAK is stimulated by the association of the kinase with its corresponding cyclin. CKI (CDK inhibitory subunit) blocks CAK's phosphorylation of CDKs by inducing conformational changes in which the activation segment is not accessible to CAK or the binding to the substrates is not allowed<sup>3,33</sup>.

On the other hand, **Myt1** and **Wee1** kinases inhibit cyclin-CDK kinase activity by phosphorylating adjacent threonine and/or tyrosine residues (Threonine 14 and/or Tyrosine 15) in the CDK subunit, preventing cell cycle progression. Removal of these phosphates by phosphatases of the **Cdc25** family is required for CDK activation and further progression through cell cycle<sup>3,12,15</sup>. Cdc25 phosphatases are found in all eukaryotic organisms except in plants. In mammalian cells, three isoforms (A, B and C) have been described, with catalytic domains quite conserved, but that differ on their activity, expression, intracellular localization and mechanisms of regulation<sup>34,35</sup>.

Due to the importance of phosphorylation and dephosphorylation of these residues for regulating CDK activity and cell cycle progression, Wee1 and Cdc25 are tightly regulated by several kinases, such as cell cycle checkpoint kinases<sup>36</sup>. In response to DNA damage, when Chk1 and Chk2 (checkpoint kinases 1 and 2) are activated, Cdc25 is inactivated<sup>36-38</sup>, while Wee1 is activated by phosphorylation<sup>39,40</sup>.

#### Regulation by CDK inhibitory proteins

The fully active cyclin-CDK complex can be turned off by **CKIs**, which can bind to CDK alone or to the CDK-cyclin complex and inactivate its activity. Two families of CDK inhibitors have been described, based on their structure and CDK specificity: the INK4 family and Cip/Kip family. The **INK4** family includes p16<sup>INK4a</sup>, p15<sup>INK4b</sup>, p18<sup>INK4c</sup> and p19<sup>INK4d</sup>, that specifically bind to CDK4 and CDK6, preventing their association with D-type cyclin by allosteric competition. The **Cip/Kip** family includes p21<sup>WAF1/Cip1</sup>, p27<sup>Kip1</sup> and p57<sup>Kip2</sup>, that bind to both cyclin and CDK subunits and disable their activity<sup>3,41-43</sup>.

Both CDK inhibitory families have multiple roles in addition to regulate cell cycle. Cip/Kip proteins play important roles in apoptosis, transcriptional regulation, cell fate determination, cell migration and cytoskeletal dynamics<sup>42</sup>. INK proteins are involved in senescence, apoptosis, DNA repair and oncogenesis<sup>44</sup>.

p21<sup>WAF1/Cip1</sup>, in particular, has various effector functions involved in gene transcription, differentiation, DNA repair, apoptosis, senescence and aging<sup>45,46</sup>. Its main transcriptional regulator is p53 transcription factor, which mediates the DNA-damage induced G1 and G2

arrest<sup>47,48</sup>. p21<sup>WAF1/Cip1</sup> has also additional CDK-independent roles for regulating cell cycle. For example, it associates with E2F<sup>49</sup> and other transcriptional factors<sup>45</sup> and suppresses their transcriptional activity.

All the mechanisms mentioned above are required to ensure a proper coordination of cyclin-CDK complexes and to safeguard a correct completion of cell cycle (**Figure 2**).

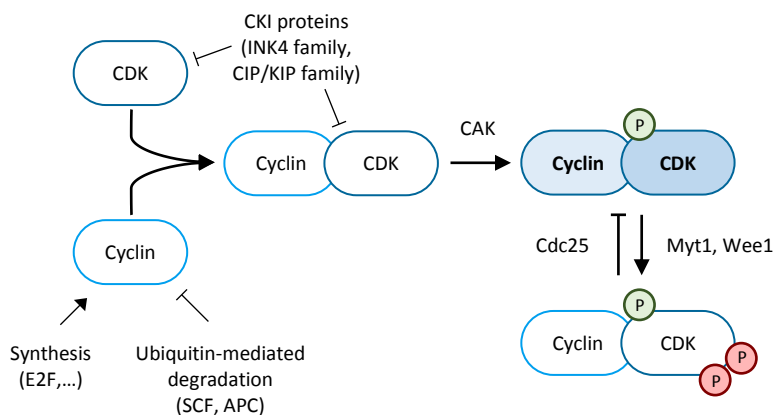


**Figure 2. Regulatory mechanisms of cyclin-CDK complexes.** Summary of the mechanisms involved in the regulation of cyclin-CDK activity explained previously. Activating phosphorylation is indicated in green, while inactivating phosphorylations are indicated in red. Active cyclin-CDK complexes are indicated in blue.

## 1.2. CELL CYCLE REGULATION BY UBIQUITIN PROTEASOME SYSTEM

The ubiquitin proteasome system (**UPS**) regulates various cellular processes including cell cycle progression by promoting the degradation of many key cell cycle regulators. Ubiquitylation consist on the covalent attachment of small ubiquitin polypeptide of 76 amino acids to a target protein<sup>8</sup>.

The different ubiquitin signals that are linked to proteins determine their fate. A single protein can be modified on one or more lysine residues with a single ubiquitin (monoubiquitylation) or with several ubiquitin molecules (polyubiquitylation). The lysine residue of ubiquitin where polyubiquitylation occurs is also important: for example, polyubiquitylation at Lys-48 (best characterized) and Lys-29 is a signal for proteasome-mediated degradation, while

polyubiquitylation at other lysine residues may act as signals for DNA repair and translation, among others. On the other hand, monoubiquitylation has other functions, as endocytosis, histone regulation and virus budding<sup>50-52</sup>.

Importantly, ubiquitylation is a reversible process due to deubiquitylating enzymes (**DUBs**), thiol proteases that catalyse the breaking of the peptide bond between the ubiquitin and proteins, and from residual peptides, and disassemble multi-ubiquitin chains. Their function is to ensure that highly ubiquitylated proteins preferentially remain associated with proteasome and prevent the accumulation of residual multi-ubiquitin chains at proteasomes<sup>50</sup>.

Ubiquitylation occurs in three consecutive steps, involving three types of enzymes. First, the ubiquitin is covalently linked and activated by an **E1** ubiquitin activating enzyme. Second, the ubiquitin is relocated to an **E2** ubiquitin conjugating enzyme. Finally, the ubiquitin is transferred by an **E3** ubiquitin ligase from the E2 enzyme to a specific lysine of the target protein<sup>8,51</sup>.

The E3 enzyme is the one that determines specificity for substrate recognition<sup>50</sup>. These enzymes can be subdivided into two major classes, **HECT** (homologous to E6-AP carboxyl terminus) family E3 ligases and **RING** (really interesting new gene) family E3 ligases. The HECT ligases form a transient covalent linkage with ubiquitin during the ubiquitylation process, while RING ligases only mediate the transference of ubiquitin from E2 enzyme to the substrate.

The RING family can be divided into single and multi-subunit E3 ligases. Single-subunit E3 contains both RING and substrate adaptor domains on the same polypeptide, while multi-subunit E3 includes a RING finger protein and a substrate adaptor protein in a complex<sup>8,50</sup>. One of the best described multi-subunit RING E3 ligases is the **CRL** (cullin RING ligase) superfamily, which includes the SCF and the APC/C E3 ligases<sup>8</sup>.

### 1.2.1. SCF COMPLEX

The SCF complex is a multi-subunit RING E3 ligase and consists of three constant subunits: the cullin subunit **Cul1**, that functions as a scaffold, and interacts simultaneously with the adaptor subunit **Skp1** (S-phase-kinase-associated protein-1) and the RING-finger protein **Rbx1**, which

interacts with the E2 ubiquitin conjugating enzyme (UBC/E2). Skp1 also binds to one variable component, known as an F-box protein, which binds through its F-box motif to Skp1 and is responsible for substrate recognition (**Figure 3**).

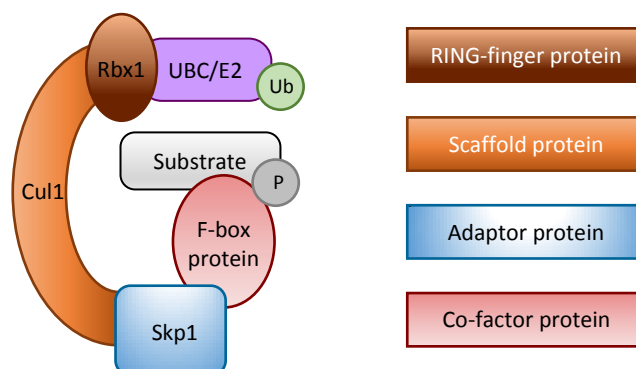


**Figure 3. Structure of SCF ubiquitin ligase.** The SCF E3 ligase is a member of the CRL superfamily. Cul1 is the scaffold protein of SCF and it binds, on one end, to Rbx1, a RING finger protein, which recruits the E2 ubiquitin conjugating enzyme (UBC, in purple). On their other end, it binds to the substrate specific unit, through an F box protein (in light red). Adapted from “The ubiquitin-proteasome system”<sup>8</sup>.

The mammalian **F-box proteins** are classified according to the structural class of their substrate-binding domains. One class is FBXW (“FBX” for F-box and “W” for WD-40 repeat domain) and seems to recognize specific Ser/Thr phosphorylation consensus sequences. The second class is FBXL (“L” for leucine-rich repeat) and seems to involve substrate phosphorylation for their interaction. And the third and last class is FBXO, which does not have WD-40 repeats or leucine-rich repeat and has different protein-protein interaction domains<sup>31,53</sup>.

Three F-box proteins, Skp2 (FBXL1), Fbw7 (FBXW7) and  $\beta$ -TrCP ( $\beta$ -transducin repeat-containing protein, also named FBXW1/11), are involved in cell-cycle control<sup>31,53</sup>. The **SCF<sup>Skp2</sup>** complex targets p27<sup>Kip1</sup><sup>54</sup>, p21<sup>WAF1/Cip1</sup><sup>55</sup> and p57<sup>Kip2</sup><sup>56</sup> CKIs and p130 pocket protein for degradation. So, it executes the transition to S phase by degrading these CDK inhibitors and maintains CDK1 and CDK2 activities. It has also been reported that this complex targets D-type and free E-type cyclins, E2F1, ORC1 and Cdt1, among other proteins<sup>57</sup>. The **SCF<sup>Fbw7</sup>** complex targets E-type cyclin, JUN and Myc for degradation<sup>31,57</sup>. The **SCF <sup>$\beta$ -TrCP</sup>** complex targets crucial cell-cycle regulators such as Wee1<sup>58</sup> and Cdc25<sup>59</sup>, and it also induces the degradation of Emi1 (APC/C inhibitor)<sup>60</sup>, allowing the correct degradation of A-type and B-type cyclins at the onset of

mitosis<sup>31,53,57</sup>. Finally, SCF<sup>β-TrCP</sup>-mediated Claspin degradation is important for recovery after a replication stress or DNA damage<sup>61</sup>.

SCF complex is active from late G1 to early mitotic entry, although it is thought to primary act at the G1-S transition<sup>31,50,53</sup>.

### 1.2.2. APC/C COMPLEX

The APC/C complex is a multi-subunit RING E3 ligase, structurally similar to SCF complex, but more sophisticated due to its large complex. It is a ubiquitin ligase of 1.5 megadaltons, forming a complex of 15 different proteins in vertebrates, including the scaffold Cul1-related protein (**Apc2**), the RBX1-related RING-finger protein (**Apc11**), which interacts with the E2/UBC enzyme, and at least 12 other components with unknown role. The variable component, known as co-factor or activator, confers specificity to APC/C complex, in the same way that F-box proteins do in the SCF complex. In mitotically cycling cells, APC/C is activated by its association with **Cdc20** (cell division cycle 20) and **Cdh1** (Cdc20-homologue 1, also known as Fzr1). There are other APC/C activators that function during meiosis and in non-dividing cells<sup>31,62</sup>. In humans, there are two E2 enzymes identified, UBCH10 and UBE2S, as a crucial regulators of cell division and identified as potential signalers for APC/C-mediated degradation (**Figure 4**)<sup>62,63</sup>.

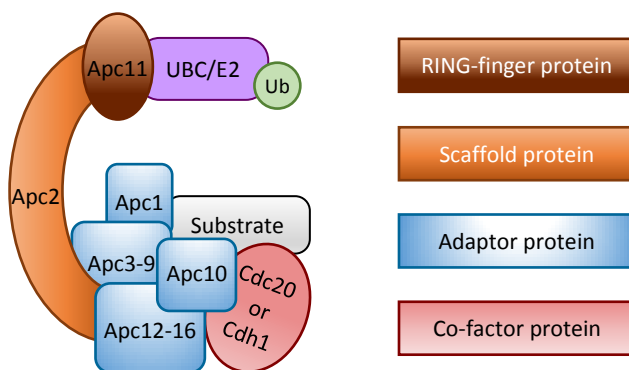


**Figure 4. Structure of APC ubiquitin ligase.** The APC E3 ligase is a member of the CRL superfamily. Apc2 is the scaffold protein of APC/C and it binds, on one end, to Apc11, a RING-finger protein, which recruits the E2 ubiquitin conjugating enzyme (UBC, in purple). On their other end, it binds to the substrate specific unit, through several proteins (in blue) and the co-factor protein (in light red). Adapted from “The ubiquitin-proteasome system”<sup>8</sup>.

Some motifs are important for substrate recognition by the APC/C E3 ligase. Chd1 and Cdc20 recognize short destruction motifs or **degron** on target substrates. The classical APC/C degron is the destruction box or **D-box**, a nine-residue motif with the consensus sequence RxxLxxI/VxN. Another APC/C degron, the **KEN motif** is a seven-residue motif with the consensus sequence KENxxxN/D<sup>63,64</sup>. Efficient ubiquitylation of substrates that harbour D and KEN motifs is dependent on both degrons. However, the substrates that contain only one of them, give some specificity on APC/C E3 ligase, since APC/C<sup>Cdc20</sup> preferentially recognizes the D-box, while APC/C<sup>Cdh1</sup> recognizes both degrons. Some substrates lack both degrons, indicating that a class of non-canonical APC/C recognition motifs contributes to APC/C-dependent substrate ubiquitylation that does not involve the co-activators in substrate recognition<sup>31,64,65</sup>.

### Regulation of APC/C

The APC/C E3 ligase is active from mitosis till the end of G1 phase. Although Cdc20 protein levels begin to accumulate in S phase, APC/C<sup>Cdc20</sup> becomes active in anaphase and drives mitotic exit by inactivating CDK1, while APC/C<sup>Cdh1</sup> ensures a G1 maintenance by a low activity of cyclin-CDK complexes<sup>66</sup>.

APC/C is activated in early mitosis by **phosphorylation** mediated by protein kinases CDK and PLK1 (polo-like kinase 1)<sup>67,68</sup>. A second mechanism to control APC/C activity is the reversible phosphorylation of co-activators: whereas the phosphorylation of APC/C is required to allow the activity of APC/C<sup>Cdc20</sup>, CDK-mediated phosphorylation of Cdh1 prevents its binding to APC/C and activation<sup>69,70</sup>. Direct phosphorylation of substrates is a third mechanism of control APC/C activity, since it hinders or reduces the APC/C ubiquitylation and subsequent degradation of some substrates, such as Cdc6<sup>71</sup> or securin<sup>72</sup>.

Another level of APC/C regulation is the presence of pseudo-substrate-based inhibitors. The major APC/C inhibitor protein, **Emi1** (also known as FBXO5), was initially discovered in preventing premature APC/C activation in early mitosis<sup>73</sup>, but some years later it was recognized as a repressor of APC/C<sup>Cdh1</sup> activity during G2<sup>74</sup>. Emi1 levels are regulated during the cell cycle. Its transcription increases at the end of G1 phase induced by E2F transcription factors and rapidly stabilises APC/C<sup>Cdh1</sup> targets such as cyclin A<sup>75</sup>. Emi1 switches from being a substrate in G1 with low Emi1 levels to acting as an inhibitor of APC/C<sup>Cdh1</sup> during S and G2

phases with high Emi1 levels<sup>76,77</sup>. Emi1 degradation is produced in prophase, after it is phosphorylated by PLK1, generating a phospho-degron that is recognized by SCF<sup>β-TrCP</sup> ubiquitin ligase<sup>60,78</sup>. To avoid Emi1 degradation, its binding partner, the **Evi5** oncoprotein blocks PLK1-dependent phosphorylation, avoiding its ubiquitination by SCF<sup>β-TrCP</sup><sup>79</sup>.

Another mechanism of control is the spindle assembly checkpoint (**SAC**), that inhibits APC/C<sup>Cdc20</sup> activity until all the kinetochores have been attached to spindle microtubules, to avoid securin and cyclin B1 degradation, both inhibitors of separase, required for a proper segregation of sister chromatids during mitosis<sup>64,80</sup>.

Finally, the linkage between APC/C activity and ubiquitin-conjugating enzyme E2 provides another mechanism of regulation. UBCH10, an E2 for human APC/C, is a target of APC/C<sup>Cdh1</sup> activity, and its degradation inactivates APC/C at the end of G1 phase, once the high affinity substrates as cyclins have been ubiquitylated<sup>64,81</sup>.

#### Functions of APC/C during mitosis and G1 phases

APC/C is inactive during G2. The increase in CDK1 and PLK1 activities at the beginning of mitosis produces the phosphorylation events required for APC/C interaction with Cdc20<sup>67,68</sup>. As a result, **APC/C<sup>Cdc20</sup>** is activated and induces A-type cyclin degradation in prometaphase<sup>82-84</sup>. Once metaphase is completed, APC/C<sup>Cdc20</sup> promotes securin degradation<sup>85,86</sup>. Securin is a chaperone that binds and inhibits separase, an enzyme capable of cleaving cohesins to liberate sister chromatids at the anaphase onset<sup>87</sup>. APC/C<sup>Cdc20</sup> also promotes B-type cyclin proteolysis<sup>82</sup>, reducing CDK1 activity at the metaphase to anaphase transition<sup>8,88</sup>, so the levels of dephosphorylated Cdh1 increase. This situation allows the formation of APC/C<sup>Cdh1</sup>, which negatively regulates APC/C<sup>Cdc20</sup> by targeting Cdc20 for degradation<sup>8</sup>. In late mitosis, besides securin and **mitotic cyclins' proteolysis**, APC/C<sup>Cdh1</sup> targets Aurora kinases<sup>89</sup> and PLK1<sup>90</sup> for ubiquitylation and degradation, which are important proteins for the **correct chromatid separation and cytokinesis**.

During G1, **APC/C<sup>Cdh1</sup>** is maintained active and is essential for the **maintenance of G1 phase**. APC/C<sup>Cdh1</sup> keeps low CDK1/2 activity during G1 phase through A-type and B-type cyclins degradation<sup>91</sup>, and through other regulators degradation, such as Skp2<sup>92,93</sup>. Repressing Skp2,

stabilizes p21<sup>WAF1/Cip1</sup> and p27<sup>Kip</sup>, which inhibit any residual cyclin-CDK complexes<sup>88</sup>. In late G1 phase, the E2F transcription factors stimulates the transcription of A-type cyclin<sup>94</sup> and Emi1<sup>75</sup>, which inhibits APC/C<sup>Cdh1</sup>, causing an increase in Skp2 levels, and a decrease in CDK inhibitors p21<sup>WAF1/Cip1</sup> and p27<sup>Kip</sup>. As a result, A-type cyclin levels increase activating CDK, and further suppress APC/C<sup>Cdh1</sup> activity by phosphorylating Cdh1.

The activity of APC/C<sup>Cdh1</sup> in G1 phase is also crucial for the **formation of pre-replicative complexes** (pre-RC) on origins of replication, where DNA polymerases initiate DNA synthesis in S phase<sup>8,31,95–98</sup>. The pre-RC assembly, known as origin licensing, involves the loading of MCM2-7 (minichromosome maintenance protein) complex in the replication origins, that requires the ORC (origin-recognition complex) and two essential factors Cdc6 (cell division cycle 6) and Cdt1 (Cdc10-dependent transcript 1). To ensure that DNA replication occurs only once per cell cycle, the assembly of pre-RC or origin licensing can occur only in a window of time with low CDK activity, during G1, and origin firing or activation can only occur after APC/C inactivation and high CDK activity, during S phase. To promote the assembly of pre-RC, APC/C<sup>Cdh1</sup> promotes the degradation of geminin<sup>99</sup>, releasing Cdt1 from its inhibition<sup>100,101</sup> and thus starting the pre-RC assembly. Furthermore, low CDK activity prevents Cdc6 phosphorylation and its consequent degradation or export from nuclei, allowing the formation of pre-RC<sup>71,96,102–104</sup>. The limitation of origin licensing to G1 phase and origin firing to S phase due to APC/C<sup>Cdh1</sup> activation is essential to prevent re-replication<sup>105</sup>. The factors involved in DNA replication and its regulation are further explained in section 2.

Besides its roles in cell cycle regulation, APC/C is also involved in other cell-cycle independent cellular functions<sup>97,98,106,107</sup>.

#### Interplay between SCF and APC during cell cycle

The previously explained regulation and functions of SCF and APC/C E3 ubiquitin ligases during cell cycle are summarized in **Figure 5**.



mechanisms previously described. The activation of APC/C<sup>Cdh1</sup> in G2 in DNA-damaged cells was described by the identification of Cdc14B phosphatase that specifically dephosphorylates and activates APC/C<sup>Cdh1</sup> upon DNA damage, after its translocation from the nucleolus to the nucleus<sup>109,110</sup>. Moreover, it was reported that p21<sup>WAF1/Cip1</sup>-dependent down-regulation of Emi1 in cells arrested in G2 by DNA damage response contributes to APC/C<sup>Cdh1</sup> activation<sup>110–112</sup>.

In the recent years, the mechanism by how APC/C<sup>Cdh1</sup> is able to control DNA damage checkpoint response is being elucidated. Many regulators of DNA damage repair and genomic stability such CtIP<sup>113,114</sup>, Claspin<sup>109,115</sup>, UPS1<sup>116</sup> and Rad17<sup>117</sup> have been characterized as Cdh1 substrates. Furthermore, G9a and GLP<sup>118</sup> have also been identified as APC/C<sup>Cdh1</sup> substrates, involving APC/C<sup>Cdh1</sup> in the regulation of senescence<sup>62,107</sup>.

## 2. DNA REPLICATION

The discovery of double-helix structure in 1953<sup>119</sup>, where two polynucleotide strands specifically paired by complementary bases, suggested how the genetic information could be copied. Some years later, Meselson and Stahl proved that replication is semiconservative in an historical experiment using density labelling<sup>120</sup>, and the first enzyme capable of synthesizing DNA was first described<sup>121</sup>. Since then, the proteins required for DNA replication, their regulation mechanisms and the coordination of DNA replication with cell cycle progression has been extensively studied<sup>122</sup>.

DNA replication consists in the duplication of the genetic material in order to obtain two copies of the same information, to finally transmit it to two daughter cells. DNA replication is a daunting process that occurs since the moment that a fertilized egg first begins to duplicate DNA to harvest a pluricellular organism, which will continue to replicate its DNA to maintain all tissue and organs. It is estimated that the human body synthesizes approximately  $2 \times 10^6$  meters of DNA in a lifetime, a distance that corresponds to 130000 times the distance between the Earth and the Sun<sup>123</sup>. So, DNA replication is an essential process that needs to be highly regulated in order to ensure the accurate duplication of the genetic material to avoid loss of information and genomic instability<sup>4,124</sup>.

Apart from copying DNA sequences, during replication, chromatin is disrupted ahead of the replication fork and must be restored behind the fork on the two newly synthesised strands. Moreover, the epigenetic marks that modulate genome accessibility also have to be maintained after DNA replication<sup>125-130</sup>.

The replication occurs in three consecutive phases (initiation, elongation and termination) that result in whole genetic material duplication. In eukaryotic cells, around 40-50 different proteins are included into the replisome<sup>131</sup>. In *Saccharomyces cerevisiae*, 42 individual proteins are sufficient to fully reconstitute DNA replication *in vitro*<sup>132</sup>.

## 2.1. DNA REPLICATION INITIATION

As previously explained, the replication origins are determined in two non-overlapping consecutive steps: a first step during G1 where pre-RCs are formed in a process known as origin licensing, and a second step during S phase where some of those pre-loaded origins are fired to duplicate the DNA. This two-stage mechanism is crucial to prevent re-replication  
105,133–135 .

The **origin licensing** requires first the recognition of origins. The main origin binding factor is the **ORC**, a conserved heterohexameric protein (ORC1-6) first identified in yeast <sup>136</sup>, which varies in its sequence specificity among different species <sup>137</sup>. Specifically, in metazoan, ORC binds to DNA without apparent sequence specificity <sup>138</sup>, but with certain characteristic elements, as nucleosome-free regions <sup>139</sup> or G-rich regions <sup>140</sup>.

Once ORC, which has ATPase activity, is recruited to replication start sites, another ATPase is bound to ORC, **Cdc6**, forming a complex required for initiation function <sup>141</sup>. In addition to ORC-Cdc6 complex, **Cdt1** is required for the assembly of pre-RC, binding to MCM2-7 and facilitating their interaction with ORC-Cdc6 complex bound at the origin <sup>122,142–145</sup>. The loading of the replicative helicase **MCM2-7** into a stable head-to-head double heterohexamer that surrounds double-stranded DNA is the defining step in origin licensing <sup>146–148</sup>. Two rounds of sequential single MCM2-7 helicase recruitment and loading at origins are required for forming a double hexamer <sup>122,144,149</sup>, resulting in the formation of pre-RCs. CDK1/2 inhibits MCM loading by phosphorylating ORC, restricting the formation of pre-RCs in G1 phase <sup>132</sup>. Subsequent events in initiation of replication do not require either ORC, Cdc6 or Cdt1, and an *in vitro* study suggest that these factors may dissociate from the DNA after MCM2-7 loading <sup>122,149</sup>.

Importantly, only a fraction of all licensed origins is activated in a cell, at different times throughout S phase, whereas other called **dormant origins** are only used to complete genome replication in conditions where S phase is affected <sup>137,150–153</sup>.

The second step is the **origin firing**, which requires high levels of CDK activity, and for this reason this process is restricted to S phase. The activation of origins is achieved by several phosphorylation events on subunits of the MCM complex mainly by the sequential action of

**DDK** (Dbf4-dependent kinase, also known as Cdc7-Dbf4 complex) and **CDK** protein kinases, required for the recruitment of **Cdc45** (cell cycle division 45) and **GINS** (go ichi ni san) for the formation of CMG complex onto chromatin<sup>154</sup>, establishing the pre-initiation complex (pre-IC)<sup>155</sup>. On their own, MCM2-7 hexamers possess little or no helicase activity, while the CMG complex possesses robust helicase activity<sup>156</sup>.

The formation of pre-IC is a process well studied in yeast, although is conserved fairly well in metazoan despite some discrepancies<sup>157</sup>. In budding yeast, first **Sld3-Sld7-Cdc45** associates with the pre-RC formed at replication origins in a DDK-dependent manner<sup>158,159</sup>. DDK phosphorylates the MCM2-7 complex, which enhances the association with Sld3-Sld7-Cdc45 and origins<sup>160,161</sup>. Secondly, CDK-mediated phosphorylation of Sld2 and Sld3<sup>162</sup> allows the association of **Sld2-Dpb11-Polε-GINS** with the origins, that are bind to Sld3 and Cdc45, to finally form an active CMG helicase<sup>163,164</sup>.

In fission yeast, the orthologs of Dpb11, Sld2 and Sld3 are well conserved, and, although DDK is needed for the association of Sld3 with origins, DDK is not as necessary in fission yeast as in budding yeast<sup>157</sup>.

Interestingly, the process of CMG complex formation seems to be quite similar also in metazoan. Although the replication machinery is well conserved in eukaryotic organisms, the regulatory components have diverged during evolution (**Figure 6**)<sup>157</sup>. Although TopBP1 (topoisomerase-binding protein 1), RecQ4 and Treslin are the functional homologues of Dpb11, Sld2 and Sld3, respectively, and are required for the initiation of replication, their requirement for pre-IC association with chromatin vary slightly. **TopBP1** is a larger and more complex protein that contains eight BRCT repeats and it is required for the loading of Cdc45<sup>165-167</sup>. **RecQ4** has been proposed as a functional homolog of Sld2, but this issue remains controversial since this protein is quite different from Sld2<sup>168,169</sup>. Although RecQ4 is dispensable for Cdc45 recruitment and formation of CMG complex, it has a role on DNA polymerase  $\alpha$  binding and DNA unwinding<sup>170,171</sup> and it is required for initiation of DNA replication<sup>172</sup>. **Treslin** was identified for its association with TopBP1 in *Xenopus* egg extracts in a CDK2-dependent manner, and required for DNA replication<sup>173,174</sup>. Other proteins are required for the formation on pre-IC: GEMC1 (geminin coiled-coil containing protein 1), which

promotes initiation of DNA replication by mediating TopBP1 and CDK2-dependent recruitment of Cdc45 into origins<sup>175,176</sup>; DUE-B (DNA unwinding element), which is able to interact with both Cdc45 and TopBP1<sup>177</sup>; and Mcm10, which is another protein required for initiation of replication<sup>178–183</sup> that interacts with RecQ4<sup>171,184</sup> and several replication factors<sup>185</sup>. Furthermore, Claspin, a protein present in the replisome that have a role in replication checkpoint activation, may play a new role in regulating the origin firing through its interaction with Cdc7<sup>186</sup>, which is also referred to as DDK<sup>187</sup>.

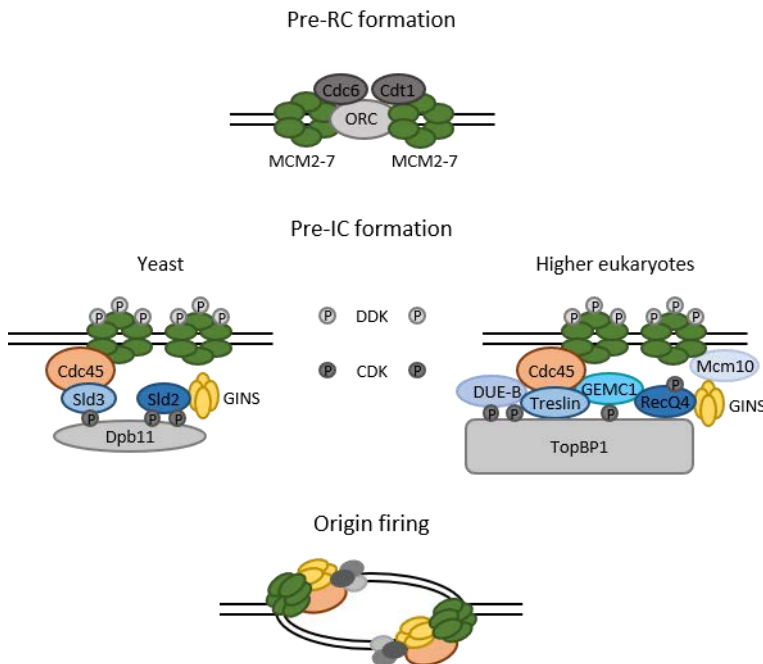


**Figure 6. Replication origins are licensed after the loading of MCM2-7 helicase complexes.** This process is conserved in all eukaryotes and requires the action of ORC, Cdc6 and Cdt1, recruited in G1 to form the pre-RC. In S phase, sequential phosphorylations of DDK and CDK (labelled with light grey and dark grey, respectively) allow the recruitment of Cdc45, GINS and additional factors to form the pre-IC. In yeast, Sld2, Sld3 and Dpb11 are the main factors leading to Cdc45 and GINS recruitment and origin firing. In higher eukaryotes, TopBP1, RecQ4 and Treslin are the functional homologs for the Cdc45 and GINS recruitment, and also other factors are required, such as GEMC1, DUE-B and Mcm10, to initiate replication. Helicase activation induces the recruitment of other proteins (labelled in grey, explained in detail in next section) at each replication fork, inducing origin firing. Adapted from “GEMC1 is a novel TopBP1-interacting protein involved in chromosomal DNA replication”<sup>176</sup> and “DNA replication origin activation in space and time”<sup>135</sup>.

## 2.2. DNA REPLICATION ELONGATION

Once the pre-RC is assembled, CMG helicase complex starts to unwind the DNA in the formation of two bidirectional replication forks together with replisome components (**Figure 7**). The initiation of DNA synthesis requires also RPA (replication protein A) and DNA polymerase alpha ( $\alpha$ )<sup>122,188,189</sup>. **RPA** is a heterotrimeric protein that consists of 70kDa, 32kDa and 14kDa subunits, which have been termed RPA1 (RPA70), RPA2 (RPA32) and RPA3 (RPA14), respectively. RPA is a single-stranded DNA (ssDNA)-binding protein that binds to ssDNA with high affinity to protect it from nucleases degradation or to avoid the formation of spontaneous duplex DNA<sup>190–192</sup>. After the DNA unwinding by CMG helicase, the ssDNA regions produced are rapidly coated by RPA. Apart from protecting this ssDNA, its function is to recruit the **DNA polymerase  $\alpha$  - primase** to the replication origins since RNA priming is required to initiate leading and lagging strand synthesis<sup>131,190</sup>. During elongation, RPA is thought to play a role in stimulating DNA polymerases delta ( $\delta$ ) and epsilon ( $\epsilon$ ) by its PCNA interaction<sup>131,190</sup>.

The major eukaryotic replicases, **DNA polymerases  $\alpha$ ,  $\delta$  and  $\epsilon$** , catalyse the formation of phosphodiester linkages of an incoming dNTP by the 3'-OH end of a growing chain. Thus, the synthesis of DNA occurs in a 5'-to-3' direction. Due to the structure of DNA, forming antiparallel double helix, when replication origins are activated, two replication forks proceed from each origin, one in each direction. In each replication fork, one chain is the **leading strand**, which is replicated continuously by DNA polymerase  $\epsilon$ ; while the other is the **lagging strand**, which is repeatedly primed and synthesized by DNA polymerase  $\alpha$  and  $\delta$ , respectively, as discontinuous fragments known as Okazaki fragments<sup>189,193</sup>. This model, which has been supported by several studies and widely accepted<sup>194,195</sup>, has been recently challenged by some studies that suggest an alternate arrangement of polymerases at the fork, concluding that DNA polymerase  $\delta$  synthesizes both strands<sup>196,197</sup> and that primers are elongated across the origin by DNA polymerase  $\delta$  until the ends are coupled to DNA polymerase  $\epsilon$  at the advancing replication forks<sup>198</sup>.

Many models of DNA replication postulate that the DNA synthesis of leading- and lagging-strands is coordinated. Due to the several additional steps that require more time occurring during lagging synthesis, it has been proposed that lagging-strand polymerase copies DNA

faster than leading-strand polymerase<sup>199</sup>. However, a recent study indicates that the average rate of both polymerases is similar, and that replication is kinetically discontinuous and disrupted by distinct pauses and rate-switches. During these pauses, helicase slows DNA unwinding to prevent the uncoupling of helicase and polymerases activities, suggesting that replication is more dynamic than previously thought<sup>200</sup>.

The efficient elongation of leading and lagging strands requires other factors. The clamp loader **RFC** (replication factor C) assembles the sliding clamp **PCNA** (proliferating cell nuclear antigen), conferring high processivity to DNA polymerases, and allowing the switch from DNA polymerase  $\alpha$  to DNA polymerase  $\delta$ <sup>122,201</sup>. The DNA unwinding during DNA elongation generates supercoils in front of the fork, which are removed by either **type I or type II topoisomerases**, being the type I the essential one; and the intertwining of daughter strands, known as pre-catenanes (behind the fork) that can only be removed by type II topoisomerases<sup>122</sup>.

During maturation of Okazaki fragments, PCNA recruits **FEN1** (flap endonuclease 1), which catalyses cleavage of the flap structure, removing the initiator RNA to make a nick<sup>201,202</sup>. To complete the maturation process of Okazaki fragments, the nick is sealed by **DNA ligase I**, which is also recruited by its interaction with PCNA<sup>122,201</sup>.

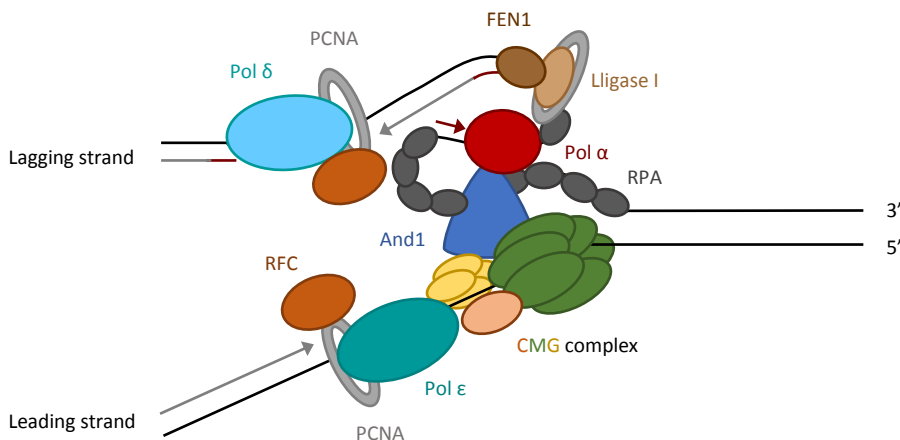


**Figure 7. Replication fork structure.** Parental strands (in black) and nascent DNA strands (in grey) are represented. The RNA primer synthesized by DNA polymerase  $\alpha$ -primase is represented in red. The proteins that compose the replisome are shown. The lagging strand is shown forming a loop so that

polymerases  $\alpha$  and  $\epsilon$  move in the same direction, in a complex composed by CMG and And1. CMG complex: MCM, Cdc45 and GINS. Pol: DNA polymerase.

In order to prevent excessive unwinding, the activities of polymerases and helicase at the replication fork are coupled by the action of the **replication pausing complex**, which travels with the replisome and is composed by **Tim1**, **Tipin**, **Claspin** and **And1** proteins. These proteins interact with several replisome components, including CMG helicase complex and polymerases<sup>203–207</sup>. These proteins are part of a larger **replisome progression complex**, which contains FACT, Mcm10 and type I topoisomerase<sup>122,208</sup>.

Moreover, during replication fork progress, a physical link between sister chromatids resulted from duplication is required to maintain them together for its correct segregation in mitosis. This link is mediated by cohesin complex, a ring-shaped multiprotein that consist of four proteins: **SMC1** (structural maintenance chromosomes protein 1), **SMC3** (structural maintenance chromosomes protein 3), Rad21 and SA1/2. This complex is not only relevant for proper segregation but also for homologous recombination (HR)-mediated repair<sup>209,210</sup>.

### 2.3. DNA REPLICATION TERMINATION

Replication termination is a process that occurs along the entire S phase, when two replication forks from neighbouring origins converge and the duplication of the DNA fragment among both origins is tidily completed. The termination includes five processes (**Figure 8**). The first process involves the relaxation of supercoils ahead of the fork mainly by type I topoisomerases. The second process is the encounter of converging forks, sliding on opposite strands of DNA (leading strand of each fork). Third, replisomes dissociate from DNA in a process known as disassembly, which requires SCF<sup>Dia2</sup>/CRL2<sup>LRR1</sup>-mediated ubiquitylation and removal from chromatin by p97/VCP/Cdc48 segregase<sup>211</sup>. Fourth, synthesis of DNA is completed through gap filling between the end of leading strand and the last Okazaki fragment of the opposing fork. Finally, copying the last turn of parental strand generates a new catenanes, that must be resolved before chromosome segregation<sup>122,212</sup>.

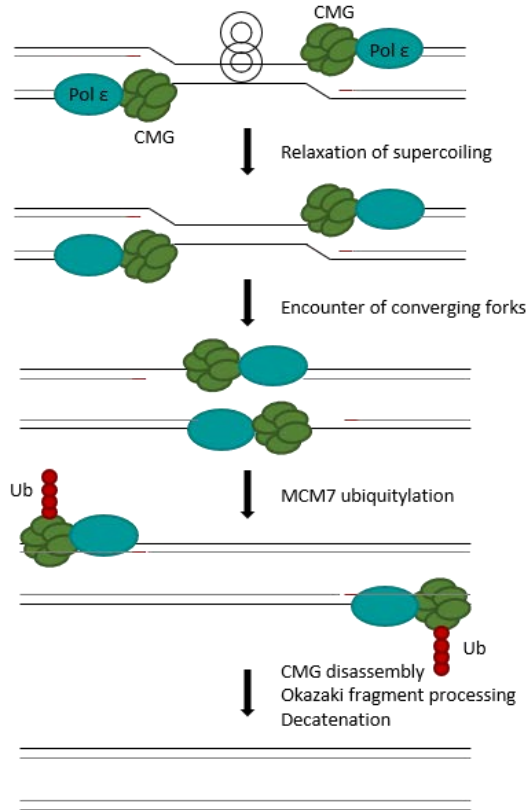


**Figure 8. DNA replication termination.** The different steps by which replication is terminated in eukaryotic model is represented. Adapted from “Mechanisms of DNA replication termination”<sup>212</sup>.

## 2.4. DNA REPLICATION ORGANIZATION

As mentioned previously, during replications, cells maintain their proper organization into chromatin (**Figure 9**) and some evidence suggest that the spatial organization of the genome is relevant<sup>213</sup>.

The first level of organization in DNA replication process is the formation of **pre-RCs** at all potential replication origins in a cell. From all the MCM2-7 complexes loaded in excess onto DNA, just 10% are being used in an unperturbed S phase. The rest normally remain dormant and are passively replicated by oncoming forks, but occasionally fire as backups to resolve problems that impede fork progression<sup>150,214</sup>.

The second level is the **replicon**, which consist in 50-120kb in metazoan cells and includes several pre-RC, of which only one is activated to replicate the stretch of DNA conforming the replicon.

The third level is the **replication domain**, which consist in 400kb to 1Mb in mammalian cells and contains several replicons in replication clusters. The replication domains adopt a structure in which replicons are separated into loops by cohesin rings. The active origins included into a replication domain fire synchronously at defined points during S phase. **Early replication** is observed in transcriptionally active gene-rich domains mainly located at the centre of the nucleus in contrast to **late replication**, which is observed in origin-poor regions enriched of repressive epigenetic marks and are located within lamina-associated domains (nuclear periphery)<sup>126,135,214,215</sup>.

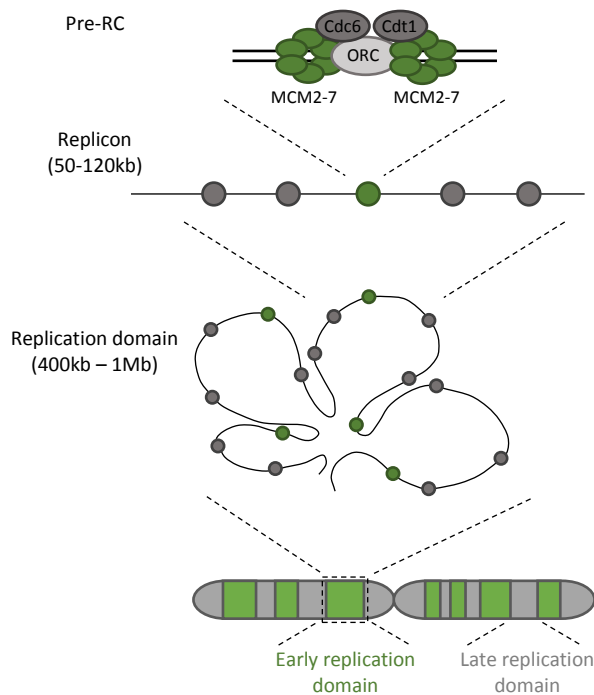


**Figure 9. Genome organization.** Pre-RCs are assembled on both active and dormant origins, but only a subset is fired in S phase. A replicon corresponds to a DNA fragment that is replicated by a single origin (active origin in green, dormant origins in grey). Adjacent replicons that fire simultaneously formed a replication domain. Each domain can replicate at different times during S phase. Adapted from “Chromatin replication and epigenome maintenance”<sup>126</sup>.

### 3. REPLICATION STRESS

The definition of **replication stress** is constantly evolving. First, it was used to define the aberrant events in cells undergoing rapid proliferation<sup>216</sup>. Later on, it was described as “the vulnerability to genotoxic insults and other stochastic events that impede the proper replication and segregation of their genomes to daughter cells”<sup>217</sup>. In recent years, replication stress has been referred to as DNA replication conflicts that generate stretches of ssDNA that is protected by RPA<sup>218</sup>. And finally, it has been described as “the slowing or stalling of replication fork progression and/or DNA synthesis”<sup>219–221</sup>.

Cells respond to replication stress by activating several mechanisms that coordinate fork stabilization and repair with cell cycle arrest to prevent cell division with unreplicated or damaged DNA. In this sense, cells try to overcome the cause of replication stress to promote replication resumption and cell cycle progression<sup>219,222–225</sup>.

In most cases, the replication stress leads to a transient pausing or **stalling** of the replisome until the stress is overcome by the checkpoint activation. Sometimes, the stalling can be more persistent and the failure to stabilize the stalled forks can lead to its collapse, which means that forks have lost their ability to replicate DNA. **Fork collapse** has been described as a process which includes replisome dissociation and the formation of double-strand breaks (DSB) at stalled forks<sup>226,227</sup>.

#### 3.1. DNA REPLICATION STRESS CAUSES

DNA replication is constantly challenged and arrested by DNA lesions induced by endogenous or exogenous agents. The hindrances can be chromosomal fragile sites, secondary DNA structures, existing DNA damage lesions, proteins tightly bound to DNA, collisions between replication and transcription machineries, insufficient nucleotides for DNA replication or oncogene activation.

### Chromosomal fragile sites

Common fragile sites (**CFSs**) are specific regions prone to exhibit gaps and breaks on metaphase following partial inhibition of DNA synthesis. Due to their genomic elements, CFSs are regions in risk for the DNA replication machinery. For example, AT-rich regions found at some CFSs can form secondary structures that stall replication forks<sup>228</sup>. Moreover, some CFSs are located at longest genes in which collisions with replication and transcriptions are produced during S phase<sup>229</sup>. Furthermore, some CFSs have low fork density and are prone to breakability because replication forks have to cover long distances<sup>230</sup>.

### Obstruction of replication fork barriers

A wide variety of hindrances can impede fork progression, either by altering the helicase activity or the ability of DNA polymerases to incorporate nucleotides, resulting in a fork slowdown and stalling. These impediments are referred to as replication fork barriers (RFB) and include DNA sequences prone to form secondary DNA structures, DNA lesions and DNA-protein complexes<sup>223</sup>.

In DNA, there are some DNA sequences that are intrinsically challenging for the replication machinery, which includes repetitive sequences and DNA regions that potentially form **secondary structures**, such as G quadruplexes, hairpins or cruciforms, that are natural barriers for replication fork progression<sup>219,221,231</sup>. To resolve or remove these obstacles, some DNA helicases are involved, such as WRN (Werner syndrome) helicase, BLM (Bloom's syndrome) protein and PIF1. Also, topoisomerases are required to remove DNA supercoils generated by the normal unwinding of DNA to replicate the region and to alleviate torsional stress<sup>221,225</sup>.

Another barrier for replication fork progression is the presence of **damaged DNA**, which is not recognized as valid template by replicative DNA polymerases. There are a variety of endogenous or exogenous sources of DNA damage, such as products of cellular metabolism (for example, reactive aldehydes), ultraviolet light and chemical mutagens. To deal with DNA lesions, DNA repair pathways and translesion DNA synthesis (**TLS**) are activated to avoid replication inhibition<sup>219,225</sup>. TLS polymerases are able to tolerate DNA template lesions, that DNA replicative polymerases do not, to resume replication<sup>232</sup>.

**Proteins tightly bound to DNA** can obstruct fork progression, generating replication stress. Although is a process described in yeast, it is not clear if these regions represent a challenge for the replisome in mammals<sup>221</sup>.

#### Replication-transcription conflicts

The transcription machinery is a natural barrier to replication fork progression, since they share the same DNA template and collisions between them are an important source of replication stress. Therefore, cells have evolved mechanisms to limit both processes in space and time to avoid collisions: most transcription occurs in G1 while replication occurs in S phase<sup>233</sup>.

On the one hand, some studies suggested that replication stress appears before **replication and transcription machineries' collision**, which is likely due to topological stress generated between them. For this reason, topoisomerases are essential to prevent genomic instability<sup>221,234</sup>.

On the other hand, the collision between both machineries forms a DNA-RNA hybrid, called **R-loop**. The generation of R-loops is limited by the THO complex, that targets the nascent RNA to the RNA processing machinery and to the nuclear pore<sup>224,235</sup>. Several factors are involved in the resolution of R-loop, including RNase H enzymes and RNA helicases such as senataxin, which remove the R-loop by degrading the RNA strand or undoing the hybrid, respectively<sup>224,225</sup>.

#### Down-regulation of limiting factors of replication

Faithful DNA replication requires numerous factors, and their down-regulation can result in the slowing or stalling of replication fork. The pool of nucleotides (dNTPs), components of replisome, histones and histone chaperones are some of these replication factors<sup>236-238</sup>.

An **excess of replication origin firing** provokes the exhaustion of essential factors for DNA replication, including RPA. Certainly, the level of RPA, which protects any form of ssDNA from breakage, becomes limiting when additional origins become active, leading to fork collapse<sup>227,239</sup>.

The balance of dNTP pools, due to the coordination of their synthesis and degradation, determines the accuracy during S phase. **Small perturbations in the dNTP pools** substantially affect fork progression<sup>240–243</sup>. A decrease in the levels of dNTPs by oncogene expression has been proposed to induce oncogene transformation, since exogenously supplied nucleosides rescue this phenotype<sup>242</sup>. Remarkably, a decrease in the pool of dNTPs can be induced by hydroxyurea (**HU**, also called hydroxycarbamide), which inhibits the ribonucleotide reductase enzyme causing replication inhibition due to lack of substrate<sup>244</sup>. HU is an antineoplastic agent, which was used as treatment for several types of solid tumours and for infectious disease. Although newer and more efficient agents have replaced HU, it is still used for the treatment of head and neck cancers and chronic myeloid leukaemia<sup>231,245–247</sup>.

### Oncogene expression

Overexpression or constitutive activation of oncogenes, such as HRas<sup>248</sup>, Myc<sup>249</sup> and cyclin E<sup>250</sup>, is another source of replication stress. Oncogenes shorten the length of G1, which can disrupt replication dynamics altering origin licensing and induce more conflicts between replication and transcription machineries<sup>251,252</sup>. Fewer licensed origins means a reduction in dormant origins, required when replication forks stall. Increased replication initiation can disrupt the temporal pattern of origin firing and may deplete the dNTP pools in a cell<sup>242</sup>, leading a persistent replication stress<sup>253</sup>.

## **3.2. CELL-CYCLE CHECKPOINTS**

As previously mentioned, cells have developed several mechanisms called **checkpoints** to ensure the fidelity of division and monitor successful completion of cell cycle events, which must occur in the proper order. When a cell cycle event has not been successfully completed, checkpoints sense the defects in the process and delay cell cycle progression until the previous step is correctly completed<sup>2,9,254</sup>.

The checkpoint pathways acts as a signal transduction cascade, that includes three groups of proteins: 1) **sensor** proteins that recognize damaged DNA or abnormalities and initiates a biochemical cascade; 2) **transducer** proteins, which are usually protein kinases that amplify

the signal from sensor by phosphorylating downstream target proteins; and 3) **effector** proteins, which include the most downstream targets and are regulated to avoid cell cycle progression<sup>4,254</sup>.

The checkpoint pathways operate during the entire cell cycle and interrupt cell cycle progression at any point during the four phases. The sensor proteins are shared by the various checkpoints, similarly as the transducing proteins; the effector proteins, which inhibit phase transition, are the proteins that give each checkpoint its identity<sup>254</sup>. In this sense, checkpoints can be classified according to the cell cycle phase in which they are activated or upon the transition that is being inhibited: G1/S checkpoint, S-phase checkpoint, G2/M checkpoint and mitotic or spindle checkpoint<sup>254–256</sup>.

In this thesis, we focused on the mechanisms activated in S phase, which is the most vulnerable phase for the acquisition of DNA damage. As explained previously, several causes can induce fork stalling during S phase, which provokes the accumulation of ssDNA. This results in **DNA replication checkpoint** activation in order to ensure the fidelity of the copied DNA to avoid genomic instability and loss of information<sup>222</sup>. If this stalling persists, replication forks are prone to collapse, and cells accumulate DSBs. When this happens, the **DNA damage checkpoint** is activated. The roles of these checkpoints are maintenance of fork stability and coordination of cell cycle delay and repair of DNA lesions with resumption of DNA replication<sup>222,225,254,257</sup>.

Three members of PIKKs (phosphoinositide 3-kinase-related kinases), **DNA-PK** (DNA-dependent protein kinase), **ATM** (ataxia-telangiectasia mutated) and **ATR** (ATM and Rad3-related), are the main sensors of DNA damage and replication stress. DNA-PK and ATM kinases are primarily activated by DSBs being ATM the main kinase involved in checkpoint response and DNA-PK in regulating DNA repair by the non-homologous end-joining (NHEJ) pathway, while ATR kinase is activated by ssDNA or replication fork arrest<sup>9,254,256,258–261</sup>.

Although both mechanisms are required to preserve genome integrity, ATR is essential for cell survival, since its deletion results in embryonic lethality<sup>262,263</sup>. However, a recent work has described that, in contrast to ATM depletion, which is not lethal<sup>264,265</sup>, point mutations in ATM that inactivate its kinase activity also result in embryonic lethality in mice<sup>266</sup>.

Although the three members of PIKK family are large kinases with significant sequence homology and they target an overlapping set of substrates<sup>259,267</sup>, they are activated by different signals and specialized in their responses so they present a low level of functional redundancy between them<sup>268</sup>. All three PIKK family members phosphorylate preferentially serine/threonine residues followed by a glutamine (S/T-Q)<sup>269</sup>. They share some common substrates, such as the phosphorylation of the histone variant H2AX on the Ser139 and phosphorylation of distinct sets of RPA32. The foci formed by phosphorylated H2AX (**γH2AX**) has been commonly used as a DSB marker<sup>257,270,271</sup>, although recent evidences indicates that only a small variable fraction of γH2AX foci in fact represents DSBs, when colocalizing with 53BP1 foci<sup>272</sup>. Another PIKK target is **RPA**, the heterotrimeric protein that accumulates on long stretches of ssDNA at stalled and collapsed forks. In response to replication stress, DNA-PK and ATR phosphorylate the RPA32 subunit<sup>273,274</sup>, while in response to DSBs are the kinases ATM and DNA-PK the ones that phosphorylate RPA32<sup>275,276</sup>.

### 3.2.1. DNA REPLICATION CHECKPOINT

The slowing or stalling of replication fork progression may expose significant amounts of ssDNA, generated by the uncoupling of helicase and polymerases activities or due to the uncoupling of leading and lagging strands synthesis<sup>124,200,232,277–279</sup>. This ssDNA becomes coated by **RPA** acting as a platform for the recruitment of many proteins important to induce the DNA replication checkpoint (**Figure 10**)<sup>267,280–282</sup>. One protein required for ATR recruitment to stressed replication fork is **ATRIP** (ATR-interacting protein)<sup>283</sup>, although it is not enough for ATR activation<sup>218</sup>. ATRIP deacetylation by Sirtuine-2 is required for ATRIP-ATR binding to RPA<sup>284</sup>. Furthermore, **ATR** kinase activation depends on conformational changes mediated by the binding of ATR to activator proteins<sup>282</sup>. In vertebrates, two ATR activators have been identified: **TopBP1**, which interacts with both ATR and ATRIP<sup>285,286</sup>, and **ETAA1** (Ewing tumour-associated antigen 1), which is recruited through direct interactions with RPA<sup>287–290</sup>. TopBP1 recruitment depends on Rad9-Hus1-Rad1 (**9-1-1**) checkpoint clamp complex<sup>291,292</sup>, which is loaded onto DNA by the RPA-recruited **Rad17-RFC** clamp loader<sup>293,294</sup>. After TopBP1 recruitment on 9-1-1 clamp complex, which is partially dependent on **MRN** (Mre11-Rad50-Nbs1) complex<sup>295,296</sup> and on **RHINO** (Rad9-Hus1-Rad1-interacting nuclear orphan)<sup>297,298</sup>, TopBP1 interacts with ATR-ATRIP to stimulate ATR activation<sup>299</sup>.

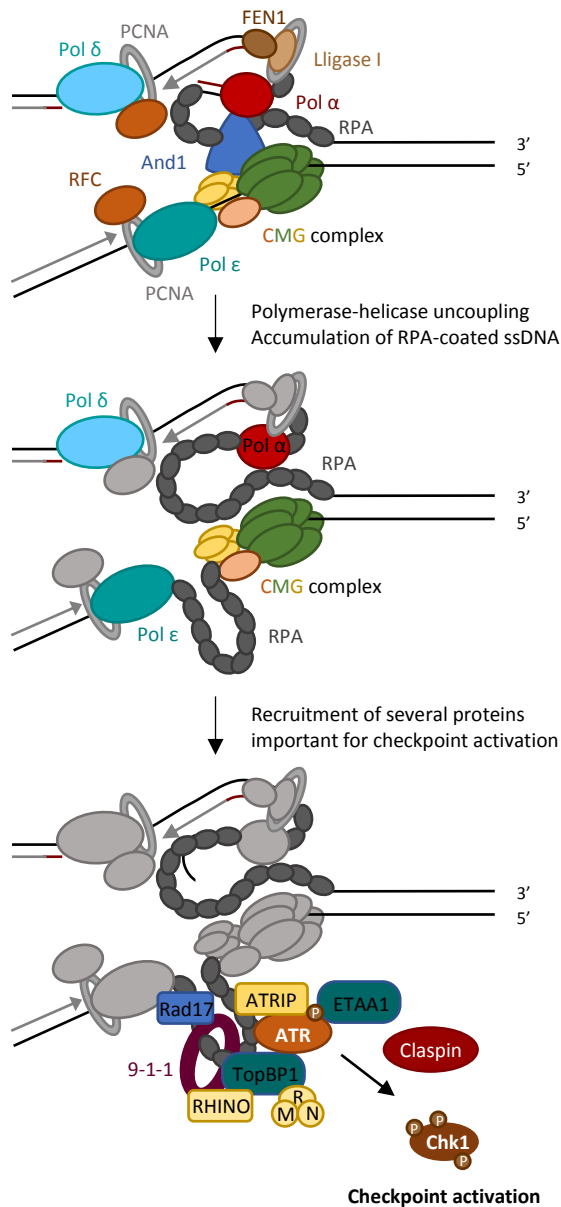


**Figure 10. A model for replication checkpoint activation.** ssDNA produced by the uncoupling of helicase and polymerases activity is coated by RPA, which acts as a platform for the recruitment of several proteins important to attract ATR, such as its regulatory unit ATRIP and regulatory factors, such as Rad17, TopBB1, the 9-1-1 complex to the replication fork. All these proteins stimulate ATR activity, and with the help of mediator proteins such as Claspin, the activation of Chk1 and the entire checkpoint pathway.

Once activated, when ATR is autophosphorylated in Thr1989<sup>300</sup>, ATR phosphorylates a large number of substrates. The main effector protein of ATR is **Chk1**. Chk1 is phosphorylated by ATR on Ser317 and Ser345<sup>301,302</sup>, inducing a conformational change on Chk1 that allows its autophosphorylation on Ser296<sup>303</sup> to further activate this effector kinase. The ATR-mediated phosphorylation of Chk1 involves several mediator proteins, such as Claspin<sup>304</sup>, Tim/Tipin<sup>305</sup> or PARP1<sup>306</sup>.

**Claspin** is phosphorylated in response to replication stress by CK1  $\gamma$ 1 (casein kinase 1  $\gamma$ 1)<sup>307</sup> allowing the association of Claspin with Chk1<sup>308-310</sup>. Activation of Chk1 is enhanced under those conditions, since ATR shows a higher affinity for the Chk1-Claspin complex, than for Chk1 alone<sup>311</sup>.

It should be noted that ATR or its main downstream effector Chk1 have effect on unperturbed cells during S phase, where they regulates origin firing<sup>312-314</sup>, although Chk1 is not strongly phosphorylated by ATR. The basal level of activity may be enough to their roles in normal conditions.

#### Functions of DNA replication checkpoint

As mentioned previously, DNA replication checkpoint is activated in response to an accumulation of ssDNA. When this happens, ATR is activated to control checkpoint activation, to promote a reversible cell cycle arrest to prevent mitotic entry with unreplicated DNA, to inhibit late origin firing and to maintain fork stability to recover replication when the stress is overcome. Additionally, this checkpoint regulates fork restart or DNA repair mechanisms to safeguard genomic integrity. The mechanisms involved in the most important functions of DNA replication checkpoint are explained below.

- **Cell cycle arrest.** One important function of ATR/Chk1 pathway is to arrest cell cycle when replication fork progression is compromised. Once Chk1 is activated, it phosphorylates and activates Wee1 kinases<sup>39,40</sup>, which phosphorylate CDKs and inhibit their activity, and phosphorylates and inactivates Cdc25 phosphatases<sup>37,40</sup>, which are required to remove inhibitory phosphorylations of CDKs<sup>34</sup>, leading to cell cycle arrest. Chk1 controls Cdc25

phosphatases by the binding of Cdc25C to 14-3-3 proteins that sequester the phosphatase in the cytoplasm or the induction of Cdc25A and Cdc25B proteasome-mediated degradation<sup>35</sup>.

- **Regulation of origin firing.** Inhibition of origin firing is another mechanism used by replication checkpoint to prevent cell cycle progression and to arrest cells in S phase. During an unperturbed S phase, ATR and Chk1 are negative regulators of origin firing, preventing excessive activation of origins<sup>312,315</sup>. ATR has also a crucial role on blocking origin firing in response to replication stress<sup>316–318</sup> to prevent RPA exhaustion that leads to fork breakage<sup>227,239</sup>. As mentioned previously, origin firing requires the loading of Cdc45 and GINS to the MCM2-7 complex, which is dependent of DDK and CDK kinases. As explained in the previous point, Chk1 phosphorylates Wee1 and Cdc25 that leads to inhibition of CDK2<sup>40</sup>. Another mechanisms by which ATR-Chk1 blocks origin firing is ATR-mediated phosphorylation and stabilization of the histone MLL (methyltransferase myeloid/lymphoid)<sup>319</sup> that methylates histone H3 Lys4, and Chk1-mediated phosphorylation of Treslin<sup>320</sup>, both preventing the loading of Cdc45 at replication origins. In addition, ATR regulates Rif1 (Rap1-interacting factor), which dephosphorylates MCM2-7 complex through directing protein phosphatase 1 to counteract DDK activity to restrain replication initiation<sup>135,321</sup>.

Although replication checkpoint suppresses origin firing under replication stress conditions, it allows dormant origin firing locally as a backup to complete replication in these regions<sup>322</sup>. The reason why local dormant origins are activated whereas global origin firing is inhibited by replication checkpoint is unknown<sup>153</sup>. A recent study suggests that regulation of origin firing by ATR depends on the level of replication stress: during low levels of replication stress, FANCI binds to unfired origin and directs DDK-dependent phosphorylation of MCM2-7 complex promoting dormant origin firing, while moderate-high levels of replication stress result in a more sustained ATR activation, leading to FANCI phosphorylation and reduced origin firing<sup>323</sup>.

- **Maintaining replication fork stability.** Replication fork stabilization has been described as an important function of the replication checkpoint and it is defined as the maintenance of the ability of stalled forks to restart DNA synthesis after removal or bypass the block of DNA replication<sup>282</sup>. Once replication forks lose the ability to restart, forks collapse, which usually involves the formation of DSBs.

It is known that ATR is essential for stabilization of stressed replication forks<sup>324</sup>. On the one hand, studies of chromatin immunoprecipitation performed in yeast show that replisome is disassembled in the absence of checkpoint kinases after HU, indicating a possible role for ATR in replisome stabilization<sup>325–327</sup>. On the other hand, ATR signalling promotes the association of FAND2 with the MCM2-7 complex, restraining replisome function and preventing the accumulation of ssDNA upon HU exposure<sup>328</sup>. Moreover, cohesins are thought to participate in fork protection and stability maintenance<sup>329,330</sup>. A recent study in yeast showed that the ATR-mediated ubiquitination of cohesins induces their mobilization to nascent DNA to stabilize stalled replication forks<sup>331</sup>.

Another mechanism of fork stabilization in response to genotoxic stresses that is rapidly emerging is **replication fork reversal**<sup>332</sup>. This model was first observed in 1976 as a fork remodelling process<sup>333</sup>. It is defined as the conversion of a replication fork, a three-way junction, into a four-way junction by the annealing of the two newly synthesized strands and the re-annealing of the parental strands forming a “chicken foot” structure<sup>334</sup>. During the last years, it has been demonstrated that fork reversal is a very common event in response to various types of DNA replication stress, from which replication can be restarted<sup>332</sup>. SMARCAL1 is a translocase of SWI/SNF protein family, which is required for reversed fork formation<sup>335,336</sup>. ATR-mediated phosphorylation of SMARCAL1 limits its fork remodelling activity and prevents aberrant fork cleavage by SKX4 and CtIP nucleases<sup>337,338</sup>. But it has to be considered that other authors show that SMARCAL1 depletion leads to the activation of an alternative mechanism involving Mus81-dependent fork cleavage<sup>339</sup>. On the other hand, Chk1 mediates the protection of replication forks by preventing fork collapse due to the inhibition of different nucleases<sup>340</sup>, such as Mus81<sup>341</sup> and Mre11<sup>342</sup>.

- **Regulation of DNA repair mechanisms.** Replication checkpoint activates, if needed, DNA repair pathways to guarantee genomic stability. The repair mechanisms induced by replication stress are one-ended DSBs. Since DSBs can also be sensed by DNA damage checkpoint (explained in section 3.2.2), there is a crosstalk between both pathways at this point<sup>222,247</sup>. ATR is described to be more implicated in HR repair than non-homologous end joining (NHEJ) repair of DSBs<sup>343</sup>. For example, ATR regulates BRCA1 (breast cancer type 1)<sup>344,345</sup>, a protein

directly involved in HR-mediated repair<sup>346</sup>. Furthermore, it is described that Chk1 interacts and phosphorylates RAD51, stimulating HR pathway<sup>347</sup>.

Apart from HR, ATR might play an important role on Fanconi anaemia (FA) pathway, involved in the repair of DNA interstrand crosslinks. ATR-mediated phosphorylation of FANCI<sup>348</sup>, which leads to FANCD2 mono-ubiquitination by the core complex<sup>349</sup>, activates the FA pathway<sup>350</sup>. Moreover, ATR phosphorylates FANCM, which allows its recruitment to the site of interstrand crosslinks and is also required for an efficient activation of ATR<sup>348,351</sup>.

- **Regulation of replication fork restart.** In addition to the replication checkpoint-mediated fork stabilization to prevent fork collapse, the replication checkpoint also regulates the pathways that promote fork restart<sup>282</sup>. Several pathways are involved in fork restart: 1) repriming by PrimPol ahead of stalled polymerase<sup>352–354</sup>, 2) bypass the damage with a TLS polymerase<sup>355</sup> or 3) template switching, using the undamaged sister chromatid as template for replication, 4) fork reversal<sup>334</sup>, and 5) cleavage of the reversed or stalled fork by endonucleases to facilitate HR-mediated mechanisms of fork restart<sup>356–358</sup>.

ATR phosphorylates Rev1 (reversionless1) and polymerase  $\eta$ , two of the translesion polymerases<sup>359–362</sup>. Moreover, ATR/Chk1-dependent recruitment of polymerase  $\eta$  and Rad18 into chromatin<sup>363</sup>, being the last one an important ubiquitin ligase that promotes PCNA mono-ubiquitination, which is an important step for TLS<sup>364</sup>, suggest a role of replication checkpoint in promoting TLS.

In addition, ATR phosphorylates RPA<sup>365,366</sup>, PALB2<sup>367</sup> and XRCC3<sup>368</sup>, while Chk1 phosphorylates RAD51<sup>347</sup> and BRCA2 (breast cancer type 2)<sup>369</sup>, all of which promotes RAD51 recruitment to stalled or collapsed forks<sup>357,370</sup>. Furthermore, ATR phosphorylates BLM<sup>371</sup> and WRM<sup>372</sup>, which promotes replication restart and prevents the formation of DSBs at stalled forks. All these substrates promote **RAD51**-dependent replication fork restart through diverse mechanisms, including template switching, fork reversal and HR<sup>282</sup>.

A detailed description of replication fork restart will be further explained in section 3.3.

### 3.2.2. DNA DAMAGE CHECKPOINT

When the DNA damaged is sensed, a DNA damage response (DDR) is activated (**Figure 11**) to detect the lesions, signal its presence and promote their repair in coordination with the inhibition of cell cycle progression to avoid mitotic entry with damaged DNA, which is promoted by DNA damage checkpoint <sup>373</sup>.

The DNA damage can be produced by physical or chemical sources, such as ionizing radiation (IR), ultraviolet (UV) light, alkylating agents (methyl methanesulfonate), crosslinking agents (mitomycin C, cisplatin, psoralen) or topoisomerase inhibitors (camptothecin, etoposide). To counteract DNA damage, repair mechanisms specific for different type of lesions have evolved: 1) mismatch repair (MMR) when mispaired bases are replaced with the correct bases, 2) base excision repair (BER) to recognize and repair small chemical alterations of DNA bases, 3) nucleotide excision repair (NER) to correct pyrimidine dimers, 3) interstrand crosslink (ICL) repair to deal with ICL with the assistance of FA proteins, 4) single-strand break (SSB) repair to repair SSB, and 5) NHEJ or HR to process DSBs <sup>373,374</sup>. In this thesis, we will focus on DSBs, since they can be generated by replication stress in S phase, as a result of collapsed forks <sup>219,222,224,225,257</sup>.

DSBs can be sensed by **MRN** mediator complex <sup>375-377</sup>: **Mre11**, which has endonuclease and 3'-5'-exonuclease activities, forms a complex with **Rad50**, a member of SMC family with ATPase activity that associates with DNA ends of DSBs, and **Nbs1**, which regulates the activities of Mre11 and Rad50 and contains additional protein-protein interaction domains important for MRN function <sup>374,377,378</sup>. Nbs1 associates with ATM, promoting its recruitment to DSBs and activation <sup>374,379</sup>, with the help of **53BP1** (p53-binding protein 1) and **BRCA1** <sup>376,380</sup>. ATM protein is predominantly nuclear, where it exists as a catalytically inactive noncovalent homodimer. DNA damage turns it into an active monomer by ATM autophosphorylation at Ser1981 in the FAT domain <sup>381,382</sup>. Additional ATM autophosphorylations, as well as **Tip60**-mediated acetylation at Lys3016, were identified for an optimal ATM-mediated response <sup>376,378,382-386</sup>. Moreover, dephosphorylation events, by PP2A44 and PP5 phosphatases, might also contribute to ATM activation <sup>376</sup>.

Once activated, **ATM** phosphorylates a large number of substrates, involved in cell-cycle checkpoints and DNA repair <sup>378,387</sup>. The main transducer protein of ATM is **Chk2**, which is phosphorylated on Thr68 by ATM <sup>254,388</sup>. As explained before, and together with other PIKKs, ATM also phosphorylates H2AX histone variant on Ser139 <sup>270,389,390</sup>, which acts as a signal amplifier: **γH2AX** is recognized by MDC1 (mediator of DNA damage checkpoint 1) protein, which in turn is stabilized on chromatin and phosphorylated by ATM, leading to further recruitment of ATM and additional **γH2AX** formation along chromatin, amplifying DDR signalling <sup>269,391</sup>. ATM-mediated phosphorylation of MDC1 allows RNF8 retention on damaged chromatin <sup>392,393</sup>, stimulating ubiquitylation of linker histone H1 <sup>394</sup>. Ubiquitylated H2 is recognized by another ubiquitin ligase, RNF168, that ubiquitylates H2A-type histones to promote recruitment of **53BP1** to repair toward NHEJ <sup>30,394</sup>. The signal amplification of ATM is important for correct DNA damage checkpoint activation, but also for **BRCA1** phosphorylation on multiple residues and recruitment at sites of damage <sup>269,374,395</sup>.

In **HR** repair pathway, DSBs are resected to generate 3'-ssDNA. This resection is promoted by MRN complex and **CtIP** (CtBP-interacting protein), and a further resection is carried out by **Exo1** (exonuclease 1), **BLM** and **DNA2** <sup>396-401</sup>. The ssDNA generated by the resection is coated by **RPA**, which activates **ATR** via ATRIP, activating the checkpoint response <sup>267</sup>. Finally, RPA is exchanged for **RAD51** to promote strand invasion, HR repair and resolution of intermediates. HR is restricted to S and G2 phases because it uses sister-chromatid sequences as the template to mediate repair <sup>373</sup>, and although it is typically viewed as an error-free pathway, it often requires error-prone polymerases <sup>402</sup>.

During **NHEJ**, the **Ku70/80** heterodimers recognize and bind to DSB ends to protect them from degradation. This complex also recruits and activates **DNA-PK** and the endonuclease Artemis, which removes the excess of ssDNA to generate a proper substrate by **DNA ligase IV**, with the help of additional factors involved in this pathway. NHEJ is considered an error-prone repair pathway since it involves direct ligation with little (less than 10pb) or no homology between joined ends. During cell cycle, this repair pathway occurs predominantly in G1 phase, but also in G2 phase <sup>403-406</sup>.

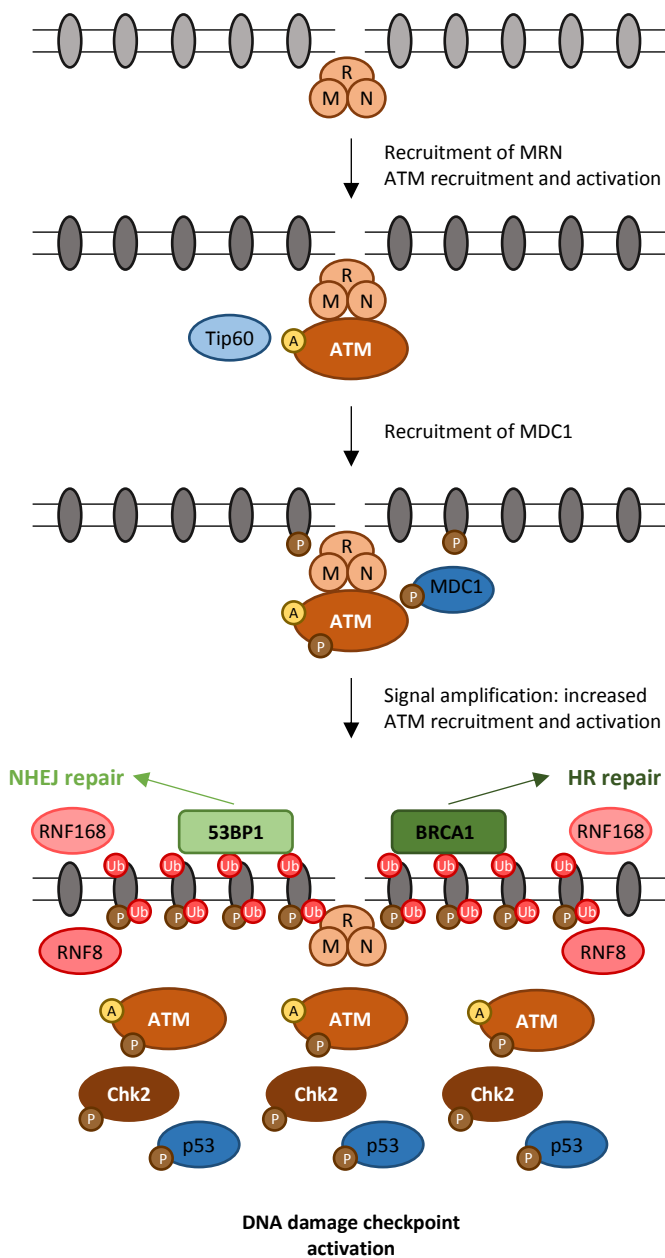


**Figure 11. A model for DDR activation and signal amplification in response to DSB.** MRN complex are recruited at DSBs. Post-translational modifications (autophosphorylation and acetylation) induce ATM activation. Once activated ATM phosphorylates several substrates, which leads to a further recruitment and activation of ATM, amplifying DDR signalling. Phosphorylation is indicated in brown circles, acetylation is indicated in yellow circles and ubiquitylation is indicated in red circles.

Several factors regulate the DNA 3' end resection, since it is the earliest divergent step between both pathways: BRCA1, in complex with MRN, promotes DNA end resection, while 53BP1 plays an important role restricting this process<sup>407,408</sup>. It is thought that in NHEJ-mediated DSB repair, 53BP1 is phosphorylated by ATM, which allows the interaction with its downstream targets such as Rif1. Rif1 suppresses 53BP1 repositioning, protecting DSBs from resection and allowing NHEJ. When 53BP1 is dephosphorylated by phosphatases, it causes Rif1 release from chromatin, which results in a reposition of 53BP1 allowing nucleases to access DNA damage sites and promoting resection for HR<sup>403,409</sup>. A recent study suggests a role of APC/C<sup>Cdh1</sup> in choosing the repair pathways in S/G2 phases. They demonstrate that the activation of APC/C<sup>Cdh1</sup> leads to USP1 destruction and the recruitment of BRCA1, which expels Rif1 and reinforces end resection promoting HR repair<sup>410</sup>.

#### Functions of DNA damage checkpoint

As it has been mentioned, different types of repair pathways that act into DSB repair are sensed by specific complexes that result in the activation of ATM, ATR and DNA-PK. The signal is transduced downstream by a kinase cascade. ATM activation results in the activation of Chk2, while ATR results in the activation of Chk1.

These kinases stabilize effector proteins like Cdc25 by phosphorylation, inhibiting CDK activity as an early response to DNA damage<sup>9,34,411</sup>. p53 transcriptional factor is a target of both sensor kinases (ATM/ATR) and effector kinases (Chk2/Chk1)<sup>412-414</sup>. Moreover, MDM2, the ubiquitin ligase responsible for p53 degradation, is targeted after DNA damage by both ATM/ATR as well as Chk2/Chk1, contributing to stabilization and accumulation of p53<sup>414,415</sup>. The key transcriptional target of p53 is p21<sup>WAF1/Cip1</sup><sup>416,417</sup>, an inhibitor of CDK activity which causes cell cycle arrest<sup>9,412</sup>. Moreover, it has been reported that p21<sup>WAF1/Cip1</sup> down-regulates Emi1 in G2 arrested cells after DNA damage, activating APC/C and degrading A-type and B-type cyclins<sup>109,111,112</sup>. Participation of p21<sup>WAF1/Cip1</sup> in DNA repair process was first suggested by its interaction with PCNA, resulting in the competition and displacement of other PCNA-interacting proteins, such as TLS polymerases, which leads to DNA replication inhibition and regulation of the repair processes<sup>418-424</sup>.

Apart from inducing cell cycle arrest, target genes of the activated cascade in response to DNA damage coordinate DNA repair. Moreover, in response to persistent damage, cells are withdrawn from the cell cycle by p53-mediated apoptosis or senescence in order to avoid cell division with damaged or unrepliated DNA<sup>425</sup>. While cellular senescence response arrests cell cycle permanently, cell death response facilitates the destruction of the damaged cell. Since senescent cells secrete pro-inflammatory cytokines, which represent a threat for the organism, cell death seems to be the safest response<sup>411</sup>.

### 3.3. REPLICATION RESTART OR REPAIR PATHWAYS

In response to replication stress, replication checkpoint tries to maintain the stability of replication forks to resume DNA duplication once the block is released<sup>222,426</sup>. Restart from the same replication fork guarantees replication of the whole genome. If the same fork cannot be restarted, **activation of dormant origins** preserves genomic integrity<sup>137,150–153</sup>, since dormant origins are located in the same replicon and their activation does not alter the replication timing program<sup>126,427,428</sup>. However, when dormant origin firing allows resumption of replication after replication fork collapse<sup>370</sup>, it might contribute to the acquisition of genomic instability<sup>226</sup>.

It has to be noted that the presence of DNA damage in the leading- or lagging-strand templates has different consequences for the replication fork. If unwinding by helicase is not impaired, damage in the lagging-strand does not hamper replication fork progression, because replication is constantly initiated on this strand generating new Okazaki fragments. On the other hand, damage in the leading-strand template is more problematic and the mechanisms described below are triggered to prevent genomic instability at this stalled fork<sup>232,278</sup>.

As mentioned previously, multiple processes have been suggested to promote fork restart: repriming, lesion bypass by translesion synthesis or template switching, fork reversal or the break-induced replication (BIR) after the cleavage of endonucleases<sup>219,282</sup>. All these mechanisms (**Figure 12**) are further explained below.

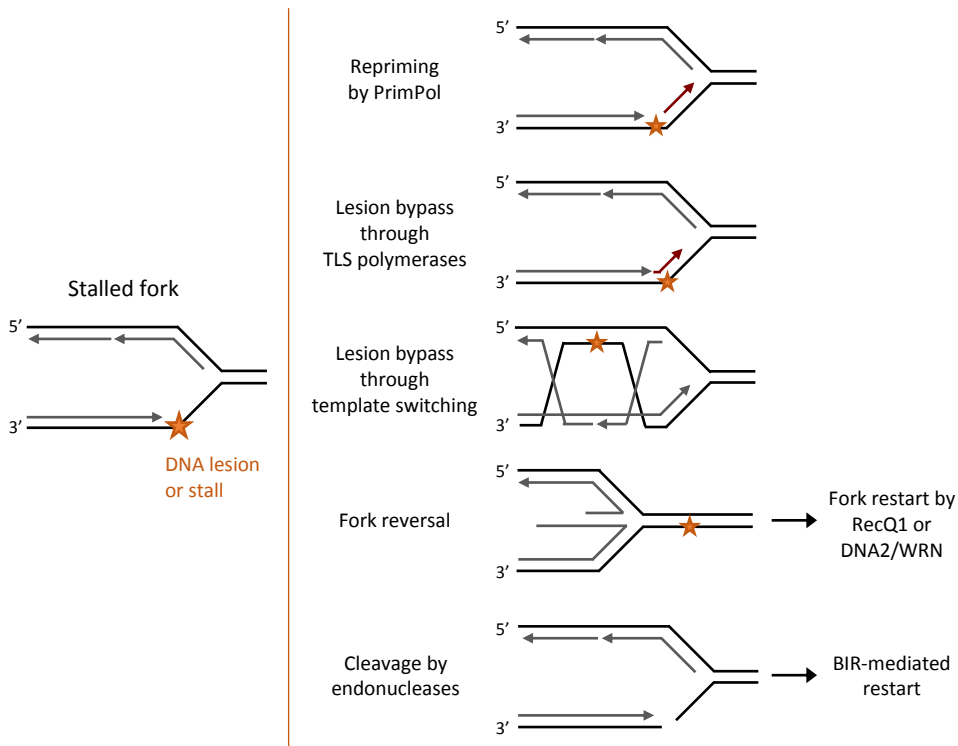


**Figure 12. Mechanisms involved in fork restart.** The mechanisms used to restart replication after fork stalling, or the presence of DNA lesion, are represented.

### Fork repriming

Lesion on DNA template can cause the uncoupling of unwinding from DNA synthesis. In this case, the replisome may skip the damaged DNA, leaving an unreplicated ssDNA gap behind that must be repaired after replication. The replisome is able to reinitiate DNA synthesis downstream of the lesion in the leading strand by a *de novo* repriming event and the continuance of unwinding of the template strands<sup>429–432</sup>.

Repriming in mammalian cells is performed by **PrimPol**, the second human archaeon-eukaryotic primase family identified<sup>433</sup>. This enzyme has RNA/DNA primase activities and polymerase and TLS activities<sup>353</sup>. The human PrimPol ensures resumption of DNA synthesis after UV irradiation<sup>434</sup>, oxidative lesions<sup>435</sup> and under conditions of dNTP depletion<sup>352</sup>, acting as both a TLS polymerase and a repriming enzyme<sup>353</sup>. A recent report suggests that PrimPol's

repriming activity plays a central role in replication reinitiation downstream of DNA lesions *in vitro* that cannot be bypassed by its TLS activity<sup>436</sup>.

A plausible pathway for repriming after leading-strand template damage could be as follows: polymerase  $\epsilon$  would stall whereas CMG would continue to unwind the parental strands and polymerase  $\alpha$ /primase and polymerase  $\delta$  would continue with replication of lagging-strand. Probably, polymerase  $\epsilon$  might move away from the lesion with the progressing CMG complex<sup>437</sup>, while PrimPol could reprime downstream of the damage on the leading-strand template<sup>232</sup>. Then, polymerase  $\delta$  could extend from the new primer until catching up with the progressing CMG-polymerase  $\epsilon$  complex, dissociating by collision with the slower CMG complex<sup>232,437</sup>.

#### Direct bypass of damage

DNA lesions represent a threat for replicative DNA polymerases, the ones that are part of the replisome and synthesize the bulk of undamaged DNA templates. These polymerases are highly accurate but do not tolerate DNA template lesions. Otherwise, the **TLS polymerases** have a larger catalytic site to bypass DNA lesions<sup>438,439</sup>. There are many TLS polymerases in mammalian cells, being the important ones polymerase  $\zeta$ , polymerase  $\eta$ , polymerase  $\kappa$ , polymerase  $\iota$  and Rev1. All these TLS polymerases are error-prone polymerases that lack proofreading activity and have lower nucleotide selectivity than the replicative polymerases. Otherwise, several studies suggest that correct selection of the TLS polymerase to accurately bypass the DNA lesion is crucial to prevent elevated mutagenesis<sup>439–443</sup>.

As mentioned previously, the recruitment of TLS polymerases to stalled replication forks is promoted by Rad18-mediated PCNA mono-ubiquitination<sup>364,444,445</sup>. However, several studies suggest that PCNA ubiquitination is important for efficient recruitment and synthesis of TLS polymerases in normal cells, but it is not essential, since TLS can occur in the absence of PCNA mono-ubiquitination<sup>446–449</sup>.

Many models suggest that replicative polymerases switch at the stalled fork for TLS polymerases to bypass the lesion. However, recent studies suggest that replicative polymerase  $\alpha$  is able to replicate and bypass lesion directly in the replisome, without the recruitment and

activation of error-prone polymerases<sup>450,451</sup>. In eukaryotic cells it is unlikely that polymerase  $\epsilon$  would be able to bypass damaged DNA, similarly of polymerase  $\alpha$ , which would release at the block and would rebind ahead of it to synthesize a new primer<sup>232</sup>. However, bypassing a lesion by TLS could involve DNA polymerase  $\delta$ , specifically the POLD3 subunit<sup>452,453</sup>.

### Template switching

Another way to bypass DNA lesions is template switching, which uses the nascent DNA strand as template to avoid damaged DNA<sup>442</sup>. Template switching is mediated by poly-ubiquitination<sup>454</sup> and SUMOylation of PCNA<sup>442,455</sup>.

This mechanism requires the unwinding of nascent strands from parental strands and the annealing of both nascent strands to overcome DNA lesions. A DNA helicase, a DNA translocase able to perform branch migration, a DNA recombinase and a DNA polymerase to extend the stalled nascent DNA are required<sup>232</sup>.

There are two models of template switching: one model proposes that replication can resume downstream of DNA lesion, leaving a ssDNA gap to be filled postreplicatively, while the second model proposes that stalled replication fork can be remodelled into reversed fork to facilitate damage bypass<sup>456,457</sup>. The second model will be further explained in the next section.

In relation to the first model, it is a process well studied in bacteria<sup>458</sup> and yeast<sup>456,457,459</sup>. Studies in budding yeast have allowed the visualization and identification of DNA structures involved in this process<sup>460</sup>. RAD51 and other mediators, such as Rad55 and Rad57, bind to the ssDNA gaps behind replication forks to allow recombination<sup>459</sup>. The recombination reaction is initiated by Exo1-mediated gap processing, causing exposure of the newly synthesized strand for DNA synthesis<sup>459,460</sup>. The D-loop is matured into a double Holliday Junction-like structure, by the annealing of parental strands and the annealing of nascent strands<sup>457,460</sup>. The DNA synthesis depends on polymerase  $\delta$ <sup>459</sup>. The intermediates are resolved by the action of the Sgs1-Top3-Rmi1 (STR) complex in yeast or BLM-TOP3 $\alpha$ -RMI1/2 complex in humans<sup>457,459-461</sup>.

### Fork reversal

The other model of template switching proposes the remodelling of stalled fork into a reversed fork<sup>457</sup>. Fork reversal is defined as the transformation of a typical fork structure, a three-way junction, into a four-way junction forming a “chicken foot” structure, by the annealing of the nascent DNA strands and the re-annealing of the parental strands<sup>221,334,457</sup>. It was first described as a pathological consequence of replication inhibition, but recent evidences have indicated that fork reversal is an important mechanism of protection when replication forks encounter DNA lesions. This mechanism enables replication fork to pause and restart without chromosomal breakage. However, fork reversal also can lead to chromosomal instability if the reannealing causes misalignments or the four-way junction undergoes by uncontrolled nucleolytic cleavage<sup>334</sup>.

It has been demonstrated that fork reversal is a global response to a wide spectrum of DNA-damaging and fork stalling agents<sup>462</sup>. During the last years, compelling evidences have contributed to the understanding of the reversed-fork formation. Several enzymes have been shown to exhibit fork reversal activity *in vitro*, including the DNA translocases Rad54<sup>463</sup>, SMARCAL1<sup>339</sup>, FANCM<sup>464</sup>, ZRANB3<sup>465,466</sup> and HLTf<sup>467–469</sup> and the DNA helicases FHB1<sup>470</sup>, RECQ5<sup>471</sup>, BLM and WRN<sup>472</sup>. The enzymes that are reported to catalyse fork reversal *in vivo* are DNA translocases SMARCAL1<sup>335,336</sup>, ZRANB3<sup>473</sup> and the DNA helicase **FHB1**<sup>470</sup>. The central recombinase factor **RAD51** is also involved in the formation of reversed forks<sup>462</sup>, but since it does not have fork-remodelling activity on its own, it may stimulate fork reversal through other proteins<sup>463,474</sup>.

RAD51 binds to both ssDNA and dsDNA with a modest affinity, so RAD51 requires a mediator to access the RPA-bound ssDNA. In mammalian cells, the main mediator is the tumour suppressor BRCA2<sup>474,475</sup>. However, BRCA2 is dispensable for the role of RAD51 in fork reversal, although it seems relevant for the assembly of RAD51 nucleofilaments on regressed arms to protect them from Mre11-dependent degradation<sup>335,476–478</sup>. Additional proteins are implicated in fork protection, such as BRCA1 and FANCD2 by preventing Mre11-dependent degradation<sup>479</sup> or BOD1L by stabilizing RAD51 on ssDNA and preventing DNA2-mediated degradation<sup>480</sup>.

Regarding replication fork restart from reversed forks in human cells, two different pathways have been described (**Figure 13**). The first pathway has as a central player the human helicase **RECQ1**. In this case, RECQ1 drives the restart of reversed forks, and its function is inhibited by PARP1 (poly(ADP-ribose) polymerase 1) until the damage is repaired or the stress is overcome<sup>481</sup>. The second pathway involves the **DNA2** nuclease and **WRN** helicase in cooperation to process and restart reversed forks. Both DNA2 nuclease and WRN helicase promote a 5'-3' resection creating a 3' overhang and promoting fork restart, by strand invasion that could be mediated by RAD51. In this case RECQ1 limits DNA2 activity by preventing excessive nascent DNA degradation. Moreover, DNA2 role in the restart of reversed forks is not accomplished by other nucleases, such as Exo1, Mre11 and CtIP<sup>220,482</sup>.

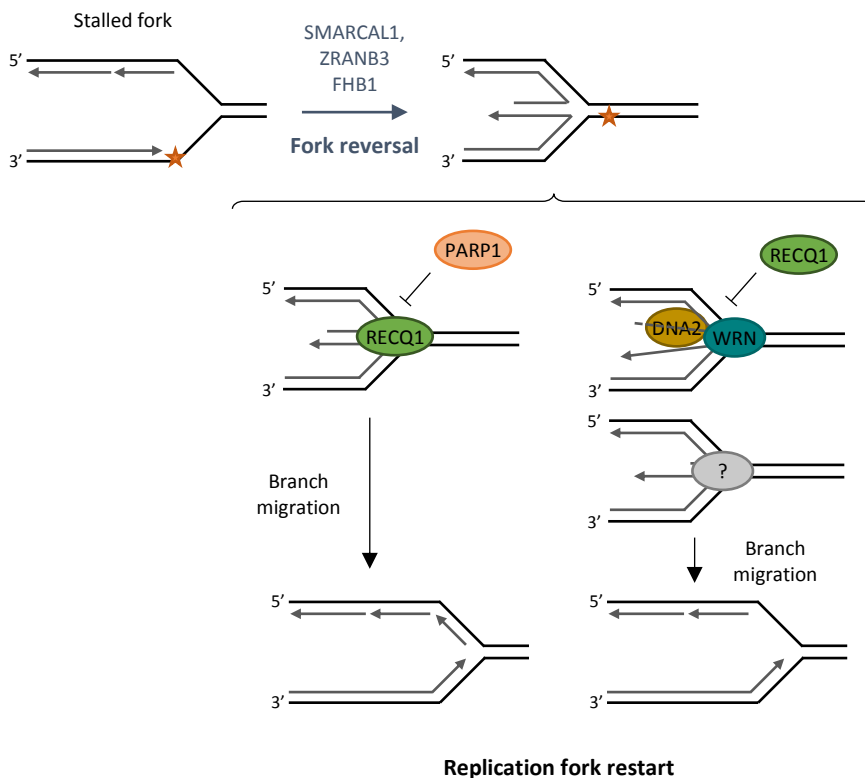


**Figure 13. Mechanisms of reversed forks processing and restart.** Two mechanisms are described for the resolution of reversed forks, one dependent on RECQ1 helicase and the other on DNA2 nuclease and WRN helicase. Adapted from "Replication stress: getting back on track"<sup>220</sup> and "DNA2 drives processing and restart of reversed replication forks in human cells"<sup>482</sup>.

### Break-induced replication

Another mechanism for replication fork restart is mediated by the cleavage of reversed or stalled forks by endonucleases. When a stalled fork is processed by structure-specific endonucleases, such as Mus81-Eme1, a one-ended DSB is generated<sup>483,484</sup>. However, DSBs are not terminal events for replication forks, since these breaks can be solved by an HR pathway known as break-induced replication (**BIR**). BIR initiates by strand-invasion of a broken DNA end into a homologous template followed by initiation of DNA synthesis that can copy hundreds of kilobases of DNA. This process is particularly important to complete replication close to telomeric ends, but for this thesis its relevance lies in its role in recovering collapsed replication forks<sup>220,485,486</sup>. BIR is associated with a high frequency of mutations and chromosomal rearrangements, making this unusual mode of DNA replication an important source of genomic instability<sup>487</sup>.

In *Escherichia coli*, where replication involves two replication forks moving in opposite direction from a single origin and terminating at a single locus, broken replication forks must be repaired by a process like BIR. In eukaryotes, BIR is also involved in the restart of collapsed forks, although cells are less dependent on BIR due to the presence of dormant origins. However, the relevance of BIR in the repair and restart of damaged forks has been recently confirmed in human cells<sup>488</sup>.

BIR begins with DNA end resection followed by RAD51-mediated strand invasion to form a D-loop, before replication fork assembly and extensive DNA synthesis (**Figure 14**)<sup>489</sup>. From studies done in yeast, it has been reported that leading-strand synthesis proceeds in migrating D-loop, while lagging-strand synthesis occurs in a conservative manner in which the nascent ssDNA is used as a template<sup>490-492</sup>. In human cells, BIR depends on Rad52<sup>493</sup> and POLD3, a mammalian homolog for the BIR-specific polymerase  $\delta$  subunit Pol32<sup>486,488,492,494</sup>.

Reversed replication forks that are unable to restart might represent a proper substrate for structure-specific endonucleases and might use this mechanism to reinitiate replication. In fact, Mus81 nuclease is involved in DSBs formation in response to replication inhibition<sup>483</sup> and a recent study suggest its role in the cleavage of reversed forks to promote BIR-dependent

fork restart<sup>495</sup>. Moreover, SLX4 endonuclease can cleave similar structures under unregulated checkpoint<sup>496</sup>.

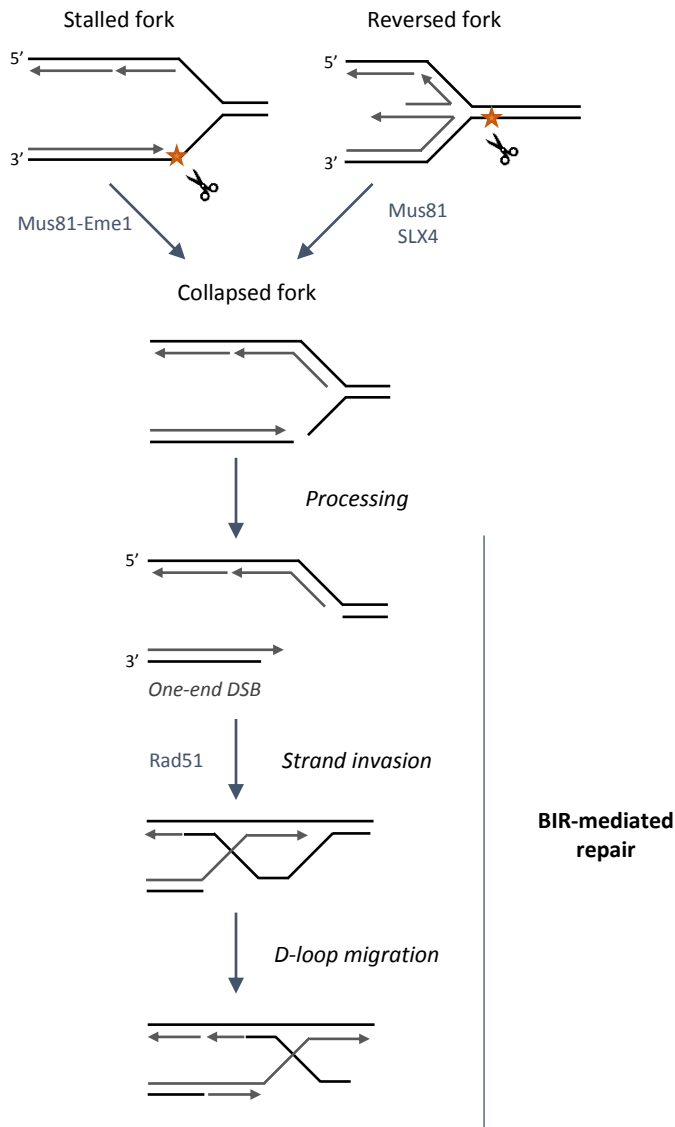


**Figure 14. BIR-mediated restart from collapsed forks.** The mechanism used to resume replication from the nuclease-mediated cleavage of stalled or reversed forks. Collapsed forks are processed to generate a one-end DSBs. After that, RAD51-mediated strand invasion event forms a D-loop and DNA synthesis proceeds in the migrating D-loop.

## 4. REPLICATION STRESS AND CANCER

The relevance of the cellular responses to replication stress is highlighted by a collection of cancer-prone genetic diseases that are caused by alterations in genes that participate in these responses (**Table 1**)<sup>221,225</sup>.

For example, mutations in the pre-replication factors ORC1, ORC4, ORC6 and Cdt1, Cdc6, which affect origin licensing in DNA replication<sup>497</sup>, and mutations in the Cdc45, an essential component of pre-IC and CMG helicase complex<sup>498</sup>, are associated with the Meier–Gorlin Syndrome, a disease characterized by severe growth retardation and developmental malformations.

Loss of ATR represents one of the most severe perturbations, as it is a key initiating event in replication-stress response. Mutation, splicing defects or protein expression reduction of ATR or mutations in ATR's binding partner, ATRIP, are associated with Seckel syndrome<sup>499–502</sup>, which is characterized by developmental delay, microcephaly and mental retardation. Loss of the MRN complex, which activates ATR during replication stress but is also required for DSB repair, is also associated with several developmental disorders<sup>219</sup>. Mutations in the RNase H2 gene cause the Aicardi-Goutieres syndrome, which is characterized by severe neurological dysfunction and a congenital infection-like phenotype<sup>503</sup>.

Mutations in proteins involved in chromatin remodelling during DNA replication have also been associated with human disorders. Mutations in the SMARCAL1 are associated with the Schimke immune-osseous dysplasia<sup>504–506</sup>. Mutations that affect the RECQ family DNA helicases (WRN, BLM and RECQL4), which play an important role in the efficient resolution of replication intermediates and arrested forks, are responsible for the genetic syndromes Werner, Bloom and Rothmund-Thomson, respectively<sup>507</sup>. Moreover, mutations in the FA complementation groups are responsible for the Fanconi Anaemia disease<sup>508</sup>, due to its failure to repair ICLs, which elevates their genome instability. Finally, mutations in TLS polymerase  $\eta$  are linked to Xeroderma pigmentosum, which increases photosensitivity and skin cancer predisposition<sup>509</sup>.

**Table 1. Human diseases associated with defective proteins involved in the replication stress response.** Adapted from “Causes and consequences of replication stress”<sup>219</sup>. Proteins that are not mentioned in this thesis are written in grey.

Human disease	Defective protein(s)	Affected pathway	Characteristics
<b>Aicardi-Goutieres syndrome</b>	RNase H2, TREX1, SAMDH1	Removal of ribonucleotides, RNA-DNA hybrids	Neurological dysfunction, appearance of chilblains
<b>Amyotrophic lateral sclerosis 4</b>	Senataxin	Resolution of RNA-DNA hybrids, transcription termination	Childhood- or adolescent-onset degeneration of motor control
<b>Ataxia-ocular apraxia 2</b>			Adolescent-onset cerebellar ataxia
<b>Ataxia-telangiectasia-like disease</b>	Mre11	MRN complex; ATR/ATM activation	Neurodegeneration, ataxia
<b>Bloom syndrome</b>	BLM	DNA remodelling, replication fork structure resolution	Premature aging, growth retardation, cancer predisposition
<b>Cancer</b>	Many	Many	Uncontrolled cell growth, leading to organ failure
<b>Fanconi anaemia</b>	FANC family proteins	DNA inter-strand crosslink repair	Heterogenous: bone marrow failure, skeletal defects, hypopigmentation, cancer predisposition
	FANCD2, BRCA2	Replication fork protection	
<b>Meier-Gorlin syndrome</b>	ORC1, ORC4, ORC6, Cdt1, Cdc6, Cdc45	Origin licensing, centrosome maintenance, origin firing	Growth retardation, microcephaly
<b>Nijmegen breakage syndrome</b>	Nbs1	MRN complex; ATR/ATM activation	Microcephaly, growth retardation, cancer predisposition
<b>Nijmegen breakage syndrome-like disorder</b>	Rad50	MRN complex; ATR/ATM activation	Microcephaly, growth retardation, mental retardation
<b>Rothmund-Thomson syndrome</b>	RecQL4	DNA remodelling, replication fork structure resolution	Premature aging, growth retardation, cancer predisposition
<b>Schimke immunosseous dysplasia</b>	SMARCAL/HARP	Replication fork stabilization and reversal; DNA re-annealing	Dwarfism, skeletal abnormalities, renal failure, immunodeficiency
<b>Seckel syndrome</b>	ATR, ATRIP, CENPJ, CEN152, PCNT	ATR signalling	Growth retardation, dwarfism, microcephaly, mental retardation
<b>Werner syndrome</b>	WRN	DNA remodelling, replication fork structure resolution	Premature ageing, growth retardation, cancer predisposition
<b>Xeroderma pigmentosum - variant</b>	Polymerase $\eta$	Translesion synthesis	Cancer predisposition (especially skin cancer)

Apart from the genetic conditions described previously, replication stress induces genomic instability and potentiates cell transformation and cancer predisposition. In this sense, Hanahan and Weinberg modified their original hallmarks of cancer<sup>510</sup> to add the enabling characteristic of “genome instability and mutation”, among others, to their list<sup>511</sup>. Moreover, DNA damage and DNA replication stress have been proposed as additional hallmarks of cancer that describe the state of cancer cells rather than their functional capabilities<sup>425,512</sup>.

Upon oncogene expression, DNA damage response and replicative stress response are activated in precancerous lesions<sup>513,514</sup>, inducing senescence or apoptosis programs in damaged cells<sup>515</sup>. Some cells may evade this barrier by various mechanisms (for example, p53 mutations) to facilitate cancer development<sup>516</sup>. Interestingly, no significant incidence of mutations in ATR or Chk1 is found on human tumours<sup>517,518</sup>, although their expression are frequently upregulated in cancer, probably to deal with the enhanced levels of replication stress in tumour cells<sup>224</sup>. Remarkably, a recent study has demonstrated that cancer risk is correlated with the number of stem cell divisions in different tissues, that became due to stochastic problems arising during DNA replication<sup>519</sup>.

Several mechanisms might enhance replication stress specifically in tumour cells. Some years ago, it was thought that the enhanced replication stress stemmed from the rapid proliferation and the need to replicate DNA of tumour cells, while differentiated cells rarely or never divided. Nowadays, the activity of oncogenes, such as HRas<sup>248</sup>, Myc<sup>249</sup> and cyclin E<sup>250</sup>, has a more important role in the contribution to replication stress. Furthermore, tumour cells often lack efficient DNA repair mechanisms, so some general DNA repair deficiency syndromes are associated with increased cancer incidence<sup>520</sup>.

DNA replication process has been a target of cancer treatment for many years. In this sense, DNA replication inhibition is broadly applied due to the high proliferative state of cancer cells. Conventional chemotherapy objective is to induce DNA damage by producing replication stress (**Table 2**), leading to programmed cell death<sup>247,520</sup>.

**Table 2. Conventional chemotherapy targeting DNA replication or damaging DNA.** Adapted from “Cellular responses to replication stress: Implications in cancer biology and therapy”<sup>247</sup>.

Mechanism to induce replication stress	Drug	Application
<b>Nucleotide synthesis inhibitors</b>	Hydroxyurea	Chronic myelogenous leukaemia, head and neck cancer
	Methotrexate	Acute lymphoblastic leukaemia, non-Hodgkin lymphoma
	5-Fluorouracil	Gastrointestinal cancers, head and neck cancer
	6-Mercaptopurine	Acute lymphoblastic leukaemia
	Fludarabine	Leukaemia, lymphoma
<b>Chain elongation inhibitors</b>	Cytarabine (Ara-C®)	Leukaemia, lymphoma
	Gemcitabine (Gemzar®)	Lung, breast, ovarian, or pancreatic cancer
<b>Topoisomerase inhibitors</b>	Topoisomerase I inhibitor: irinotecan, topotecan	Ovarian, lung or colon cancer
	Topoisomerase II inhibitor: etoposide, teniposide, mitoxantrone	Leukaemia, lymphoma, sarcoma, brain tumour, lung cancer
<b>Alkylating agents</b> (DNA base modification)	Nitrogen mustards	Leukaemia, lymphoma, Hodgkin disease, multiple myeloma, sarcoma, carcinoma
	Nitrosoureas	
	Alkyl sulfonates	
	Triazines	
<b>Platinum compounds</b> (DNA base modification)	Ethylenimines	Lymphoma, sarcoma, cervical cancer Lymphoma,
	Cisplatin, carboplatin, oxaliplatin	
<b>Anti-tumour antibiotics</b> (DSBs formation)	Bleomycin	Lymphoma, sarcoma, testicular or ovarian cancer, malignant pleural effusion
	Anthracyclines	Leukaemia, lymphoma, multiple myeloma, sarcoma or carcinoma
	Mitomycin C	Stomach or pancreatic adenocarcinoma

However, even though prolonged replication stress caused by conventional chemotherapy increases genomic instability, it promotes cell adaptation. To deal with this problem, small molecule inhibitors of specific proteins related to replication stress and cell cycle, such as ATR, Chk1, Wee1, PLK1 or CDKs inhibitors, are recently being used in clinical trials for cancer treatment in combination with conventional agents. The conventional therapy causes replication stress and these inhibitors eliminate the cellular responses of tumour cells to cause synthetic lethality<sup>247</sup>. Another strategy that is being carried out in cancer treatment is to promote mitotic catastrophe by eliminating the checkpoint barrier<sup>521</sup>.

The ATR/Chk1 pathway is crucial for cellular response to replication stress. Different studies in preclinical phase show that ATR and Chk1 inhibitors increase sensitization of different types of cancer to a variety of chemotherapies<sup>522,523</sup>, and that is why ATR and Chk1 inhibitors are being tested in clinical trials, alone or in combination with conventional chemotherapy agents<sup>524-528</sup>.

## *INTRODUCTION*

Since all the agents mentioned are related to replication stress and work through different mechanisms, it is worth exploring the optimal combinations of conventional and emerging agents, as well as the combination of different novel strategies. Further studies are needed to identify the most promising targeting inhibitors combinations to determine their mechanism and clinical usage.

Besides ATR/Chk1 pathway, the ATM/Chk2 pathway and DNA-PK are also important targets activated by DNA replication stress, due to DSBs formation when replication forks collapse. In this sense, inhibitors of ATM, Chk2 or DNA-PK, and their downstream targets, could potentiate replication stress<sup>529,530</sup>. Moreover, targeting DNA repair pathway and proteins, such as RAD51, could be also an interesting approach<sup>531-535</sup>.

## **OBJECTIVES**



Our laboratory has focused on studying the replication stress response induced with HU, a ribonucleotide reductase inhibitor that promotes a deoxyribonucleotide depletion in the cells and inhibits replication due to lack of substrate.

Previous results from our group showed that the competence to restart is maintained in non-transformed human cells after acute HU-induced replication stress. However, after a prolonged HU-induced replication stress, resumption of DNA replication is compromised due to APC/C<sup>Cdh1</sup> activation in S phase, which causes new origin firing inhibition<sup>536</sup>. On the other hand, the proteins present on nascent DNA were analysed in order to characterize replication stress-induced changes at replication fork level in non-transformed human cells (unpublished data).

The general aim of this thesis was to study the HU-induced replication stress response in a prolonged and an acute HU treatment that contributes to regulate DNA replication re-initiation and to preserve genomic integrity. Three specific objectives were defined for this thesis:

1. To study the contribution of APC/C<sup>Cdh1</sup> activation after a prolonged HU-induced replication stress to preserve genomic integrity.
2. To analyse the HU-induced changes at replication fork level in non-transformed human cells.
3. To characterize the role of specific proteins present at replication forks in response to HU-induced replication stress.



## **RESULTS**



# CHAPTER 1

## LACK OF APC/C<sup>CDH1</sup> ACTIVATION IN S PHASE AFTER A SEVERE REPLICATION STRESS ALLOWS RESUMPTION OF DNA SYNTHESIS IN TUMOUR CELLS

The results presented in this chapter have been obtained working in collaboration with Amaia Ercilla, PhD, and they were published in *Ercilla et al., NAR, 2016*.



## PREVIOUS DATA

LOSS OF REPLICATION RECOVERY COMPETENCE IN RESPONSE TO A PROLONGED REPLICATION INHIBITION IS APC/C<sup>CDH1</sup>-DEPENDENT IN hTERT-RPE CELLS

During DNA replication, cells are susceptible to acquire DNA damage and chromosomal instability, a hallmark of cancer<sup>511</sup>. Therefore, cells have developed several mechanisms or checkpoints to ensure the proper completion of each cell cycle phase and coordinate DNA repair pathways<sup>9,254,256</sup>. Increasing evidences indicate that oncogene overexpression causes replication stress in non-transformed human cells, inducing DNA damage and oncogene-induced senescence (OIS)<sup>515,537,538</sup>. In this regard, our group has focused on the analysis and characterization of the replication stress response<sup>219</sup> induced by HU in non-transformed human cells, to understand the alterations that tumour cells suffer to bypass OIS.

Previous results of our group showed that upon prolonged replication stress (10mM of HU for 14 hours), the resumption of DNA replication and mitotic entry were both compromised in non-transformed human cells. By contrast, cells were able to recover replication and entry into mitosis after an acute replication stress (10mM of HU for 2 hours). The used model was hTERT-RPE cell line, a human retinal pigment epithelial cells line immortalized with hTERT (Figure 15).

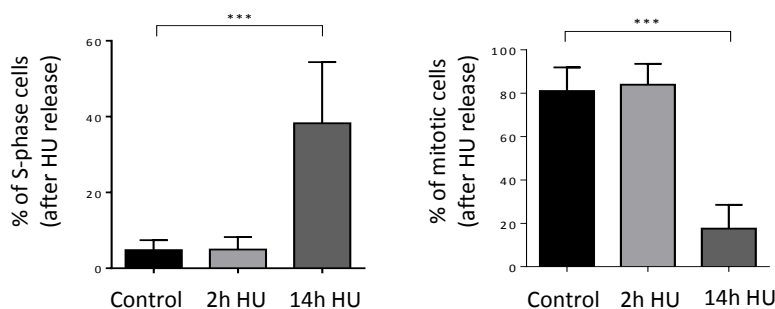


**Figure 15. Replication resumption and mitotic entry are compromised after a prolonged replication stress in hTERT-RPE cells.** Cells were pulse-labelled with BrdU for 30 minutes and then treated with 10mM HU for the indicated times or left untreated (control). After HU treatment, cells were released into nocodazole-containing media for 24 hours. The average percentage of BrdU positive cells that remain in S phase (left panel) or that enter into mitosis (right panel) after HU release are shown in the graphs. Error bars represent standard deviation (paired *t*-test, n=6).

*PREVIOUS DATA*

Cyclin A2 and Cyclin B1, which are important for cell-cycle progression<sup>3</sup>, were accumulated during an unperturbed S-phase (data not shown), but their levels decreased in response to a prolonged HU treatment, although cells were arrested in S-phase. The decrease in cyclins levels, which started after 12 hours of HU treatment, correlated with the loss of replication recovery competence (**Figure 16A**). This decrease was due to APC/C<sup>Cdh1</sup>-dependent degradation, since Cdh1 depletion restored their levels. Moreover, the levels obtained with Cdh1 depletion were the same as the obtained with the addition of MG132 proteome inhibitor, indicating that this ubiquitin ligase was the one responsible for their degradation (**Figure 16B**). Furthermore, we showed that APC/C<sup>Cdh1</sup> activation was at least in part responsible for the S phase arrest observed after a prolonged HU treatment, since Cdh1 depletion significantly rescued replication recovery competence after 14 hours of HU treatment (**Figure 16C**).

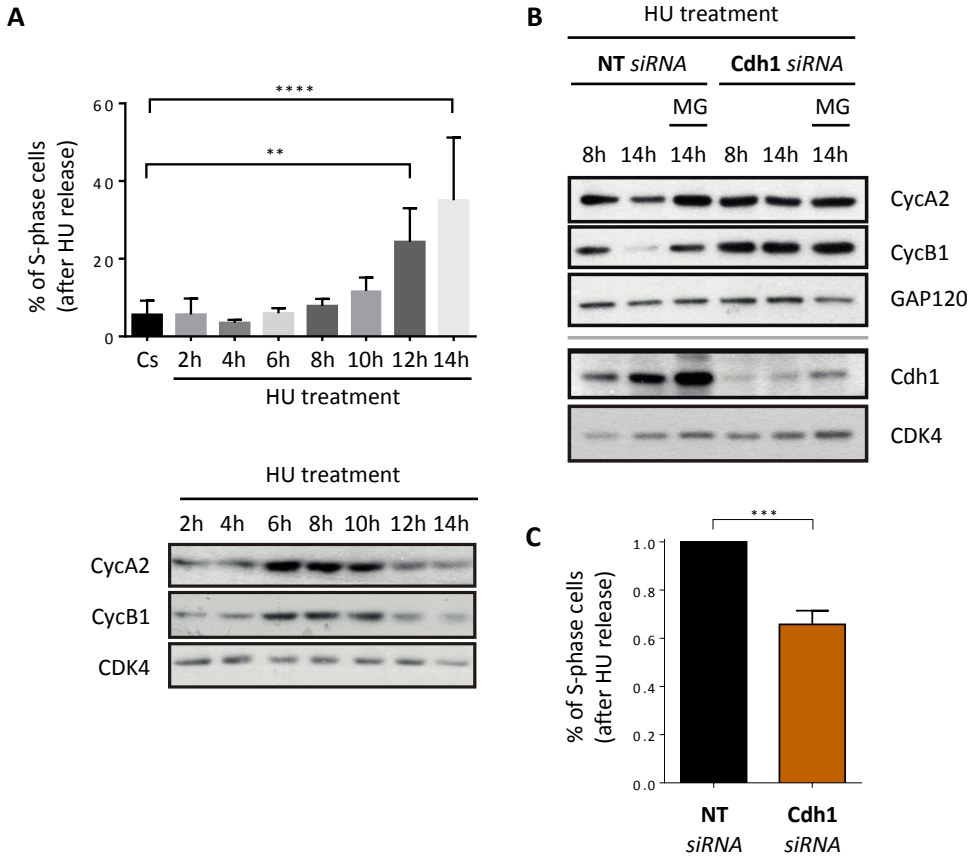


**Figure 16. Replication recovery competence is lost in response to a prolonged HU treatment due to APC/C<sup>Cdh1</sup> activation in hTERT-RPE cells.** (A) S-phase synchronized hTERT-RPE cells were treated during the indicated times with 10mM HU or left untreated (Cs) and then harvested for Western Blot (WB) analysis (bottom panel) or released into nocodazole-containing fresh media for 24 hours. DNA content was used to determine the number of cells that remained in S-phase after HU release (upper panel, paired *t*-test, *n*=4; \*\* P value < 0.01, \*\*\*\* P value < 0.0001). (B) hTERT-RPE cells were transfected with the indicated siRNA and then synchronized in S phase before HU treatment. Cells were harvested during the indicated times and harvested for WB analysis. MG132 (MG) was added during the last 6h of treatment where indicated. GAP120 and CDK4 were used as a loading control. (C) hTERT-RPE transfected cells were synchronized in S phase and treated during 14 hours with HU and then released into nocodazole-containing media during 24 hours. DNA content was analysed by flow cytometry to quantify the number of cells that remain arrested in S phase after HU release. Means and standard deviation (bars) of the fold increase relative to non-target (NT) siRNA are shown in the graph (unpaired *t*-test, \*\*\* P value < 0.001). Cdc: Cyclin.

Consistently, the levels of Emi1, an APC/C inhibitor that is implicated in the regulation of this ubiquitin ligase during a normal cell cycle<sup>73,76,77,539,540</sup>, decrease upon a prolonged HU replication stress, correlating with the timing of APC/C<sup>Cdh1</sup> activation in hTERT-RPE cells (**Figure 17**).

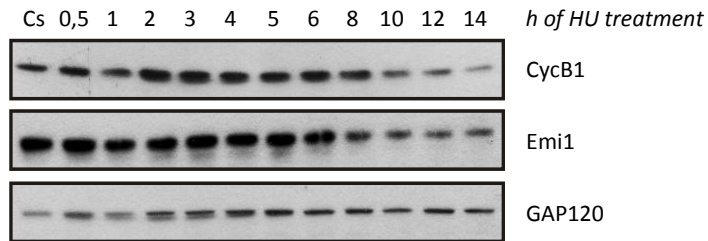


**Figure 17. APC/C<sup>Cdh1</sup> activation correlates with a decrease in Emi1 levels in response to HU treatment.** hTERT-RPE cells were synchronized in S phase and then treated with 10mM HU during the indicated times or left untreated (Cs). Whole cell lysates were analysed by WB with the indicated antibodies. GAP120 was used as a loading control.

### **APC/C<sup>Cdh1</sup> INHIBITS NEW ORIGIN FIRING IN S PHASE AFTER A PROLONGED REPLICATION STRESS IN hTERT-RPE CELLS**

Once it was determined that the capacity of replication recovery was lost after a prolonged HU treatment, due to the APC/C<sup>Cdh1</sup> activation in S-phase, we used DNA fiber assay to analyse the effect of Cdh1 depletion in replication recovery. To do so, hTERT-RPE cells were labelled with CldU for 30 minutes, then treated with 10mM of HU (a dose of HU which completely stalls replication forks) during 2 hours or 14 hours, and finally cells were labelled with IdU for 1 hour more.

A 14 hours of HU treatment caused a decrease in the number of restarted forks and a concomitant increase in the number of stalled forks, both in non-target and Cdh1 siRNA transfected cells. Interestingly, Cdh1 depletion strongly increased new origin firing events after prolonged HU treatment, suggesting that a deficient origin firing was causing the loss of replication recovery competence in hTERT-RPE cells (**Figure 18**).

On the other hand, after an acute replication stress, where it had been demonstrated that cells were able to recover replication and entry into mitosis (**Figure 15**), and APC/C<sup>Cdh1</sup> was not activated yet (**Figure 16**), replication forks restarted after HU release (**Figure 18**).

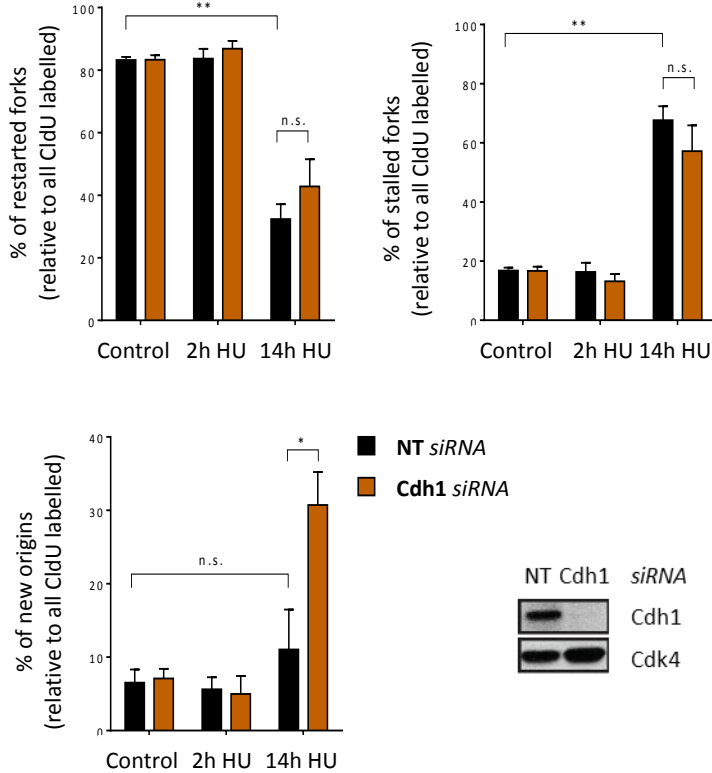


**Figure 18. APC/C<sup>Cdh1</sup> inhibits new origin firing in S phase after a prolonged HU treatment in hTERT-RPE cells.** Cells were transfected with the indicated siRNA and synchronized in S phase before DNA fiber labelling. Then cells were treated with 10mM HU during the times indicated or left untreated (control). The percentage of replication fork restart (upper-left panel), stalled forks (upper-right panel) and new origin firing events (bottom-left panel) relative to total CldU (first labelling) is shown in the graphs. More than 1000 fibers from three independent experiments were counted in each condition. Means and standard deviation (bars) are shown (paired *t*-test, n.s.: non-statistically significant, \* P value < 0.05, \*\* P value < 0.01). S-phase synchronized untreated cells were harvested for WB analysis, with the indicated antibodies (bottom-right panel).

## RESULTS

### 1.1. TUMOUR CELL LINES ARE PREDOMINANTLY DEFICIENT IN APC/C<sup>Cdh1</sup> ACTIVATION IN S PHASE AND ARE ABLE TO RESUME REPLICATION IN RESPONSE TO A PROLONGED HU TREATMENT

To analyse the contribution of APC/C<sup>Cdh1</sup> activation towards preservation of genomic integrity, we studied the effect of replication inhibition on cells that, in contrast to hTERT-RPE cells<sup>536</sup>, did not activate APC/C<sup>Cdh1</sup> in response to a prolonged HU treatment. To this end, a panel of tumour cell lines, which presents a less robust replication checkpoint response<sup>541,542</sup>, was analysed in order to evaluate if this mechanism was activated in response to a prolonged replication stress.

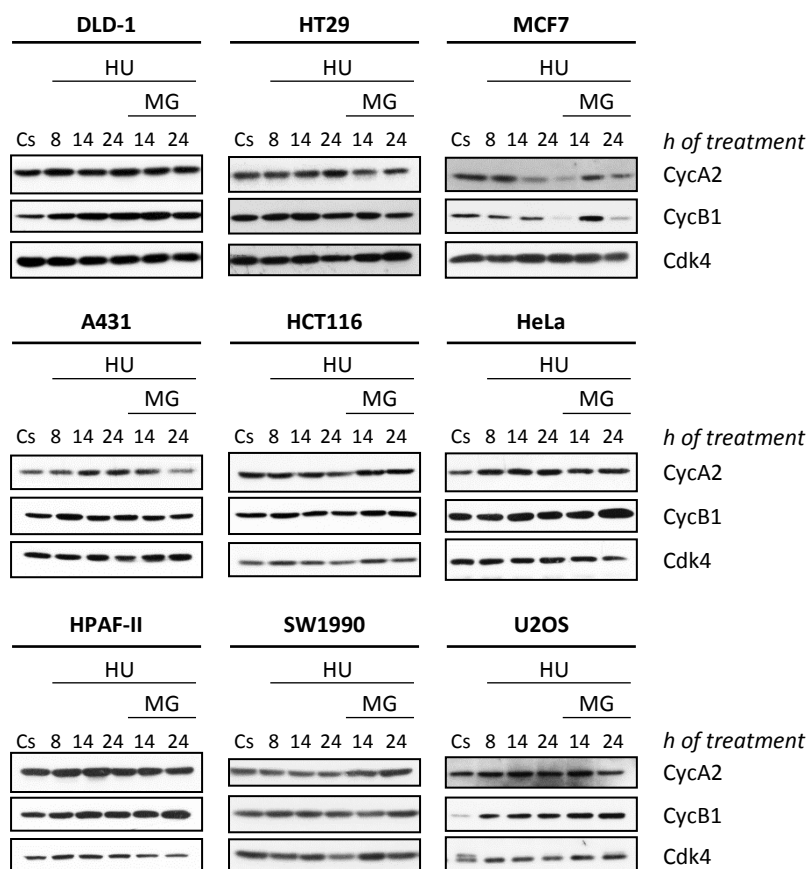


**Figure 19. Tumour cell lines are predominantly deficient in APC/C<sup>Cdh1</sup> activation in S-phase in response to a prolonged HU treatment.** Human tumour cell lines were synchronized in S phase by single thymidine block and then treated with 10mM HU during the indicated time or left untreated (Cs). Whole cell

extracts were prepared and analysed by WB with the indicated antibodies. MG132 (MG) was added during the last 6 hours of treatment in the case of 14h MG or during the last 10 hours of treatment in the case of 24h MG. The panel of cell tumour cell lines included human cervix epithelial cancer cells (HeLa), colorectal cancer cells (DLD-1, HT29, HCT116), breast cancer cells (MCF7), squamous cancer cells (A431), pancreatic cancer cells (HPAF-II, SW1990) and osteosarcoma cells (U2OS). Cyc: cyclins.

Interestingly, as shown in **Figure 19**, from all the analysed cell lines, only one, MCF7, activated APC/C<sup>Cdh1</sup> in response to a prolonged HU treatment, as shown by Cyclin A2 and Cyclin B1 degradation, and their correct protein levels recovery when MG132 (proteasome inhibitor) was added. In conclusion, tumour cell lines are predominantly deficient in APC/C<sup>Cdh1</sup> activation after a prolonged HU treatment.

We next wondered if these tumour cell lines were able to resume replication after a severe replication stress. To this end, tumour cells were pulse-labelled with BrdU during 30 minutes in order to mark cells in S phase. Then, cells were treated with 10mM of HU during 14 hours and, after treatment, they were released into nocodazole-containing media for 12 hours. After that, cells were collected and analysed by flow cytometry in order to evaluate S-phase resumption after HU release.

In accordance with our previous results, the correlation between APC/C<sup>Cdh1</sup> activation and loss of replication recovery was supported by these results in tumour cell lines, since most of them did not activate APC/C<sup>Cdh1</sup> after a prolonged HU treatment, and six of these nine cell lines were able to reinitiate replication when they were released from this replication stress (**Figure 20**).

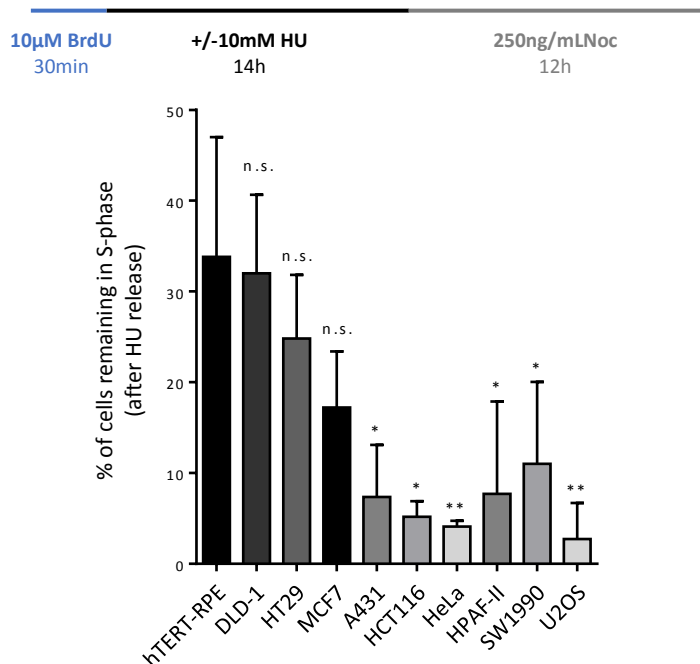


**Figure 20. Tumour cells lines are predominantly able to resume replication after a prolonged HU treatment.** Asynchronously growing cells were pulse labelled for 30 minutes with BrdU and then treated with 10mM HU for 14 hours. Cells were finally released into nocodazole-containing fresh media during 12 hours (24 hours in the case of hTERT-RPE cells). The labelling and treatment protocol was shown (upper panel). DNA content (PI staining) of BrdU positive population was analysed by flow cytometry to quantify the average percentage of BrdU positive cells that remain arrested in S phase after release (normalized by untreated (control) cells) is shown in the graph (n=3). Means and standard deviation (bars) are shown (paired *t*-test, n.s.: non-statistically significant, \* P value < 0.05, \*\* P value < 0.01).

## 1.2. NEW ORIGIN FIRING CONTRIBUTES TO REPLICATION RECOVERY IN HCT116 CELLS AFTER A PROLONGED HU TREATMENT

We already knew that the activation of APC/C<sup>Cdh1</sup> in S phase inhibited origin firing in hTERT-RPE cells, which prevented replication recovery in those cells. Thus, we decided to analyse replication dynamics after a prolonged HU treatment in a previously analysed tumour cell line, which did not activate APC/C<sup>Cdh1</sup> and resumed DNA replication after replication stress release. To this end, we chose HCT116 cell line.

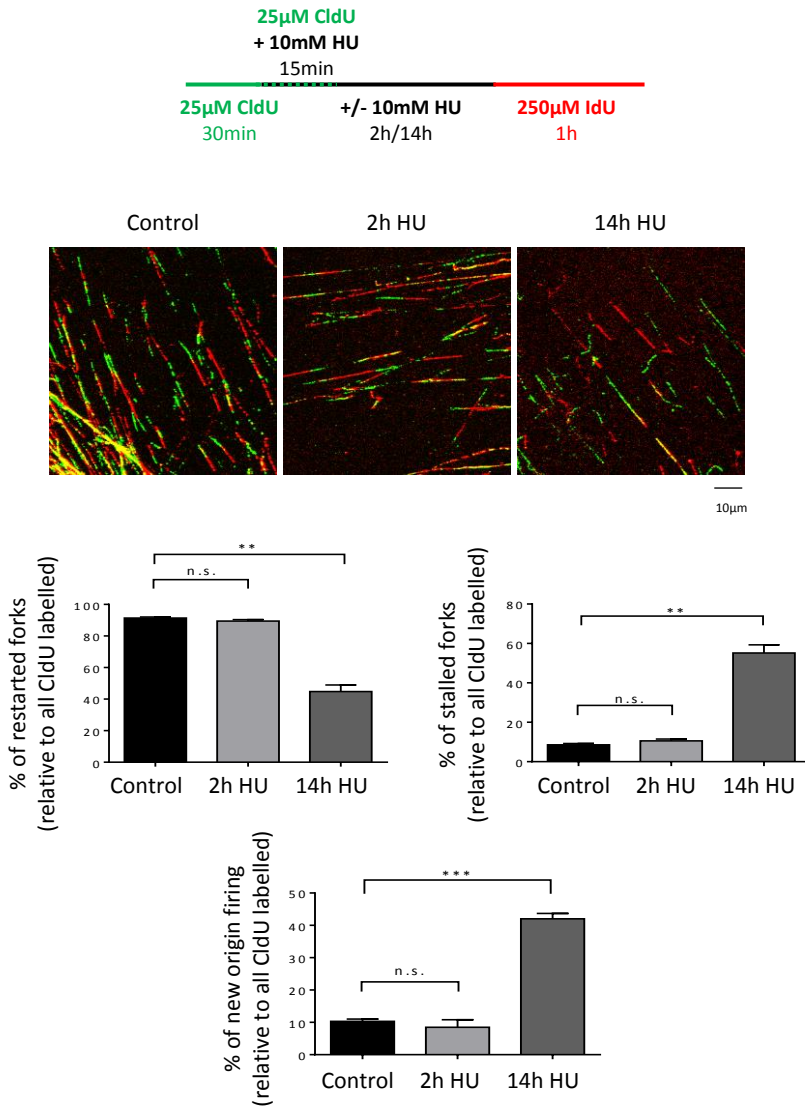


**Figure 21. HCT116 cell line activates new origin firing after a prolonged HU treatment.** S-phase synchronized (by single thymidine block) HCT116 cells were treated as indicated and then DNA fibers were prepared and labelled with anti-BrdU antibodies. A scheme of the labelling protocol is shown (upper panel). Representative images are shown (middle panel). The percentage of replication fork restart, stalled replication forks and new origin firing events relative to total CldU labelled fibers are shown in the graphs (bottom panel). At least 1500 fibers from three independent experiments were counted in each condition. Means and standard deviation (bars) are shown (paired t-test, n.s.: non-statistically significant, \*\* P value < 0.01, \*\*\* P value < 0.001).

The CldU analogue was maintained in the media during the first 15 minutes of HU treatment, since it was the time needed to completely stall replication forks<sup>536</sup>. The second labelling period was longer since replication forks needed some time to recover replication after HU release.

DNA fiber assay allows us to discern different replication dynamics after replication inhibition caused by HU<sup>243</sup>: restarting forks are represented by replication tracks that have incorporated both analogues, stalled forks correspond to CldU only tracks, and new origin firing events correspond to IdU only tracks<sup>543</sup>.

As shown in **Figure 21**, HCT116 cells resume replication mainly by restarting replication forks after an acute replication stress (10mM HU during 2 hours), as hTERT-RPE cells (shown in **Figure 18**). By contrast, after a prolonged replication stress (10mM HU during 14 hours), there was a defect in fork restart, observed by a decrease in the number of restarted forks and a concomitant increase in the number of stalled forks. In contrast to what happened in hTERT-RPE cells, replication restart defect was mainly compensated by increasing the number of new origin firing events (**Figure 21**).

### 1.3. HCT116 CELLS ACQUIRE GENOMIC INSTABILITY AFTER A PROLONGED HU TREATMENT

To analyse the role of APC/C<sup>Cdh1</sup> activation in S phase in preventing genomic instability, we first analysed the capacity of HCT116 cells to resume cell cycle and proliferate once released from a prolonged replication stress. To this end, colony formation assays were performed. The results indicated that HCT116 cell line maintained the ability to resume replication when stress was removed, and that those cells were able to proliferate and form colonies, in sharp contrast to what happened in hTERT-RPE cells (**Figure 22**).

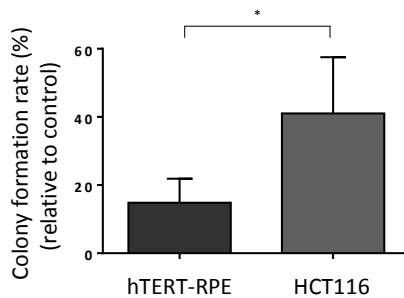


**Figure 22. HCT116 cells maintain the competence to recover from a prolonged HU treatment.** HCT116 and hTERT-RPE cells were synchronized in S phase and then treated during 14 hours with 10mM HU or left untreated (control, not shown). Cells were then released into fresh media for 12 hours and diluted (250 cells per well on 6-well plates) for colony formation assay. Colonies were harvested 8 days later. The average percentage of colonies in HU-treated relative to control was calculated in each case. Means and standard deviation (bars) from three independent experiments are shown (unpaired *t*-test, \* P value < 0.05)

Then, we analysed the acquisition of DNA damage or genomic instability, as measured by the presence of G1 cells (analysed by Cyclin D1 positive cells) with 53BP1 foci<sup>544-546</sup> and of cells presenting micronuclei<sup>547</sup>. Interestingly, after a prolonged HU treatment, HCT116 cells were able to reach the next G1 phase with damage, since there was an increase in the percentage of cells with 53BP1 foci in the next G1 and an increase in the number of cells presenting micronuclei (**Figure 23**).

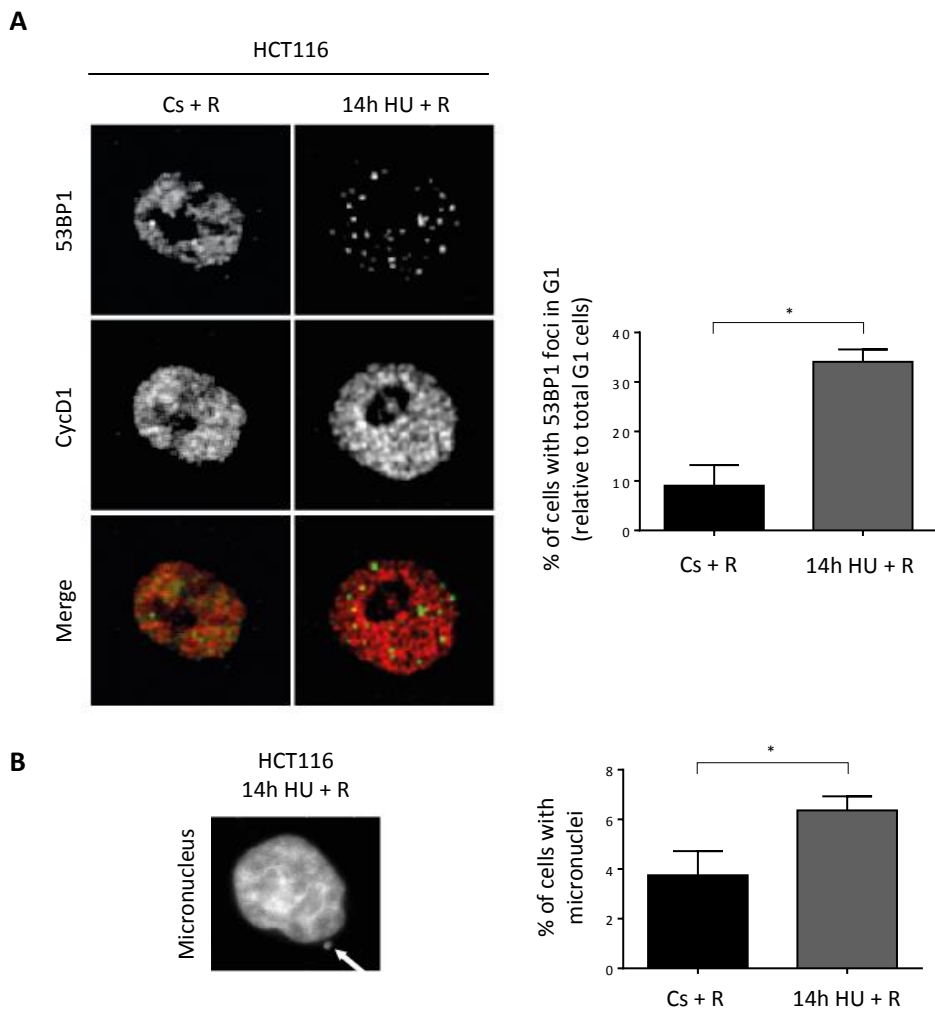


**Figure 23. HCT116 cells acquire genomic instability after a prolonged HU treatment.** Cells were synchronized in S phase by single thymidine block, treated with HU during 14 hours or left untreated and then released (R) into fresh media during 12 hours, after which cells were fixed and immunostained with 53BP1 and Cyclin D1 antibodies. Representative images (A, left panel) and the average percentage of cells with more than six 53BP1 foci from G1 (Cyclin D1 positive) population (A, right panel) from three independent experiments are shown. DNA was counterstained with DAPI to analyse the presence of micronuclei. A representative image (B, upper panel) and the average percentage of cells with micronuclei (B, bottom panel) of three representative experiments are shown. Means and standard deviation (bars) are shown. Values marked with asterisks are statistically significant (paired *t*-test \* P value < 0.05).

#### 1.4. EMI1 DEPLETION-INDUCED APC/C<sup>Cdh1</sup> ACTIVATION COMPROMISES REPLICATION RESUMPTION AND GENOMIC INSTABILITY ACQUISITION IN HCT116 CELLS

The previous results showed the correlation between APC/C<sup>Cdh1</sup> activation and the loss of replication recovery after a prolonged replication stress. To analyse the influence of S-phase arrest on the maintenance of genomic integrity, we decided to activate APC/C<sup>Cdh1</sup> artificially in HCT116 cells and analyse genomic instability.

Emi1 depletion had been reported to be enough to induce APC/C<sup>Cdh1</sup> activation<sup>76,548,549</sup>. Consistently, Emi1 depletion, after thymidine synchronization, induced an artificial APC/C<sup>Cdh1</sup> activation in S phase (shown by Cyclin A2 and Cyclin B1 degradation) in HCT116 cells (**Figure 24**). Moreover, this activation compromised the ability to resume replication after a prolonged HU treatment, as shown by an increase of cells remaining in S phase after HU release (**Figure 24**).

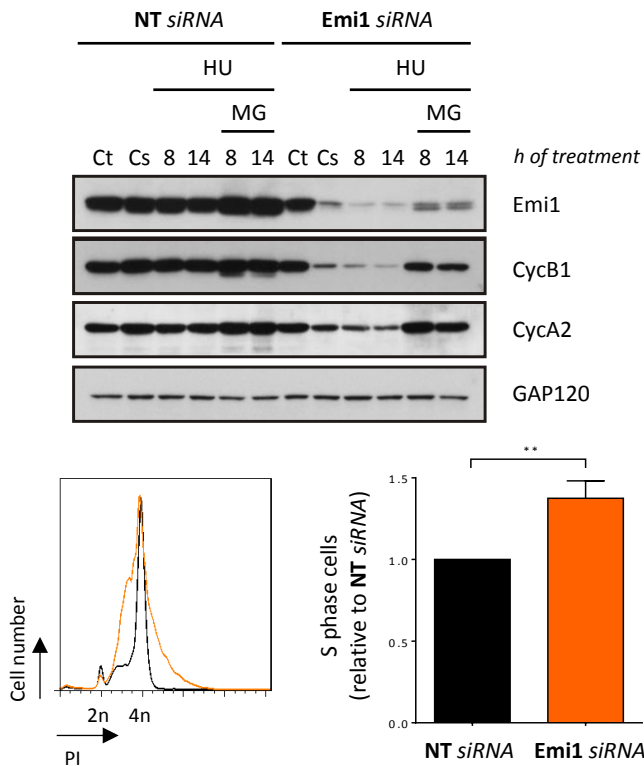


**Figure 24. Emi1 depletion activates APC/C<sup>Cdh1</sup> in S phase and revokes replication resumption in HCT116 cells.** HCT116 cells were transfected with the indicated siRNA and 4 hours later (Ct), thymidine was added to synchronize the cells in S phase during 20-24 hours. Then cells were released from thymidine and treated with 10mM HU during the indicated time or left untreated (Cs). Whole cell extracts were

prepared and analysed by WB with the indicated antibodies (upper panel). After 14 hours of HU treatment, cells were released into nocodazole-containing fresh media during 12 hours. DNA content (PI: propidium iodide) was analysed by flow cytometry. The histograms were overlaid matching the maximum point (bottom-left). Means and standard deviation (bars) of S-phase arrested cells (relative to NT siRNA) from three independent experiments are shown (bottom panel, unpaired *t*-test, \*\* P value < 0.01).

Then, we analysed the acquisition of DNA damage or genomic instability, as measured by the presence of G1 cells (analysed by Cyclin D1 positive population) with 53BP1 foci<sup>544–546</sup> and of cells presenting micronuclei<sup>547</sup> in Emi1-depleted cells after a release from a prolonged replication stress. Interestingly, Emi1 depletion resulted in a decrease in the number of cells with 53BP1 foci in the next G1 phase, and also a decrease in the number of cells presenting micronuclei under those conditions (**Figure 25**).

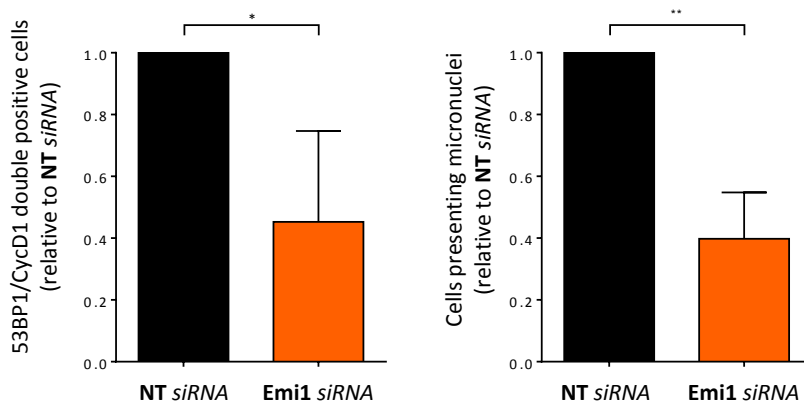


**Figure 25. Emi1 depletion contributes to safeguard genomic stability in HCT116 cells.** Cells were transfected with the indicated siRNA and 4 hours later, thymidine was added to synchronize the cells in S phase. Cells were treated with 10mM HU during the 14 hours and then cells were released into fresh media during 12 hours, and finally immunostained for 53BP1 and Cyclin D1 analysis. DNA was counterstained with DAPI. The average percentage of cells with more than six 53BP1 foci in G1 (left panel) and the average percentage of cells with micronuclei (right panel) relative to NT siRNA from three independent experiments are shown. Error bars represent standard deviation. Values marked with asterisks are statistically significant (unpaired *t*-test, \* P value < 0.05, \*\* P value < 0.01).

Moreover, the capacity of Emi1-depleted cells to divide and proliferate in a long term after a prolonged replication stress was analysed by colony formation assay. The results showed that HU treatment or Emi1 depletion decreased the capacity of colony formation, and the decrease was even more pronounced when both conditions occurred at the same time (**Figure 26**).

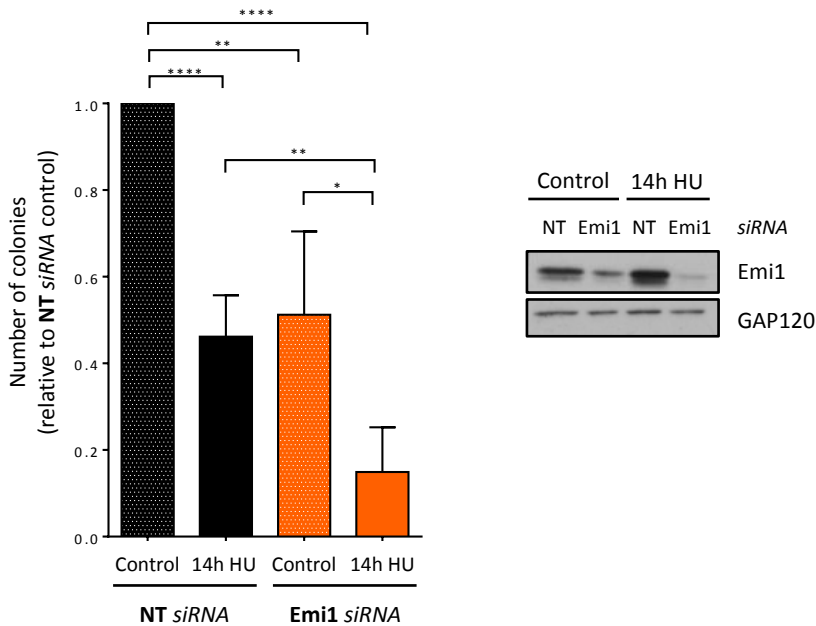


**Figure 26. Emi1 depletion compromises colony formation capacity in HCT116 cells.** Cells were transfected with the indicated siRNA and 4 hours later, cells were treated with 10mM HU during 14 hours or left untreated (control). 12 hours later, cells were diluted and seeded at 250 cells per well (6-well plates). After incubation for 8 days, cells were harvested and stained to visualize the number of colonies in each condition. Number of colonies relative to NT siRNA control of four independent experiments is shown in the graph. Means and standard deviation (bars) are shown. Values marked with asterisks are statistically significant (unpaired *t*-test, \* P value < 0.05, \*\* P value < 0.01, \*\*\*\* P value < 0.0001).

Collectively, all the data presented in this chapter support the idea that the activation of APC/C<sup>Cdh1</sup> in S phase compromises the ability to resume replication and contributes to safeguard genome integrity after a prolonged replication stress. Additionally, our results indicate that tumour cells have developed mechanisms to avoid APC/C<sup>Cdh1</sup> activation upon a prolonged replication stress, and consequently these cells are able to resume replication despite acquiring more genomic instability.



# **CHAPTER 2**

## **FORK REMODELLING AFTER AN ACUTE HU-INDUCED REPLICATION STRESS**

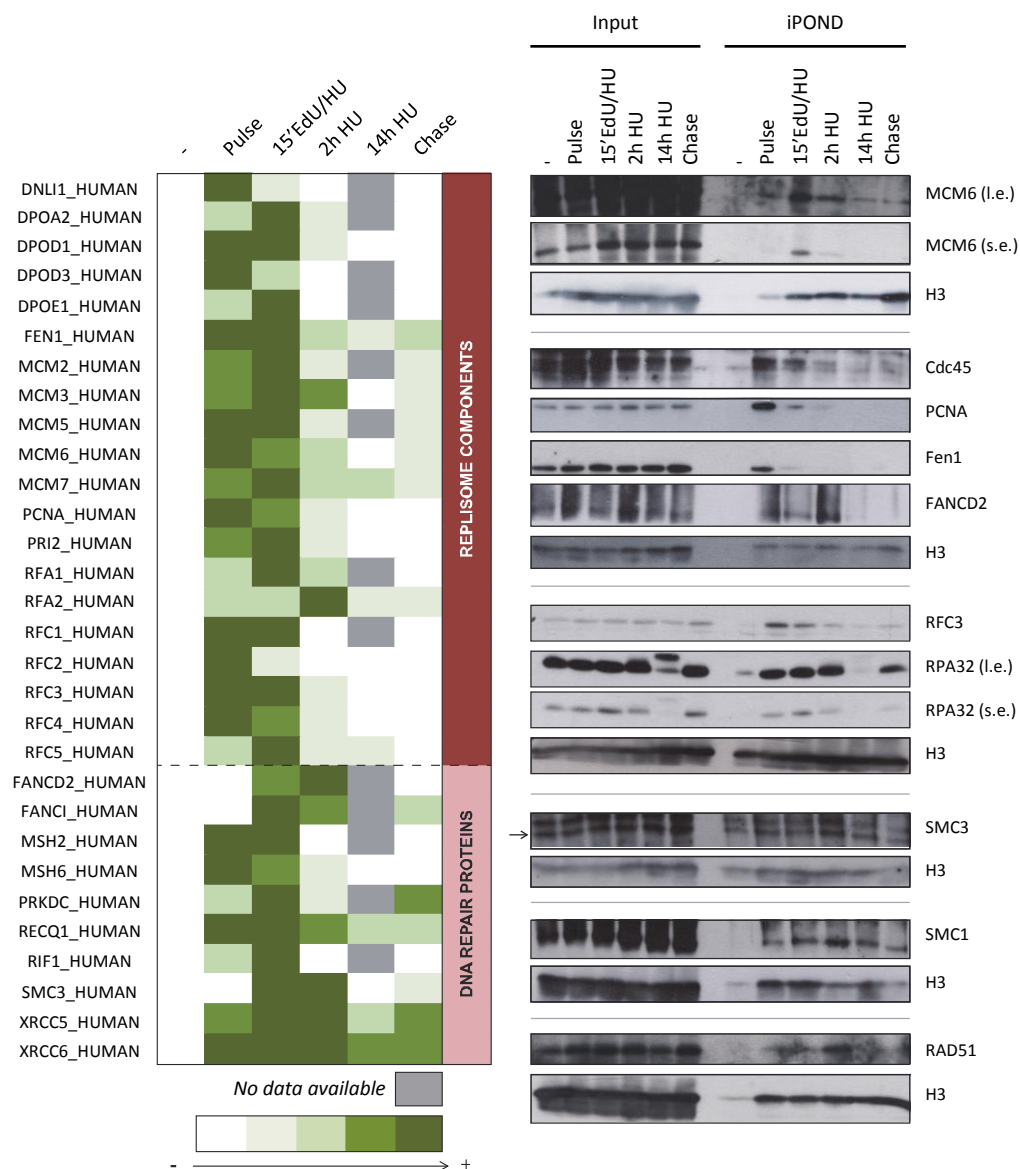
The results presented in this chapter have been obtained working in collaboration with Amaia Ercilla, PhD. The results shown in the previous data section are comprised at Amaia Ercilla's PhD thesis.



## PREVIOUS DATA

### REPLISOME IS DISENGAGED FROM NASCENT DNA UPON AN ACUTE HU TREATMENT, BUT MAINTAINS ITS ASSOCIATION WITH CHROMATIN IN hTERT-RPE CELLS

With the aim to characterize HU-induced replication stress changes at replication fork level in non-transformed human cells, an isolation of proteins present on nascent DNA (iPOND), of hTERT-RPE cells, was performed after an acute (2 hours) or a prolonged (14 hours) HU treatment, using a dose (10mM) that completely stalls replication forks. The iPOND technique allows the isolation of protein complexes crosslinked to EdU thymidine analogue-containing fragments that are located at active replication forks<sup>550-552</sup>. This experiment was performed in collaboration with Sergi Aranda, PhD, and Prof. Patrik Ernfors, PhD. As expected, the iPOND experiment showed that most of the replisome components were enriched at nascent DNA in the pulse and 15'EdU/HU conditions, both in MS and in WB analysis (**Figure 27**). Surprisingly, the results showed that replisome components were displaced away from nascent DNA after an acute replication stress induced by HU (**Figure 27**), but they remained associated to chromatin under this condition (**Figure 28**). Remarkably, proteins involved in maintaining fork stability and promoting their restart, such as RAD51, FANCD2 and SMC1/3 cohesins<sup>329,330,476,479,553</sup>, increased their presence in nascent DNA after an acute replication stress (**Figure 27**).



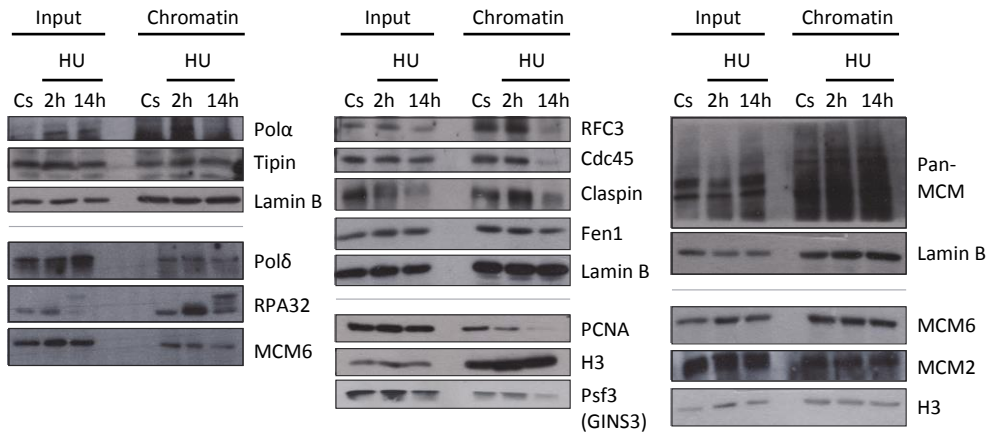


**Figure 28. Replisome components are associated with chromatin after an acute replication stress in hTERT-RPE cells.** Cells were synchronized in S phase and then treated during the indicated time with 10mM of HU or left untreated (Cs). Chromatin extracts were prepared and analysed by WB with the indicated antibodies. Input: whole cell lysates. Lamin B1, MCM6 and Histone 3 (H3) were used as a loading control.

### REVERSED REPLICATION FORKS ARE PRESENT AFTER AN ACUTE REPLICATION STRESS IN hTERT-RPE CELLS

The fact that replisome components were not associated to nascent DNA but they remained associated to chromatin after an acute HU treatment make us wondered whether the replication forks might be reversed. To test this, the formation of these structures was analysed indirectly under those conditions. BrdU immunofluorescence under native conditions has been described to be a sensitive and quick *in situ* method to analyse the accumulation of single-stranded DNA (ssDNA)<sup>554</sup>. Reversed forks expose a fragment of ssDNA on the 3' end of leading strand, due to DNA2 degradation of reversed forks with a 5'-to-3' polarity in the lagging strand and forming a newly 3' overhang in the leading one<sup>482</sup>. This formed ssDNA can be detected by BrdU antibodies under nondenaturing conditions, if nascent DNA was previously labelled for 10 minutes with BrdU analogue<sup>337,470</sup>.

DSBs could interfere with this assay but our group had already validated that replication forks were not processed into DSBs after an acute replication stress (data not shown). Thus, the presence of single-stranded nascent DNA might most likely be due to fork reversal.

The results of this experiment showed that hTERT-RPE cells presented an increase in single-stranded nascent DNA after an acute replication stress, which was more pronounced upon severe replication stress (**Figure 29**). Notably, replication forks are processed into DSBs (data not shown) explaining the increase in native BrdU levels upon 14h HU treatment.

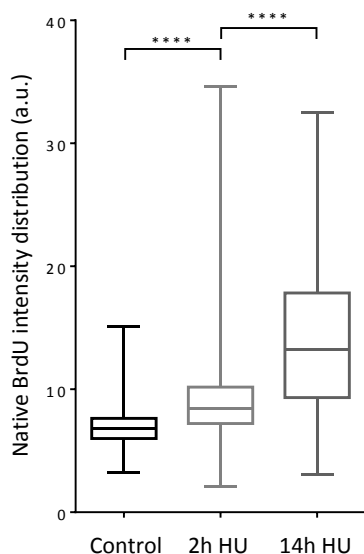


**Figure 29. Acute replication stress generates single-stranded nascent DNA in hTERT-RPE cells.** Cells synchronized in S phase were labelled for 10 minutes with BrdU and treated with 10mM HU during the indicated time before performing BrdU immunofluorescence under native conditions. BrdU analogue was maintained in the media during the first 15 minutes of HU treatment. The relative native BrdU intensities (in arbitrary units (a.u.)), of more than 700 cells from four independent experiments were measured in each condition. Box and whiskers show: min, max, median and first quartiles (unpaired *t*-test, \*\*\*\* P value < 0.0001).

Consistent with the accumulation of single-stranded nascent DNA observed in **Figure 29**, we observed an increase in the chromatin-bound RPA levels upon an acute HU treatment (**Figure 28**).

### STALLED REPLICATION FORKS ARE ABLE TO RESTART AFTER AN ACUTE REPLICATION STRESS WITHOUT COMPROMISING GENOMIC INTEGRITY IN hTERT-RPE CELLS

As explained in previous results of chapter 1, replication forks of hTERT-RPE cells are able to restart after an acute, but not a prolonged HU treatment (**Figure 18**). At this point, it was already known that replisome components were displaced away from nascent DNA, but they maintained their association with chromatin. Our group next wondered if the previously observed restart<sup>536</sup> was due to the activation of nearby origins that could not be distinguished in the fiber assay<sup>135</sup> or if the previously formed CMG complexes were reused to resume replication. Thus, to study the real fork restarting, a DNA fiber assay was performed using roscovitine, a CDK inhibitor<sup>555</sup>, to inhibit CDK2-mediated phosphorylations of replisome components, essential for origin firing<sup>156,173,174</sup>. The efficiency of roscovitine was corroborated by the reduction in the number of new origins and the shortening of IdU track length (data not shown), due to the previously described role of CDKs in fork progression<sup>556</sup>. Remarkably, the number of restarted forks was maintained despite roscovitine addition after an acute replication stress in hTERT-RPE cells, indicating that restart was not due to nearby fired origins (**Figure 30**).

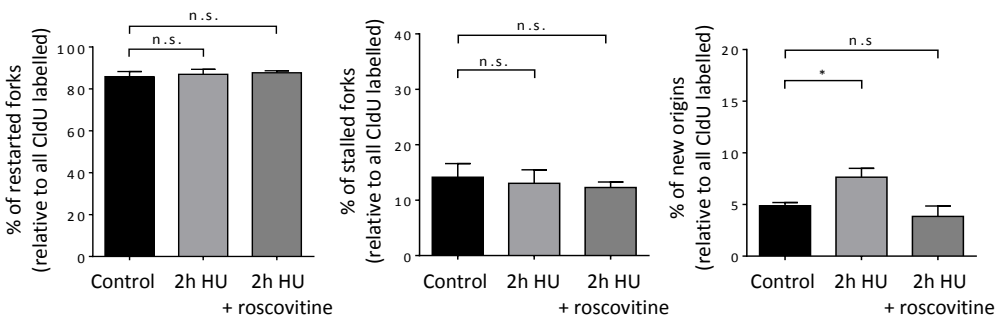


**Figure 30. Replication forks are able to restart after an acute replication stress in the absence of CDK activity in hTERT-RPE cells.** Asynchronously cells were labelled with CldU for 30 minutes, then cells were treated with 10mM of HU in the presence or absence of roscovitine for 2 hours. CldU was maintained in the media during the first 15 minutes of HU treatment. Finally, cells were incubated with IdU in the presence or absence of roscovitine for 1 hour more. DNA fibers were prepared and stained with BrdU antibodies. Around 1500 fibers from three independent experiments were counted in each condition. The percentage of stalled and restarted forks and new origin firing events, relative to total CldU labelled fibers, are shown. Error bars represent standard deviation (paired *t*-test, n.s.: non-statistically significant, \* *P* value < 0.05).

*PREVIOUS DATA*

The results from the presence of single-stranded nascent DNA suggested that replication forks could be reversed after acute HU treatment and that replication was restarted from the same forks. The group had already demonstrated that cells were able to recover replication and arrive in mitosis after an acute replication stress induced by 10mM of HU treatment <sup>536</sup> (previous data in chapter 1, **Figure 15**). The possible acquisition of genomic instability under those conditions was studied by analysing the number of cells with 53BP1 foci in the next G1 phase <sup>544-546</sup>. Notably, the percentage of G1 cells with 53BP1 foci did not significantly increase upon a release from acute HU treatment (data not shown). These results support the idea that replication restart from reversed forks does not compromise genomic integrity.

## RESULTS

### 2.1. CMG HELICASE MAINTAINS ITS INTEGRITY AND ASSOCIATION WITH CHROMATIN AFTER AN ACUTE REPLICATION STRESS IN hTERT-RPE CELLS

From previous data, we already knew that CMG was disengaged from nascent DNA. This raised the question of how replication forks restarted after an acute replication stress, since the assembly of new origins is restricted to G1 phase of the cell cycle, and the activation of new origins is impaired under HU conditions, due to the need of CDK activity to fire the pre-replicative complexes<sup>187,557</sup> and the fact that CDK is inhibited under these conditions<sup>34,558–561</sup>.

Since we had already demonstrated that replisome components preserved their association with chromatin, we wanted to analyse the integrity of CMG complex under this condition. We performed a co-immunoprecipitation experiment of MCM3 which demonstrated that the integrity of CMG complex in chromatin was maintained upon an acute HU treatment (**Figure 31**).

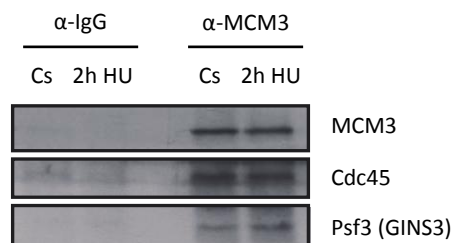


**Figure 31. CMG helicase maintains its integrity after an acute HU treatment in hTERT-RPE cells.** S-phase synchronized cells were treated with 10mM HU during 2 hours or left untreated (Cs). Chromatin fractions were incubated with antibodies against MCM3 or non-specific IgG. Protein immunocomplexes were pulled down and analysed by WB with the indicated antibodies.

## 2.2. CMG HELICASE IS DISENGAGED FROM NASCENT DNA AFTER AN ACUTE REPLICATION STRESS INDIFFERENTLY OF CDK ACTIVITY IN hTERT-RPE CELLS

Our previous results showed that replication forks could restart upon acute HU treatment, even when CMG complex was disengaged. To prove that the observed restart was real and not an artifact due to dormant origins activation, we added CDK inhibitor, roscovitine, during DNA synthesis reinitiation and we checked that a real restart was observed under these conditions (**Figure 30**).

We next wondered if in CDK inhibition conditions, replication forks could be stabilized, and replisome components could not be disengaged from nascent DNA after an acute replication stress. To analyse it, we performed the iPOND technique to corroborate that CDK inhibition did not alter the changes that we observed upon acute HU treatment in replication forks and that CMG complex was still disengaged from nascent DNA.

The results in **Figure 32** showed that the helicase complex was displaced away from nascent DNA upon HU treatment in hTERT-RPE cells, even in the absence of CDK activity. The efficiency of roscovitine was corroborated by the reduction of CMG complex in control condition (pulse condition with roscovitine) due to the impairment of firing new origins.

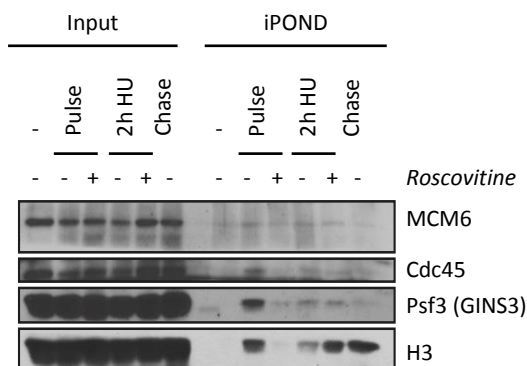


**Figure 32. CMG complex is disengaged from nascent DNA upon HU treatment even in the absence of CDK activity in hTERT-RPE cells.** S-phase synchronized cells were treated and harvested for iPOND. Roscovitine was added where indicated. The proteins present on iPOND extracts were analysed by WB with the indicated antibodies. (-): no EdU. Input: nuclear extract. Histone 3 (H3) was used as an immunoprecipitation control. Notice that, as expected, roscovitine addition before the EdU pulse compromised EdU incorporation and, thus, protein immunoprecipitation by iPOND.

### 2.3. FBH1 DEPLETION REDUCES THE AMOUNT OF SINGLE-STRANDED NASCENT DNA, BUT DOES NOT IMPAIR REPLICATION FORK RESTART IN hTERT-RPE CELLS

The previous results indicated that replication forks were remodelled after an acute replication stress, and seemed to point out that, after 2 hours of HU treatment, replication forks were regressed into chicken foot structures<sup>462,562,563</sup>. To study this, we focused on FBH1, since it was the unique helicase that had been demonstrated to have the capacity to promote fork reversal *in vivo*<sup>470</sup> at the time these experiments were performed. Since then, several other replication fork remodellers have been proposed to have a role on fork reversal, as RAD51<sup>462</sup>, SMARCAL1<sup>335,339</sup>, polyUB-PCNA and ZRANB3<sup>473</sup> or HLF<sup>469,564</sup>.

We analysed if the increase in single-stranded nascent DNA after an acute HU treatment (**Figure 29**) was due to FBH1-dependent fork reversal. To this end, the analysis of ssDNA accumulation in the nascent DNA by native BrdU staining<sup>337</sup> was performed in FBH1-depleted cells.

The results of this experiment showed an increase in nascent ssDNA upon acute HU treatment, which decreased upon FBH1 depletion (**Figure 33**). This indicates that replication stress induced by an acute HU treatment leads to fork reversal in hTERT-RPE cells, with FBH1 playing a role in this process. However, even though FBH1 depletion decreases the amount of single-stranded nascent DNA, native BrdU intensity is still higher than control conditions (**Figure 33**). Thus, it has to be considered that fork reversal could be performed by other remodellers. On the other hand, this ssDNA analysis is an indirect method to analyse fork reversal and changes in the presence of ssDNA could be explained by other processes, such as resection.

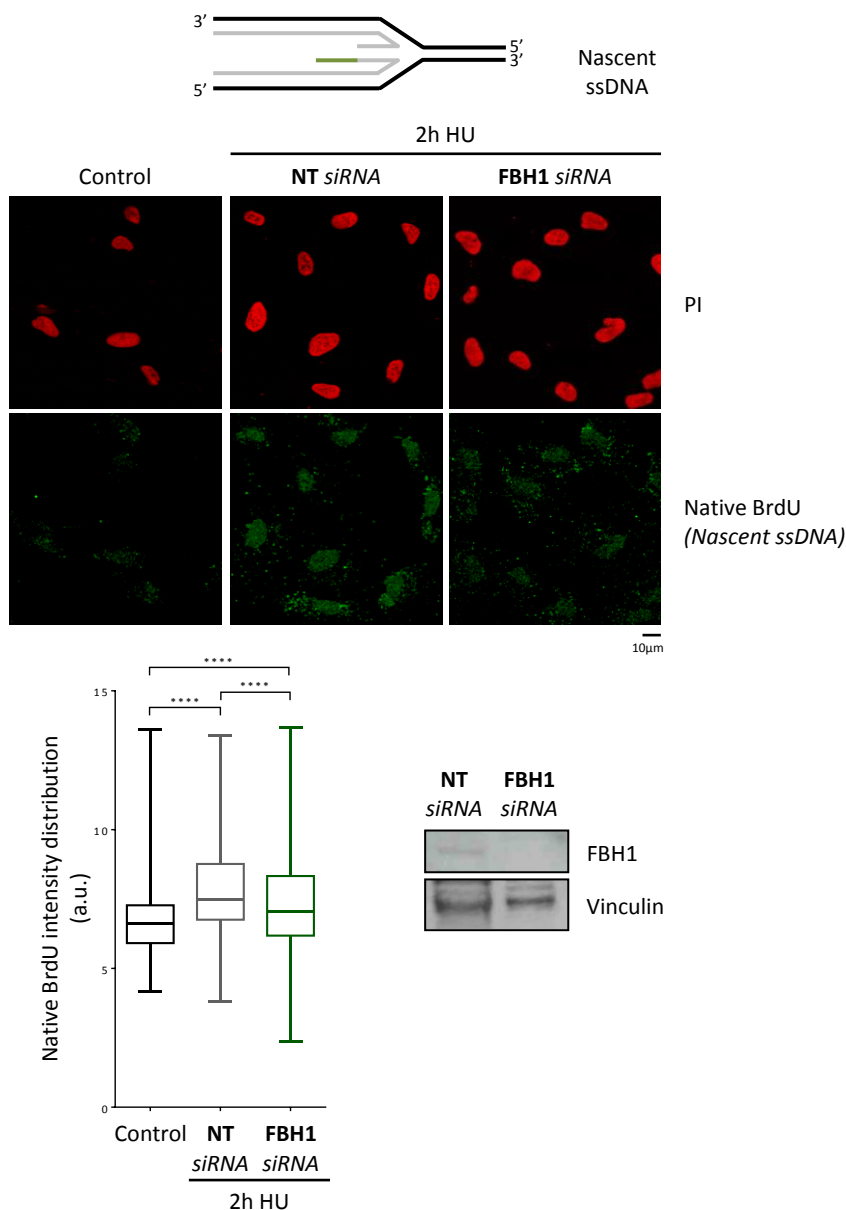


**Figure 33. FBH1 depletion decreases nascent ssDNA upon acute HU treatment in hTERT-RPE cells.** Cells were transfected with the indicated siRNA (NT: non-target) and then synchronized in S phase. After that, cells were labelled for 10 minutes with BrdU and treated with 10mM HU during 2 hours (maintaining BrdU during the first 15 minutes) before performing BrdU immunofluorescence under native conditions. If forks are reversed as indicated, BrdU antibody can label the ssDNA present on the 3' end of the leading strand (indicated in green in the upper panel). DNA was counterstained with PI. Representative images are shown (middle panel). The relative BrdU intensities (in arbitrary units (a.u.)) of more than 600 cells was measured in each condition. Box and whiskers show: min, max, median and first quartiles (bottom-left panel, unpaired *t*-test, \*\*\*\* *P* value < 0.0001). In parallel, whole cells extracts were analysed by WB with the indicated antibodies (bottom-right panel). Vinculin was used as loading control. *The WB was performed by Sólveig Hlín Brynjólfsdóttir, PhD (in the laboratory of Prof. Claus Storgaard Sørensen, PhD).*

Initially, the reversed forks were associated with the accumulation of toxic intermediates<sup>278,496,562,565,566</sup>, but more recently it is being considered whether fork reversal may have a protective role, safeguarding genome integrity<sup>334</sup>. Furthermore, replication restart from reversed forks has been described<sup>481,482,567</sup>. Thus, considering that fork reversal could have a protective role, we next wondered if FBH1 depletion could have an effect on replication fork restart after an acute HU treatment. We analysed this hypothesis by DNA fiber assay and, in order to study the real fork restart, we performed the experiment using roscovitine<sup>555</sup>. Interestingly, the number of restarted forks was maintained despite FBH1 depletion after an acute replication stress in hTERT-RPE cells, indicating that restart was maintained in conditions where the number of reversed forks had decreased (**Figure 34**).

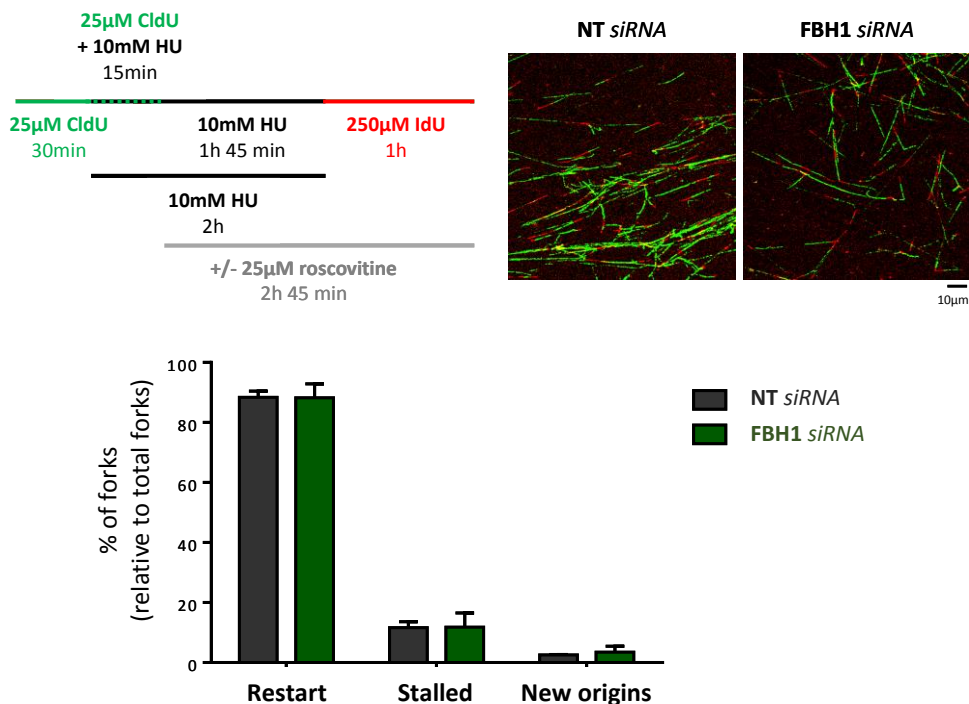


**Figure 34. FBH1 depletion does not impair replication fork restart after an acute HU treatment in hTERT-RPE cells.** Cells transfected with the indicated siRNA (NT: non-target) were labelled as indicated (upper-left panel) and DNA fibers were prepared and stained with anti-BrdU antibodies. Representative images are shown (upper-right panel). At least 300 fibers were counted in each condition for each experiment. The percentage of stalled and restarted forks and new origin firing events, relative to total forks, of two independent experiments are shown. Error bars represent standard deviation (bottom panel). The knockdown was shown in Figure 33.

Next, we wondered if the cells, whose replication forks restarted after an acute replication stress without being reversed, could resume cell cycle and arrive into mitosis. To answer this question, cells in S phase were pulse-labelled with a BrdU pulse for 30 minutes; then they were treated with HU during 2 hours and released from the stress into nocodazole-containing medium. After 12 hours of release, cells were harvested, and cell cycle was analysed by cell cytometer.

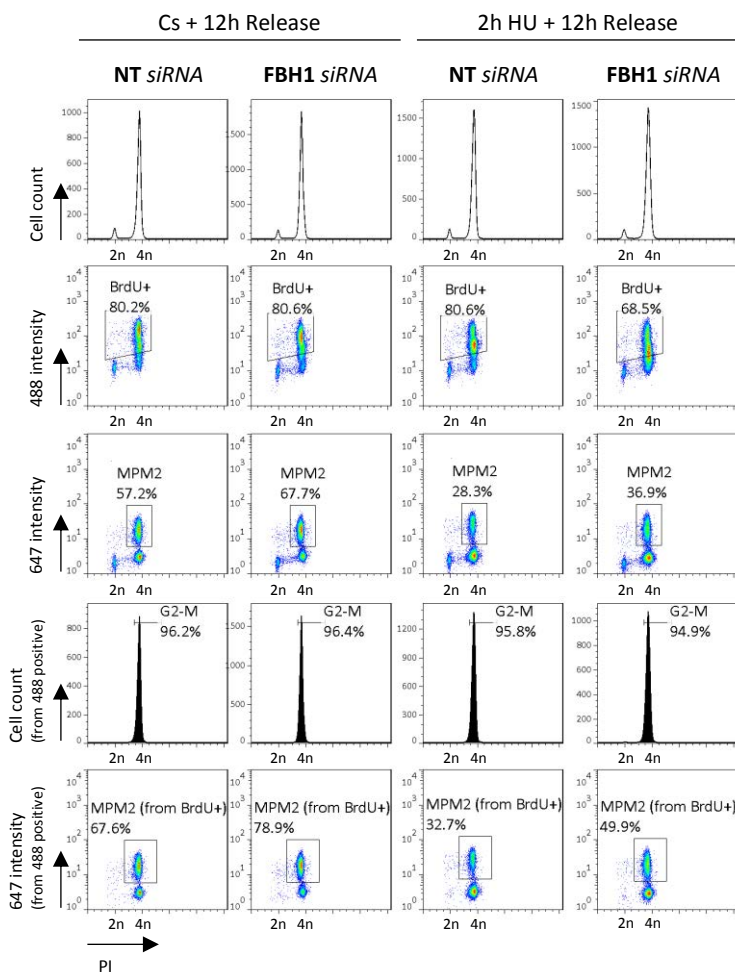


**Figure 35. FBH1 depletion does not impair mitotic entry after an acute HU treatment in hTERT-RPE cells.** Cells were transfected with the indicated siRNA (NT: non-target) and 48 hours later cells were labelled with BrdU and then treated with 10mM HU or left untreated (12h release) for 12 hours, and then released into nocodazole-containing fresh medium for 12 hours. Flow cytometry analysis of approximately 15000 cells was performed to analyse the S-phase arrested (BrdU-488 positive) cells after 12 hours of HU treatment, and the recovery from this stress measuring mitotic (MPM2-647 positive) cells from BrdU positive population. The experiment was performed once under those conditions (we performed the experiment with different times of HU treatment and the results were the same). The knockdown was shown in Figure 33.

The results above show that FBH1-depleted cells resumed replication after an acute replication stress could arrive into G2-M phases and entered into mitosis, even in a higher percentage than cells treated with non-targeted siRNA (**Figure 35**).

All these results indicate that even though fork reversal was impaired by FBH1 depletion, the cells could restart replication forks, resume cell cycle and enter into mitosis without impairment.

#### 2.4. REPLISOME DISENGAGEMENT FROM NASCENT DNA CORRELATES WITH LARGE AMOUNTS OF SINGLE-STRANDED PARENTAL DNA AND RPA ACCUMULATION

After having seen that despite the impairment of fork regression by FBH1 depletion, replication forks were able to restart, we wondered how these replication forks look like.

It has been reported by Zellweger *et al.* that in human cells, especially in non-transformed hTERT-RPE cells, several genotoxic agents that interfere with DNA synthesis (such as HU) caused two types of fork-remodelling events: on the one hand a replication fork uncoupling between helicase and polymerases, and on the other hand, fork reversal, neither of them compromising fork integrity<sup>462</sup>.

At this point, we analysed if under our conditions, where reversed forks are present, the replication fork uncoupling was also produced. The functional uncoupling of helicases and polymerases is expected to cause an accumulation of large amounts of single-stranded parental DNA, while fork reversal generates accumulation of single-stranded nascent DNA (**Figure 36**).

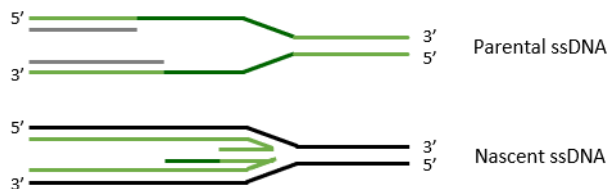


**Figure 36. Fork remodelling events that generates ssDNA, that can be detected by BrdU immunofluorescence under native conditions.** Asynchronously growing cells were labelled for 48 hours (parental) or 15 minutes (nascent) with BrdU. The presence of ssDNA is detected by BrdU immunofluorescence under native conditions. The BrdU-labelled DNA is indicated in light green and the ssDNA that is generated in each case is indicated in dark green.

We analysed if fork uncoupling was an event that could also occur upon acute HU treatment in hTERT-RPE cells. To determine this, we analysed the accumulation of ssDNA on parental strands and on nascent strands by quantitative image-based cytometry (QIBC)<sup>239</sup>.

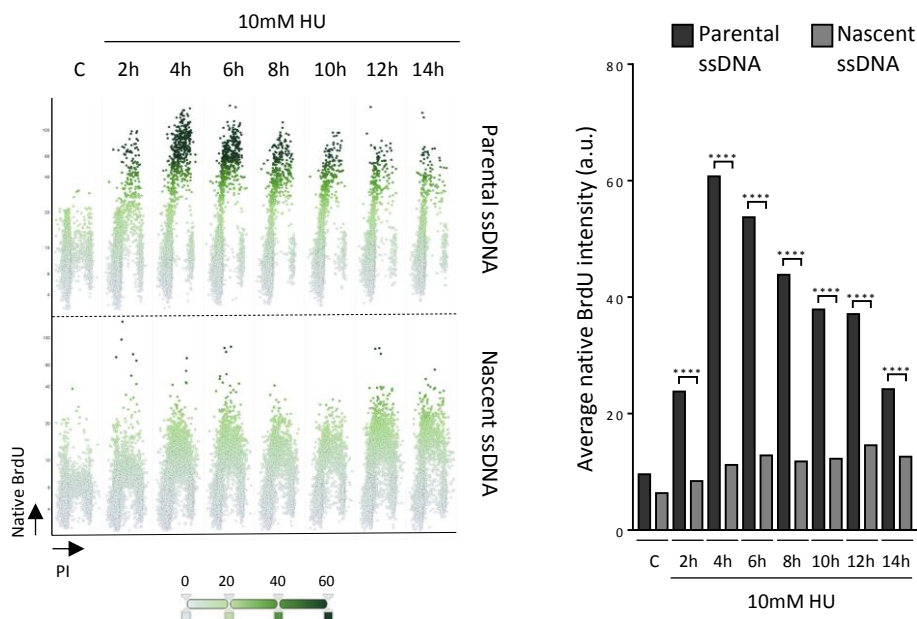


**Figure 37. Acute HU treatment generates fork reversal and functional helicase-polymerases uncoupling.** Asynchronously growing cells were labelled for 48 hours (parental ssDNA) or 15 minutes (nascent ssDNA) with BrdU and treated for the indicated time with 10mM HU or left untreated (C). For parental ssDNA detection, cells were released overnight in 10 $\mu$ M thymidine before HU treatment. For nascent ssDNA detection, BrdU was maintained in the media for the first 15 minutes of HU treatment. BrdU under native conditions was analysed by QIBC. Cells were counterstained with DAPI. The relative BrdU intensities (in arbitrary units (a.u.)) of at least 5000 cells were measured in each condition (unpaired *t*-test, \*\*\*\* P value < 0.0001). The experiment was performed in Centre for Chromosome Stability (CCS) by Amaia Ercilla, PhD.

The results above show a slight increase in nascent ssDNA upon an acute HU treatment (also shown in **Figure 29** and **Figure 33**), but they also reflect a much higher accumulation of ssDNA in parental strands under the same conditions (**Figure 37**), indicating that fork uncoupling is a predominant event also occurring upon acute HU treatment.

We already knew that upon an acute replication stress, large amounts of RPA bound to chromatin were accumulated (**Figure 28**). We wanted to determine if the increase in chromatin-bound RPA correlated better with an increase of parental ssDNA or of nascent ssDNA. The results showed that chromatin-bound RPA showed a better correlation with the amount of ssDNA detected by native BrdU staining in the parental strands, than with the amount of ssDNA in the nascent strands (**Figure 38**).

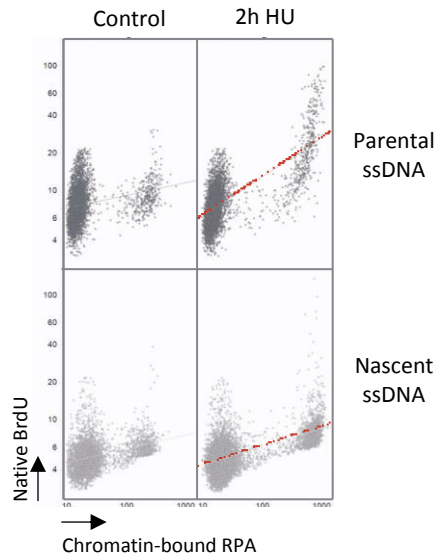


**Figure 38. Cells with more parental ssDNA have more chromatin-bound RPA after an acute HU treatment in hTERT-RPE.** Asynchronously growing cells were labelled for 48 hours (parental ssDNA) or 15 minutes (nascent ssDNA) with BrdU and treated for the indicated time with HU or left untreated (control). For parental ssDNA detection, cells were released overnight in 10 $\mu$ M thymidine before HU treatment. For nascent ssDNA detection, BrdU was maintained in the media for the first 15 minutes of HU treatment. BrdU under native conditions and chromatin-bound RPA were analysed by QIBC. Cells were counterstained with DAPI. *The experiment was performed in Centre for Chromosome Stability (CCS) by Amaia Ercilla, PhD.*

## 2.5. NASCENT DNA IS NOT DEGRADED BY MRE11 AFTER AN ACUTE REPLICATION STRESS IN hTERT-RPE CELLS

The results above indicated that the accumulation of ssDNA was more pronounced in the parental strands, suggesting that fork uncoupling was the predominant event. But ssDNA at parental DNA strands could result from resection of nascent DNA. Mre11-dependent degradation of nascent DNA has been well described<sup>335,476,495,568,569</sup>. To discard that the

## RESULTS

presence of ssDNA in the parental strands was due to nascent DNA degradation, we performed a DNA fiber assay, labelling the nascent DNA before acute HU treatment. When cells were treated with HU, in the presence of the second analogue, mirin, a Mre11 inhibitor, was also added in the indicated condition<sup>495,570</sup>. If under this condition, nascent DNA would be degraded by Mre11, a decrease in the IdU track length would be obtained. This decrease should be rescued by the addition of mirin.

The results of this experiment demonstrated that nascent DNA was not degraded by Mre11 upon acute HU treatment, since no increase was obtained when mirin was added (**Figure 39A**). The condition of 14 hours of HU was used as a positive control for mirin, since we already knew that under this condition nascent DNA was degraded<sup>536</sup>, and this experiment showed that the degradation is Mre11-dependent after a prolonged HU treatment (**Figure 39B**).

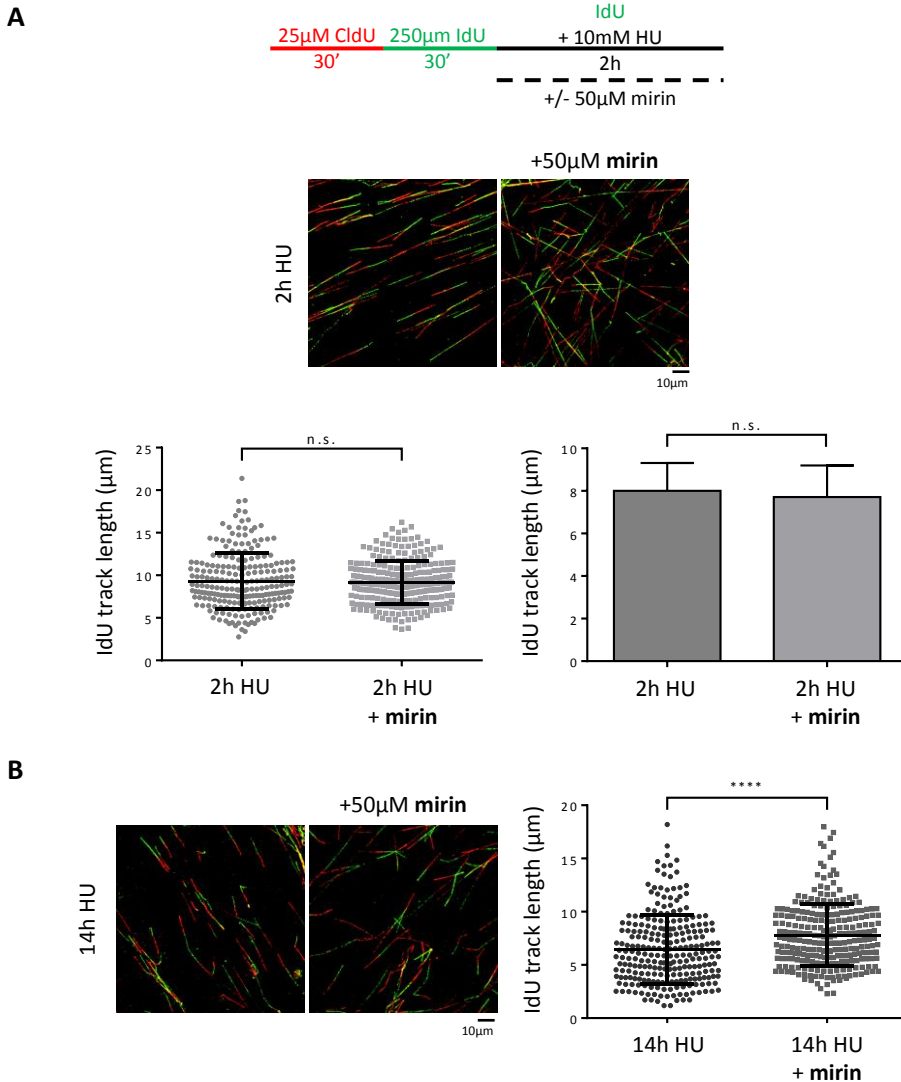


**Figure 39. Nascent DNA is not degraded by Mre11 after an acute HU treatment in hTERT-RPE cells. (A)** Asynchronously growing cells were labelled and treated as indicated (upper panel). DNA fibers were prepared and stained. Around 750 fibers were counted in each condition. IdU track length distribution and statistical analysis are shown. Scatter plot with mean and SD of a representative experiment is shown (bottom-left panel, Mann-Whitney test, n.s.: non-statistically significant). Column graph with mean and SD of different experiments is shown (bottom-right panel, paired *t*-test, n=4, n.s.: non-statistically significant). **(B)** Cells were treated as in (A) and DNA fiber assay was performed in 14 hours of 10mM HU treatment, to used is as a positive control for Mirin<sup>536</sup>. Representative images are shown (left panel). Scatter plot with mean and SD of one experiment is shown (right panel, Mann-Whitney test, \*\*\*\*P value < 0.0001).

## 2.6. REPLICATION RESUMPTION OCCURS WITHOUT LONG STRETCHES OF SINGLE-STRANDED PARENTAL DNA IN hTERT-RPE CELLS

The information above indicates that, in line with previous reports <sup>462</sup>, replication stress induced by HU can cause fork remodelling, both functional helicase-polymerases uncoupling and fork reversal, which does not compromise fork restart. It should be noticed that the amount of ssDNA in parental strands suggests that the most predominant event is fork uncoupling. Moreover, our data suggest that replication forks restart from the same CMG complexes that have been disengaged from nascent DNA. To define how uncoupled forks could resume replication, we analysed the parental ssDNA disappearance and the chromatin-bound RPA levels upon release from acute HU treatment. The results show that the amount of parental ssDNA decreases almost completely after 30 minutes of HU release (**Figure 40A**). Consistently, chromatid-bound RPA levels decrease to levels similar to the control after 30 minutes to 1-hour release from acute HU treatment (**Figure 40B**).

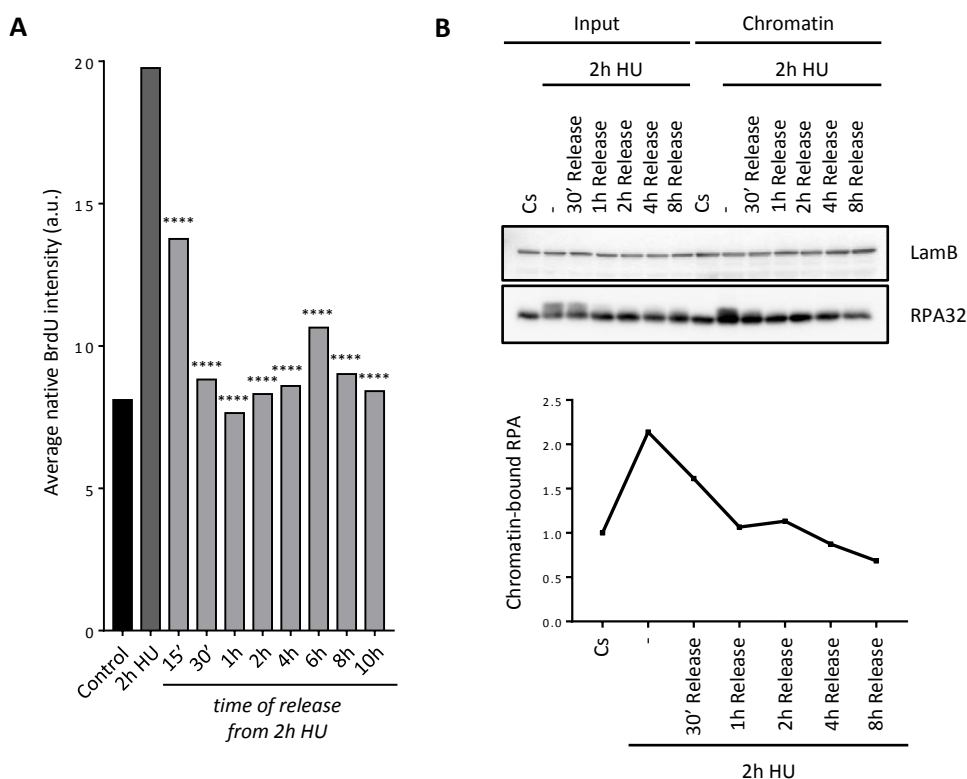


**Figure 40. Parental ssDNA and chromatin-bound RPA levels decrease almost completely after 30 minutes or 1 hour from HU release in hTERT-RPE cells. (A)** Asynchronously growing cells were labelled for 48 hours with BrdU and released overnight in 10 $\mu$ M thymidine before 10mM HU treatment. After

that, cells were treated for 2 hours with 10mM HU and then released into fresh media for the indicated time. BrdU under native conditions was analysed by QIBC. Cells were counterstained with DAPI. The relative BrdU intensities (in arbitrary units (a.u.)) of at least 5000 cells were measured in each condition (unpaired *t*-test, relative to 2h HU, \*\*\*\* P value < 0.0001). *The experiment was performed in Centre for Chromosome Stability (CCS) by Amaia Ercilla PhD.* **(B)** Synchronic S-phase cells were treated with 10mM HU for 2 hours (-) or left untreated (Cs). After HU treatment, cells were released into fresh media for the indicated time. Chromatin-enriched fractions were obtained and analysed by WB with the indicated antibodies. Lamin B (LamB) was used as a loading control (upper panel). Quantification of chromatin-bound RPA of two different experiments is shown (bottom panel).

Taken together, the results presented in this chapter indicate that two fork remodelling events are occurring upon acute replication stress. On the one hand, fork reversal occurs under these conditions, since FBH1 depletion decreases the amount of single-stranded nascent DNA. On the other hand, helicase-polymerases uncoupling also occurs, since a large amount of single-stranded parental DNA is obtained upon an acute replication stress, being this last one the predominant event. Moreover, the presence of ssDNA in the parental strands does not involve nascent DNA degradation by Mre11. And most interestingly, the uncoupled forks present assembled CMG complexes, which are disengaged from nascent DNA, but are able to reinitiate DNA synthesis upon HU removal, with the rapid disappearance of single-stranded parental DNA.



# **CHAPTER 3**

## **ROLE OF RAD51 IN REPLICATION FORKS IN RESPONSE TO REPLICATION STRESS**



## RESULTS

### 3.1. RAD51 DEPLETION DOES NOT AFFECT THE NUMBER OF RESTARTED FORKS, BUT IMPAIRS FORK PROGRESSION AFTER AN ACUTE REPLICATION STRESS IN hTERT-RPE CELLS

IPOND analysis of replication forks showed a recruitment of RAD51 upon 2 hours of 10mM HU treatment (previous data shown in chapter 2, **Figure 27**). Under this condition, as it was shown in chapter 2, hTERT-RPE cells recover from this HU-induced replication stress mainly by restarting replication forks. The aim of this study was to analyse the relevance of RAD51 under these conditions.

First, we wondered if RAD51 was necessary for replication fork restart after acute HU treatment. To do so, non-transformed human hTERT-RPE cells were depleted of RAD51 and their replication dynamics was analysed. To this end, cells were labelled during 30 minutes with the first analogue, CldU, then treated with 10mM of HU for 2 hours, and finally labelled during 1 hour with the second analogue, IdU. CldU was maintained in media during the first 15 minutes of HU treatment, since it was the time needed to completely stall replication forks<sup>536</sup>.

As shown in **Figure 41**, the number of restarted forks after 2 hours of 10mM HU treatment was not affected upon RAD51 depletion. But DNA fiber assay did not allow us to distinguish between restart and activation of nearby origins<sup>135</sup>. Thus, to study the real fork restart, we also performed the DNA fiber assay using roscovitine, a CDK inhibitor<sup>555</sup>, to inhibit CDK2-mediated phosphorylations of replisome components, essential for origin firing<sup>156,173,174</sup>. As shown in **Figure 41**, 90% of forks with real restart (the one observed with roscovitine) was maintained despite RAD51 depletion. A slight decrease in the new origin firing events was obtained with roscovitine addition, indicating that origin firing was inhibited under roscovitine conditions. The results indicate that RAD51 depletion does not affect the number of forks able to restart after an acute HU treatment.

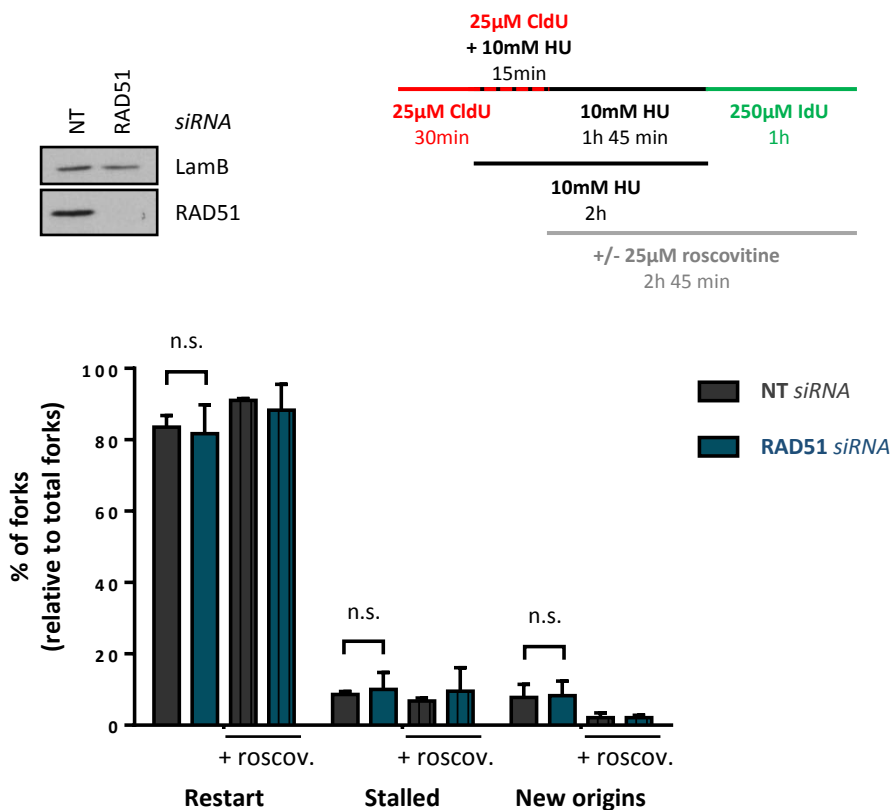


**Figure 41. RAD51 depletion does not affect fork restart after an acute HU treatment in hTERT-RPE cells.** Cells were transfected with the indicated siRNA (NT: non-target) and 48 hours later cells were harvested for WB analysis with RAD51. Lamin B (LamB) was used as a loading control (upper-left panel). hTERT-RPE transfected cells were labelled as indicated (upper-right panel). After labelling, cells were harvested and prepared for DNA fiber analysis. At least 200 fibers of each condition in each experiment were used to calculate the percentage of restart, stalled forks and new origin firing events relative to total forks. Means and standard deviation (bars) of three experiments without roscovitine and two experiments with roscovitine (+roscov.) are shown (bottom-right panel). The statistical analysis was performed just in HU-treated cells (paired *t*-test, n.s.: non-statistically significant).

Then, fork progression after replication restart from the same experiments was analysed, measuring the IdU (second analogue) track length in fibers that had incorporated both analogues. As shown in **Figure 42**, while with RAD51 depletion there were no differences in fork progression, the addition of roscovitine in RAD51-depleted cells showed a significant reduction in fork progression after an acute HU treatment.

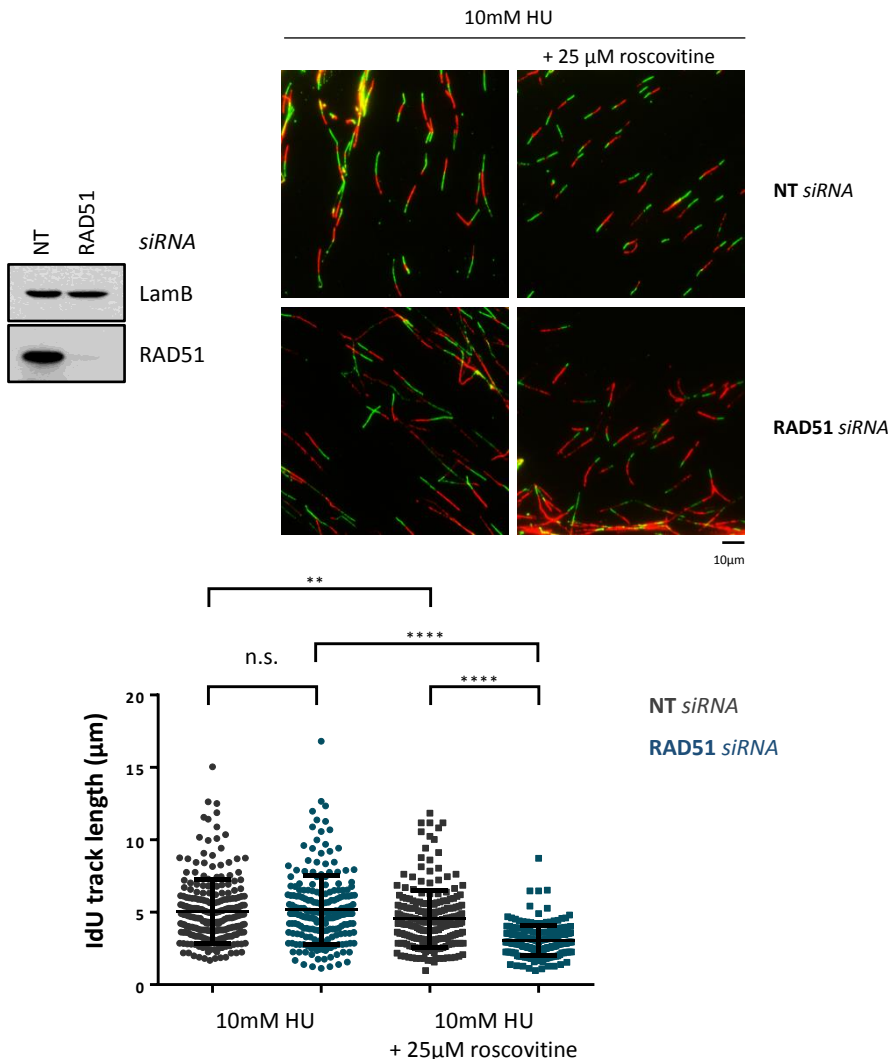


**Figure 42. RAD51 depletion impairs fork progression after replication restart in hTERT-RPE cells.** Cells were transfected with the indicated siRNA (NT: non-target) and 48 hours later cells were harvested for WB analysis with RAD51. Lamin B (LamB) was used as a loading control (upper-left panel). DNA fibers for Figure 41 were used to measure IdU track length. Representative images are shown (upper-right panels). At least 200 fibers of each condition in each experiment were measured. Means and standard deviation (bars) of one representative experiment out of two is shown (bottom panel, Mann-Whitney test, n.s.: non-statistically significant, \*\* P value < 0.01, \*\*\*\* P value < 0.0001).

The results above indicate that, although RAD51 depletion does not have effect in the number of restarted forks, it impairs fork progression after an acute replication stress. In HU-treated conditions, this effect would be compensated by dormant origins that cannot be distinguished by DNA fiber assay.

### 3.2. RAD51 DEPLETION DOES NOT CAUSE FORK DEGRADATION AFTER AN ACUTE REPLICATION STRESS IN hTERT-RPE CELLS

Multiple HR proteins protect the nascent DNA at replication forks from nucleases degradation<sup>370,476,477,479</sup>. In order to know if RAD51 was necessary to protect DNA from degradation of for DNA stabilization upon acute HU treatment, the degradation of nascent DNA in RAD51-depleted cells was analysed. To do so, siRNA transfected-cells were labelled with CldU for 30 minutes and with IdU for 30 minutes more. Then cells were treated with 10mM of HU during 2 hours.

The analysis of IdU track length showed that no significant differences were obtained between non-targeted and RAD51-depleted cells after an acute replication stress (**Figure 43**), which indicates that RAD51 is not required at replication forks under these conditions to protect nascent DNA.

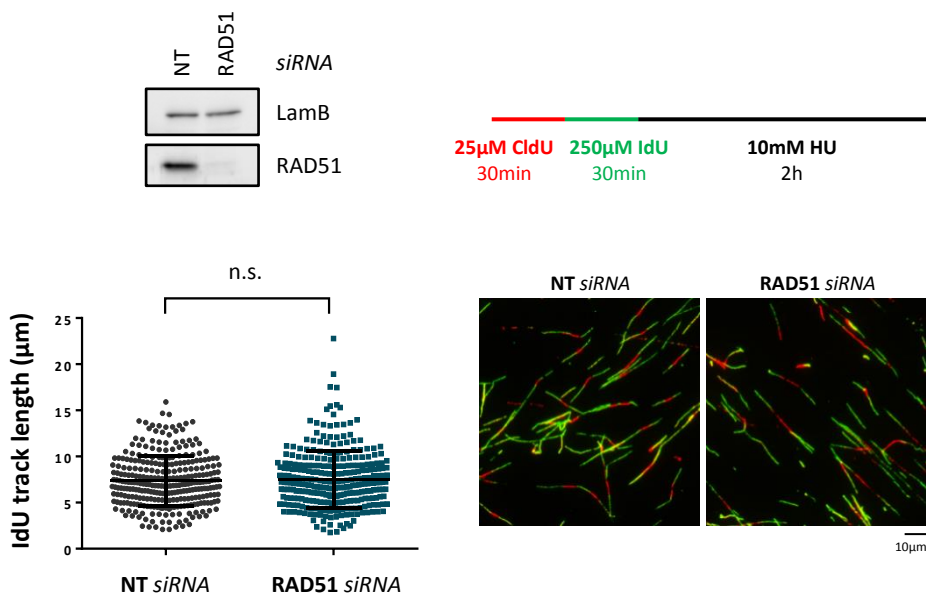


**Figure 43. RAD51 depletion does not cause fork degradation upon acute HU treatment in hTERT-RPE cells.** Cells were transfected with the indicated siRNA (NT: non-target) and 48 hours later cells were harvested for WB analysis with RAD51 antibody. Lamin B (LamB) was used as a loading control (upper-left panel). hTERT-RPE transfected cells were labelled as indicated (upper-right panel). After labelling, cells were harvested and prepared for DNA fiber analysis. Representative images are shown (bottom-right panels). The IdU track length was measured. At least 300 fibers of each condition in each experiment were measured. One representative experiment out of three is shown (bottom-left panel, Mann-Whitney test, n.s.: non-statistically significant).

### **3.3. RAD51 DEPLETION DOES NOT IMPAIR REPLICATION RECOVERY AFTER AN ACUTE REPLICATION STRESS IN hTERT-RPE CELLS**

We next wondered if RAD51-depleted cells, which were able to restart after an acute replication stress, were able to finish S phase and entry into mitosis. To analyse it, cell cytometer analysis was performed. hTERT-RPE cells were transfected and 48h later a BrdU pulse was done in order to label cells in S phase and analysed their progression through cell cycle. Then, cells were treated with 10mM of HU or left untreated in nocodazole-containing media (control situation). After HU treatment, cells were released in nocodazole-containing media during 12 hours. As shown in **Figure 44**, RAD51-depleted cells were not affected by acute replication stress (2h HU + 12h release), since they were able to finish replication as in a control situation (12h release). Remarkably, RAD51 depletion had a strong effect in cell cycle, since an accumulation of cells in G2 phase was obtained. These data are in agreement with another report, which demonstrate that RAD51 inactivation does not affect S phase but provokes a G2 arrest<sup>571</sup>.

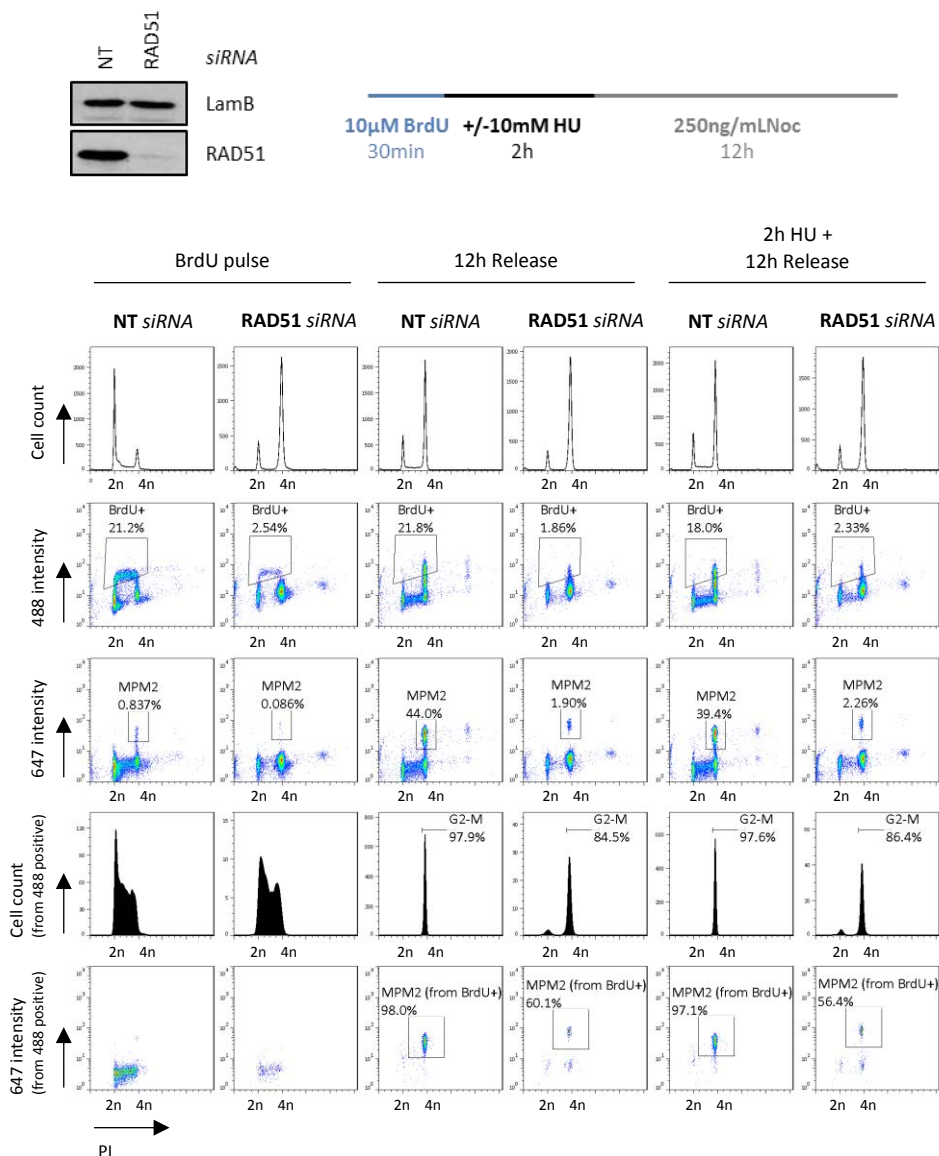


**Figure 44. RAD51 depletion does not impair replication recovery after an acute HU treatment in hTERT-RPE cells.** Cells were transfected with the indicated siRNA (NT: non-target) and 48h later cells were labelled with BrdU and then treated with 10mM HU or left untreated (12h release) into nocodazole-containing media for 12 hours. HU-treated cells were then released into nocodazole-containing fresh medium for 12 hours (2h HU + 12h release). Flow cytometry analysis of approximately 15000 cells was performed to analyse the S-phase arrested (BrdU-488 positive) cells after HU treatment, and the recovery from this stress measuring mitotic (MPM2-647 positive) cells from BrdU positive population. One representative experiment out of two is shown.

### 3.4. RAD51 DEPLETION INCREASES GENOMIC INSTABILITY IN hTERT-RPE CELLS

The previous data showing the effect of RAD51 depletion in replication fork progression after acute HU treatment made us wonder if RAD51 depletion would affect genomic stability. To analyse this fact, immunofluorescence of 53BP1 was performed. 53BP1 is described as a marker of DSB<sup>572</sup> or under-replicated regions of DNA<sup>544–546</sup>. The results suggested that RAD51 depletion increased the presence of DNA damage, and this increase was more noteworthy after acute HU treatment (**Figure 45**).

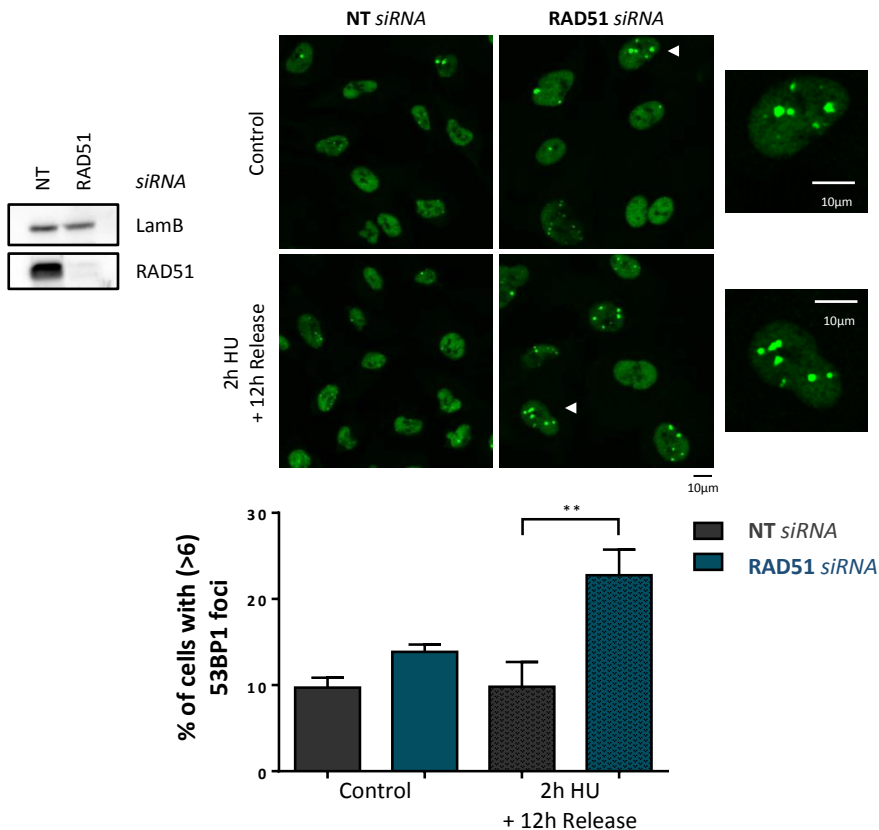


**Figure 45. RAD51 depletion increases 53BP1 foci after an acute HU treatment in hTERT-RPE cells.** Cells were transfected with the indicated siRNA (NT: non-target) and 48 hours later cells were treated with 10mM HU for 2 hours or left untreated for 12 hours (Control). After HU treatment, cells were released into fresh medium for 12 hours. Finally, 53BP1 immunofluorescence was performed. The control for KD was shown (upper-left panel). Representative images from each condition are shown (upper-middle panels). Two cells with more than six 53BP1 foci, indicated with a white arrowhead in the representative images from RAD51-depleted population, are shown in more detail (upper-right panels). At least 500 cells were counted for NT-depleted cells and 200 cells were counted for RAD51-depleted cells in each experiment. Means and standard deviation (bars) of percentage of cells presenting more than six 53BP1 foci of two experiments in control and three experiments in HU conditions are shown (bottom-right panel). The statistical analysis was performed just in HU-treated cells (unpaired *t*-test, \*\* *P* value < 0.01).

### 3.5. RAD51 INHIBITION DOES NOT AFFECT FORK PROGRESSION IN hTERT-RPE CELLS

The results above showed that RAD51 depletion had a strong effect in cell cycle, and an accumulation of cells in G2 phase was obtained. Thus, the analysis of fork progression was performed with a few cells present in S phase (seen by BrdU pulse condition in **Figure 44**). To avoid this problem, we chose to study the effect of RAD51 inhibition by using B02, a recently described RAD51 inhibitor, which was identified by high throughput screening<sup>531</sup> and acts by disrupting RAD51 binding to DNA and formation of the nucleofilament protein<sup>532</sup>.

First, we analysed if RAD51 inhibition had an effect in fork progression under unperturbed conditions in non-transformed human cells. To do so, a DNA fiber assay was performed by adding the inhibitor during the second analogue in order to avoid no labelling if RAD51 inhibition had a significant effect. The results showed that RAD51 inhibition had no effect in replication fork progression under normal conditions since IdU (second analogue) track length was maintained (**Figure 46**).

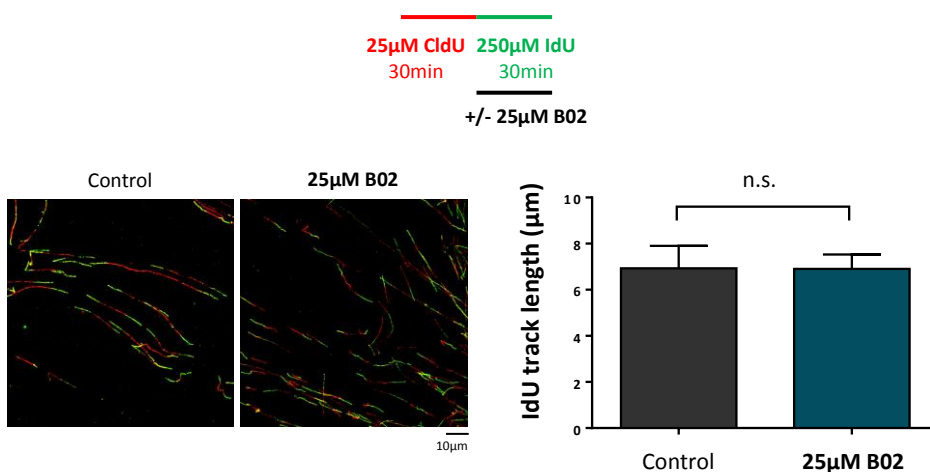


**Figure 46. RAD51 inhibition by B02 does not affect replication fork progression under normal conditions in hTERT-RPE cells.** Cells were labelled as indicated (upper panel), adding the B02 inhibitor with the second analogue. After labelling, cells were harvested and prepared for DNA fiber analysis. Representative images are shown (bottom-left panels). The IdU track length was measured. At least 200 fibers of each condition in each experiment were measured. Means and standard deviation (bars) of three experiments are shown (bottom-right panel, paired *t*-test, n.s.: non-statistically significant).

### 3.6. RAD51 INHIBITION DOES NOT AFFECT THE NUMBER OF RESTARTED FORKS, BUT IMPAIRS FORK PROGRESSION AFTER AN ACUTE REPLICATION STRESS IN hTERT-RPE CELLS

In order to validate the results obtained with RAD51 depletion, we first analysed the effect of RAD51 inhibition in replication dynamics after acute replication stress. To do so, non-transformed human hTERT-RPE cells were labelled during 30 minutes with the first analogue CldU, then treated with 10mM of HU for 2 hours with or without B02, and finally labelled during 1 hour with the second analogue IdU with or without B02. From now on, CldU was maintained during HU treatment to label DNA till replication forks were completely stalled.

As shown in **Figure 47**, the number of restarted forks after 2 hours of 10mM HU treatment, which stalls replication forks, was not affected upon RAD51 inhibition with B02, neither in roscovitine-treated conditions. The results validated the previous ones indicating that RAD51 depletion does not affect the number of restarted forks after an acute HU treatment.

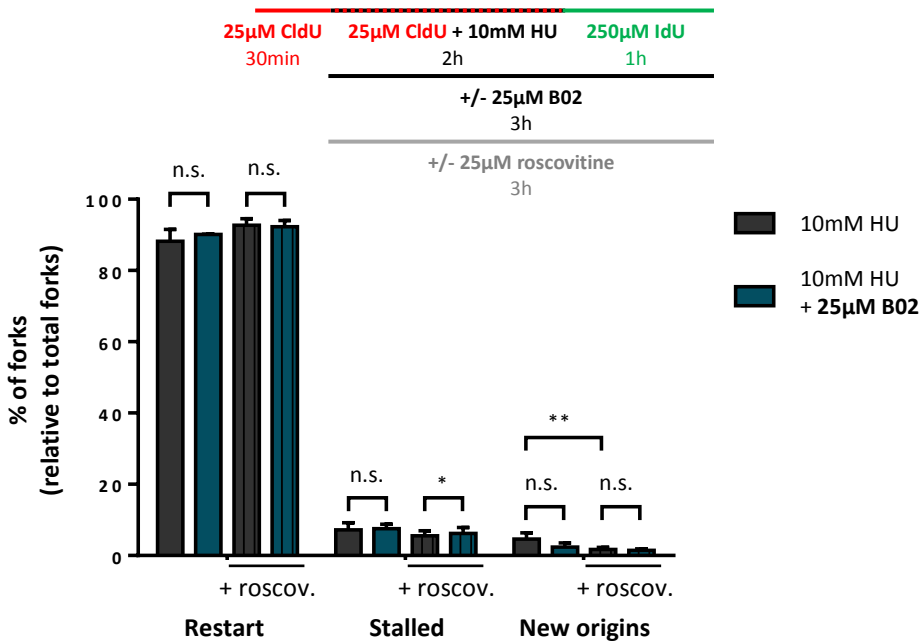


**Figure 47. RAD51 inhibition by B02 does not affect fork restart after an acute HU treatment in hTERT-RPE cells.** Cells were labelled as indicated (upper panel), adding the B02 inhibitor and roscovitine with HU and the second analogue. After labelling, cells were harvested and prepared for DNA fiber analysis. At least 200 fibers of each condition in each experiment were used to calculate the percentage of restart, stalled forks and new origin firing events relative to total forks. Means and standard deviation (bars) of three experiments with (+roscov.) or without roscovitine are shown (bottom-right panel, paired *t*-test, n.s.: non-statistically significant, \* *P* value < 0.05, \*\* *P* value < 0.01).

Then, fork progression after fork restart from the same experiments was analysed, measuring the IdU (second analogue) track length in fibers labelled with both analogues. As shown in **Figure 48**, RAD51 inhibition with B02, with or without roscovitine, showed a significant reduction in fork progression after 2 hours of HU treatment.

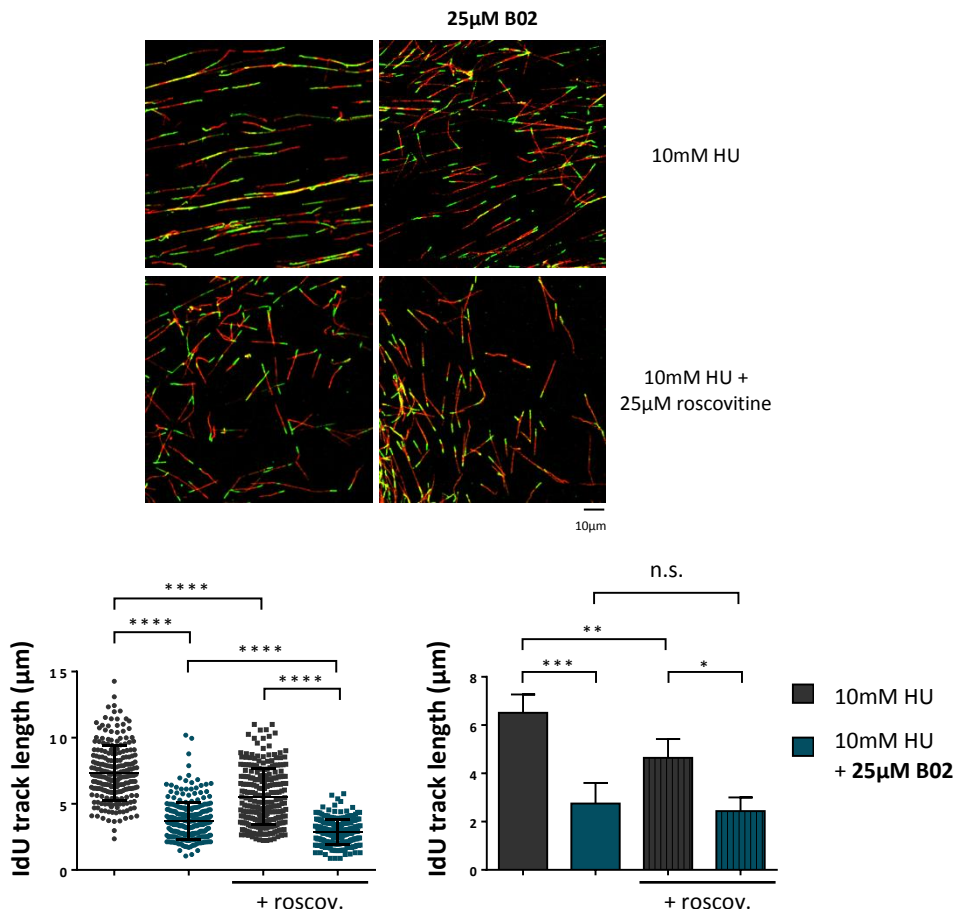


**Figure 48. RAD51 inhibition by B02 impairs fork progression after replication restart in hTERT-RPE cells.** DNA fibers for Figure 47 were used to measure IdU track length (second analogue). Representative images are shown (upper panels). At least 200 fibers of each condition in each experiment were measured. One representative experiment out of three is shown (bottom-left panel, Mann-Whitney test, \*\*\*\* P value < 0.0001). Means and standard deviation (bars) of three experiments with (+roscov.) or without roscovitine are shown (bottom-right panel, paired *t*-test, n.s.: non-statistically significant, \* P value < 0.05, \*\* P value < 0.01, \*\*\* P value < 0.001).

The efficiency of roscovitine was corroborated by the reduction in the number of new origins (**Figure 47**) and the shortening of IdU track length (**Figure 48**), due to the previously described role of CDKs in fork progression<sup>556</sup>.

### 3.7. RAD51 INHIBITION DOES NOT CAUSE FORK DEGRADATION AFTER AN ACUTE REPLICATION STRESS IN hTERT-RPE CELLS

In order to know if the inhibition of RAD51 during HU treatment was not affecting the nascent DNA, as we had seen in RAD51-depleted cells, we used the same experiments of DNA fiber assay performed previously (Figure 47 and Figure 48). The CldU (first analogue) was measured to analyse the stability of nascent DNA, since it labelled the replicated DNA just before the replication stress agent was added. The analysis of CldU track length showed that no significant differences were obtained with or without RAD51 inhibitor (Figure 49), which indicated that its inhibition during an acute replication stress and after its release, did not affect the stability of nascent DNA.

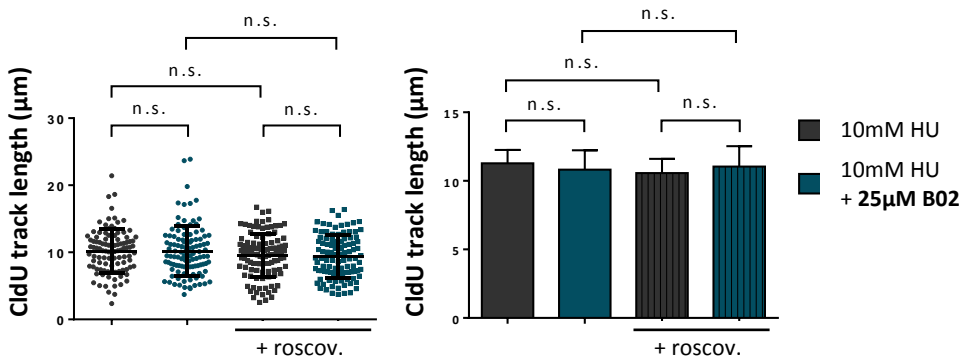


**Figure 49. RAD51 inhibition by B02 does not affect stability of nascent DNA after an acute HU treatment in hTERT-RPE cells.** DNA fibers for Figure 47 and Figure 48 were used to measure CldU track length (first analogue). At least 300 fibers of each condition were measured. One representative experiment out of three is shown (left panel, Mann-Whitney test, n.s.: non-statistically significant). Means and standard deviation (bars) of three experiments with (+roscov.) or without roscovitine are shown (right panel, paired *t*-test, n.s.: non-statistically significant).

### 3.8. RAD51 IS NECESSARY FOR AN EFFICIENT FORK RESTART AND PROGRESSION AFTER AN ACUTE REPLICATION STRESS IN hTERT-RPE CELLS

Due to the fact that RAD51 inhibition did not affect the number of restarted forks but its fork progression was impaired, we wanted to know if RAD51 was involved in fork progression after its restart or in replication restart efficiency after an acute replication stress. To elucidate this, a DNA fiber assay was performed, adding the B02 inhibitor at different times. In the first condition, we added B02 during the last 30 minutes of IdU labelling, to distinguish if RAD51

RESULTS

activity is important for the progression of restarted forks, since we already knew that replication forks needed 30 minutes to restart from an acute replication stress (data not shown). In the second condition, we added B02 during the last 15 minutes of HU treatment and during the hour of IdU labelling, in order to know if RAD51 activity is important for an efficient fork restart.

As shown in **Figure 50**, the addition of B02 during the last 30 minutes of IdU labelling decreased the IdU track length. But the addition of B02 during the last minutes of HU treatment and during the IdU labelling decreased the IdU track length even more, maybe due to the sum of both effects. The results showed that fork progression and effective fork restart were both affected due to RAD51 inhibition.

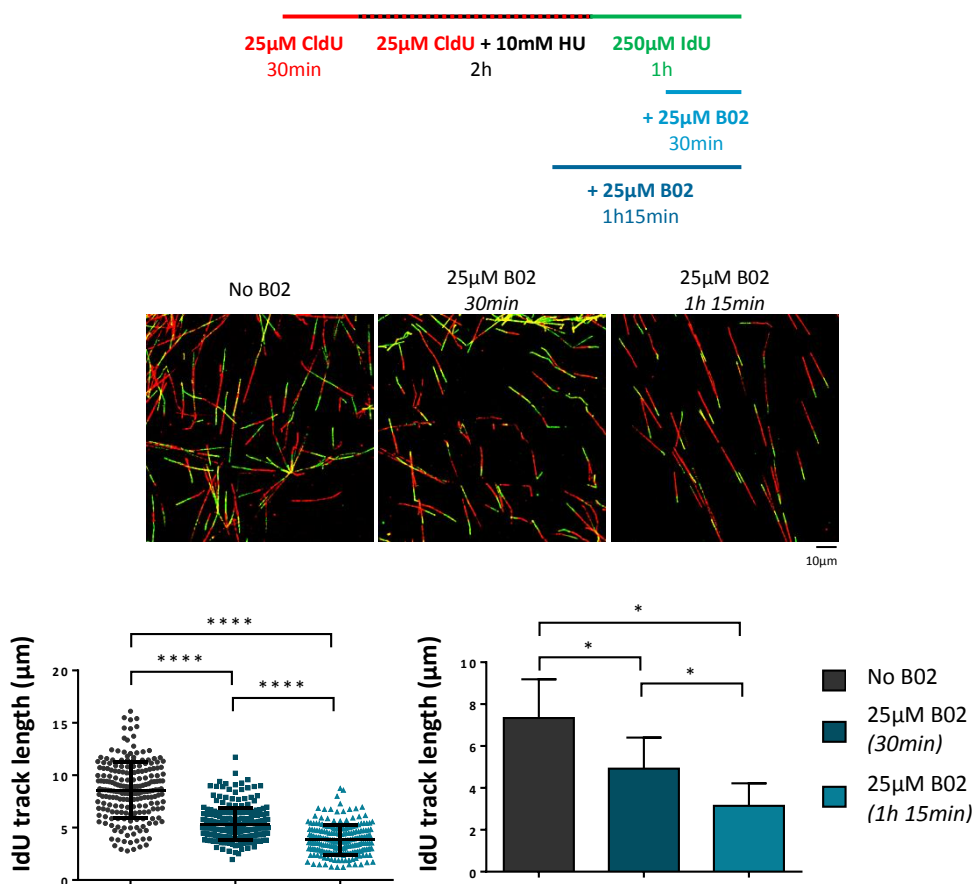


**Figure 50. RAD51 is necessary for efficient fork restart and progression after an acute HU treatment in hTERT-RPE cells.** Cells were labelled as indicated (upper panel), adding the B02 inhibitor where indicated. After labelling, cells were harvested and prepared for DNA fiber analysis. Representative images are

shown (middle panels). At least 200 fibers of each condition in each experiment were measured. One representative experiment out of three is shown (bottom-left panel, Mann-Whitney test, \*\*\*\* P value < 0.0001). Means and standard deviation (bars) of three experiments are shown (bottom-right panel, paired *t*-test, \* P value < 0.05).

### 3.9. RAD51 INHIBITION AFFECTS CELL CYCLE PROGRESSION IN hTERT-RPE CELLS

To analyse the effect of RAD51 inhibition in cell cycle progression, a cell cytometer analysis was performed. hTERT-RPE cells were pulse-labelled with BrdU, in order to label cells that were in S phase and analyse its progression through cell cycle.

On the one hand, to analyse the effect of B02 inhibitor in a control situation, cells were left untreated in nocodazole-containing media after BrdU pulse, with or without RAD51 inhibitor, for 12 hours. As shown in **Figure 51**, the entry into mitosis of population that initially was in S phase (BrdU-488-positive population) after a period of 12 hours was significantly affected when B02 was added in an unperturbed situation. It should be noted that arrival into G2-M phases (shown by black DNA profiles) was not affected.

On the other hand, to analyse the effect of B02 in a replication stress situation, cells were treated with 10mM of HU after BrdU pulse during 2 hours, and then released in nocodazole-containing media for 12 hours. During this release, B02 was added to the media at different times (using the same as in **Figure 50**): in one condition B02 was added 30 minutes after HU release, and in the other condition B02 was added during the last 15 minutes of HU treatment and maintained during the HU release. As shown in **Figure 52**, recovery of acute replication stress was impaired when B02 was added, regardless of when the inhibitor was added.

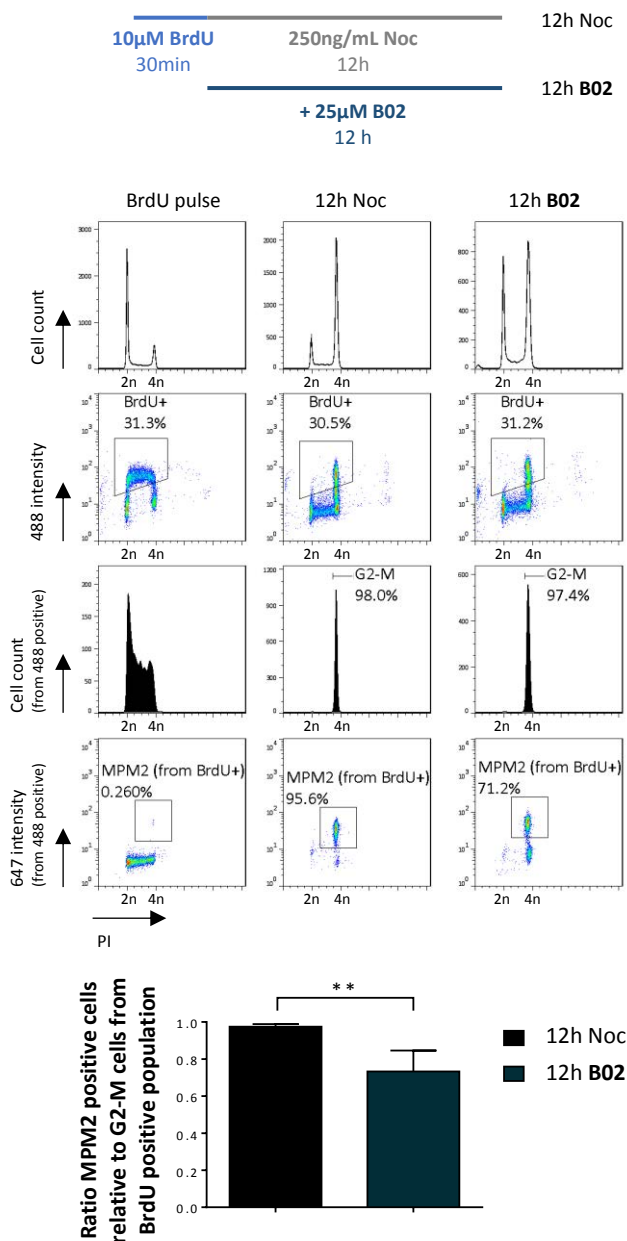


**Figure 51. RAD51 inhibition by B02 affects mitotic entry under unperturbed conditions in hTERT-RPE cells.** Cells were labelled with BrdU and then left untreated for 12 hours into nocodazole-containing fresh medium, without (12h Noc) or with RAD51 inhibitor (12h B02) (upper panel). Flow cytometry analysis of approximately 15000 cells was performed to analyse the S-phase population, initially labelled with BrdU analogue (BrdU-488 positive cells) after 12 hours. Cell cycle progression was analysed by measuring mitotic cells (MPM2-647 positive from BrdU-488-positive population) relative to cells into G2-M phases (obtained by black DNA profiles from BrdU-488-positive population). A representative experiment is shown (middle panel). Means and standard deviation (bars) of six experiments are shown (bottom panel, paired *t*-test, \*\* P value < 0.01).

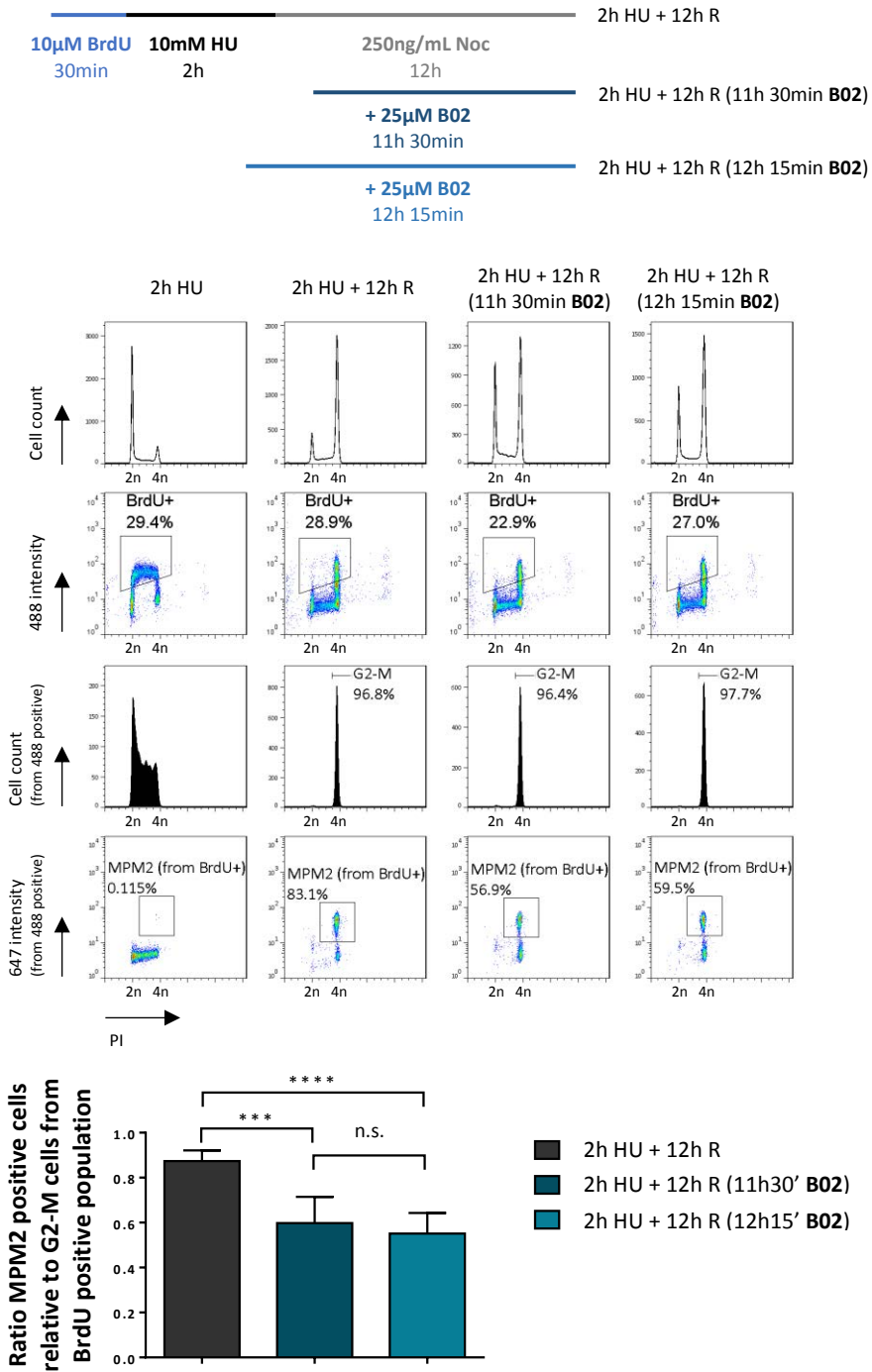
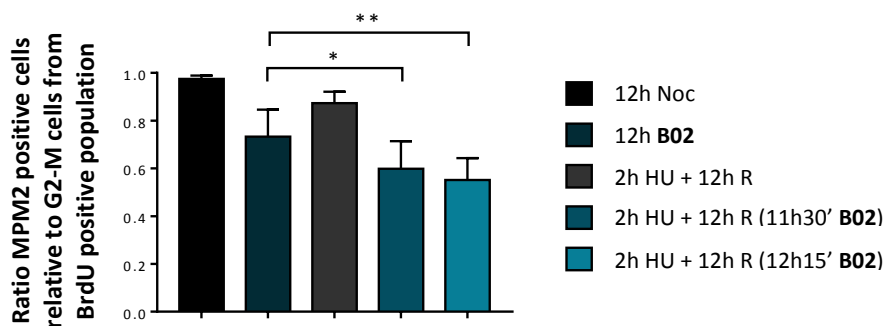


Figure 52. RAD51 inhibition by B02 affects mitotic entry after an acute HU treatment in hTERT-RPE cells. Cells were labelled with BrdU and then treated with 10mM HU during 2 hours. Then, cells were released (R) into nocodazole-containing fresh medium for 12 hours, adding RAD51 inhibitor, B02, at the

indicated times (upper panel). Flow cytometry analysis of approximately 15000 cells was performed to analyse the S-phase arrested (BrdU-488 positive) cells after 2 hours of HU treatment, and the recovery from this stress measuring, within the BrdU-positive population, the relation between mitotic cells relative to the cells in G2-M phases. A representative experiment is shown (middle panel). Means and standard deviation (bars) of six experiments are shown (bottom panel, paired *t*-test, n.s.: non-statistically significant, \*\*\* P value < 0.001, \*\*\*\* P value < 0.0001).

Remarkably, the impairment of mitotic entry when B02 was used increased significantly after an acute replication stress response compared to the control situation (**Figure 53**).



**Figure 53. RAD51 inhibition by B02 has a higher effect on mitotic entry after an acute HU treatment in hTERT-RPE cells.** Data from Figure 51 and Figure 52 were used to compare the B02 conditions in control situation and after an acute replication stress. Means and standard deviation (bars) of six experiments are shown (bottom panel, paired *t*-test, \* P value < 0.05, \*\* P value < 0.01).

### 3.10. RAD51 INHIBITION INCREASES GENOMIC INSTABILITY AFTER AN ACUTE REPLICATION STRESS IN hTERT-RPE CELLS

The previously results described the effect on mitotic entry when RAD51 was inhibited after an acute replication stress, so the next objective was analysed its contribution on genomic instability. To do so, the presence of 53BP1 foci was analysed in non-treated cells compared with HU-treated cells, with or without RAD51 inhibitor. In this case, an EdU pulse was performed before HU treatment in order to label S-phase cells to analyse them.

As shown in **Figure 54**, the analysis of cells positives both for EdU and 53BP1 foci relative to the population that was in S phase initially (EdU-labelled) increased significantly when RAD51 inhibitor was added during the release of 12 hours from an acute HU treatment.

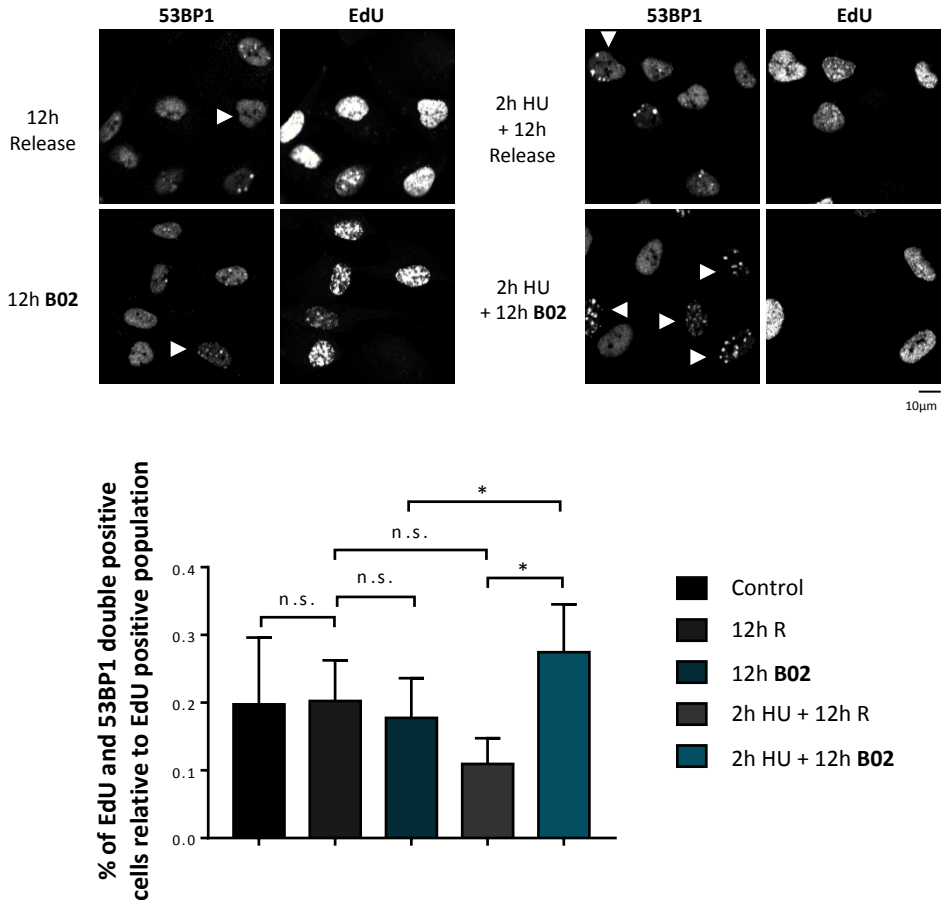


**Figure 54. RAD51 inhibition increases genomic instability after an acute HU treatment in hTERT-RPE cells.** Cells were pulse-labelled with EdU analogue during 30 minutes (Control). Then, cells were treated with 10mM HU for 2 hours or left untreated for 12 hours, without or with B02 inhibitor (12h R or 12h B02, respectively). After 2 hours, the HU-treated cells were released (R) into fresh medium for 12 hours, without or with B02 inhibitor (2h HU + 12h R or 2h HU + 12h B02, respectively). Finally, click reaction and 53BP1 immunofluorescence were performed. Representative images are shown (upper panels). At least 100 cells were counted for condition in each experiment. Means and standard deviation (bars) of three experiments in control and four experiments in other conditions are shown. The percentage of cells presenting both EdU and 53BP1 foci (more than six) relative to EdU positive cells is shown (bottom panel, paired *t*-test, n.s.: non-statistically significant, \* *P* value < 0.05, \*\* *P* value < 0.01).

### 3.11. RAD51 INHIBITION AFFECTS FORK PROGRESSION DURING A MILD REPLICATION STRESS IN hTERT-RPE CELLS

Due to the consequences that RAD51 inhibition had on acute replication stress response, we wondered if it would have an effect in a mild replication stress response, where replication forks could progress. To do so, a DNA fiber assay was performed upon 1mM HU treatment. hTERT-RPE cells were pulse labelled with the first analogue CldU, and then the second analogue IdU was added during the HU treatment. This mild replication stress allows IdU incorporation, but the labelling time is much longer to be able to analyse the IdU track length, since fork progression is undoubtedly impaired under these conditions.

As shown in **Figure 55**, IdU track length during a mild replication stress decreases when B02 is added. Thus, replication fork progression is impaired when RAD51 is inhibited during a mild replication stress caused by 1mM HU treatment.

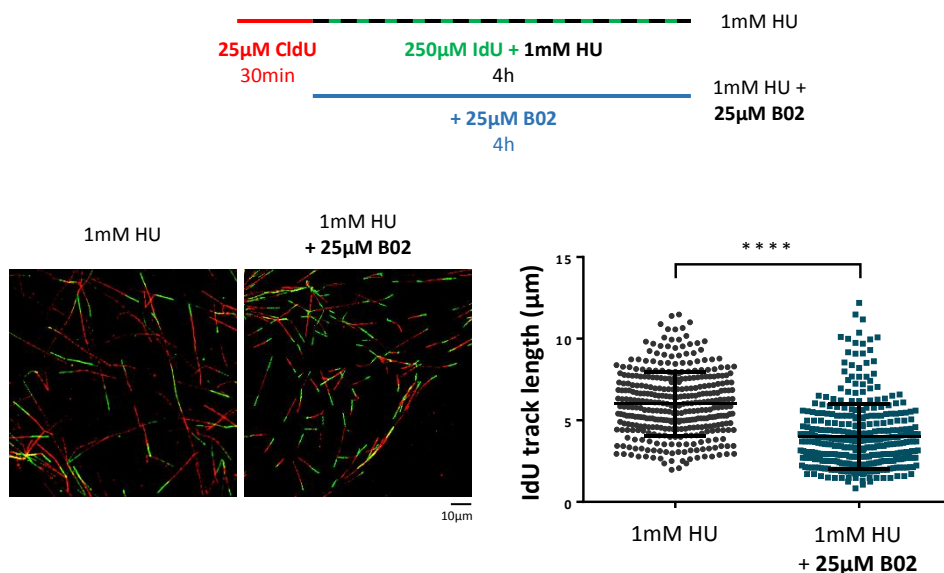


**Figure 55. RAD51 inhibition by B02 impairs fork progression during a 1mM HU treatment in hTERT-RPE cells.** Cells were labelled as indicated (upper panel), adding the B02 inhibitor during the second analogue and HU treatment. After labelling, cells were harvested and prepared for DNA fiber analysis. Representative images are shown (bottom-right panels). At least 300 fibers of each condition in each experiment were measured. One representative experiment out of two is shown (bottom-left panel, Mann-Whitney test, \*\*\*\* P value < 0.0001).

Since 1mM of HU treatment is a mild replication stress that slows the replication fork progression in a significant manner, we decided to use a 0.1mM of HU treatment, which we consider that represents a more physiological replication stress. First of all, we analysed if hTERT-RPE cells activated replication checkpoint (by analysing phosphorylated Chk1) upon a 0.1mM of HU treatment. As shown in **Figure 56**, Chk1 is not phosphorylated in Ser296 upon a replication stress induced by 0.1mM of HU, neither in synchronic nor asynchronous conditions, while 10mM of HU had already induced checkpoint activation in 1 hour of treatment, in both conditions. In this sense, we defined this 0.1mM HU treatment as a bearable replication stress, since no replication checkpoint response was observed.

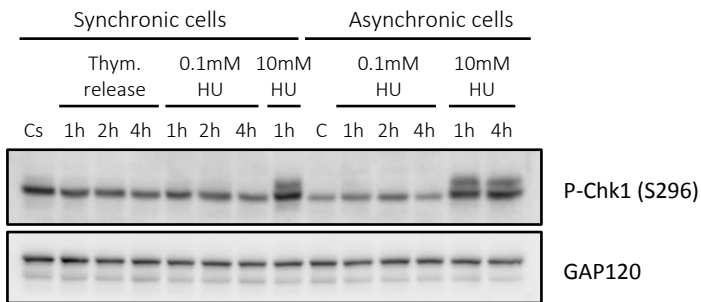


**Figure 56. Replication checkpoint is not activated upon a 0.1mM of HU treatment in hTERT-RPE cells.** Cells were synchronized in S-phase were indicated or left asynchronous. Then cells were treated with HU with the doses indicated during the indicated times or left untreated (S-phase synchronic cells (Cs) or asynchronous cells (C)). Whole cell extracts were prepared and analysed by WB with the indicated antibodies. GAP120 was used as a loading control.

After that, we analysed if under a bearable replication stress, RAD51 inhibition had an effect in fork progression in hTERT-RPE cells by performing a DNA fiber assay with 0.1mM of HU treatment. As shown in **Figure 57**, the addition of RAD51 inhibitor B02 impaired fork progression significantly also during a bearable replication stress, shown as a shorter IdU track length under those conditions.

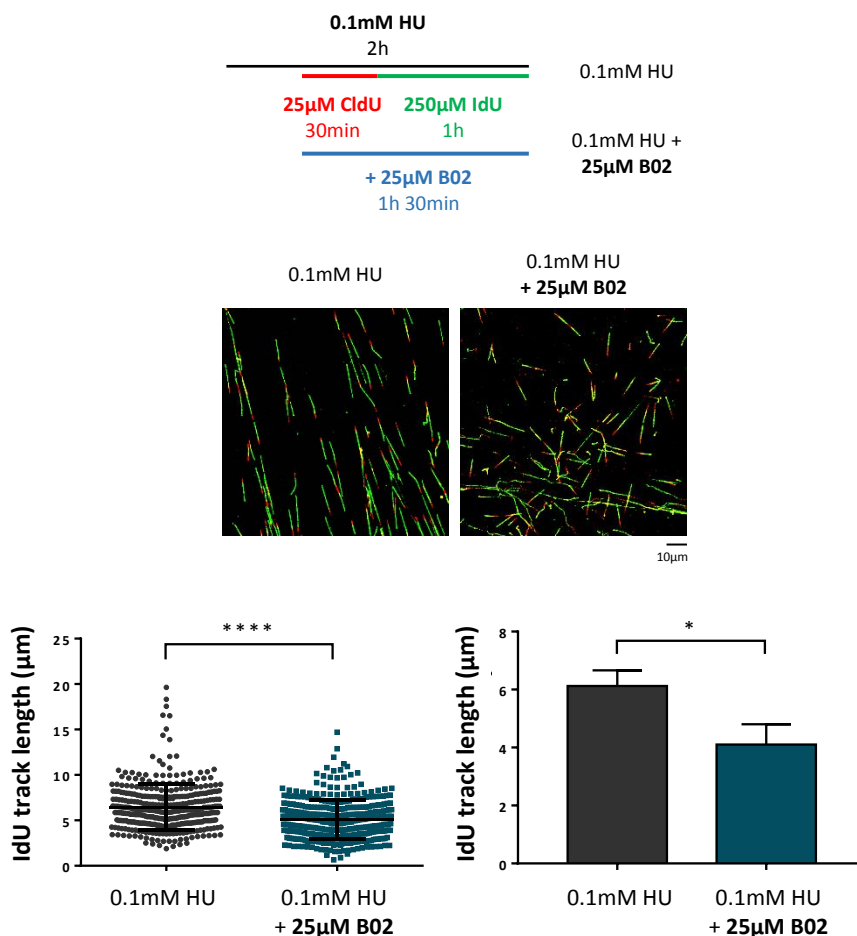


**Figure 57. RAD51 inhibition by B02 impairs fork progression during a 0.1mM HU treatment in hTERT-RPE cells.** Cells were labelled as indicated (upper panel). HU was added 30 minutes before labelling, since the dose of HU used is supposed to not have a strong effect on replication. The B02 inhibitor was added where is indicated. After labelling, cells were harvested and prepared for DNA fiber analysis. Representative images are shown (middle panels). At least 250 fibers of each condition in each experiment were measured. One representative experiment out of four is shown (bottom-left panel, Mann-Whitney test, \*\*\*\* P value < 0.0001). Means and standard deviation (bars) of four experiments are shown (bottom-right panel, paired t-test, \* P value < 0.05).

### 3.12. RAD51 INHIBITION AFFECTS FORK PROGRESSION IN COLORECTAL CANCER CELLS

Recent findings indicate that replication stress is a feature present in most cancers<sup>425,516</sup>. Since we had demonstrated that RAD51 had a role in fork progression during a mild and bearable replication stress, we wondered if RAD51 inhibition could influence fork progression in unperturbed conditions in cancer cells, with a basal increased replication stress.

To analyse this issue, we chose a colorectal cancer cell line as a model: HCT116 cell line with a functional p53 gene. First of all, the levels of phosphorylated Chk1 in this cell line were compared with hTERT-RPE cell line and we verified that this cell line presented an increased replication stress compared with the non-transformed cell line, hTERT-RPE, under unperturbed conditions (**Figure 58**).

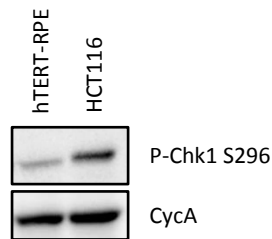
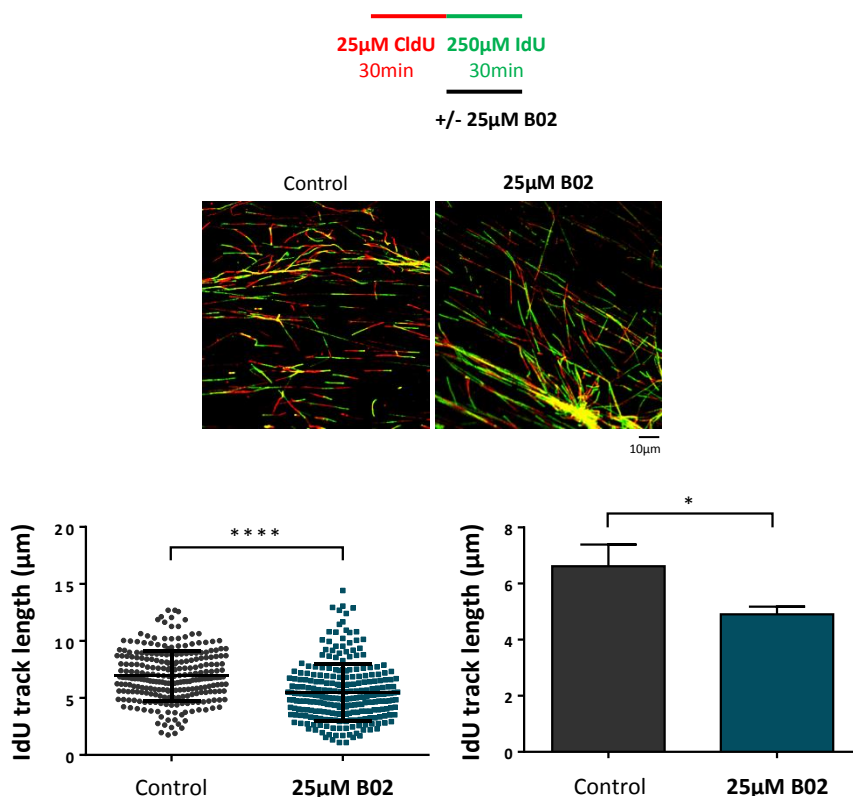


**Figure 58. HCT116 cell line presents an increased replication stress compared to non-transformed hTERT-RPE cell line.** HCT116 and hTERT-RPE cell lines were seeded and 48 hours later cells were harvested and analysed by WB with the indicated antibodies. Cyclin A (CycA) was used as a control of S-phase cells.

Since HCT116 cell line presented an increased replication stress, we studied the effect of RAD51 in replication fork progression in this tumour cell line under unperturbed conditions. To do so, DNA fiber assay was performed, by adding the inhibitor during the second analogue. The results showed that RAD51 inhibition decreased replication fork progression under normal conditions in HCT116 cell line (**Figure 59A**). On the other hand, the replication dynamics were not affected by the inhibition of RAD51 (**Figure 59B**).

A



B

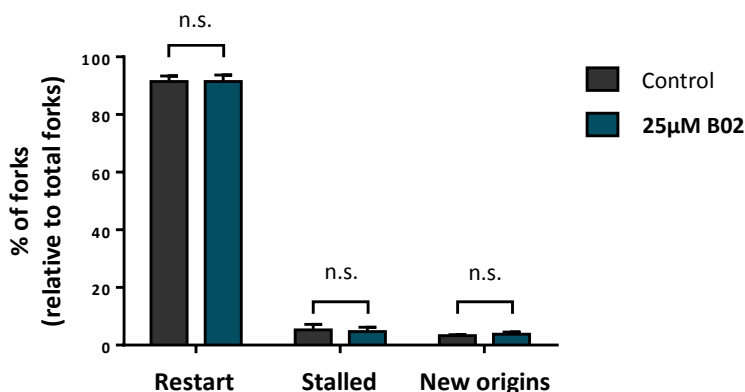


**Figure 59. RAD51 inhibition by B02 reduces fork progression in HCT116 cell line but does not affect replication dynamics under normal conditions.** (A) Cells were labelled as indicated (upper panel), adding the B02 inhibitor with the second analogue. After labelling, cells were harvested and prepared for DNA fiber analysis. Representative images are shown (middle panels). The IdU track length was measured. At least 250 fibers of each condition in each experiment were measured. One representative experiment out of three is shown (bottom-left panel, Mann-Whitney test, \*\*\*\* P value < 0.0001). Means and standard deviation (bars) of three experiments are shown (bottom-right panel, paired *t*-test, \* P value < 0.05). (B) DNA fibers were used to calculate the percentage of restart, stalled forks and new origin firing events relative to total forks. Around 1500 fibers from three independent experiments were counted in each condition. The average of those experiments is shown. Error bars represent standard deviation (paired *t*-test, n.s.: non-statistically significant).

Collectively, the data presented in this chapter support the idea that RAD51 is important to maintain replication fork progression after acute replication stress. Although the number of restarted forks is not impaired with RAD51 depletion or inhibition, RAD51 is necessary for efficient fork restart and progression after an acute replication stress in hTERT-RPE cells. In contrast to what is thought, in our conditions RAD51 depletion or inhibition does not cause fork degradation after an acute replication stress.

Moreover, RAD51 inhibition has an effect on cell cycle progression, which is more pronounced after acute HU treatment. In addition, after acute replication stress conditions, RAD51 inhibition increases genomic instability.

Interestingly, RAD51 is also relevant for replication fork progression during a mild or bearable replication stress, in HU-treated hTERT-RPE cells or untreated HCT116 cells, which presents a higher basal replication stress. The physiological relevance of RAD51 under those conditions has not been elucidated yet.



# **CHAPTER 4**

## **OZF IS ESSENTIAL TO MAINTAIN FORK PROGRESSION RATE UNDER REPLICATION STRESS CONDITIONS**

The results shown in the previous data section are comprised  
at Alba Llopis's PhD thesis.



## PREVIOUS DATA

## CLASPIN INTERACTS WITH OZF

Due to the role of Claspin on the activation of replication checkpoint<sup>304,308,573,574</sup> and to discover new Claspin-interacting proteins, a two-hybrid system was performed in the laboratory of Prof. Raimundo Freire, PhD. The experiment was done with a Claspin-encoding cDNA fragment that codifies for the last 347 amino acids of the protein. The results showed that 9 of 39 positive hits obtained were proteins with multiple zinc-finger (ZnF) domains of the Krüppel subfamily, which was discovered in 1991<sup>575</sup> (**Figure 60**).

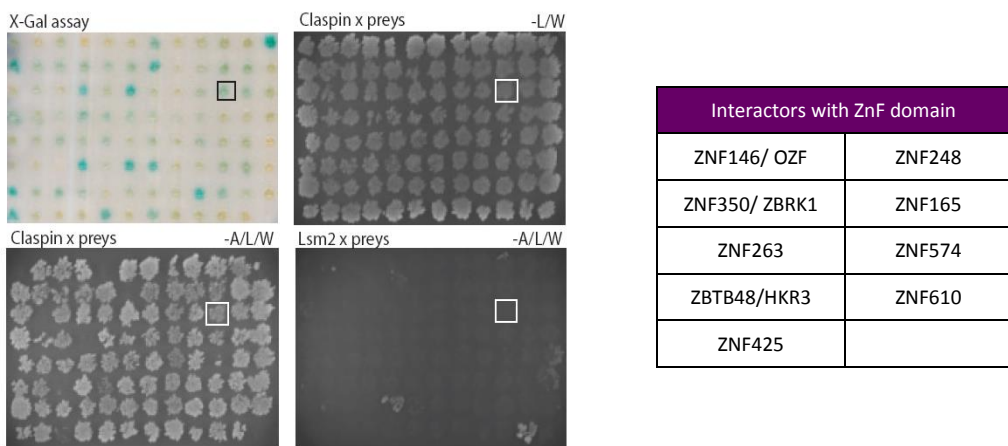


**Figure 60. Two-hybrid system to discover new Claspin-interacting proteins.** Detail of the results obtained from the analysis with the C-terminal domain of Claspin. *Experiments performed by Prof. Raimundo Freire, PhD.*

The main focus was set on ZNF146/OZF (Only zinc-finger) protein, since it was an only zinc finger protein that was described as a nuclear protein of 33kDa which binds to DNA. It consists of ten consecutive ZnF domains of C<sub>2</sub>H<sub>2</sub><sup>576,577</sup>. In contrast to the other members of the Krüppel subfamily, it does not contain a transactivation domain<sup>576,577</sup>. With an unknown function, it has been shown to interact with a telomeric protein, hRap1, and with the SUMO-1 conjugating enzyme UBC9<sup>578,579</sup>.

The interaction of Claspin and OZF was confirmed by co-immunoprecipitation of exogenously expressed proteins, and also of the endogenous ones (**Figure 61**). The interaction of OZF and Claspin was maintained even under replication stress conditions (**Figure 61C**).

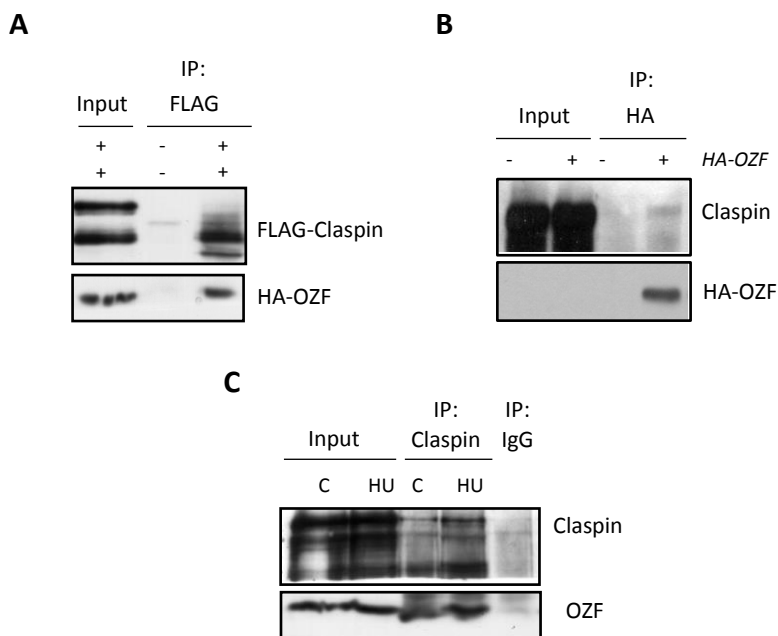


**Figure 61. OZF interacts with Claspin.** (A) HEK293T cells were transfected with both FLAG-Claspin and HA-OZF. FLAG-Claspin was immunoprecipitated from nuclear extracts and FLAG and HA were detected by WB. (B) HEK293T cells were transfected with HA-OZF, and it was immunoprecipitated from nuclear extracts. HA and endogenous Claspin were detected by WB. (C) HEK293T cells were enriched in S phase and treated with 1.5mM HU during 7 hours (HU) or left untreated (C), and immunoprecipitation of Claspin was performed. Endogenous Claspin and OZF were detected by WB. *Experiments performed by Alba Llopis, PhD.*

## OZF LOCALIZES AT ONGOING REPLICATION FORKS

In order to gain insight into the OZF role, their protein levels during cell cycle were analysed. For this purpose, different cell lines were used, and it was found that OZF protein levels were low during G<sub>0</sub> (cells in serum starvation), while their levels increased after the addition of serum during S phase, reaching its maximum in G<sub>2</sub>/M phases (results not shown).

It was already known that OZF is a nuclear protein, so cell fractionation experiments were performed to know if it was bound or not to chromatin. The results showed that OZF was a chromatin-bound protein, as well as Claspin, which was according with literature<sup>580-584</sup> (**Figure**

**62A).** It was already known that Claspin is found in replication forks and that it interacts with different components of the replisome<sup>580-582</sup>. To analyse the presence of OZF in replication forks, the iPOND technique was used. This technique allows the isolation of protein complexes crosslinked to EdU thymidine analogue-containing fragments that are located at active replication forks<sup>550-552</sup>. The results indicated that OZF interacted with nascent DNA together with Claspin or PCNA, demonstrating the presence of OZF in ongoing replication forks (**Figure 62B**).

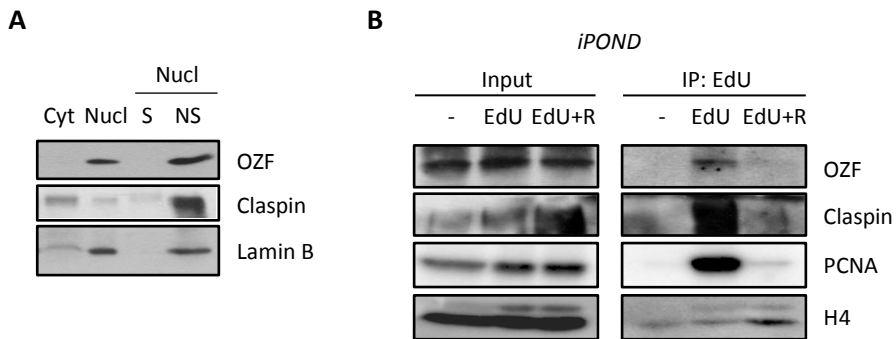
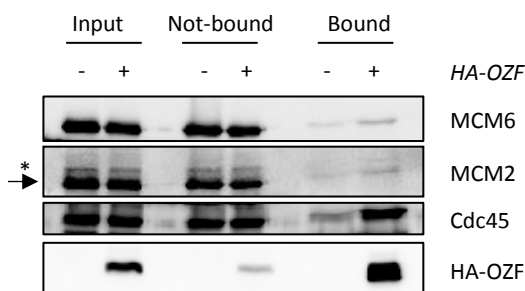


**Figure 62. OZF and Claspin colocalize in the replication forks.** (A) Cell fractionation from HEK293T cells. The levels of OZF, Claspin and LaminB were analysed by WB. Cyt: cytoplasm; Nucl: nuclei; S: soluble; NS: non-soluble. *Experiment performed by Alba Llopis.* (B) hTERT-RPE cell lines were treated, where indicated, with EdU for 15 minutes. EdU was immunoprecipitated and the associated proteins were analysed by WB. *Experiment performed by Amaia Ercilla, PhD.*

## RESULTS

### 4.1. OZF INTERACTS WITH CDC45 AND MCM

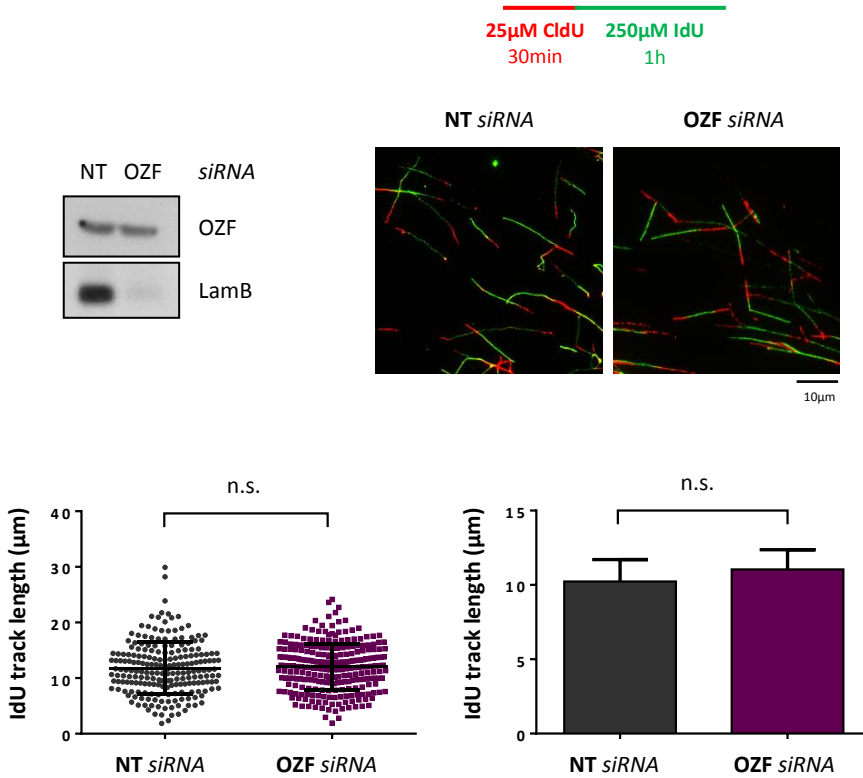
Since we already knew that OZF was located in replication forks, its interaction with Claspin, and the interaction of Claspin with diverse replisome components, we investigated if OZF could interact with some replisome components by performing chromatin-bound OZF immunoprecipitation. The results showed that OZF interacted with Cdc45, MCM6 and MCM2, all components of CMG complex (**Figure 63**). Co-immunoprecipitation between OZF with Cdc45, a part of the MCMs, indicates that OZF interacts with activated origins, not just licensed.



**Figure 63. OZF interacts with components of CMG complex.** HEK293T cells were transfected with HA-OZF. HA-OZF was immunoprecipitated from nuclear extracts and HA and different replisome components were detected by WB. The arrow indicates the specific band corresponding to MCM2. The asterisk indicates the band corresponding to MCM6.

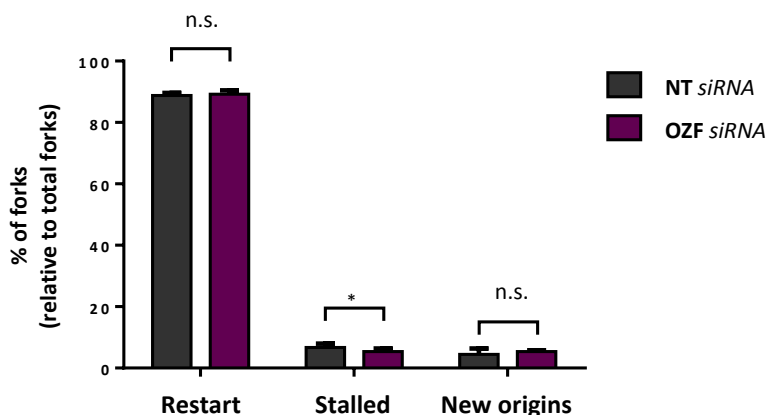
### 4.2. OZF IS NOT ESSENTIAL FOR REPLICATION IN hTERT-RPE CELLS

Due to OZF presence in replication forks and its interaction with some replisome components and the role of Claspin in a normal S-phase progression, we studied the effect of OZF in fork progression in non-transformed human cells under unperturbed conditions. To do so, hTERT-RPE cells were depleted of OZF and, approximately 48 hours after siRNA transfection, DNA fiber assay was performed. The results showed that OZF depletion had no effect in replication fork progression under normal conditions since IdU (second analogue) track length was maintained (**Figure 64**).



**Figure 64. OZF depletion does not affect replication fork progression under unperturbed conditions in hTERT-RPE cells.** Cells were transfected with the indicated siRNA (NT: non-target) and 48 hours later cells were harvested for WB analysis with OZF. Actin was used as a loading control (middle-left panel). hTERT-RPE transfected cells were labelled as indicated (upper panel). After labelling, cells were harvested and prepared for DNA fiber analysis. Representative images are shown (middle-right panels). The IdU track length was measured. At least 250 fibers of each condition in each experiment were measured. One representative experiment out of three is shown (bottom-left panel, Mann-Whitney test, n.s.: non-statistically significant). Means and standard deviation (bars) of three experiments are shown (bottom-right panel, paired *t*-test, n.s.: non-statistically significant).

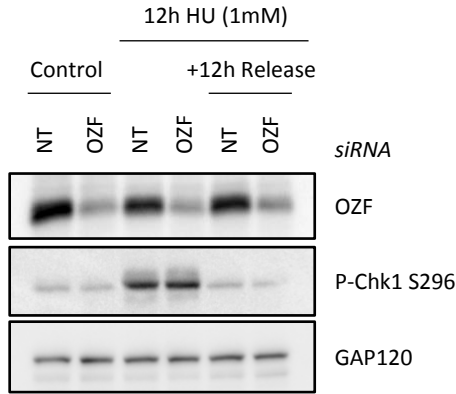
It has been recently proposed that Claspin has a function in DNA replication origin firing via its interaction with Cdc7<sup>187,585</sup>, so replication dynamics were analysed after OZF depletion under unperturbed conditions to know if this Claspin-interacting protein may participate on this role. No differences were found between non-target and OZF-depleted hTERT-RPE cells in new origin firing events and the number of restarted forks (**Figure 65**).



**Figure 65. OZF depletion does not affect replication dynamics under normal conditions in hTERT-RPE cells.** DNA fibers for Figure 64 were used to measure the percentage of restart, stalled forks and new origin firing events relative to total forks. Around 1500 fibers from three independent experiments were counted in each condition. The average of those experiments is shown. Error bars represent standard deviation (paired *t*-test, n.s.: non-statistically significant, \* P value < 0.05).

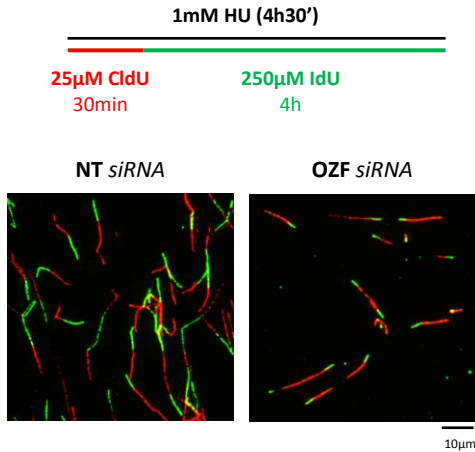
#### 4.3. OZF DEPLETION REDUCES FORK PROGRESSION UNDER MILD REPLICATION STRESS CONDITIONS IN hTERT-RPE CELLS

After analysing the effect of OZF depletion in unperturbed conditions, the role of OZF under mild replication stress conditions, which allows replication fork progression, was analysed. For this reason, 1mM of HU was used. Due to the role of Claspin in the activation of Chk1 by ATR<sup>586</sup>, we first analysed whether OZF was involved in this process. The WB analysis shows that OZF depletion did not prevent Chk1 phosphorylation after 12 hours of HU treatment (**Figure 66**). It should be noted that 12 hours after HU release, the phosphorylated Chk1 decreased until control levels in both cases, indicating a recovery from this mild replication stress. The results showed that OZF did not have a role in checkpoint activation upon 1mM HU treatment.



**Figure 66. OZF is not essential for checkpoint activation upon 1mM HU treatment in hTERT-RPE cells.** Cells were transfected with the indicated siRNA (NT: non-target) and 48h later cells were treated with 1mM HU or left untreated (Control) for 12 hours, and then released into fresh medium for 12 hours. Whole cell extracts were prepared and analysed by WB with the indicated antibodies. GAP120 was used as a loading control.

To further analyse if OZF had a role in fork progression under replication stress conditions, DNA fiber assay was performed upon 1mM HU treatment. As shown in **Figure 67**, OZF depletion resulted in a significant reduction in replication fork progression during this mild replication stress, shown by a shorter IdU track length.



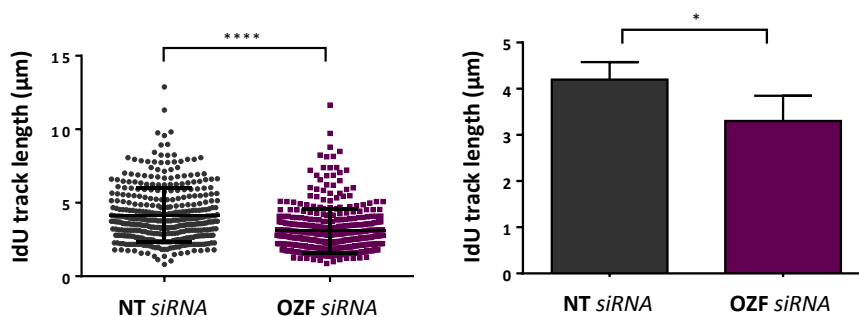


**Figure 67. OZF depletion reduces fork progression during 1mM HU treatment in hTERT-RPE cells.** Cells were transfected with the indicated siRNA (NT: non-target) and 48 hours later cells were treated and labelled as indicated (upper panel). After labelling, cells were harvested and prepared for DNA fiber analysis. Representative images are shown (middle panels). The IdU track length was measured. At least 250 fibers of each experiment were measured. One representative experiment out of three is shown (bottom-left panel, Mann-Whitney test, \*\*\*\* P value < 0.0001). Means and standard deviation (bars) of three experiments are shown (bottom-right panel, paired *t*-test, \* P value < 0.05). The siRNA transfection control is shown in Figure 66.

Under these conditions, replication dynamics were analysed. The results indicated that OZF depletion, although it had an effect in fork progression, did not alter replication dynamics upon 1mM HU treatment (**Figure 68**).

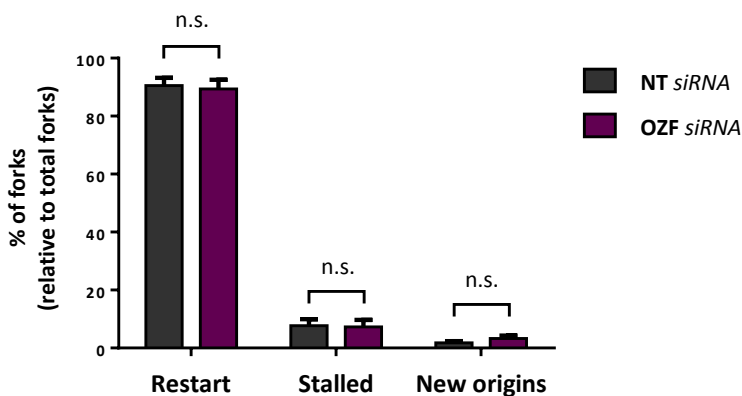


**Figure 68. OZF depletion has no effect in replication dynamics during 1mM HU treatment in hTERT-RPE cells.** DNA fibers for Figure 67 were used to measure the percentage of restart, stalled forks and new origin firing events relative to total forks. Around 1500 fibers from three independent experiments were counted in each condition. The average of those experiments is shown. Error bars represent standard deviation (paired *t*-test, n.s.: non-statistically significant).

Since 1mM of HU treatment is a mild replication stress that slows the replication fork progression in a significant manner, we did the DNA fiber assay with 0.1mM of HU treatment, which represents a bearable replication stress that does not activate replication checkpoint (**Figure 56**). As shown in **Figure 69**, OZF depletion resulted in a significant reduction in replication fork progression upon a 0.1mM HU treatment, shown as a shorter IdU track length.

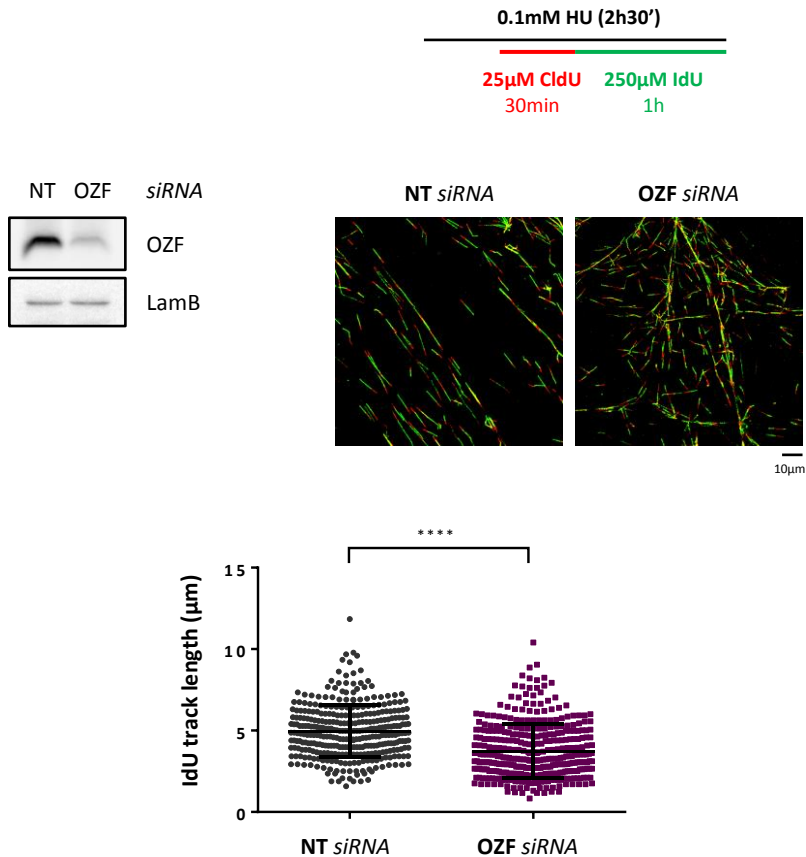


**Figure 69. OZF depletion reduces fork progression during 0.1mM HU treatment in hTERT-RPE cells.** Cells were transfected with the indicated siRNA (NT: non-target) and 48 hours later cells were harvested for WB analysis with the indicated antibodies. Lamin B (LamB) was used as a loading control (middle-left panel). hTERT-RPE transfected cells were labelled as indicated (upper panel). After labelling, cells were harvested and prepared for DNA fiber analysis. Representative images are shown (middle-right panels). The IdU track length was measured. At least 300 fibers from one experiment were measured (bottom-left panel, Mann-Whitney test, \*\*\*\* P value < 0.0001).

#### 4.4. OZF DEPLETION DOES NOT INCREASE GENOMIC INSTABILITY IN hTERT-RPE CELLS

The previous data showing the effect of OZF depletion in replication fork progression upon 1mM HU treatment made us wonder if OZF silencing would affect genomic stability. First, we studied the mitotic entry after 12 hours of release from 1mM HU treatment. S phase cells were labelled with BrdU analogue and then cells were followed through cell cycle after HU release.

As it was seen in **Figure 70**, 1mM of HU treatment slowed replication noticeably, since BrdU positive cells remained in S phase after 12 hours of 1mM HU treatment, and remained there even after 72 hours (data not shown). After this mild replication stress, cells seemed to recover replication, to finish S phase and to arrive into G2-M phases due to the presence of nocodazole (as it was shown by DNA profiles). The entry in mitosis, shown as MPM2 positive cells, did not seem to be affected by OZF depletion (even there were some more mitotic cells under those conditions).

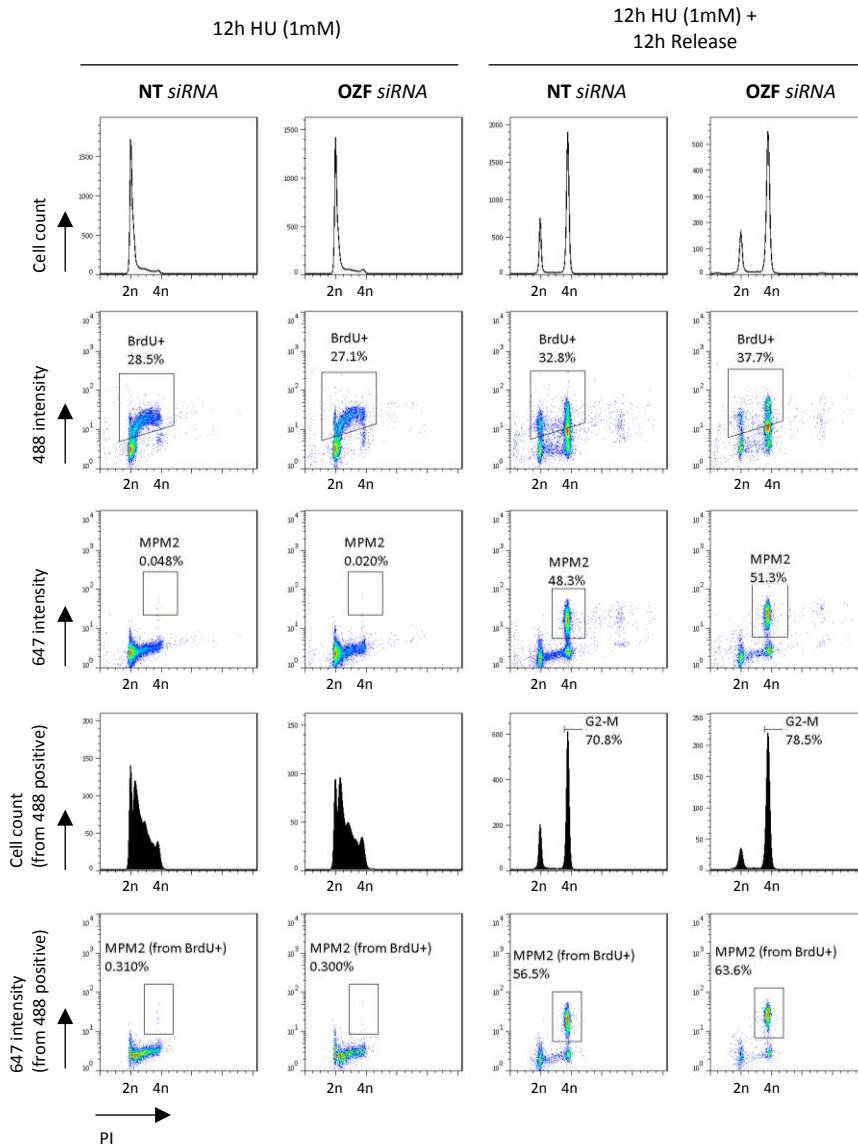


**Figure 70. OZF depletion does not affect mitotic entry after 12 hours release from 1mM HU treatment in hTERT-RPE cells.** Cells were transfected with the indicated siRNA (NT: non-target) and 48 hours later cells were labelled with BrdU and then treated with 1mM HU for 12 hours or left untreated (Control), and then HU-treated cells were released into nocodazole-containing fresh medium for 12 hours. Flow cytometry analysis of more than 10000 cells was performed to analyse the S-phase arrested (BrdU-488 positive) cells after 12 hours of HU treatment, and the recovery from this stress measuring mitotic (MPM2-647 positive) cells from BrdU positive population. The experiment shown was performed once, and the KD control is shown in Figure 66.

Due to the fact that no noteworthy effect was seen in mitotic entry, we wondered if there was some effect in DNA damage that could stem from the slowing of replication fork progression. To analyse this, we performed an immunofluorescence of 53BP1 and  $\gamma$ H2AX, both markers of DNA damage. The results suggested that no substantial differences in the percentage of cells presenting both 53BP1 and  $\gamma$ H2AX foci appeared when OZF was depleted after a mild replication stress (**Figure 71**).

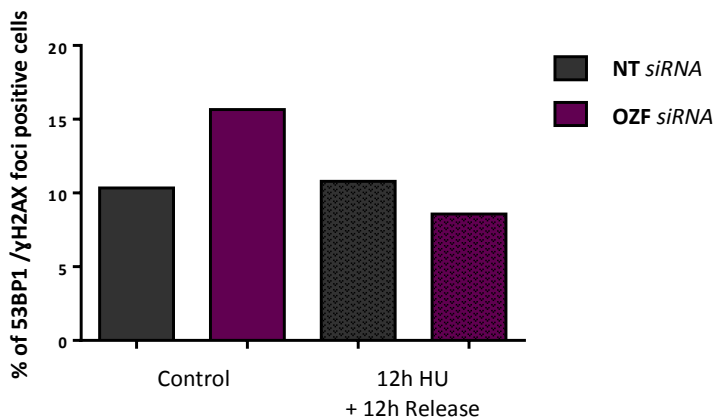


**Figure 71. OZF depletion does not have an effect in DNA damage after 1mM HU treatment in hTERT-RPE cells.** Cells were transfected with the indicated siRNA (NT: non-target) and 48 hours later cells were treated with 1mM HU or left untreated (Control) for 12 hours, and then HU-treated cells were released into fresh medium for 12 hours. Finally, 53BP1 and  $\gamma$ -H2AX immunofluorescences were performed. At least 200 cells were counted for each condition. The percentage of cells presenting more than six 53BP1 and more than ten  $\gamma$ -H2AX foci is shown. The experiment shown was performed once, and the KD control is shown in Figure 66.

In order to evaluate the long-term viability after treatment, colony formation was analysed under those condition. OZF depletion did not seem to affect colony formation capacity, neither in control conditions (these results were already obtained in our lab) nor after 1mM HU treatment (**Figure 72**).

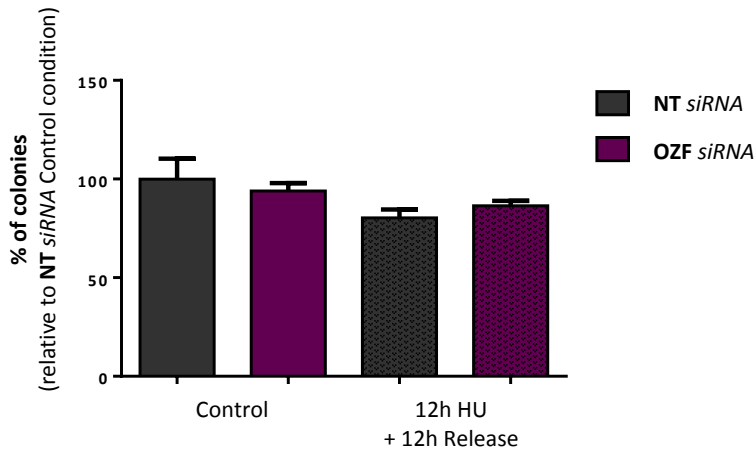


**Figure 72. OZF depletion does not have an effect in colony formation after 1mM HU treatment in hTERT-RPE cells.** Cells were transfected with the indicated siRNA (NT: non-target) and 48 hours later cells were treated with 1mM HU for 12 hours or left untreated (Control), and then released into fresh medium for 12 hours. Finally, cells were plated diluted (200 cells per well on 6-well plate, in triplicate) for colony formation assay. Colonies were harvested and stained 7 days later. The average percentage of colonies of three plates was calculated in each case, and the graph shows the percentage of colonies relative to NT siRNA control situation. The experiment shown was performed once, and the KD control is shown in Figure 66. *Experiment performed by Fernando Unzueta, PhD student.*

The analyses of genomic stability by cell cycle analysis, the presence of DNA damage or long-term viability, indicated that no effect was obtained from OZF depletion after HU treatment, despite its effect in fork progression. It has to be noted that all the analyses were performed in one specific time after release (12h), which does not exclude a possible delay in cell cycle progression.

#### 4.5. OZF DEPLETION REDUCES FORK PROGRESSION IN COLORECTAL CANCER CELLS

Previous studies of OZF described its overexpression in pancreatic cancer<sup>587</sup> and in more than 80% of colorectal cancer<sup>588</sup>. In this last case OZF overexpression was already observed in low-grade adenomas, indicating that occurs in an primary stage of tumour progression<sup>588</sup>. Moreover, OZF is a c-Myc oncogene-target gene<sup>589</sup>.

## RESULTS

Since it was already described that DNA replication stress is a feature present in most cancers<sup>425,516</sup>, we wondered if OZF depletion could have an effect on colorectal cancer cells.

To study this matter, we chose a colorectal cancer cell line, HCT116, as a model, which has a functional p53 gene. First of all, the levels of OZF protein were analysed in this cell line compared with hTERT-RPE cell line, and it was verified that this cell line presented OZF overexpression (**Figure 73**).

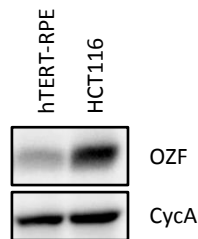


**Figure 73. OZF is overexpressed in HCT116 cell line compared to non-transformed hTERT-RPE cell line.** HCT116 and hTERT-RPE cell lines were seeded and 48 hours later cells were harvested and analysed by WB with the indicated antibodies. Cyclin A (CycA) was used as a control of S-phase cells.

Since HCT116 cell line presented an increased basal replication stress (chapter 3, **Figure 58**), we studied the effect of OZF in fork progression in this tumour cell line under unperturbed conditions. To do so, HCT116 cells were depleted of OZF and, approximately 48 hours after siRNA transfection, DNA fiber assay was performed. The results showed that OZF depletion decreased replication fork progression under normal conditions, shown as a shorter IdU track length (**Figure 74A**), but did not affect replication dynamics (**Figure 74B**).

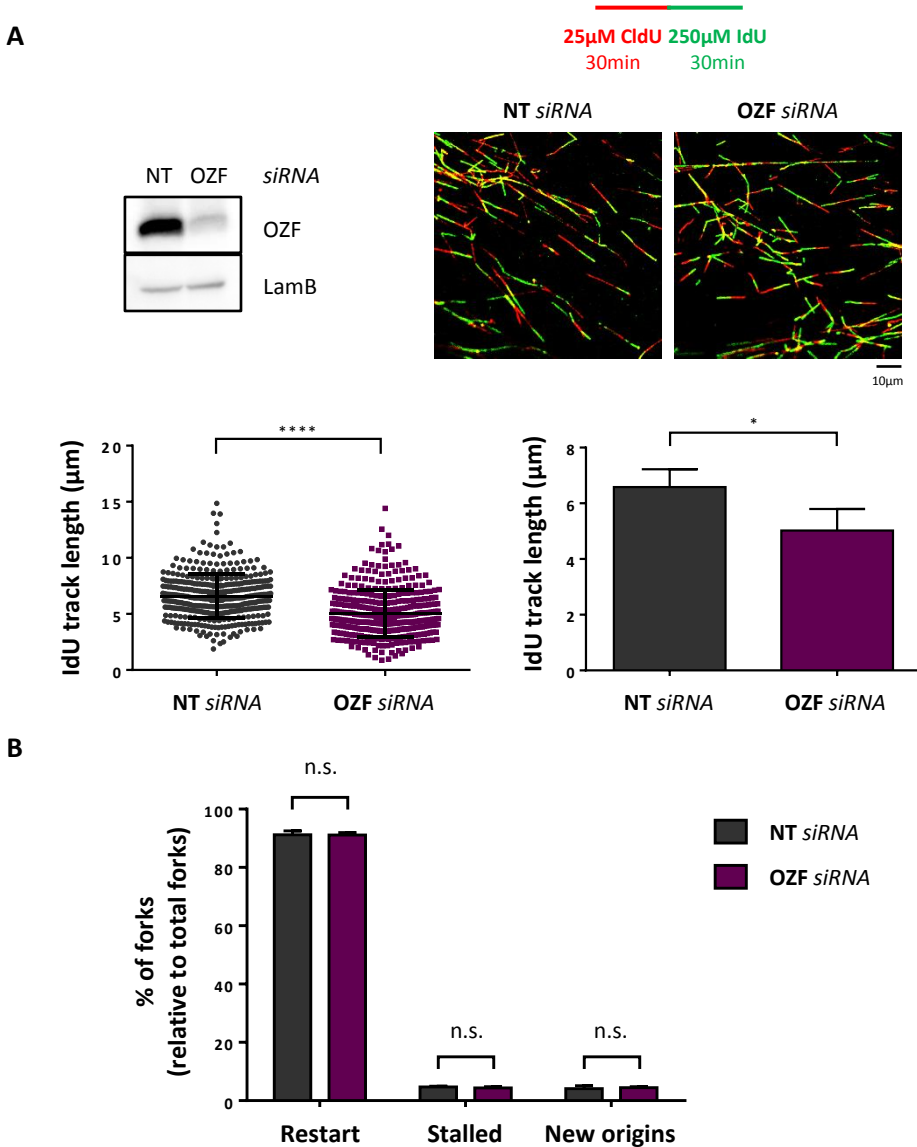


**Figure 74. OZF depletion reduces fork progression in HCT116 cell line but does not affect replication dynamics under normal conditions.** (A) Cells were transfected with the indicated siRNA (NT: non-target) and 48 hours later cells were harvested for WB analysis with OZF. Lamin B (LamB) was used as a loading control (middle-left panel). HCT116 transfected cells were labelled as indicated (upper panel). After labelling, cells were harvested and prepared for DNA fiber analysis. Representative images are shown (middle-right panel). The IdU track length was measured. At least 250 fibers of each condition in each experiment were measured. One representative experiment out of three is shown (bottom-left panel, Mann-Whitney test, \*\*\*\* P value < 0.0001). Means and standard deviation (bars) of three experiments are shown (bottom-right panel, paired *t*-test, \* P value < 0.05). (B) DNA fibers were used to measure the percentage of restart, stalled forks and new origin firing events relative to total forks. Around 1500 fibers from three independent experiments were counted in each condition. The average of those experiments is shown. Error bars represent standard deviation (paired *t*-test, n.s.: non-statistically significant).

## *RESULTS*

Taken together, the results presented in this chapter demonstrate that OZF, a novel Claspin-interacting protein, is found on replication forks and interacts with components of CMG complex, although its depletion does not affect DNA replication under unperturbed conditions in hTERT-RPE cells. Interestingly, OZF depletion impairs replication fork progression in cells under replication stress, such as HU-treated hTERT-RPE cells or HCT116 cells with higher basal replication stress, although its physiological relevance has not been elucidated yet.

## **DISCUSSION**



DNA replication is an essential process that has to be properly and accurately completed only once per cell cycle to avoid loss of information and the acquisition of genomic instability, a hallmark of cancer<sup>4,5</sup>. Several endogenous and exogenous factors challenge DNA duplication, inducing replication stress. In this sense, cells have developed mechanisms or checkpoints to monitor the fidelity of copying DNA. In fact, kinases involved in DNA replication checkpoint are active in a non-perturbed S phase in a basal level<sup>282</sup>, and their depletion results in embryonic lethality<sup>262,263</sup>, which indicates their relevance in preserving genome integrity.

In response to replication stress, replication checkpoint is activated to maintain fork stability and to coordinate the reversible cell cycle arrest and DNA repair with the resumption of DNA replication<sup>222,225,257</sup>. The role of this checkpoint is the prevention of cell cycle progression until the stress is overcome. If the arrest persists for a long period of time, replication forks collapse, causing DSBs. In the cases of persistent damage, cells withdraw from cell cycle by apoptosis or senescence to avoid cell division with damaged or unreplacated DNA<sup>219,221,223-225,425</sup>.

Replication checkpoint mechanisms are essential to maintain genomic integrity and, thus, to avoid cancer development<sup>9</sup>. Hence, DNA damage response has been well studied in transformed cells, and replication stress response has attracted much attention in the recent years, especially in transformed cells. For this reason, during the last years, our group has focused in defining and characterizing the replication stress response pathways that contribute to preserve genomic integrity of non-transformed human cells.

During this thesis, and the previous ones of the group, we have focused on studying the response of non-transformed human cells after an acute (2h) or a prolonged (14h) replication inhibition induced by 10mM HU. After an acute replication stress, cells are able to restart and resume cell cycle progression without the acquisition of genomic instability, while after a prolonged replication stress, cells have lost the capacity to recover DNA replication<sup>536</sup>. With these premises, we have tried to define the mechanisms involved in such processes.

## **I. LACK OF APC/C<sup>Cdh1</sup> ACTIVATION IN S PHASE AFTER A SEVERE REPLICATION STRESS ALLOWS RESUMPTION OF DNA SYNTHESIS IN TUMOUR CELLS**

Previous data from our group demonstrated that, after a prolonged HU treatment, non-transformed human cells are not able to recover replication due to activation of APC/C<sup>Cdh1</sup> in S phase, which inhibits origin firing<sup>536</sup>.

It is well known that oncogene expression induces replication stress. Replication stress and DNA damage responses are activated to act as a tumorigenic barrier<sup>516,590</sup>. The data presented in chapter 1 from this thesis indicates that APC/C<sup>Cdh1</sup> is a new element of this barrier. Consistently, APC/C presents heterozygous mutations in human colon cancer cells<sup>591</sup>.

In this sense, our results indicate that tumour cells are predominantly deficient in APC/C<sup>Cdh1</sup> activation in S phase in response to a prolonged HU treatment. Moreover, these tumour cell lines are predominantly able to resume replication after a prolonged replication stress<sup>536</sup>. Taking the HCT116 colorectal cancer cell line as a model, the results indicate that HCT116 cells resume replication after a prolonged HU treatment and these cells are able to divide in spite of the presence of DNA damage, as observed by the presence of 53BP1 foci in the next G1 phase, and the presence of genomic instability, as observed by the presence of cells with micronuclei.

The kinases essential for the induction of origin firing in S phase are Cdk2/A-type cyclin and Cdc7/Dbf4<sup>158</sup>, the regulatory subunits of which are substrates of APC/C<sup>Cdh1</sup><sup>83,84,363</sup>. Since APC/C<sup>Cdh1</sup> is not activated in tumour cells, a possible explanation for their recovery was the activation of new origins. We corroborated this hypothesis in HCT116 cells by DNA fiber assay, where we showed that after a prolonged HU treatment the activation of new origins was produced. Related with this result, a recent study showed that a release from an aphidicolin-induced replication stress results in a marked increase in the number of initiation sites detected by nascent strand abundance sequencing<sup>592</sup>.

A similar observation was shown in U2OS cells, in which most stalled forks are inactivated after a long HU-mediated replication stress and replication is resumed by new origin firing. Under these conditions, replication forks of U2OS cells are collapsed and DSBs need to be repaired by HR to prevent genomic instability<sup>370</sup>. Under our conditions, we do not know if DSBs are present due to fork collapse in HCT116 cells, although this would explain the genomic

instability that these cells acquire after a prolonged HU treatment. Moreover, in the case that stalled forks were processed into DSBs, a recent study suggests the role of APC/C<sup>Cdh1</sup> in choosing the repair pathways. The inactivity of APC/C<sup>Cdh1</sup> promotes the DSBs repairing by NHEJ, an error-prone mechanism, since the deubiquitinating enzyme USP1, which removes the poly-ubiquitin chains on histones that promotes BRCA1 recruitment, is not degraded by APC/C<sup>Cdh1</sup> 410.

We next studied the contribution of APC/C<sup>Cdh1</sup> activation in genomic stability. Since Emi1 depletion has been reported to be enough to induce APC/C<sup>Cdh1</sup> activation<sup>76,548,549</sup>, we artificially induced APC/C<sup>Cdh1</sup> activation during S phase by depleting Emi1 in HCT116 cells. It has to be noted that Emi1 depletion promotes rereplication<sup>548</sup>, which undergoes to DNA damage<sup>549,593</sup>. To prevent rereplication, Emi1 was depleted in S-phase arrested cells, first by a thymidine block after siRNA transfection and then by HU treatment. Nevertheless, the presence of cells with a DNA content higher than 4n observed in the flow cytometry analysis (**Figure 24**) suggests that, after HU release, Emi1-depleted cells that maintain the ability to resume replication are actually able to rereplicate. Despite this pool in the Emi1-depleted population, the rest of the cells are arrested in S phase due to APC/C<sup>Cdh1</sup> activation upon a prolonged HU treatment. Moreover, induced APC/C<sup>Cdh1</sup> activation in HCT116 cells by Emi1 depletion decreases the number of cells that divide with the presence of DNA damage or genomic instability, indicating its contribution to safeguard genomic stability.

Finally, the capacity to proliferate was analysed by colony formation assay. In this sense, Emi1 depletion promotes by itself a decrease in the number of colonies, similar to the one induced by prolonged HU treatment in HCT116 cells. But, if we add to Emi1-depleted cells a prolonged replication stress, an additive effect was observed, inducing a significant decrease in the proliferation.

Collectively, our results suggest that the activation of APC/C<sup>Cdh1</sup> after a prolonged replication stress is a mechanism activated in non-transformed human cells that contributes to safeguard genomic stability, although it compromises the ability to resume replication. Transformed human cells have incorporated mechanisms to avoid APC/C<sup>Cdh1</sup> activation upon a prolonged HU treatment and, consequently, tumour cells are able to recover replication by activating

## DISCUSSION

new origins and resume cell cycle progression, despite the acquisition of more genomic instability.

Tumour cells might have developed several mechanisms to avoid APC/C<sup>Cdh1</sup> activation. On the one hand, overexpression of its regulators, such as Emi1, which is frequently overexpressed in malignant tumours<sup>594</sup>. Moreover, it has been recently demonstrated that Emi1 overexpression promotes chromosome instability and the formation of multiple solid tumours *in vivo*, which are more proliferative and metastatic than control tumours<sup>595</sup>. These results are in accordance with ours, where we show that APC/C<sup>Cdh1</sup> inactivation promotes cell cycle resumption upon release from replication stress but with an increase in markers of DNA damage or genomic instability. Since *EMI1* mutations or genomic amplifications are rare in human solid cancers, it is likely that this overexpression occurs through a defective pRb pathway signalling<sup>75,596</sup> or through its stabilization by Evi5 oncogene<sup>79</sup>.

On the other hand, other proteins could be responsible for low APC/C activity in tumour cells. Conceivably, deubiquitinases like USP28<sup>109,597</sup> are found to be overexpressed in colon and breast carcinomas<sup>598,599</sup>, and also in non-small cell lung cancer, where they were correlated with low survival rate<sup>600</sup>. Another possibility is a low strength of premature APC/C induction<sup>112</sup>.

Finally, the fact that APC/C is mutated in some human colon cancer cells, such as HT29<sup>591</sup>, could explain the APC/C<sup>Cdh1</sup> inactivation in some cases, although the model chosen for our work, HCT116 cell line, exhibit wild-type APC/C.

Collectively, the results suggest that the forced activation of APC/C<sup>Cdh1</sup> in tumour cells in response to a prolonged replication stress induces an irreversible cell cycle exit. This could provide an opportunity to develop new strategic therapies and Emi1 represents a potential target for cancer therapy, as its inhibition could enhance the effect of chemotherapy directed to induce replication stress by an irreversible cell cycle exit.

## II. FORK REMODELLING AFTER AN ACUTE HU-INDUCED REPLICATION STRESS

As previously explained, replication forks stall for different causes, such as replication and transcription machineries collision, the presence of DNA damage or insufficient nucleotides. One of the functions of replication checkpoint is the stabilization of replication forks, although the fate of replisome is not clear.

We were interested in defining the mechanisms involved in replication fork stability and restart, which occurs after an acute HU treatment, and in the loss of replication recovery, which occurs after a prolonged HU treatment. To do so, we used the iPOND technique, which allows the isolation of protein complexes crosslinked to EdU thymidine analogue-containing fragments that are located at active replication forks<sup>128,550–552,601</sup>. This is a powerful tool to analyse the HU-induced changes in the replication forks in hTERT-RPE cells. The robust methodology of our iPOND experiments was validated by the enrichment of known replisome components in the pulse condition.

The iPOND results of non-transformed human cells showed that, after a prolonged replication stress, there is a dissociation of replisome components and also of other proteins involved in DNA repair, such as FANCD2 and RAD51, both in the replication forks and in chromatin. This would explain the lack of replication fork restart under these conditions. Moreover, the lack of repair proteins BRCA2<sup>477</sup>, FAND2<sup>479</sup> and RAD51<sup>476</sup> would promote the Mre11-dependent degradation of nascent DNA that we observe under these conditions (**Figure 39**). In addition, it has been recently described the role of mitotic regulators, such as Aurora A, in protecting DNA replication forks<sup>602</sup>. Aurora A, as a substrate of APC/C<sup>Cdh1</sup>, is degraded after a prolonged HU-induced replication stress, which would cause a deprotection of replication forks and induce their degradation<sup>602</sup>. Nascent DNA degradation could promote the dissociation of replisome components and other proteins from chromatin after a prolonged replication stress.

Surprisingly, the iPOND results also show that replisome components are dissociated from nascent DNA already after an acute replication stress, but this does not result in the dissociation of those proteins from chromatin at this time. These results suggest that replisome components are displaced away from nascent DNA more than dissociated from replication forks after an acute replication stress. Moreover, proteins involved in maintaining

## DISCUSSION

fork stability and promoting fork restart, such as RAD51, FANCD2 and SMC1/3 cohesins<sup>329,330,476,479,553</sup>, are recruited in nascent DNA after an acute replication stress. Under these conditions, replication forks present single-stranded nascent DNA. Restart from the same replication forks occurs without compromising genome integrity in hTERT-RPE cells.

It was previously reported that replisome components were stably bound to nascent DNA upon HU treatment<sup>426</sup>. The discrepancy with our results could be clarified by several explanations. On the one hand, the cellular model used is different: while we use hTERT-RPE cells, Dungrawala *et al.* used HEK293T cells. On the other hand, the dose of HU used is different in both cases: our work was done with a dose of 10mM HU, which completely stalls replication after 15 minutes of HU addition<sup>536</sup>, while they used a lower dose of HU (3mM HU), which does not completely block EdU incorporation. Thus, EdU was maintained in the media during the HU treatment.

Previous results showed that replication forks of hTERT-RPE cells maintain the competence to restart, even in the presence of CDK inhibitor roscovitine, after an acute HU treatment and that replisome is displaced away from nascent DNA. In this thesis we have showed that, despite the addition of roscovitine, replication forks are not altered, and CMG complex maintains its disengagement from nascent DNA. Moreover, the loading of MCM helicases is impaired under HU conditions in which cells are arrested in S phase. We have also demonstrated that CMG helicase maintains its integrity and association with chromatin after an acute replication stress. This, together with the fact that replication forks are able to restart after HU release, reinforces the idea that CMG maintains its association with chromatin in order to be reused to restart DNA replication.

The previous results suggested that there was a remodelling event after an acute replication stress. The presence of single-stranded nascent DNA suggested that fork reversal could occur under our conditions<sup>470</sup>. In this sense, the work done in this thesis with FBH1, a helicase that has been demonstrated to have the capacity to perform fork reversal *in vivo*<sup>470</sup>, confirms this hypothesis. The presence of single-stranded nascent DNA that appears after an acute replication stress decreases after FBH1 depletion in hTERT-RPE cells. Under these conditions, where fork reversal is impaired, replication forks are also able to restart, and cell cycle progression is resumed. It has to be noted that although single-stranded nascent DNA

decreases after acute replication stress in FBH1-depleted cells, it is still significantly different from control conditions. In this sense, there are several remodellers that can also have a role in fork reversal in our conditions, as SMARCAL1<sup>335,336</sup> or ZRANB3<sup>473</sup>.

Another possible remodelling event is the uncoupling of helicase and polymerase activities. To investigate it, the ssDNA in nascent and parental strands was analysed. The larger amount of single-stranded parental DNA obtained upon an acute replication stress suggests that the helicase-polymerases uncoupling is the predominant remodelling event under these conditions. This could also explain the increased chromatin-bound RPA after acute replication stress, which could not be explicated by reversed forks.

The presence of single-stranded parental DNA after acute replication stress in non-transformed cells could be due to resection. In this sense, Mre11-dependent degradation may cause an accumulation of single-stranded parental DNA<sup>476</sup>. But our results show that an acute replication stress does not cause Mre11-dependent DNA degradation in non-transformed human cells, contrary to what happens after a prolonged replication stress.

Actually, uncoupling of helicase and polymerases activities in replication forks have been described to occur in response to several replication stresses agents<sup>279,462</sup>. Moreover, some studies suggest that this uncoupling generates RPA-ssDNA, which was required for checkpoint activation<sup>277,279</sup>. But, the current accepted model of the uncoupling of helicase and polymerases activities does not include the disengagement of replisome components from nascent DNA, and consequently reinitiation could easily occur. Our proposed models are based on the observation that upon 2 hours of HU treatment, replisome components do not interact with nascent DNA, although they are bound to chromatin, and that CMG integrity is maintained and can be reused once replication stress is removed. On the one hand, the presence of nascent ssDNA that decreases after FBH1 depletion indicates that reversed forks are present in our conditions. And, on the other hand, the accumulation of long stretches of parental ssDNA indicates that there is a functional uncoupling between helicase and polymerases activities which results in replisome disengagement from nascent DNA (**Figure 75**).

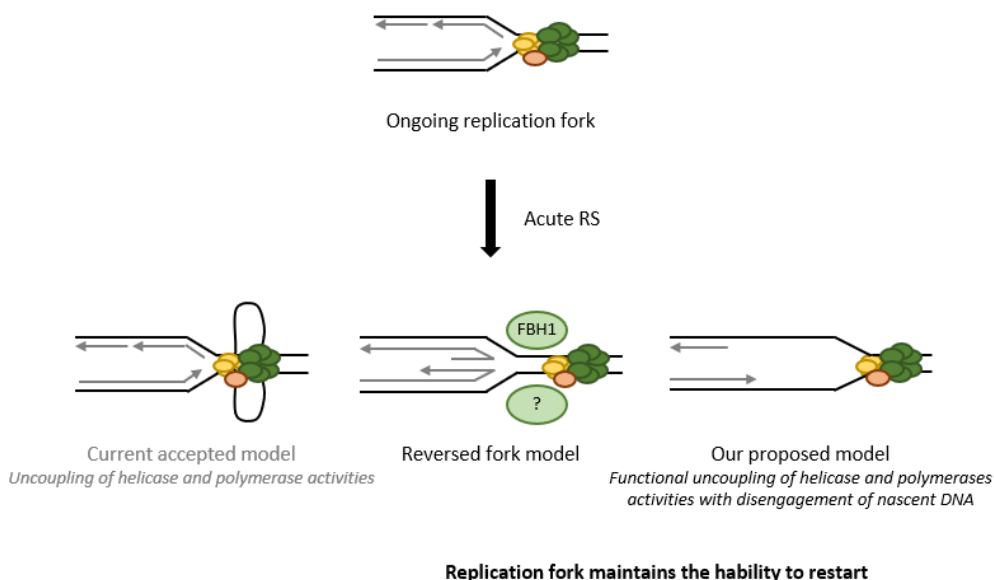


**Figure 75. Our proposed model after an acute replication stress induced by HU.** Under our conditions, hTERT-RPE cells remodel their ongoing forks after an acute replication stress. Our results suggest that there are two proposed models based on our observations: the reversed forks and the functional uncoupling of helicase and polymerases activities with disengagement of nascent DNA. Despite this remodelling, these forks are able to restart replication by reusing the same CMG complex. RS: replication stress.

Finally, and most interestingly, our data show that the remodelled forks are able to reinitiate DNA synthesis upon HU release, although replisome components are displaced away from nascent DNA, without compromising genomic stability.

In the reversed forks, replication fork restart would occur through two different pathways. The first pathway has as a central player RECQ1 helicase, which drives fork restart of reversed forks by branch migration<sup>481</sup>. The second pathway includes DNA2 nuclease and WRN helicase that process reversed forks and a branch migration factor, such as RAD51, would be needed to induce replication fork restart<sup>482</sup>.

In the proposed model, in which there is a functional uncoupling of helicase and polymerases activities and a disengagement of replisome from nascent DNA, the possible mechanisms of replication fork restart are only hypothesis. As explained in the introduction, the lagging-strand synthesis could be easily reinitiated by the polymerase  $\alpha$  binding *de novo* to the replisome after HU release<sup>232,278</sup>. On the other hand, reinitiation of leading-strand synthesis

could be more complex: the 3' end of nascent DNA has to be carried to the replisome by some linker molecule or some polymerase has to work independently of the replisome. Since our data show that the bulk of single-stranded parental DNA and phosphorylated chromatin-bound RPA disappeared rapidly once replication is restarted, a possible explanation could be fork repriming by PrimPol or DNA polymerase  $\alpha$ . Moreover, RAD51 is also recruited in nascent DNA after an acute replication stress, and its interaction with polymerase  $\alpha$ <sup>335</sup> could promote replication fork restart under our conditions. Another possibility could be that the soluble (not bound to replisome) polymerase  $\delta$  would be engaged to the 3' end of nascent DNA and synthesise DNA until catches the CMG complex, when it would be dissociated by collision release<sup>437</sup>.

Interestingly, our results demonstrate that replication forks are more plastic than one could expect, and they can restart replication, even when there is a disengagement of the replisome from the nascent DNA, without inducing genomic instability.

### III. ROLE OF RAD51 IN REPLICATION FORKS IN RESPONSE TO REPLICATION STRESS

We are also interested on elucidating the mechanisms and proteins important to promote fork restart to better understand the mechanisms that cells use to deal with replication stress. Since RAD51 could be involved in the restart of the remodelled replication forks after acute HU treatment, and it is recruited to nascent DNA under these conditions, we wanted to analyse its role in replication forks under replication stress conditions.

RAD51 is a protein well conserved during evolution from its bacterial RecA to human ortholog RAD51, since it is a key element of HR, having a critical role in DNA homology search and in catalysing strand invasion<sup>603</sup>. Moreover, emerging roles in replication fork protection and restart have been identified for RAD51 and other mediators, such as BRCA2<sup>476,477,479</sup>.

The recruitment of RAD51 to nascent DNA observed after acute HU treatment make us wonder if RAD51 could have a role in fork protection<sup>335,476,479,568,604–606</sup> or in fork restart<sup>370,476</sup> in hTERT-RPE cells. The work has been done with two different approaches: on the one hand RAD51 depletion with siRNA, and on the second hand RAD51 inhibition with B02. B02 is a small molecule inhibitor of RAD51, which was identified by a high-throughput screening<sup>531</sup>. This molecule specifically inhibits the strand exchange activity of RAD51, inhibiting the HR repair mechanism and increasing sensitivity to DNA damage agents<sup>532–534</sup>.

First, we analysed if RAD51 had a role in replication fork restart after acute replication stress. The two approaches (both RAD51 silencing or inhibition by B02) does not affect the number of restarted forks, although the IdU (second analogue) track length is impaired under these conditions. Thus, RAD51 seems to be important for efficient fork restart or progression after an acute replication stress. In RAD51 silencing, the impairment in fork progression is obtained only when roscovitine is added to avoid the activation of new origins. In HU conditions without roscovitine, dormant origins that cannot be distinguish by DNA fiber assay would compensate replication. This does not happen with RAD51 inhibition, since the impairment is already observed in conditions without roscovitine. These differences could be explained for the timing of RAD51 silencing or inhibition: the siRNA transfection takes place 48 hours before the DNA labelling, so cells might have adapted by the time DNA labelling was performed, while the RAD51 inhibition is performed during DNA labelling, with no time for adaptation. Moreover, it

should be noted that the number of cells in S phase 48 hours after siRNA transfection is significantly reduced, since RAD51 depletion has a strong effect on cell cycle, generating an accumulation of cells in G2 phase, as has been previously described<sup>571</sup>.

Next, we analysed if RAD51 had a role in replication fork protection. In chapter 1, we demonstrate that there is no Mre11-dependent degradation after an acute replication stress in hTERT-RPE cells. In this sense, we analysed the nascent DNA labelled before HU addition to study RAD51 contribution in protecting nascent DNA from degradation under our conditions. Despite having an effect on efficient fork restart or progression, RAD51 depletion or inhibition does not cause fork degradation after an acute replication stress in contrast to what is described, since no decrease in nascent labelled DNA is observed under these conditions. Thus, after an acute replication stress induced by 10mM HU, RAD51 is recruited to nascent DNA to promote efficient fork restart or progression, but not to protect nascent DNA in hTERT-RPE cells.

As mentioned, RAD51 depletion had a great effect on cell-cycle, resulting in accumulation of cells in G2 phase, where it is required for HR repair, so we performed the next experiments only with RAD51 inhibitor.

RAD51 inhibition by itself has no effect on fork progression in hTERT-RPE cells, although it has an effect on mitotic entry under unperturbed conditions. As previously described, RAD51 is dispensable for DNA replication but is required in G2 to resolve DNA structures that would impede mitotic entry<sup>571,607</sup>. Moreover, it has to be noted that the mitotic entry is more impaired after an acute HU treatment, when RAD51 inhibition has an effect in replication fork progression in hTERT-RPE cells.

To decipher which role RAD51 has in fork progression after acute replication stress, we performed a DNA fiber assay, adding the B02 inhibitor at different times: during all the HU release or after 30 minutes of HU release. We already knew that most replication forks of hTERT-RPE cells need 30 minutes to restart after an acute HU treatment (data not shown), so the last condition allowed us to know if RAD51 is important for fork progression after replication fork restart. The first condition may be important for the recognition of RAD51 as an important protein for efficient replication fork restart. The results show that the labelling of

## DISCUSSION

the second analogue during HU release is impaired in both conditions, having more effect in the condition where the inhibitor is maintained through all the HU release, suggesting that both efficient fork restart and fork progression are affected due to RAD51 inhibition after an acute replication stress in hTERT-RPE cells.

Due to RAD51 role in replication forks after an acute HU treatment, we next analysed its contribution to genomic stability. In order to analyse the cells that were in S phase just before HU treatment, an EdU pulse was performed previously to label replicating cells and the presence of more than six 53BP1 foci was analysed in the S-phase population. Although RAD51 inhibition has a small effect in mitotic entry under unperturbed conditions, this was not reflected with an increase in genomic instability. Instead, after an acute HU treatment, where the effect on mitotic entry was more pronounced by RAD51 inhibition, the number of EdU-labelled cells with more than six 53BP1 foci increases significantly when RAD51 inhibitor was added during HU release in non-transformed human cells.

Finally, after analysing the consequences that RAD51 inhibition had on replication forks after an acute replication stress in hTERT-RPE cells, we analysed if this protein was also relevant for replication fork progression during a mild or bearable replication stress. As a mild replication stress, we used a lower dose of HU (1mM) that allows DNA replication in hTERT-RPE, even though fork progression is significantly impaired, activating the replication checkpoint response. As a bearable replication stress, which represents a more physiological replication stress, we used, on the one hand, an even lower dose of HU (0.1mM) in hTERT-RPE that does not activate replication checkpoint response and, on the other hand, a colorectal cancer cell line, HCT116, that presents a higher basal replication stress compared with the non-transformed human cell line hTERT-RPE. In all cases, RAD51 inhibition with B02 impairs replication fork progression. In conclusion, RAD51 is also relevant for replication fork progression during a mild or bearable replication stress, although the consequences of its inhibition on genome instability and survival have to be elucidated.

Our results are slightly misaligned with a work done by Yoon *et al.* with mouse embryonic stem cells (mESCs) that indicates that RAD51 suppression does not affect replication fork progression and speed<sup>607</sup>. It has been previously described that ESCs proliferate rapidly and exhibit a high degree of replication stress<sup>608–610</sup>. In this sense, we would expect that RAD51

suppression to have an effect in replication fork progression under basal increased replication stress conditions, as we have seen in HCT116 cell line. Instead, results from Yoon *et al.* are more similar to the ones obtained with hTERT-RPE cell line. Moreover, they suggest that replication dynamics do not differ in RAD51-depleted cells when compared with control cells<sup>607</sup>, as also shown in our data. However, Yoon *et al.* analyse the replication dynamics by IdU and CldU labelling foci, but no significant differences in IdU-CldU foci colocalization were obtained with RAD51 depletion<sup>607</sup>.

On the other hand, there is another study performed by Kim *et al.* in mESC that used two RAD51 mutants, one defective for ATP binding and one defective for ATP hydrolysis. Although they do not affect RAD51-protein interaction, ATP binding is critical for assembly and stabilization of nucleofilament, essential for proper RAD51 function. Both mutants exhibit impaired cellular proliferation and reduced replication fork restart after a mild replication stress<sup>611</sup>. Under our conditions, replication dynamics are not affected with RAD51 inhibition, although the conditions of the experiment are different. As mentioned, mESC are supposed to exhibit a higher basal replication stress<sup>608-610</sup>, and Kim *et al.* use a dose of 2mM of HU during 2 hours. The IdU labelling after HU release is very short (about 20 minutes), so it is possible that replication forks do not have time enough to restart replication. Moreover, since we know that RAD51 has a role in the efficient fork restart and progression after an acute replication stress, it is possible that this short time in IdU labelling is turned into an increase in the number of stalled forks under these conditions.

Interestingly, RAD51 is overexpressed in a wide range of human tumours, contributing to their drug resistance<sup>612-615</sup>. In this sense, tumour cells in which RAD51 expression is suppressed<sup>612,615,616</sup> or its activity is inhibited<sup>532-534,615</sup> become susceptible to DNA-damaging agents. All these studies, together with our data, suggest that RAD51 is a potential target for cancer therapy, the inhibition of which could enhance not only the effect of DNA damage-based chemotherapy but could also enhance the effect of replication stress-induced chemotherapy.

#### **IV. OZF IS ESSENTIAL TO MAINTAIN FORK PROGRESSION RATE UNDER REPLICATION STRESS CONDITIONS**

OZF was identified as a zinc-finger protein<sup>576</sup> that interacts with a telomeric protein, hRap1<sup>578</sup>, and with the SUMO-1 conjugating enzyme UBC9<sup>579</sup>, although its function remains unknown.

Previous work of our group has defined OZF as a novel Claspin-interacting protein that localizes at ongoing replication forks in control situation in hTERT-RPE cells. Since Claspin is an important protein for the correct replication in a normal cell cycle<sup>186,583,585,617,618</sup> and also for the replication checkpoint response<sup>308,574,619</sup>, it made us wonder if OZF would have a role in these processes.

Our data show that OZF interacts with Cdc45, MCM2 and MCM6, all components of CMG complex. Thus, OZF is located in activated origins, which correlates with the fact that it is also present in the ongoing replication forks. Nevertheless, its depletion does not affect fork progression neither replication dynamics under unperturbed conditions in hTERT-RPE. Hence, OZF does not have a role in replication in a control situation in non-transformed human cells.

Interestingly, OZF depletion impairs replication fork progression, but does not affect replication dynamics, under mild or bearable replication stress conditions in hTERT-RPE. On the other hand, OZF is not essential for replication checkpoint activation, since OZF-depleted cells also activate Chk1 after a mild replication stress induced by 1mM HU treatment.

Due to the effect that OZF silencing has in fork progression during a mild or bearable replication stress in hTERT-RPE cells, we analysed its contribution in genomic stability. Cell cycle progression, the presence of cells with 53BP1 and  $\gamma$ H2AX foci and colony formation were analysed after a release of 1mM HU treatment. The results show that OZF depletion does not affect cell cycle progression nor mitotic entry. These cells do not present more DNA damage, and colony formation is not affected either. Thus, the impairment in fork progression seems to have no effect on cell cycle progression, on DNA damage nor on cell viability in OZF-depleted hTERT-RPE cells, since these cells are able to deal with these differences in replication fork progression without major consequences.

Since previous studies of OZF described its overexpression in pancreatic cancer <sup>587</sup> and in colorectal cancer <sup>588</sup>, we wanted to analyse its relevance in the colorectal cancer cell line, HCT116, which exhibits a higher basal replication stress than the non-transformed human cells hTERT-RPE. Our results show that OZF depletion impairs replication fork progression in tumour HCT116 cell line under unperturbed conditions. The consequences in genomic stability, which could be different from hTERT-RPE cells, remain to be elucidated. The non-transformed human cells could deal with replication stress and could repair the DNA damage, while tumour cells could be more OZF-dependent because they might not repair the DNA damage so well.

Such as it is described, OZF overexpression is restricted to tumour cells <sup>587</sup> and is already observed in low-grade adenomas, occurring in the primary stage of tumour progression <sup>588</sup>. Moreover, OZF is a c-Myc oncogene-target gene <sup>589</sup>. A possible explanation is that c-Myc oncogene activity induces rapidly replication stress <sup>620</sup> and also could induce OZF overexpression that would maintain replication forks progression rate under replication stress conditions. Since OZF expression is dysregulated as an early event in tumour formation, it could be a potential indicator and also a therapeutic target if its physiological relevance is demonstrated.

## DISCUSSION

As a summary of all the results included in this thesis, a final model is shown (**Figure 76**). In HEK193T cells, transfected OZF interacts with several components of CMG complex. Since previous data showed that OZF was present in nascent DNA under unperturbed conditions in hTERT-RPE cells, we assume that OZF is interacting with replisome in their ongoing replication forks. In this case, OZF does not have a clear function in replication fork progression, but it could be there prepared for a replication stress situation. In case of bearable (0.1mM HU) or mild replication stress (1mM HU), during which replication forks are able to duplicate DNA, both OZF and RAD51 are important for replication forks progression in hTERT-RPE cells. Moreover, in tumour cells such as HCT116 cell line, which present a higher basal replicative stress, these proteins are also important for replication fork progression during unperturbed conditions.

After an acute replication stress (10mM HU during 2h), stalled forks are able to restart once the stress is released, both in hTERT-RPE cells and HCT116 cells. We have deeply studied the remodelling events that occur in response to acute replication stress in non-transformed human cells. In this case, HU-induced replication inhibition causes both fork reversal and, predominantly, a functional helicase-polymerases uncoupling with replisome disengagement from nascent DNA. In reversed forks we have demonstrated that FBH1 has a role in this remodelling event, although we cannot rule out that other remodellers participate in this process. Moreover, in response to acute replication stress, RAD51 is recruited to nascent DNA and our results suggest that this protein has a role in efficient fork restart and progression once HU is removed. These remodelling events do not compromise replication fork restart neither genome integrity in hTERT-RPE cells.

After prolonged replication stress (10mM HU during 14 hours), non-transformed human cells activate APC/C<sup>Cdh1</sup> during S phase, which compromises the ability to resume replication by inhibiting origin firing and contributes to safeguard genomic stability<sup>536</sup>. Moreover, replication forks collapse and nascent DNA is degraded by Mre11. Instead, transformed human cells have incorporated mechanisms to avoid APC/C<sup>Cdh1</sup> activation upon a prolonged HU treatment. Consequently, tumour cells, such as HCT116, are able to recover replication by the activation of new origins and resume cell cycle progression, despite the acquisition of genomic instability.

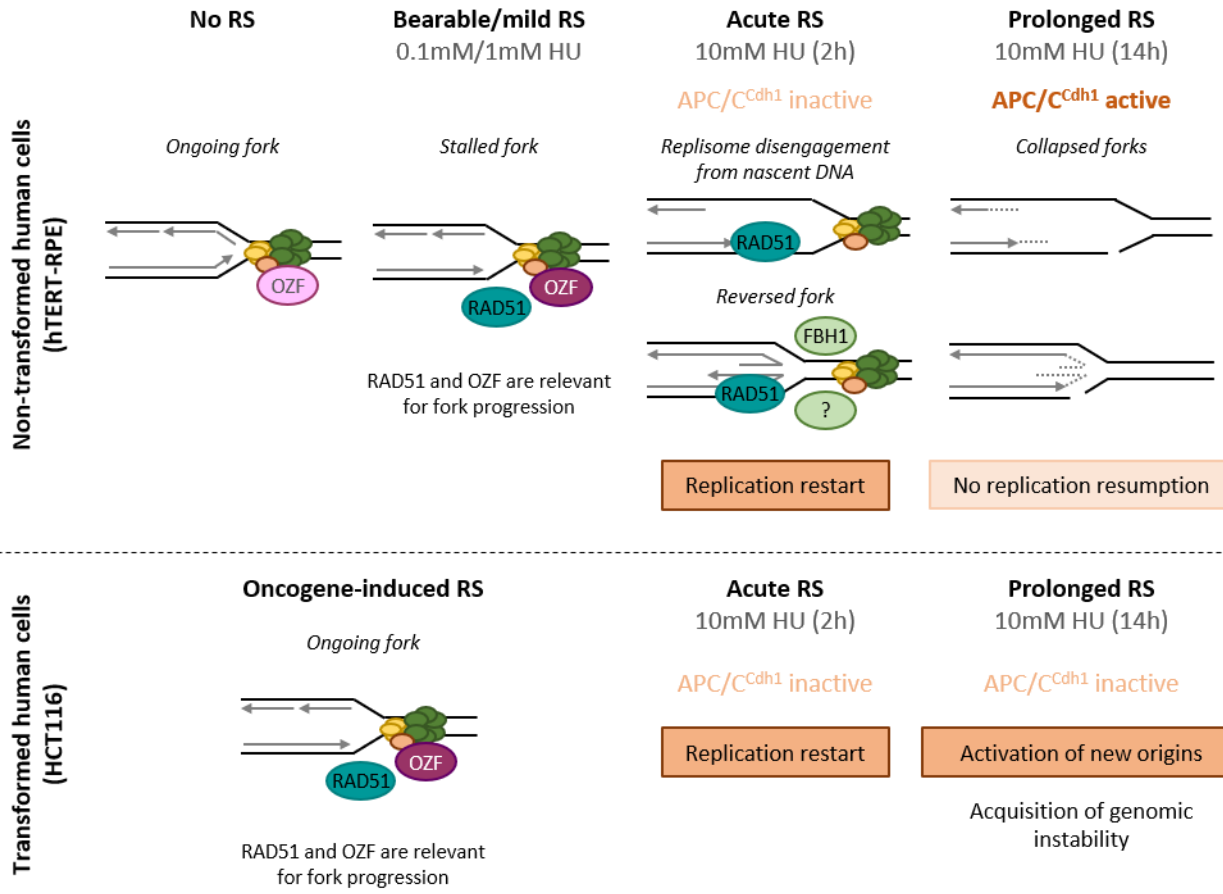


**Figure 76. Final model.**

Our results suggest that different mechanisms and molecules are involved in replication stress response. In response to a bearable or mild replication stress, RAD51 and OZF are required for fork progression in both hTERT-RPE and HCT116 cell lines. In response to acute replication stress, some remodelling events occur at replication fork level in hTERT-RPE cell line: fork reversal and, predominantly, a functional uncoupling of helicase-polymerases activities with replisome disengagement from nascent DNA. RAD51 has a role in replication fork restart after acute replication stress in hTERT-RPE cells. After a prolonged replication stress, the activation of APC/C<sup>Cdh1</sup> compromises the ability to resume replication in hTERT-RPE, while transformed cells avoid this mechanism at the expense of acquisition of genomic instability. RS: replication stress.

## *DISCUSSION*

Understanding how checkpoint mechanisms are working on non-transformed cells, and comparing them with tumour cells, can help us understand the alterations that tumour cells have acquired in order to bypass these regulations. This can aid in the discovery of new molecules relevant to deal with each S phase in tumour cells with a higher basal replication stress, and to develop new anti-tumoral therapies. Although further experimentation is needed, from this thesis we can conclude that Emi1, RAD51, and OZF are potential targets for cancer therapy, the inhibition of which could enhance the effect of chemotherapy directed to induce replication stress.

## **CONCLUSIONS**



Based on the exposed results, the general conclusions of this thesis are:

1. The lack of activation of APC/C<sup>Cdh1</sup> in S phase in HCT116 cells allows DNA replication resumption after a prolonged HU treatment by new origin activation, even though genomic instability is acquired in the process.
2. After an acute HU treatment, there is replisome disengagement from nascent DNA and functional helicase-polymerases uncoupling, but CMG complex maintains its integrity and can be reused for replication fork restart in hTERT-RPE cells.
3. RAD51 is essential for efficient fork restart and progression after both acute and mild replication stress in hTERT-RPE cells. Furthermore, RAD51 is essential for replication fork progression under unperturbed conditions in HCT116 cells, which present a higher basal replication stress.
4. OZF, which co-immunoprecipitates with CMG complex in basal conditions, is necessary for replication fork progression during a mild replication stress in hTERT-RPE cells and is important for replication fork progression under unperturbed conditions in HCT116 cells.

Based on the previously defined objectives and exposed results, the specific conclusions of this thesis are:

**I. Conclusions from the study of the contribution of APC/C<sup>Cdh1</sup> activation after a prolonged HU-induced replication stress to preserve genomic integrity.**

- 1.1) Tumour cell lines are predominantly deficient in APC/C<sup>Cdh1</sup> activation in S phase and are able to resume replication in response to a prolonged HU treatment.
- 1.2) New origin firing contributes to replication recovery in HCT116 cells after a prolonged HU treatment.
- 1.3) HCT116 cells acquire genomic instability after a prolonged HU treatment.
- 1.4) Emi1 depletion-induced APC/C<sup>Cdh1</sup> activation compromises replication resumption and genomic instability acquisition in HCT116 cells.

**II. Conclusions from the analysis of the HU-induced changes at replication fork levels in non-transformed human cells.**

- 2.1) CMG helicase maintains its integrity and association with chromatin after an acute replication stress in hTERT-RPE cells.
- 2.2) CMG helicase is disengaged from nascent DNA after an acute replication stress, indifferently of CDK activity in hTERT-RPE cells.
- 2.3) FBH1 depletion reduces the amount of single-stranded nascent DNA, but does not impair replication fork restart in hTERT-RPE cells.
- 2.4) Replisome disengagement from nascent DNA correlates with large amounts of single-stranded parental DNA and RPA accumulation.
- 2.5) Nascent DNA is not degraded by Mre11 after an acute replication stress in hTERT-RPE cells.
- 2.6) Replication resumption occurs without long stretches of single-stranded parental DNA in hTERT-RPE cells.

**III. Conclusions from the characterization of the role of specific proteins, RAD51 and OZF, at replication forks in response to HU-induced replication stress.** *The conclusions of RAD51 role are obtained from chapter 3 in the results section, while the conclusions about OZF are obtained from chapter 4 in the results section.*

- 3.1) RAD51 depletion or inhibition does not affect the number of restarted forks but impairs fork progression after an acute replication stress in hTERT-RPE cells.
- 3.2) RAD51 depletion or inhibition does not cause fork degradation after an acute replication stress in hTERT-RPE cells.
- 3.3) RAD51 depletion does not impair replication recovery, although increases genomic instability, after an acute replication stress in hTERT-RPE cells.
- 3.4) RAD51 inhibition does not affect fork progression under unperturbed conditions in hTERT-RPE.
- 3.5) RAD51 is necessary for an efficient fork restart and progression after an acute replication stress in hTERT-RPE cells.
- 3.6) RAD51 inhibition affects mitotic entry, having more effect after an acute replication stress in hTERT-RPE cells. In this last case, an increase in genomic instability is also obtained.
- 3.7) RAD51 inhibition affects fork progression under mild or bearable replication stress in hTERT-RPE cells and also during unperturbed conditions in HCT116 cells.
- 3.8) OZF interacts with components of CMG complex, although it is not essential for replication in hTERT-RPE cells under unperturbed conditions.
- 3.9) OZF depletion reduces fork progression rate under mild replication stress conditions in hTERT-RPE cells, although it is not essential for checkpoint activation.
- 3.10) OZF depletion reduces fork progression in HCT116 cells under unperturbed conditions.



# **MATERIALS AND METHODS**



# 1. CELL CULTURE

## 1.1. CELL LINES AND CULTURE CONDITIONS

The cellular models and culture conditions used in this thesis are specified below:

**Table 3. Cell lines used in this thesis.**

Cell line	Cell type	Medium	Origin
<b>hTERT-RPE</b>	Human retinal pigment epithelial cells, immortalized with hTERT	DMEM: F12 (1:1) supplemented with 7% FBS (foetal-bovine serum, Biological Industries)	ATCC
<b>HCT116</b>	Human colorectal adenocarcinoma cells	DMEM: F12 (1:1) supplemented with 7% FBS	Dr. Capellà, ICO
<b>A431</b>	Human epithelial cells from epidermoid carcinoma	DMEM supplemented with 10% FBS	ATCC
<b>DLD-1</b>	Human colorectal adenocarcinoma cells	DMEM: F12 (1:1) supplemented with 7% FBS	ATCC
<b>HeLa</b>	Human epithelial cells derived from a cervix cancer	DMEM supplemented with 10% FBS	ATCC
<b>HPAF-II</b>	Human pancreatic ductal adenocarcinoma cells	DMEM supplemented with 10% FBS	ATCC
<b>HT29</b>	Human epithelial cells from pancreatic ductal adenocarcinoma	DMEM supplemented with 10% FBS	ATCC
<b>MCF7</b>	Human epithelial cells derived from breast cancer metastasis in the pleural effusion	DMEM supplemented with 10% FBS	London (S. Guaita)
<b>SW1990</b>	Human epithelial cells derived from pancreatic ductal adenocarcinoma metastasis in the spleen	DMEM supplemented with 10% FBS	ATCC
<b>U2OS</b>	Human osteosarcoma cells	DMEM supplemented with 10% FBS	ATCC
<b>HEK293T</b>	Human embryonic kidney cells, immortalized with SV-40	DMEM supplemented with 10% FBS	ATCC

All culture media (Biological Industries, ref. 01-055-1A for DMEM and ref.01-095-1A for F12) were supplemented with 1% of non-essential amino acids (Biological Industries, ref.01-340-1B), 2mM L-Glutamine (Sigma-Aldrich, ref.49419), 1mM pyruvic acid (Sigma-Aldrich, ref.P5280), 50U/mL penicillin and 50µg/mL streptomycin (both from Biological Industries,

ref.03-031-1B). All supplements were filtered with a 2µm membrane before being added to the media in order to maintain sterility.

Cell lines were maintained at 37°C in incubators (Thermo Scientific, HERACell 150i) with humidified atmosphere of 5% CO<sub>2</sub>, which were periodically treated with biocide- and anti-mycoplasma-containing products. Manipulation of cells was always performed under sterile conditions inside a vertical laminar flow hood (Mars Safety Class 2) with previously sterilized material.

### 1.2. MAINTENANCE OF CULTURED CELLS

When cells were at around 80% of confluency, they were subcultured to prevent medium exhaustion or, in the case of normal cells, growth arrest due to contact inhibition. To do so, the medium from the flasks was removed and discarded and the cells were washed with PBS (phosphate-buffered saline) to remove any traces of serum. Cells were enzymatically dissociated by adding 0.05% trypsin (Biological Industries, ref.15400-054) for a few minutes and, once detached, fresh medium was added to inactivate the trypsin (at least twice the trypsin volume). The cell-medium mixture was homogenised by pipetting several times and a portion of cells was transferred into a new flask, where fresh culture medium was added.

PBS	131mM NaCl
	1.54mM KH <sub>2</sub> PO <sub>4</sub>
	5.06mM Na <sub>2</sub> HPO <sub>4</sub>

### 1.3. CRYOPRESERVATION

Cell lines are a valuable resource and thus, it is important to have a long-term storage system for them. When needed, cells at a low passages were cryopreserved in liquid nitrogen in complete medium with 10% dimethyl sulfoxide (DMSO; Sigma, ref.D2650), a cryoprotective agent that reduces the risk of ice crystal formation. Three cryotubes of cell suspension was prepared from each 150cm<sup>2</sup> flasks. Cells were enzymatically dissociated with trypsin (as explained before) and once detached, they were collected in a 15mL sterile tube and were centrifuged at 650g for 5 minutes at 4°C. Then, the supernatant was removed, and pellets were resuspended in 2.7mL of supplemented culture medium. Finally, cell suspension was

mixed with DMSO and the cryotubes were rapidly mixed and placed in dry ice. The vials were stored in a liquid nitrogen storage container.

On regular basis, a new vial of low passage cells was taken from the liquid nitrogen container and thawed in supplemented cultured medium. The cells were thawed slowly by pipetting small volumes of cultured medium into the cryotube, resuspending as many cells as possible and returning the solution to the 15mL tube to dilute the DMSO. The process was repeated until all cells from the cryotube were in suspension. The tube was centrifuged at 650g for 5 minutes at 4°C and the supernatant was removed. The pellet was resuspended with 13mL of fresh medium and the cells were transferred into a 75cm<sup>2</sup> flask and were incubated overnight in incubators. After that, medium was replaced and, if necessary, cells were subcultured.

#### 1.4. AGENTS USED

*Table 4. Agents used in this thesis.*

Agent	Reference	Function	Working concentration
<b>Thymidine</b>	Sigma, T1895	Deoxynucleoside	1.5mM in hTERT-RPE 2.5mM in HCT116 if not specified otherwise
<b>Hydroxyurea (HU)</b>	Sigma, H8627	Ribonucleotide reductase inhibitor	10mM to stall replication forks 1mM or 0.1mM to slow replication forks
<b>Nocodazole</b>	Sigma, M1404	Inhibitor of microtubule polymerization	250ng/mL in tumour cells 500ng/mL in hTERT-RPE
<b>MG132</b>	SelleckChem, S2619	Proteasome inhibitor	20µM
<b>BrdU</b>	Sigma, B5002	Thymidine analogue	10µM in asynchronously growing cells 20µM in synchronized cells
<b>CldU</b>	Sigma, C6891	Thymidine analogue	25µM
<b>IdU</b>	Sigma, I7125	Thymidine analogue	250µM
<b>EdU</b>	Invitrogen, A10044	Thymidine analogue	50µM
<b>Roscovitine</b>	Sigma, R7772	CDK inhibitor	25µM
<b>B02</b>	Sigma, SML0364	Rad51 inhibitor	25µM
<b>Mirin</b>	Sigma, M9948	Mre11 inhibitor	50µM

## 1.5. THYMIDINE SYNCHRONIZATION

Cell synchronization is used in order to obtain a population enriched on a specific cell cycle phase. In this thesis, cell synchronization was performed with a single thymidine block to obtain a population enriched in S-phase. As mentioned before, thymidine is a deoxynucleoside, and an excess of it can be used to inhibit DNA synthesis, thereby arresting cells either at the G1/S transition, or in S phase. This arrest can be easily reverted by removing the thymidine from the media, allowing the cells to re-enter into S phase. It should be noticed that this reversible S-phase arrest may promote replication stress, as it promotes fork stalling.

This synchronization method can be used to synchronize any cell line in S phase. To this end, cells were seeded at 60% of confluency and then thymidine was added to the media. Cells were incubated with thymidine for 20-24 hours, and finally released into fresh media for 2 hours, time at which more than 80% of the cells are in S phase.

## 1.6. DNA TRANSFECTION METHODS

### 1.6.1. CALCIUM PHOSPHATE

For transient transfection of HA-tagged proteins, HEK293T cells were transfected using calcium phosphate. Calcium phosphate facilitates the binding of the co-precipitate of condensed DNA to the cell surface, therefore DNA is able to enter into the cell by endocytosis.

Cells were seeded in a 10cm<sup>2</sup> plate and, at the time of transfection, they were at around 50% of confluency. Some hours (6 hours approximately) before transfection, the medium was replaced.

For a 10cm<sup>2</sup> plate, two tubes were prepared with the following solutions:

- A. 0,5mL of HBS2X
- B. 0,5mL of a mixture of ultrapure water with 10µg of DNA and 250mM CaCl<sub>2</sub>.

The solution B was added on top of solution A slowly (drop-wise) and stirred with a vortex. It was incubated during 10 minutes at room temperature (RT) and it was vortexed twice during that period. The mix was poured around the plate, while stirring gently. Fresh medium was added after 8-16 hours of transfection and cells were collected after 48 hours post-transfection.

<i>HBS 2X pH7 solution</i>	50mM HEPES
	10mM KCl
	280mM NaCl
	12mM Dextrosa
	1.5mM Na <sub>2</sub> HPO <sub>4</sub>

## 1.7. siRNA TRANSFECTION

Transient siRNA transfections were performed using HiPerFect Transfection Reagent (Qiagen, ref.301705) or Lipofectamine® RNAiMax (Invitrogen, ref.13778), according to manufactures guidelines.

### 1.7.1. HiPERFECT TRANSFECTION

For HiPerFect-mediated transfections, reverse-transfection protocol was used and thus, cell seeding and transfection were carried out on the same day. The number of cells used in each case was calculated according to manufacturer's guidelines. siRNA oligos were transfected at 50nM final concentration. In the case of hTERT-RPE cells, 140.000 cells were plated in a 35cm<sup>2</sup> plate for each transfection. The proper volume of siRNA was added to a sterile tube, and then the mix of HiPerFect and OptiMEM (Gibco, ref.31985-070) was prepared (indicated in **Table 5**). The mix was added to the siRNA and it was incubated for 15-30 minutes. Finally, the cells in suspension were added to the tube with the transfection reagents, carefully mixed and seeded. Filter tips and clean gloves were used in all cases.

*Table 5. Volums used in HiPerFect Transfection in a 6-well plate.*

Culture format	Equivalent volume of 20µM of siRNA stock	Volume of HiPerFect	Volume of OptiMEM	Volum of cells (in a concentration of 77777cells/mL)
<b>6-well plate (35cm<sup>2</sup> plate)</b>	5µL	15µL	200µL	1.8mL

To prevent possible off-target effects, oligo sets containing 4 different sequences (ONTARGETplus SMARTpools; Dharmacon) were used in all cases, except in the case of OZF, where a mix of 3 different sequences was used. The siRNA concentration that resulted in an efficient decrease in target protein levels was analysed for each of them before experiments were conducted. The following siRNA oligos (Dharmacon) were transfected with HiPerFect reagent in hTERT-RPE cell line:

**Table 6. siRNA sequences used in this thesis in HiPerFect transfection.**

Target protein	Reference	Sequences
<b>Non-target (NT)</b>	D-001810-10-20	5'-UGGUUUACAUGUCGACUAA-3' 5'-UGGUUUACAUGUUGUGUGA-3' 5'-UGGUUUACAUGUUUUUCUGA-3' 5'-UGGUUUACAUGUUUUCCUA-3'
<b>FBH1</b>	L-017404-00-0005	5'-CCUCAACGCUGGUCAAGUA -3' 5'-AGGGAAGGGUGGAUUCUAU-3' 5'-GUGCCUAUUUGGUGUAAGA-3' 5'-AAACAAAACCCUGUCAUUA-3'
<b>Rad51</b>	L-003530-00-0005	5'-UAUCAUCGCCCAUGCAUCA-3' 5'-CUAAUCAGGUGGUAGCUCA-3' 5'-GCAGUGAUGUCCUGGAUAA-3' 5'-CCAACGAUGUGAAGAAAUU-3'
<b>OZF</b>	J-019625-05-002	5'-GCGAGAAGCUUUUCGAAUG-3'
	J-019625-06-002	5'-GCAAUCCAACCUUACUGA-3'
	J-019625-07-002	5'-GCGAACAUACUUUUGUA-3'

### 1.7.2. LIPOFECTAMINE® RNAiMAX TRANSFECTION

For Lipofectamine® RNAiMAX-mediated transfections, forward-transfection protocol was used and thus, cells were seeded to be 60-80% confluent at the time of the transfection. The Lipofectamine® RNAiMAX reagent was diluted in OptiMEM medium. In parallel, siRNA was also diluted in OptiMEM (the volumes used in 6-well plate was indicated in Table 7). Then, diluted siRNA was added to the diluted Lipofectamine® RNAiMAX reagent (1:1 ratio), and the mix was incubated at RT for 5 minutes. Finally, the siRNA-lipid complex was added to the cells. Experiments were performed after 1-2 days of transfection.

**Table 7. Volumes used in Lipofectamine® RNAiMax Transfection in a 6-well plate.**

Culture format	Equivalent volume of 20µM of siRNA stock	Volume of OptiMEM	Volume of Lipofectamine® RNAiMAX	Volume of OptiMEM
<b>6-well plate (35cm<sup>2</sup> plate)</b>	5µL	195µL	6µL	194µL

The following siRNA oligos (Dharmacon) were transfected with Lipofectamine® RNAiMAX reagent in HCT116 cell line:

**Table 8. siRNA sequences used in this thesis in Lipofectamine® RNAiMAX transfection.**

Target protein	Reference	Sequences
<b>Non-target (NT)</b>	D-001810-10-20	5'-UGGUUUACAUGUCGACUAA-3' 5'-UGGUUUACAUGUUGUGUGA-3' 5'-UGGUUUACAUGUUUUCUGA-3' 5'-UGGUUUACAUGUUUCCUA-3'
<b>Emi1</b>	L-012434-00-0005	5'-CAACAGACACUAAUAGUA-3' 5'-CGAAGUGUCUCUGUAAUUA-3' 5'-UGUAAUUGGGUCACCGAUUG-3' 5'-GAAUUUCGGUGACAGUCUA-3'
<b>OZF</b>	J-019625-05-002	5'-GCGAGAAGCUUUUCGAAUG-3'
	J-019625-06-002	5'-GCAAAUCCAACCUUACUGA-3'
	J-019625-07-002	5'-GCGAACAUCACUAAUUGUA-3'

## **2. CELL PROLIFERATION AND SURVIVAL ASSAYS**

### **2.1. COLONY FORMATION ASSAY**

Colony formation assay is based on crystal violet-mediated proteins and DNA staining of attached cells to evaluate the cell viability after the treatment at long-term conditions.

For colony formation assays, cells were seeded in 12-well plates and treated during the indicated times with HU or left untreated. Cells were then extensively washed with PBS and then released into fresh medium without HU. After some hours of release, cells were diluted (200 cells in each well) in 6-well plates. Seven days later, cells were fixed and stained with 1% crystal violet in 70% ethanol during 5 minutes at RT and the number of colonies was counted.

### 3. ELECTROPHORESIS AND WESTERN BLOT (WB)

#### 3.1. PREPARATION OF SAMPLES

Three different type of samples have been used to perform electrophoresis and WB analysis during this thesis: whole cell lysates, chromatin enriched fractions and iPOND extracts. The preparation of each of them was performed as explained below.

##### 3.1.1. WHOLE CELL LYSATES

For whole cell lysates, cells were washed with PBS and then lysed by adding a SDS (sodium dodecyl sulphate)-containing lysis buffer. Cells were collected by scraping.

The high amount of anionic detergent denaturalizes all the proteins, and the addition of protease and phosphatase inhibitors is not required in this case. Nevertheless, SDS precipitates at low temperature and thus, samples had to be collected at RT.

After adding the lysis buffer, lysates were viscous due to DNA denaturing. To fluidify the samples and degrade the DNA, they were heated at 97°C for 15 minutes and finally stored at -20°C.

<i>Lysis buffer (pH 6,8)</i>	67mM Tris
	2% SDS

##### 3.1.2. CHROMATIN ENRICHED FRACTIONS

Chromatin extraction was performed following a modified version of the protocol described on (Méndez and Stillman, 2000)<sup>621</sup>. Samples must be kept on ice and sterile material has to be used all the time.

First, cells were harvested by scraping on ice with ice-cold PBS, and then centrifuged at 660g for 5 minutes at 4°C. Supernatant was discarded and pellets could be stored at -80°C during several weeks.

Next, cells were lysed by adding buffer A (8 times the volume of the pellet), supplemented with freshly added protease and phosphatase inhibitors and Triton X-100. The optimal

concentration of Triton X-100 and the incubation time on ice must be set up for each cell line (from 0.1% to 0.5% of Triton X-100, and from 10 to 20 minutes of incubation). To do so, the degree of lysis and purified nuclei could be observed under microscopy. In the case of hTERT-RPE, lysis was performed with 0.1% Triton X-100-containing buffer A during 20 minutes on ice. In HEK293T cells, lysis was performed in 0.1% Triton X-100-containing buffer A during 10 minutes on ice. After that, cells were centrifuged at 600g for 5 minutes at 4°C.

Supernatants (S1 fraction), corresponding to the cytoplasmic fraction of the cells, were collected in a new tube and stored at -20°C. Pellets, corresponding to nuclei, were washed with buffer A (8 times the volume of the pellet) supplemented with protease and phosphatase inhibitors but without Triton X-100, and then centrifuged at 600g for 5 minutes at 4°C.

Supernatants were discarded and pellets (nuclei) were resuspended and incubated during 10 minutes on ice with buffer B (8 times the volume of the pellet, a critical point) supplemented with protease and phosphatase inhibitors. After incubation, cells were centrifuged at 1700g for 5 minutes at 4°C.

Supernatants (S2 fraction), corresponding to the nuclear soluble fractions, were collected in new tubes and stored at -20°C. Pellets, corresponding to chromatin-associated and nuclear matrix-bound proteins, were washed with buffer B (8 times the volume of the pellet) supplemented with inhibitors until they became transparent (more than two washes are not required). Supernatants were discarded each time by centrifugation at 600g for 5 minutes at 4°C.

Finally, pellets were resuspended in lysis buffer (3 times the volume of the pellet), which is the same one used in whole cell lysates. Since samples contained SDS, they were heated at 97°C for 15 minutes and finally stored at -20°C.

<i>Buffer A</i>	10mM HEPES, pH 7.4
	10mM KCl
	1.5mM MgCl <sub>2</sub>
	0.34M sucrose
	10% glycerol
	1mM DTT
	Protease inhibitors: 21μM leupeptine, 154nM aprotinine, 1mM PMSF
	Phosphatase inhibitors: 1mM NaF, 0.1mM sodium orthovanadate

<i>Buffer B</i>	3mM EDTA
	0.2mM EGTA
	1mM DTT
	Protease inhibitors: 21μM leupeptine, 154nM aprotinine, 1mM PMSF
	Phosphatase inhibitors: 1mM NaF, 0.1mM sodium orthovanadate

### 3.2. PROTEIN QUANTIFICATION

Protein quantification was performed using two different colorimetric assays: 1) Bradford assay<sup>622</sup>, which is based in Coomassie Blue G-250 dye binding, and 2) the Lowry assay<sup>623</sup>, based on copper-protein chelation.

#### 3.2.1. BRADFORD METHOD

The Bradford method relies on the binding of the dye Coomassie Blue G250 to the proteins. The binding of the dye to a protein causes a shift in the absorbance maximum of the dye from 465 to 595nm. The increase of absorption at 595nm is monitored to determine protein concentration.

This assay has certain limitations, as it cannot be used to quantify protein when the sample contains certain substances such as EDTA or detergents such as Triton X-100 or SDS, because they interfere with the estimation of protein concentration.

This assay was performed when RIPA buffer was used. Bovine serum albumin (BSA) was used to obtain the calibration curve.

Firstly, diluted Bradford solution was prepared by diluting Protein Assay Dye Reagent Concentrate (Bio-Rad, ref.500-006) with distilled water in proportion 1:4. Then, standards and samples were prepared by following the table below (Table 9). Replicates of each standard and sample were prepared twice.

**Table 9. Volumes required to prepare standards and samples in 96-well plates.**

	$\mu\text{g}$ of BSA (stock $1\mu\text{g}/\mu\text{L}$ )	$\mu\text{L}$ of sample	$\mu\text{L}$ of lysis buffer	$\mu\text{L}$ of water
<b>Standards</b>	0	-	1	39
	1	-	1	38
	2	-	1	37
	4	-	1	35
	8	-	1	31
	16	-	1	29
<b>Samples</b>	-	1	-	39

After that,  $160\mu\text{L}$  of diluted Bradford solution was added to the wells and mixed well by pipetting up and down several times. The mix was incubated for 10 minutes at RT. Finally, the absorbance of each well was measured with a multimode plate reader (Spark<sup>®</sup>, TECAN) at 595nm and 450nm, and the ratio 595nm/450nm was used to estimate the protein concentration, since it has been demonstrated that this ratio is linearly correlated with protein concentration<sup>624</sup>.

With the absorbance values of the standards, a simple lineal regression was performed. With the absorbance values of the samples, the average of replicates was calculated, it was interpolated, and the concentration of each sample was determined.

### 3.2.2. LOWRY METHOD

The Lowry method was developed approximately 60 years ago. The Lowry reaction is based on the amplification of the Biuret reaction, in which the peptide bonds of proteins react with copper under alkaline conditions to produce  $\text{Cu}^+$ , and a subsequent reaction with the Folin-phenol reagent, consisting in the oxidation of the aromatic residues of the protein by the reagent. In the Folin-Ciocalteu reaction, the phosphomolybdate present in the reagent is reduced to heteropolymolybdenum blue, which absorbs light at 750nm.

This assay was used for protein quantification in samples lysed with buffers-containing more than 1% SDS. BSA was used to obtain the calibration curve.

First, Solution A was prepared as a reaction mixture of the reagents 1, 2 and 3, following the proportions 48:1:1. Secondly, Solution B was prepared by diluting Folin-Ciocalteu's Phenol reagent (Merck, ref.1.09001) in distilled water in proportion 1:1.

Then, the standards and the samples were prepared by following the table below (Table 10). Replicates of each standard and sample were prepared twice.

**Table 10. Volumes required to prepare standards and samples in 96-well plates.**

	$\mu\text{g}$ of BSA (stock $1\mu\text{g}/\mu\text{L}$ )	$\mu\text{L}$ of sample	$\mu\text{L}$ of lysis buffer	$\mu\text{L}$ of water
<b>Standards</b>	0	-	2	8
	0.5	-	2	7.5
	1	-	2	7
	2	-	2	6
	4	-	2	4
	8	-	2	0
<b>Samples</b>	-	2	-	8

After that,  $180\mu\text{L}$  of Solution A was added to the wells and mixed well by pipetting. The mix was incubated for 10 minutes at RT.

Then,  $20\mu\text{L}$  of Solution B was added and mixed well by pipetting. It was incubated 30 minutes at RT and the absorbance is measured at 750nm in multimode plate reader (Spark®, TECAN). With the absorbance values of the standards, a simple lineal regression was performed. With the absorbance values of the samples, the average of replicates was calculated, it was interpolated, and the concentration of each sample was determined.

<i>Solution A</i>	Solution 1: 2% of $\text{Na}_2\text{CO}_3$ in 0.1M NaOH
	Solution 2: 0.5% $\text{CuSO}_4$
	Solution 3: 1% sodium potassium tartrate

<i>Solution B</i>	Folin-Ciocalteu's Phenol reagent
	Distilled water

### 3.3. SAMPLE PREPARATION

Samples were prepared to load between 15-50 $\mu$ g of protein in each well. The volumes of the different samples were normalized between them by adding lysis buffer. Finally, loading buffer (Laemmli buffer<sup>625</sup>) was added at 1x final concentration and samples were boiled for 5 minutes at 97°C. The presence of DTT reduces any disulphide bridges present that hold together the protein tertiary structure. On the other hand, SDS is an anionic detergent which binds strongly and denatures the protein.

<i>Laemmli Buffer</i> (loading buffer)	67mM Tris-HCl, pH 6.8
	10% glycerol
	2% SDS
	10mM DTT
	0.01% Bromophenol blue

### 3.4. ELECTROPHORESIS AND WB

Electrophoresis combined with WB is a semi-quantitative method used to detect and quantify the relative abundance of proteins of interest on a certain sample. The first step consists in separating the proteins by SDS-PAGE electrophoresis. The SDS present on the samples, on the gel and on the buffers, denatures the proteins and adds negative charges on them, so they can migrate towards the positive pole, while they are separated according to their molecular weight. Separated proteins are then transferred to nitrocellulose membranes, where they are detected by incubation with primary and secondary antibodies. The primary antibodies recognize the protein of interest via the variable region (Fab), and they are recognized by secondary antibodies conjugated to HRP (horseradish peroxidase) enzyme on their constant region (Fc). Finally, these secondary antibodies are detected by the addition of peroxidase substrate ECL (enhanced chemiluminescent substrate), which reacts with the HRP enzyme present on the secondary antibody, giving a chemiluminescent substrate.

*\* The electrophoresis and WB experiments were performed at least three times in each case.*

### 3.4.1. SDS-PAGE ELECTROPHORESIS

The SDS-polyacrylamide gels can be prepared with different amounts of acrylamide, which provides different size of pores. For high molecular weight proteins, a lower amount of polyacrylamide was required to form larger pores. For low molecular weight proteins, a higher amount of polyacrylamide was used to form smaller pores. Gels have two different sections, the stacking and the resolving. While the former allows the alignment of the different samples loaded in the gels due to its larger pores, the latter is the one properly separating the proteins.

The system Mini-PROTEAN® of Bio-Rad was used in all our experiments.

**Table 11. Volumes required to prepare stacking and resolving gels.**

	Resolving gel			Stacking gel
	6%	10%	12%	
<b>Solution 1 (mL)</b>	5	5	5	-
<b>Solution 2 (mL)</b>	2	3.4	4	0.36
<b>Solution 3 (mL)</b>	-	-	-	1.5
<b>Ultrapure water (mL)</b>	3	1.6	1	1.2
<b>TEMED (μL)</b>	14	14	14	7.5
<b>1,5APS 13% (μL)</b>	50	50	50	30

*Gel solutions*

Solution 1: 0.75M Tris-HCl pH 8.8, 0.2% SDS

Solution 2: 30% Acrylamide, 0.8% Bis-acrylamide

Solution 3: 0.25M Tris-HCl pH 6.8, 0.2% SDS

The mix of resolving gels were prepared, adding the polymerizing agents last (Table 11). First, the mix of resolving gel was poured between the glasses of the structure built up to create the gels, and 1mL of ultrapure water was added slowly on top of the resolving mix, without disrupting it. Once polymerized, the ultrapure water was removed by decantation.

The mix of stacking gels was prepared (Table 11). It was poured on top of the resolving gel and immediately a gel comb was insert in order to create the loading wells. Once the stacking gel was polymerized, the glasses containing the gel were transferred from the building structure to the electrophoresis bucket. The running buffer was added until the gel was completely sunk, and the comb was removed.

<i>Electrolyte buffer</i>	25mM Tris
	192mM Glycine
	0.1% SDS

In one of the loading wells, 2.5µL of protein standard (Precision All Blue Standards (ref.1610373) or Low (ref.1610304) or High Range Unstained Standards (ref.1610303), all from Bio-Rad) was loaded. The previously prepared samples were then loaded in the rest of wells with a Hamilton syringe.

The electrophoresis bucket was plugged to the power source and set at 100V to run the gels (Figure 77). When samples reached the bottom of the bucket (it can be determined by the intense blue band of bromophenol that Laemmli buffer contained), the power source was unplugged, and the next step was performed.

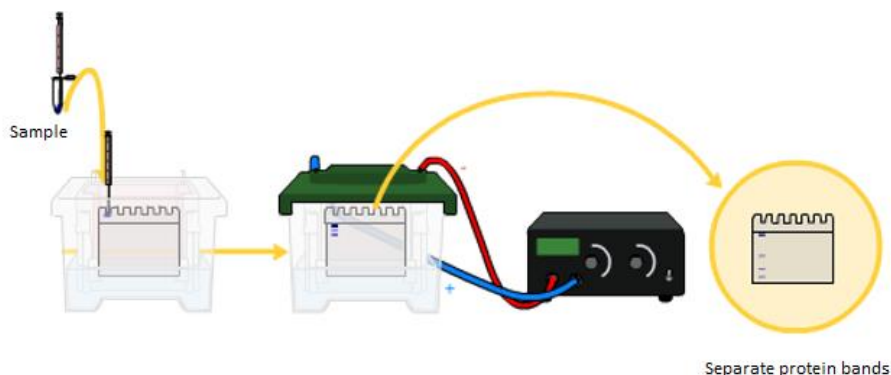


**Figure 77. Diagram of SDS-PAGE.**

### 3.4.2. TRANSFERENCE OF PROTEINS TO NITROCELLULOSE MEMBRANES

Once proteins had been properly separated according to their molecular weight, they had to be transferred into a nitrocellulose membrane to be able to incubate them with specific antibodies, avoiding the interference of diffusion and denaturing reagents.

The membranes needed to be hydrated by sinking them in transfer buffer. All the sponges, filter papers, membranes and gels were equilibrated in transfer buffer. The sandwich was assembled with the necessary parts stacked for the transference, as indicated in Figure 78. No

air bubbles could remain between the membrane and the gel. Two sponges and filter papers were used to build up pressure inside the sandwich.

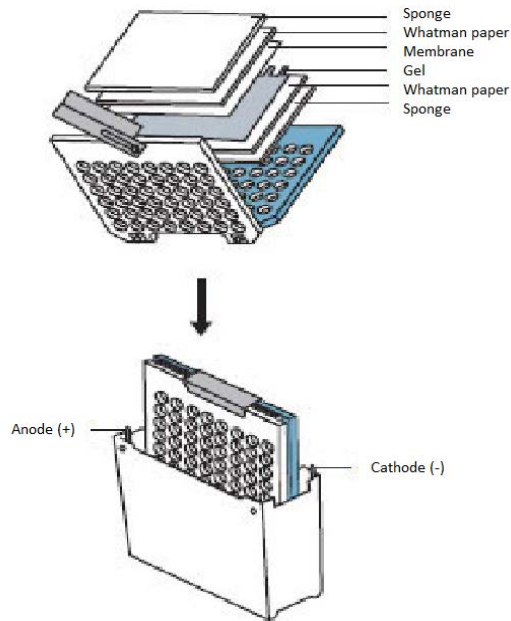


**Figure 78. Diagram of protein transference to a nitrocellulose membrane**

The sandwich was transferred to a transference bucket filled with transfer buffer. The bucket was plugged to a power source at 4°C and the desired voltage was set. During this thesis, the transference was performed during 2 hours at 70V. After this time, the membrane was dried in order to fixate the proteins. For proteins with a molecular weight higher than 120KDa, the transference was performed using a 2x transference buffer, which contains twice the SDS and electrolyte concentration.

<i>Transfer buffer</i>	25mM Tris
	192mM Glycine
	0.02% SDS
	20% Ethanol
<i>Transfer buffer</i> 2x	50mM Tris
	384mM Glycine
	0.04% SDS
	20% Ethanol

### 3.4.3. PONCEAU S STAINING

The Ponceau S is a sodium salt of a diazo dye of a light red colour, that can be used to rapidly and reversibly stain and detect protein bands on nitrocellulose membranes. Its staining allowed the determination of the efficiency of the previous steps of the WB and it could be used as a loading control.

The membrane was incubated in Ponceau S solution for 1 minute. After that, it was destained with several washes with distilled water to diminish background colour. The standard protein was marked with a pencil. Finally, the membrane was washed until it was completely destained.

<i>Ponceau Protein Stain Solution</i>	0.1% Ponceau reagent (Sigma, P3504)
	5% Acid acetic

### 3.4.4. BLOCKING

Membranes must be blocked to avoid the antibodies to be non-specifically attached to the membranes. Since the membrane has the ability to bind to proteins, it is necessary to saturate it before incubating the antibodies. Blocking of membranes was performed using 3% milk-containing Tris-Buffered Saline-Tween20 (TBS-T) for total proteins, or 3% BSA-containing TBST-T. The membranes were incubated with those blocking buffers for 1 hour while shaking at RT.

<i>TBS-T</i>	20mM Tris
	150mM NaCl
	0.05% Tween20

### 3.4.5. INCUBATION WITH PRIMARY AND SECONDARY ANTIBODIES

Blocked membranes were incubated overnight at 4°C with primary antibodies against the proteins of interest, diluted in 3% BSA-containing blocking solution. The incubation was static in a humidity chamber. The dilution used for each primary antibody was specified below (Table 12).

After that, membranes were washed three times with TBS-T (for 7 minutes each wash), and then incubated during 1h at RT with secondary antibodies against the primary ones, diluted in 5% milk-containing TBS-T in a static manner. The dilution used for each secondary antibody was specified below (Table 13). Then, the membranes were washed twice with TBS-T and once with TBS (7 minutes each).

<i>TBS</i>	20mM Tris
	150mM NaCl

### 3.4.6. DEVELOPING

Finally, the membranes were developed by adding an ECL solution (EZ-ECL; Biological Industries, ref.20-500-120) that reacts with the HRP enzyme present on the secondary antibody, giving a chemiluminescent reaction. When the substrate of peroxidase (luminol) was added, it resulted in an excited state, and when it returned to stable conditions, it emitted light, which was captured by the exposition of the membrane to a film (AGFA Cunik 60, Fujifilm) or a camera (ChemiDoc™, BioRad). The membranes were exposed different times to obtain a good visualization of the proteins.

### 3.4.7. ANTIBODIES

*Table 12. Primary antibodies with the commercial provider, reference and dilution used in this thesis for WB.*

Primary antibodies	Reference	Source	Dilution
<b>Cdc45 (H-303)</b>	Santa Cruz; sc-55569	Rabbit	1/200
<b>CDK4 (H-303)</b>	Santa Cruz; sc-709	Rabbit	1/500
<b>Cyclin A2 (H-432)</b>	Santa Cruz; sc-751	Rabbit	1/500
<b>Cyclin B1 (GNS1)</b>	Santa Cruz; sc-245	Mouse	1/200
<b>Emi1</b>	Invitrogen; 37-6600	Mouse	1/100
<b>GAP120</b>	Santa Cruz; sc-63	Mouse	1/200
<b>H3</b>	Abcam; ab1791	Rabbit	1/2000
<b>HA</b>	Sigma; H6908	Rabbit	1/1000
<b>Lamin B1 (M-20)</b>	Santa Cruz; sc-6217	Goat	1/500
<b>MCM2 (H-126)</b>	Santa Cruz; sc-10771	Rabbit	1/200
<b>MCM3</b>	Homemade (by Dr. Juan Méndez)	Rabbit	1/1000

<b>MCM6 (C-20)</b>	Santa Cruz; sc-9843	Goat	1/200
<b>OZF</b>	Sigma, HPA003358	Rabbit	1/3000
<b>P-Chk1 (S296)</b>	Cell signalling; #2349	Rabbit	1/1000
<b>Psf3 (GINS3)</b>	Bethyl Laboratories; A304-124A	Rabbit	1/2000
<b>Rad51 (H-92)</b>	Santa Cruz; sc-8349	Rabbit	1/200
<b>RPA32</b>	Cell signalling; #2208	Rat	1/1000

**Table 13. Secondary antibodies with the commercial provider, reference and dilution used in this thesis for WB.**

<b>Secondary antibodies</b>	<b>Reference</b>	<b>Dilution for whole cell lysates</b>	<b>Dilution for chromatin-enriched fractions and iPOND extracts</b>
<b>Anti-Rabbit IgG (H+L) HRP Conjugate</b>	BioRad, 1706515	1/3000	1/2000
<b>Anti-Mouse IgG (H+L) HRP Conjugate</b>	BioRad, 1706516	1/3000	1/2000
<b>Anti-Rat IgG (whole molecule) Peroxidase conjugate</b>	Sigma, A9037	1/3000	1/2000
<b>Anti-Goat IgG (whole molecule)-Peroxidase</b>	Sigma, A5420	1/10000	1/5000

## 4. IPOND: ISOLATION OF PROTEINS ON NASCENT DNA

iPOND<sup>550,551</sup> is a powerful technique to analyse the proteins bound directly or indirectly to the nascent DNA. The method is based on the isolation of proteins complexes crosslinked to EdU thymidine analogue-containing nascent DNA, which allows the conjugation of biotin through a click reaction and the purification of proteins crosslinked by high affinity interaction between biotin and streptavidin. Proteins obtained by iPOND can then be analysed by electrophoresis and WB (iPOND+WB) or by the identification/quantification by mass spectrometry (iPOND+MS). In this thesis only the analysis by WB was performed, and to do so one 100cm<sup>2</sup> plate per condition was used. The biotinylation and sonication of the samples were always validated before performing the modified version of iPOND<sup>128</sup>.

### 4.1. PREPARATION OF SAMPLES

The iPOND procedure begins by incubating cells with EdU (referenced in Table 2) for a short period of time (15 minutes) to label the replication forks, and then some dishes were treated while others were left untreated (Pulse control condition). Cells were fixed in 1% PFA-containing PBS for 10 minutes at RT. After crosslinking, PFA was quenched with 0.125mM glycine (pH 7) for 5 minutes at RT. Then, cells were washed twice with PBS and finally harvested in ice-cold PBS, supplemented with protease inhibitor cocktail (PIC, Roche 14424700), by scrapping. Cells' pellets were obtained by centrifugation at 1000g for 10 minutes at 4°C and finally stored at -80°C (during a couple of weeks).

#### 4.1.1. PROCESSING: BIOTINYLATION AND SONICATION OF SAMPLES

Cells' pellets were lysed by incubation of 500µL of lysis buffer (ChIP-IT® Express Shearing Kit, Active Motive 53032), supplemented with 0.05% PCI-containing PBS and 0.5mM PMSF, during 30 minutes on ice.

Lysates were passed 10 times through a 21-gauge needle, and then nuclei were pelleted by centrifugation at 2400g for 10 minutes at 4°C. Pellets were washed with PCI-containing PBS and centrifuged again at 2400g for 10 minutes at 4°C.

In order to conjugate biotin with the EdU incorporated into nascent DNA, click reaction was performed. This reaction is based on the presence of an alkyne functional group in EdU that allows copper-catalysed cycloaddition to a biotin azide to yield a stable covalent linkage. To this end, cells' nuclei were incubated during 30 minutes at RT with 500µL of click reaction solution.

<i>Click reaction solution</i>	100mM Tris-HCl, pH 8
	2mM CuSo4
	0.2mM biotin azide (Invitrogen B10184)
	100mM ascorbic acid

*\*Reagents must be added to ultrapure water in this order*

After click reaction, nuclei were pelleted by centrifugation, washed again as previously with PIC-containing PBS and then pelleted again by centrifugation at 2400g for 10 minutes at 4°C.

Finally, pellets were resuspended in 600µL of shearing buffer (Active Motif, ref.101231) supplemented with 0.05% PCI-containing PBS, sonicated in a water sonicator (Bioruptor, Diagenode) for 15 minutes at high intensity (30s on/30s off pulses), and centrifuged at 15000g for 20 minutes at 4°C. After that, supernatants were collected and divided it in:

- **Input:** 30µL of sample, and 30µL of lysis buffer was added. Input was boiled for 15 minutes (in case of proteins of high molecular weight, samples were boiled during 30 minutes). Input was finally quantified by Lowry assay (section 3.2.2).
- **DNA purification and validation of sonication:** 30µL of sample
- **Dot-blot:** 10µL of sample
- **iPOND extract:** 530µL of sample

The samples were stored at -20°C.

*\* Samples must be kept on ice if not specified otherwise.*

## 4.2. DNA PURIFICATION AND VALIDATION OF SONICATION

For DNA purification, 30 $\mu$ L of processed cell extracts (5%) were mixed and incubated overnight at 65°C with 170 $\mu$ L of ultrapure water, 10 $\mu$ L of 5M NaCl and 1 $\mu$ L of RNase (Active Motif, ref.101249; 10 $\mu$ g/ $\mu$ L) to reverse the crosslink.

After that, 1 $\mu$ L of Proteinase K (Ambion, AM2546; 20 $\mu$ g/ $\mu$ L) was added, and samples were incubated at 55°C during more than 4 hours. Then, 1 $\mu$ L of Glicogen (20 $\mu$ g/ $\mu$ L, no essential), 2.2 $\mu$ L of sodium acetate 3M pH 5.2 and 267 $\mu$ L of cold 100% ethanol were added into the sample and mixed. The mix was finally incubated overnight at -20°C.

After incubation, the samples were centrifuged at maximum speed during 30 minutes at 4°C. The pellet was washed once with cold 70% ethanol, and centrifuged at maximum speed during 10 minutes at 4°C. The pellet was left at 37°C to dry it, and finally it was incubated with 20 $\mu$ L of ultrapure water (previously tempered at 55°C) during 20 minutes at 55°C to elute DNA.

The obtained DNA was quantified using a nanodrop (ThermoFisher Scientific). After that, 10ng of DNA was send to Functional Genomics Facility of IDIBAPS to analyse with Bioanalyzer 2100 the fragments of DNA obtained. On the other hand, the sample left was loaded into a Red Safe (INtRON, ref. 21141)-containing 1.5% agarose gel. Finally, DNA fragments were visualized using Infinity system of gel documentation (Vilber). Fragments of 100-300bp were properly considered to perform iPOND technique.

## 4.3. DOT-BLOT

The biotinylation of the samples was analysed by dot-blot. To this end, 1 $\mu$ L of processed cell extract was spotted onto a nylon membrane (Hybond-N+, Amersham) in triplicate. As a standard, a serially diluted 5'-biotinylated oligonucleotide (5'-CTCATAGCTCACGCTGTAGGTATCTCAGTTCCGG-3') was used, and also was spotted in triplicate on the membrane. After that, membranes were air-dried at room-temperature for 15 minutes, and then DNA was crosslinked to the membrane by UV light using a GS Gene Linker UV Chamber (program C-L, 125mJ). After crosslinking, membranes were rehydrated with TBS-T, blocked with 5mg/mL salmon sperm DNA- (Sigma) containing TBS-T for 1 hour at room-temperature, and washed several times with TBS-T before incubation with primary antibody. A primary antibody against Avidin, which was already conjugated to HRP enzyme, was used in

this case. Membranes were incubated during 15 minutes at room-temperature with the primary antibody (1/1000), washed several times with TBS-T and finally developed using ECL.

#### 4.4. iPOND

The modified version of iPOND<sup>128</sup> was performed as follows. For each condition, 500µL of beads were used. Streptavidin-conjugated Dynabeads M-280 (Invitrogen) were washed three times with cold 1x ChIP buffer and then blocked during 1 hour at ROOM-TEMPERATURE with 10 mg/mL salmon sperm DNA- (Sigma-Aldrich) containing PBS. Then blocking solution was removed and beads were resuspended in 4.5mL of cold 1x ChIP dilution buffer with 10 mg/mL salmon sperm DNA. Processed cell extracts (aprox. 500µL) were then incubated with previously blocked Dynabeads (1:10) for 30 minutes at RT. Finally, beads were washed twice with low salt buffer and twice with high salt buffer (between washes, 5 minutes in rotation at RT), and then resuspended in 200µL of Laemmli buffer 2X for WB analysis. Finally, samples were boiled during 30 minutes at 97°C. Samples must be kept on ice before the addition of Laemmli buffer if not specified otherwise.

<i>1x ChIP buffer</i>	1% Triton X-100 2mM EDTA, pH 8 150mM NaCl 20mM Tris-HCl, pH 8 20mM beta-glycerol phosphate 2mM Na <sub>3</sub> VO <sub>4</sub>	
<i>Low salt buffer</i>	1% Triton X-100 2mM EDTA, pH 8 150mM NaCl 20mM Tris-HCl, pH 8	<i>High salt buffer</i>
		1% Triton X-100 2mM EDTA, pH 8 500mM NaCl 20mM Tris-HCl, pH 8

## 5. IMMUNOPRECIPITATION

In this thesis, the interaction between different proteins was analysed by immunoprecipitation, which is a small-scale affinity purification of antigens using specific antibodies that are immobilized on agarose resin.

### 5.1. IMMUNOPRECIPITATION OF HA-OZF

In this case, a pre-immobilized antibody approach was used, since anti-HA antibody was bound to agarose and was used to immobilize the protein HA- tagged OZF. This immunoprecipitation was used to check if OZF protein interacts with other replisome proteins.

The HEK293T transfected cells with HA-OZF were collected by scrapping with ice-cold PBS on ice. Cells were centrifugated at 600g during 5 minutes at 4°C and pellets.

To perform the immunoprecipitation, firstly nuclei were obtained from the samples (already explained in section 3.1.2). Cells were lysed by the addition of buffer A (8 times the volume of the pellet), supplemented with freshly added protease and phosphatase inhibitors and 0.1 % Triton X-100 in HEK293T cells, during 10 minutes on ice. After that, cells were centrifuged at 600g for 5 minutes at 4°C. Pellets were washed with buffer A (8 times the volume of the pellet), supplemented with freshly added protease and phosphatase inhibitors and without Triton X-100. Cells were centrifuged at 600g for 5 minutes at 4°C, the supernatant was discarded, and pellet corresponded to nuclei was kept.

Secondly, nuclei were lysed by resuspending the pellets by the addition of buffer RIPA250 (5 times the volume of the pellet), supplemented with DNase (8 units/100µL), and nuclei were incubated during 45 minutes at 4°C in rotation. Nuclei were centrifugated at 14100g during 10 minutes at 4°C to eliminate non-soluble fractions. Supernatants were collected (soluble fraction), and pellets were discarded. The soluble fraction of nuclei was quantified by Bradford assay (see in section 3.2.1).

Finally, immunoprecipitation was performed. Firstly, 20µg of protein was separated as INPUT, and stored at -20°C. Then, 50µL per sample of Monoclonal Anti-HA-Agarose antibody (clone HA-7, Sigma, A20956) was washed with PBS five times, and finally RIPA250 buffer was added to the initial volume taken. After that, the beads were incubated with 1000-1500µg of protein

obtained from soluble nuclei fraction (the volumes were normalized between them by adding RIPA250 buffer) during 3 hours at 4°C in rotation. After incubation, samples were centrifuged at 10000g for 30 seconds. Pellets were the bound fraction, while supernatant was kept as not bound fraction. Bound fraction was washed three times with 1mL of RIPA250. To perform the immunodetection, loading buffer 4x was added to the beads. The bound and not bound fractions were stored at -20°C since electrophoresis was performed. Samples must be kept on ice before the addition of Laemmli buffer if not specified otherwise

## **5.2. IMMUNOPRECIPITATION OF MCM3**

For MCM3 immunoprecipitation, a protocol from Dr. Juan Méndez's laboratory was used. Briefly, a free antibody approach was used: the free and unbound antibody was allowed to form immune complexes in the cell lysate and the complexes were then retrieved to the beads. In this case antibodies against MCM3 was used to purify the complexes bound to those proteins and analyse them after HU treatment. This technique was performed in hTERT-RPE cells, and the volumes indicated are for a 150cm<sup>2</sup> plate.

Firstly, chromatin solubilization was performed from samples collected as in section 3.1.2. For nuclei obtaining, cells were lysed by the addition of 400µL of buffer A, supplemented with freshly added protease and phosphatase inhibitors and 0.1% Triton X-100, and incubated for 20 minutes. After that, cells were centrifuged at 600g for 5 minutes at 4°C. Supernatants (S1 fraction), corresponding to the cytoplasmic fraction of cells, were collected in a new tube and stored at -20°C. Pellets, corresponding to nuclei, were washed with 400µL of buffer A supplemented with protease and phosphatase inhibitors but without Triton X-100, and then centrifuged at 600g for 5 minutes at 4°C. Supernatants were discarded and, to obtain soluble chromatin, pellet (nuclei) were incubated with 1mM CaCl<sub>2</sub> – containing buffer A (400 µL) and 0.2U of micrococcal nuclease (Sigma, N3755) was added. It was incubated 2 minutes at 37°C and the reaction was stopped by adding 1mM EGTA to the mix. The nuclei were collected by centrifugation as above. Finally, the pellet was resuspended and incubated during 30 minutes on ice with 400µL of buffer B supplemented with protease and phosphatase inhibitors, with occasional mild vortexing. After incubation, samples were centrifuged at 1700g for 5 minutes at 4°C. Pellet (P2 fraction) was enriched in insoluble chromatin and nuclear matrix proteins.

Supernatant (S2 fraction) corresponded to solubilized chromatin and this was used for immunoprecipitation.

Finally, MCM3 immunoprecipitation was performed. First, 20 $\mu$ L of solubilized chromatin were separated as INPUT, 20 $\mu$ L of loading buffer 4X was added to it and it was stored at -20°C. Then, half the volume of the sample (approximately 180 $\mu$ L) was incubated with 4 $\mu$ L of anti-MCM3 (homemade, from Dr. Méndez; Rabbit) and the other half (approximately 180 $\mu$ L) was incubated with 40 $\mu$ L of anti-IgG (Rabbit, Sigma, I8140) during 1 hour at 4°C in rotation.

Meanwhile, the Pierce® Protein A Agarose beads (ThermoScientific, 20333) were washed: 40 $\mu$ L of beads per condition was used, and washed with PBS five times, and finally buffer B was added to the initial volume taken.

After adding 40 $\mu$ L of beads per condition, samples were incubated for 1 hour at 4°C in rotation. Finally, samples were centrifuged at 10000g for 30 seconds. Pellets were the bound fraction, while supernatant was kept as not bound fraction. Bound fraction was washed twice with wash buffer 1. To perform the immunodetection, loading buffer 4x was added to the beads. The bound and not bound fractions were stored at -20°C since electrophoresis was performed.

<i>Wash buffer 1</i>	50mM Tris-HCl, pH 7.4
	150mM NaCl
	1mM EDTA
	1% Triton X-100
<i>Wash buffer 2</i>	50mM Tris-HCl, pH 7.4
	250mM NaCl
	1mM EDTA
	1% Triton X-100

*\* Samples must be kept on ice before the addition of Laemmli buffer if not specified otherwise.*

## 6. FLOW CYTOMETRY

Flow cytometry was used to analyse different cell features, such as DNA content, as well as to determine the number of cells in S- phase or in mitosis, by a combined analysis of DNA content, BrdU and MPM2. For this analysis, cells were incubated with BrdU-containing medium before treating them as indicated. Then cells were harvested by trypsinization and centrifuged at 660g for 5 minutes at 4°C. After that, cell pellets were washed with ice-cold PBS and centrifuged as before. Finally, cells were resuspended in ice-cold PBS, diluted 1:10 in cold-ethanol 70% and stored at -20°C during at least 2 hours to fix them. Samples can be stored at -20°C for several months.

After fixation, cells were washed with PBS-T, and then centrifuged at 660g for 5 minutes at 4°C. Then DNA was denatured by incubation with 0.1% Triton X-100-containing 2M HCl-PBS solution for 15 minutes at RT. HCl was then neutralized by washing twice with borate buffer (0.1M Na<sub>2</sub>B<sub>4</sub>O<sub>7</sub>·10H<sub>2</sub>O, being the pH adjusted to 8.5 by the addition of 0.1M boric acid solution), which was removed each time by centrifugation at 660g for 5 minutes at 4°C. After neutralization, cell pellets were rinsed with PBS-T and centrifuged as above. Then the blocking step was performed by incubation of cells with 3% BSA-containing PBS-T for 1 hour at RT. After blocking, cells were centrifugated as above and cell pellet was incubated with primary antibodies anti-BrdU (Abcam, ab6326; Rat; 1/250) and anti-MPM2 (Millipore, #05-368; Mouse; 1/250) diluted in blocking solution for 1 hour at RT in rotation. After that, cells were centrifugated as above. Finally, cell pellets were washed with PBS-T and incubated with secondary antibodies Alexa488-conjugated anti-rat (Invitrogen, A21208; 1/400) and Alexa647-conjugated anti-mouse (Invitrogen,A31571; 1/500) diluted in PBT-T for 45 minutes at RT in dark, washed again with PBT-T and finally resuspended in 1% propidium iodide-containing PBS, supplemented with 1mg/mL RNase (Sigma, ref.R4875). Cells were incubated with this solution during 30 minutes at 37°C before flow cytometry analysis with BD FACSCalibur (Cytometry and Cell Sorting Core Facility, IDIBAPS). The analysis of the data was performed with FlowJo software.

<i>PBS</i>	145mM NaCl	<i>PBS-T</i>	145mM NaCl
	6mM Na <sub>2</sub> HPO <sub>4</sub>		6mM Na <sub>2</sub> HPO <sub>4</sub>
	2.5mM NaH <sub>2</sub> PO <sub>4</sub>		2.5mM NaH <sub>2</sub> PO <sub>4</sub>
			0.05% Tween20

## 7. IMMUNOFLUORESCENCE

As flow cytometry, immunofluorescence is a useful technique to analyse several cell features. It uses the specificity of primary antibodies to their antigen, to detect them with secondary antibodies conjugated to fluorescent molecules than can be visualized by fluorescent microscopy.

For flow cytometry analysis, cells are maintained in suspension. By contrast, cells are attached to coverslips for immunofluorescence techniques and mounted onto slides with mowiol after the immunofluorescence.

Images were acquired using Leica TCS-SL or Zeiss LSM880 confocal microscopies (Confocal Microscopy Unit Core Facility, UB), and analysed using Fiji (Image J) software.

*\* Coverslips can be kept for several months at 4°C into dark chambers.*

### 7.1. 53BP1/CycD1, 53BP1/ $\gamma$ H2AX AND 53PB1 IMMUNOFLUORESCENCE

Previously grown attached in coverslips and treated, cells were rinsed with PBS and fixed with 2% PFA-containing PBS for 20 minutes at RT. After several PBS washes, cells were permeabilized with 0.2% Triton X-100-containing PBS for 10 minutes at RT and washed with PBS for 5 minutes. Then the cells were incubated with blocking solution (3% FBS- and 0.1% Triton X-100-containing PBS) for 1 hour at RT. After blocking, cells were incubated with the indicated primary antibodies anti-53BP1 (Abcam, ab36823; Rabbit; 1/500), anti-YH2AX (Millipore, #05-636; Mouse; 1/3000) or anti-CycD1 (DCS-6, sc-20044; 1/100) diluted in blocking solution for 45 minutes at 37°C. After 15 minutes washing in blocking solution at RT in agitation, cells were incubated with Alexa488-, Alexa555-, or Alexa647-conjugated secondary antibodies (Invitrogen, 1/500) diluted in blocking solution for 20 minutes at 37°C. Then, cells were washed again with blocking solution at RT and DNA was counterstained with DAPI (Sigma-Aldrich, ref.D9564). Finally, coverslips were mounted onto slides with mowiol-containing media (Sigma-Aldrich, ref.81381). Cells counterstained with DAPI were used to analyse the presence of micronuclei, where indicated.

For EdU staining, the click reaction was performed previously to immunofluorescence. To this end, cells were incubated during 30 minutes at RT with 500 $\mu$ L of click reaction solution.

<i>Click reaction solution</i>	100mM Tris-HCl, pH 8
	2mM CuSO <sub>4</sub>
	1 $\mu$ M Alexa488- azide (Invitrogen, A10266)
	100mM ascorbic acid

*\*Reagents must be added to ultrapure water in this order*

## 7.2. ssDNA ANALYSIS BY BRdU IMMUNOFLOUORESCENCE UNDER NATIVE CONDITIONS

To analyse the accumulation of ssDNA in the nascent or parental DNA, a BrdU immunofluorescence was performed under native conditions. For nascent ssDNA detection, the BrdU incorporation in replication forks was done just for 10 minutes to label nascent DNA recently synthesized in cells previously attached to coverslips. For parental ssDNA detection, the BrdU incorporation was done for 48 hours and then released overnight in 10 $\mu$ M thymidine before HU treatment. After HU treatment, cells were rinsed with PBS, permeabilized with 0.5% Triton X-100-containing PBS for 10 minutes at RT and fixed with 3% PFA/2% sucrose-containing PBS solution for 10 minutes at RT. After several PBS washes, cells were incubated with blocking solution with 3% BSA/0.05% Tween 20-containing PBS during 1 hour at RT. Cells were incubated with the anti-BrdU (Becton Dickinson; 347580; Mouse; 1/50) antibody diluted in blocking solution for 1 hour at 37°C. After 15 minutes washing in blocking solution at RT in agitation, cells were incubated with Alexa488-conjugated anti-mouse secondary antibody (Invitrogen, A21202; 1/500) diluted in blocking solution for 20 minutes at 37°C. Then, cells were washed again with blocking solution at RT and DNA was counterstained with 1% propidium iodide-containing PBS supplemented with 0.1mg/mL RNase (Sigma, ref. R4875) during 15 minutes at 37°C or with DAPI (Sigma-Aldrich, ref. D9564). Finally, coverslips were mounted onto slides with mowiol (Sigma-Aldrich, ref.81381).

## 8. QUANTITATIVE IMAGE-BASED CYTOMETRY (QIBC)

QIBC experiments were performed by Amaia Ercilla PhD at the Centre for Chromosome Stability (University of Copenhagen) as described in (Toledo *et al.*, 2013)<sup>239</sup>. Briefly, cells were seeded in 96-well plates, treated as indicated and collected for immunofluorescence. Cells were incubated with 0.5% Triton X-100-containing PBS for 1 minute at 4°C to pre-extract the soluble proteins. After that, cells were fixed in 4% PFA-containing PBS for 10 minutes at RT. After fixation, cells were incubated with anti-BrdU (Becton Dickinson, 347580; Mouse; 1/50) or/and anti-RPA (homemade; Rabbit; 1/1000) primary antibodies for 1 hour at RT. Finally, cells were incubated with Alexa Fluor Plus secondary antibodies for 1 hour at RT. Images were acquired by a motorized Olympus IX-81 wide-field microscope and analysed with the ScanR Acquisition software.

## 9. DNA FIBER ANALYSIS

DNA fiber assay<sup>626</sup> is a powerful technique to analyse replication dynamics<sup>543</sup>. DNA fibers are labelled with two different thymidine analogues (CldU and IdU), which are visualized by incubation with different anti-BrdU antibodies that present different specificity for each of them. The incubation of cells with the different analogues, before and after 10mM HU treatment (which stalls replication forks and replication did not continue), allowed us to determine the number of stalled forks (labelled only with the first analogue), restarted forks (labelled with both analogues) and new origin firing events (labelled only with the second analogue) in each case. The incubation with both analogues, before and during 1mM HU treatment, allowed us to determine the replication speed during a perturbing condition that slows replication.

100000 cells were seeded on a 6-well plate (two wells per condition, one labelled and the other unlabelled). After pulse-labelling cells with CldU and IdU and treating as indicated (in the labelled well), cells were washed with cold PBS, harvested by trypsinization mixing labelled and unlabelled cells (in a 1:1 ratio), centrifuged at 660g for 5 minutes at 4°C and resuspended in 200µL of ice-cold PBS.

After that, DNA spreading was performed. To this end, 4µL of the cell suspension were spotted onto glass slides and cells were lysed with 8µL of spreading buffer directly on the cell drop and mixed carefully with the pipet tip. Slides were incubated for 2 minutes at RT (in flat position), and then were tilted at a 15° angle, allowing the drop to flow along the slide slowly. The stream of DNA was air-dried briefly during 10 minutes and then fixed with a freshly prepared mix of methanol:acetic acid (3:1) during 10 minutes. Once fixed, slides could be stored in a fridge for one month.

After fixation, the slides were washed three times with PBS. Then, they were washed once with denaturation buffer (2.5M HCl in ultrapure water) and incubated in denaturation buffer for 80 minutes at RT. After this time, HCl was removed from the slides by washing four times with PBS (incubating slides 5 minutes in the last wash).

After that, slides were washed once with blocking buffer (1% BSA- and 0.1% Tween20-containing PBS solution), and then were incubated with blocking solution on parafilm in dark and humid container during 30 minutes at RT.

Once blocked, slides were incubated with anti-BrdU primary antibody for CldU (Abcam, ab6326; Rat; 1/250) diluted in blocking solution for 75 minutes at RT. After that, slides were washed once with 0.1% Tween20-containing PBS and twice with PBS.

Then, slides were fixed with 4% PFA-containing PBS for 10 minutes at RT, washed again three times with PBS and incubated with secondary antibody Alexa555-conjugated anti-rat (Invitrogen, A21434; 1/500) diluted in blocking buffer for 60 minutes at RT. From this point on, slides were protected from light.

After incubation, slides were washed three times with PBS and incubated overnight with anti-BrdU primary antibody for IdU (Becton Dickinson, 347580; Mouse; 1/200) diluted in blocking solution at 4°C. After that, slides were washed once with 0.1% Tween20-containing PBS and twice with PBS and incubated with secondary antibody Alexa488-conjugated anti-mouse (Invitrogen, A21202; 1/500) diluted in blocking buffer for 60 minutes at RT. Then, slides were washed five times with PBS and mounted with Mowiol-containing media.

During the next 48 hours, images were acquired using Leica TCS-SL or Zeiss LSM880 confocal microscopies (Confocal Microscopy Unit Core Facility, UB). The analysis of images was performed using Fiji (Image J) software.

<i>Spreading buffer</i>	200mM Tris-HCl, pH 7.4
	50mM EDTA
	0.5% SDS

*\* All material and reagents used for DNA fiber assay were previously sterilized.*

## 10. STATISTICAL ANALYSIS

Statistical analysis was always performed using GraphPad Prism T software (version 6.1). Paired or unpaired *t*-test analyses were performed as indicated. Mann-Whitney test was performed in IdU or CldU track length analysis, where values do not follow a Gaussian distribution. Values marked with asterisks are significantly different: \**p* < 0.05, \*\**p* < 0.01, \*\*\**p* < 0.001, \*\*\*\**p* < 0.0001. “n.s.” was used to indicate absence of statistical significance.

## **BIBLIOGRAPHY**



1. Alberts, B. *et al.* *Molecular biology of the cell*. Garland Publishing, Inc. (1994).
2. Salazar-Roa, M. & Malumbres, M. Fueling the Cell Division Cycle. *Trends Cell Biol.* **27**, 69–81 (2017).
3. Vermeulen, K., Van Bockstaele, D.R., Berneman, Z. N. The cell cycle: a review of regulation, deregulation and therapeutic targets in cancer. *Cell Prolif.* **36**, 131–149 (2003).
4. Branzei, D. & Foiani, M. Maintaining genome stability at the replication fork. *Nat. Rev. Mol. Cell Biol.* **11**, 208–19 (2010).
5. Mazouzi, A., Velimezi, G. & Loizou, J. I. DNA replication stress: Causes, resolution and disease. *Exp. Cell Res.* **329**, 85–93 (2014).
6. Spencer, S. L. *et al.* The proliferation-quiescence decision is controlled by a bifurcation in CDK2 activity at mitotic exit. *Cell* **155**, 369–383 (2013).
7. Cappell, S. D., Chung, M., Jaimovich, A., Spencer, S. L. & Meyer, T. Irreversible APCdh1 Inactivation Underlies the Point of No Return for Cell-Cycle Entry. *Cell* **166**, 167–180 (2016).
8. Bassermann, F., Eichner, R. & Pagano, M. The ubiquitin proteasome system — Implications for cell cycle control and the targeted treatment of cancer. *BBA - Mol. Cell Res.* **1843**, 150–162 (2014).
9. Kastan, M. B. & Bartek, J. Cell-cycle checkpoints and cancer. *Nature* **432**, 316–323 (2004).
10. Lim, S. & Kaldis, P. Cdks, cyclins and CKIs: roles beyond cell cycle regulation. *Development* **140**, 3079–3093 (2013).
11. Cao, L. *et al.* Phylogenetic analysis of CDK and cyclin proteins in premetazoan lineages. *BMC Evol. Biol.* **14**, 10 (2014).
12. Malumbres, M. Cyclin-dependent kinases. *Genome Biol.* **15**, 1–10 (2014).
13. Malumbres, M. Physiological Relevance of Cell Cycle Kinases. *Physiol. Rev.* **91**, 973–1007 (2011).
14. Malumbres, M. & Barbacid, M. Cell cycle, CDKs and cancer: a changing paradigm. *Nat. Rev. Cancer* **9**, 153–166 (2009).
15. Malumbres, M. & Barbacid, M. Mammalian cyclin-dependent kinases. *Trends Biochem. Sci.* **30**, 630–641 (2005).
16. Satyanarayana, A. & Kaldis, P. Mammalian cell-cycle regulation: Several cdk, numerous cyclins and diverse compensatory mechanisms. *Oncogene* **28**, 2925–2939 (2009).
17. Hohegger, H., Takeda, S. & Hunt, T. Cyclin-dependent kinases and cell-cycle transitions : does one fit all ? *Nat. Rev. Mol. Cell Biol.* **9**, (2008).
18. Ortega, S. *et al.* Cyclin-dependent kinase 2 is essential for meiosis but not for mitotic cell division in mice. *Nat. Genet.* **35**, 25–31 (2003).
19. Berthet, C., Aleem, E., Coppola, V., Tessarollo, L. & Kaldis, P. Cdk2 Knockout Mice Are Viable. *Curr. Biol.* **13**, 1775–1785 (2003).
20. Tsutsui, T. *et al.* Targeted disruption of CDK4 delays cell cycle entry with enhanced p27(Kip1) activity. *Mol. Cell. Biol.* **19**, 7011–9 (1999).
21. Rane, S. G. *et al.* Loss of Cdk4 expression causes insulin-deficient diabetes and Cdk4 activation results in  $\beta$ -islet cell hyperplasia. *Nat. Genet.* **22**, 44–54 (1999).
22. Malumbres, M. *et al.* Mammalian cells cycle without the D-type cyclin-dependent kinases Cdk4 and Cdk6. *Cell* **118**, 493–504 (2004).
23. Santamaría, D. *et al.* Cdk1 is sufficient to drive the mammalian cell cycle. *Nature* **448**, 811–815 (2007).
24. Obaya, A. J. & Sedivy, J. M. Regulation of cyclin-Cdk activity in mammalian cells. *Cell. Mol. Life Sci.* **59**, 126–142 (2002).
25. Attwooll, C., Denchi, E. L. & Helin, K. The E2F family: Specific functions and overlapping interests. *EMBO J.* **23**, 4709–4716 (2004).
26. Wong, J. V., Dong, P., Nevins, J. R., Mathey-Prevot, B. & You, L. Network calisthenics: Control of E2F dynamics in cell cycle entry. *Cell Cycle* **10**, 3086–3094 (2011).
27. Chong, J. L. *et al.* E2f1-3 switch from activators in progenitor cells to repressors in differentiating cells. *Nature* **462**, 930–934 (2009).
28. Dimova, D. K. & Dyson, N. J. The E2F transcriptional network: Old acquaintances with new faces. *Oncogene* **24**, 2810–2826 (2005).
29. Morgan, D. O. CYCLIN-DEPENDENT KINASES : Engines , Clocks , and Microprocessors. *Ann. Rev. Dev. Biol.* (1997).

30. Fradet-Turcotte, A. *et al.* 53BP1 is a reader of the DNA-damage-induced H2A Lys 15 ubiquitin mark. *Nature* **499**, 50–4 (2013).
31. Nakayama, K. I. & Nakayama, K. Ubiquitin ligases: Cell-cycle control and cancer. *Nat. Rev. Cancer* **6**, 369–381 (2006).
32. Kaldis, P. The cdk-activating kinase (CAK): From yeast to mammals. *Cell. Mol. Life Sci.* **55**, 284–296 (1999).
33. Lolli, G. & Johnson, L. CAK-Cyclin-dependent activating kinase. *Cell Cycle* **4**, 572–577 (2005).
34. Boutros, R., Dozier, C. & Ducommun, B. The when and wheres of CDC25 phosphatases. *Curr. Opin. Cell Biol.* **18**, 185–191 (2006).
35. Boutros, R., Lobjois, V. & Ducommun, B. CDC25 phosphatases in cancer cells: Key players? Good targets? *Nat. Rev. Cancer* **7**, 495–507 (2007).
36. Perry, J. A. & Kornbluth, S. Cdc25 and Wee1: Analogous opposites? *Cell Div.* **2**, 1–12 (2007).
37. Karlsson-Rosenthal, C. & Millar, J. B. A. Cdc25: mechanisms of checkpoint inhibition and recovery. *Trends Cell Biol.* **16**, 285–292 (2006).
38. Harashima, H., Dissmeyer, N. & Schnittger, A. Cell cycle control across the eukaryotic kingdom. *Trends Cell Biol.* **23**, 345–356 (2013).
39. Vera, J. *et al.* Chk1 and Wee1 control genotoxic-stress induced G2-M arrest in melanoma cells. *Cell. Signal.* **27**, 951–960 (2015).
40. López-Contreras, A. J. & Fernandez-Capetillo, O. The ATR barrier to replication-born DNA damage. *DNA Repair (Amst).* **9**, 1249–1255 (2010).
41. Malumbres, M. M. & Barbacid, M. M. To cycle or not to cycle: a critical decision in cancer. *Nat. Rev. Cancer* **1**, 222–231 (2001).
42. Besson, A., Dowdy, S. F. & Roberts, J. M. CDK Inhibitors: Cell Cycle Regulators and Beyond. *Dev. Cell* **14**, 159–169 (2008).
43. Quereda, V., Porlan, E., Canámero, M., Dubus, P. & Malumbres, M. An essential role for Ink4 and Cip/Kip cell-cycle inhibitors in preventing replicative stress. *Cell Death Differ.* **23**, 430–441 (2016).
44. Cánepa, E. T. *et al.* INK4 proteins, a family of mammalian CDK inhibitors with novel biological functions. *IUBMB Life* **59**, 419–426 (2007).
45. Abbas, T. & Dutta, A. P21 in cancer: Intricate networks and multiple activities. *Nat. Rev. Cancer* **9**, 400–414 (2009).
46. Jung, Y. S., Qian, Y. & Chen, X. Examination of the expanding pathways for the regulation of p21 expression and activity. *Cell. Signal.* **22**, 1003–1012 (2010).
47. Waldman, T., Kinzler, K. W. & Vogelstein, B. p21 Is Necessary for the p53-mediated G1 Arrest in Human Cancer Cells. *Cancer Res.* **55**, 5187–5190 (1995).
48. Bunz, F. *et al.* Requirement for p53 and p21 to Sustain G2 Arrest After DNA Damage. *Science* **282**, 1497–1501 (1998).
49. Delavaine, L. & La Thangue, N. B. Control of E2F activity by p21(Waf1/Cip1). *Oncogene* **18**, 5381–5392 (1999).
50. Weissman, A. M. Themes and variations on ubiquitylation. *Nat. Rev. Mol. Cell Biol.* **2**, 169–178 (2001).
51. Hochstrasser, M. *et al.* The Ubiquitin-Proteasome System. *J. Biosci.* **31**, 137–155 (2006).
52. Hicke, L. Protein regulation by monoubiquitin. *Nat. Rev. Mol. Cell Biol.* **2**, 195–201 (2001).
53. Cardozo, T. & Pagano, M. The SCF ubiquitin ligase: Insights into a molecular machine. *Nat. Rev. Mol. Cell Biol.* **5**, 739–751 (2004).
54. Tsvetkov, L. M., Yeh, K. H., Lee, S. J., Sun, H. & Zhang, H. p27(Kip1) ubiquitination and degradation is regulated by the SCF(Skp2) complex through phosphorylated Thr187 in p27. *Curr. Biol.* **9**, 661–664 (1999).
55. Bornstein, G. *et al.* Role of the SCFSkp2 ubiquitin ligase in the degradation of p21Cip1 in S phase. *J. Biol. Chem.* **278**, 25752–25757 (2003).
56. Kamura, T. *et al.* Degradation of p57Kip2 mediated by SCFSkp2-dependent ubiquitylation. *Proc. Natl. Acad. Sci.* **100**, 10231–10236 (2003).
57. Nakayama, K. I. & Nakayama, K. Regulation of the cell cycle by SCF-type ubiquitin ligases. *Semin. Cell Dev. Biol.* **16**, 323–333 (2005).

58. Watanabe, N. *et al.* M-phase kinases induce phospho-dependent ubiquitination of somatic Wee1 by SCF $\beta$ -TrCP. *Proc Natl Acad Sci* **101**, 4419–4424 (2004).
59. Busino, L. *et al.* Degradation of Cdc25A by  $\beta$ -TrCP during S phase and in response to DNA damage. *Nature* **426**, 87–91 (2003).
60. Margottin-Goguet, F. *et al.* Prophase destruction of Emi1 by the SCF $\beta$ TrCP/Slimb ubiquitin ligase activates the anaphase promoting complex to allow progression beyond prometaphase. *Dev. Cell* **4**, 813–826 (2003).
61. Peschiaroli, A. *et al.* SCF-betaTrCP-Mediated Degradation of Claspin Regulates Recovery from the DNA Replication Checkpoint Response. *Mol. Cell* **23**, 319–329 (2006).
62. Zhou, Z., He, M., Shah, A. a & Wan, Y. Insights into APC/C: from cellular function to diseases and therapeutics. *Cell Div.* **11**, 9 (2016).
63. Sivakumar, S. & Gorbosky, G. J. Spatiotemporal regulation of the anaphase-promoting complex in mitosis. *Nat. Rev. Mol. Cell Biol.* **16**, 82–94 (2015).
64. Barford, D. *Structure, function and mechanism of the anaphase-promoting complex. Quarterly Reviews of Biophysics* **44**, (2011).
65. Teixeira, L. K. & Reed, S. I. Ubiquitin Ligases and Cell Cycle Control. *Annu. Rev. Biochem.* **82**, 387–414 (2013).
66. Bochis, O. V., Fetica, B., Vlad, C., Achimas-cadariu, P. & Irimie, A. THE IMPORTANCE OF UBIQUITIN E3 LIGASES, SCF AND APC/C, IN HUMAN CANCERS. *Clujul Med.* **88**, 9–14 (2015).
67. Kraft, C. *et al.* Mitotic regulation of the human anaphase-promoting complex by phosphorylation. *EMBO J.* **22**, 6598–6609 (2003).
68. Golan, A., Yudkovsky, Y. & Hershko, A. The cyclin-ubiquitin ligase activity of cyclosome/APC is jointly activated by protein kinases Cdk1-cyclin B and Plk. *J. Biol. Chem.* **277**, 15552–15557 (2002).
69. Rudner, A. D. & Murray, A. W. Phosphorylation by Cdc28 activates the Cdc20-dependent activity of the anaphase-promoting complex. *J. Cell Biol.* **149**, 1377–1390 (2000).
70. Kramer, E. R., Scheuringer, N., Podtelejnikov, A. V., Mann, M. & Peters, J.-M. Mitotic Regulation of the APC Activator Proteins CDC20 and CDH1. *Mol. Biol. Cell* **11**, 1555–1569 (2000).
71. Mailand, N. & Diffley, J. F. X. CDKs promote DNA replication origin licensing in human cells by protecting Cdc6 from APC/C-dependent proteolysis. *Cell* **122**, 915–926 (2005).
72. Holt, L. J., Krutchinsky, A. N. & Morgan, D. O. Positive feedback sharpens the anaphase switch. *Nature* **454**, 353–357 (2008).
73. Reimann, J. D. R. *et al.* Emi1 is a mitotic regulator that interacts with Cdc20 and inhibits the anaphase promoting complex. *Cell* **105**, 645–655 (2001).
74. Di Fiore, B. & Pines, J. Defining the role of Emi1 in the DNA replication-segregation cycle. *Chromosoma* **117**, 333–338 (2008).
75. Hsu, J. Y., Reimann, J. D. R., Sørensen, C. S., Lukas, J. & Jackson, P. K. E2F-dependent accumulation of hEmi1 regulates S phase entry by inhibiting APC(Cdh1). *Nat. Cell Biol.* **4**, 358–366 (2002).
76. Miller, J. J. *et al.* Emi1 stably binds and inhibits the anaphase-promoting complex / cyclosome as a pseudosubstrate inhibitor. *Genes Dev.* **20**, 2410–2420 (2006).
77. Cappell, S. D. *et al.* EM11 switches from being a substrate to an inhibitor of APC/CCDH1 to start the cell cycle. *Nature* **558**, 313–317 (2018).
78. Hansen, D. V, Loktev, A. V., Ban, K. H. & Jackson, P. K. Plk1 Regulates Activation of the Anaphase Promoting Complex by Phosphorylating and Triggering SCF-betaTrCP- dependent Destruction of the APC Inhibitor Emi1. *Mol. Biol. Cell* **15**, 5623–5634 (2004).
79. Eldridge, A. G. *et al.* The Evi5 oncogene regulates cyclin accumulation by stabilizing the anaphase-promoting complex inhibitor Emi1. *Cell* **124**, 367–380 (2006).
80. Alfieri, C. *et al.* Molecular basis of APC / C regulation by the spindle assembly checkpoint. *Nature* **536**, 431–436 (2016).
81. Rape, M. & Kirschner, M. W. Autonomous regulation of the anaphase-promoting complex couples mitosis to S-phase entry. *Nature* **432**, 588–595 (2004).
82. Glotzer, M., Murray, A. W. & Kirschner, M. W. Cyclin is degraded by the ubiquitin pathway. *Nature* **349**, 132–138 (1991).
83. Geley, S. *et al.* Anaphase-promoting Complex / Cyclosome – dependent Proteolysis of Human

- Cyclin A Starts at the Beginning of Mitosis and Is Not Subject to the Spindle Assembly Checkpoint. *J Cell Biol.* **153**, 137–147 (2001).
84. Elzen, N. Den & Pines, J. Cyclin A is destroyed in prometaphase and can delay chromosome alignment and anaphase. *J. Cell Biol.* **153**, 121–135 (2001).
  85. Hagting, A. *et al.* Human securin proteolysis is controlled by the spindle checkpoint and reveals when the APC/C switches from activation by Cdc20 to Cdh1. *J. Cell Biol.* **157**, 1125–1137 (2002).
  86. Zur, A. & Brandeis, M. Securin degradation is mediated by fzy and fzr, and is required for complete chromatid separation but not for cytokinesis. *EMBO J.* **20**, 792–801 (2001).
  87. Hauf, S., Waizenegger, I. C. & Peters, J. M. Cohesin cleavage by separase required for anaphase and cytokinesis in human cells. *Science* **293**, 1320–1323 (2001).
  88. Pines, J. Cubism and the cell cycle: The many faces of the APC/C. *Nat. Rev. Mol. Cell Biol.* **12**, 427–438 (2011).
  89. Floyd, S., Pines, J. & Lindon, C. APC/CCdh1 Targets Aurora Kinase to Control Reorganization of the Mitotic Spindle at Anaphase. *Curr. Biol.* **18**, 1649–1658 (2008).
  90. Lindon, C. & Pines, J. Ordered proteolysis in anaphase inactivates Plk1 to contribute to proper mitotic exit in human cells. *J. Cell Biol.* **164**, 233–241 (2004).
  91. Sigrist, S. J. & Lehner, C. F. Drosophila fizzy-related down-regulates mitotic cyclins and is required for cell proliferation arrest and entry into endocycles. *Cell* **90**, 671–681 (1997).
  92. Wei, W. *et al.* Degradation of the SCF component Skp2 in cell-cycle phase G1 by the anaphase-promoting complex. *Nature* **428**, 194–198 (2004).
  93. Bashir, T., Dorello, H. V., Amador, V., Guardavaccaro, D. & Pagano, M. Control of the SCFSkp2-Cks1 ubiquitin ligase by the APC/CCdh1 ubiquitin ligase. *Nature* **428**, 190–193 (2004).
  94. Schulze, A. *et al.* Cell cycle regulation of the cyclin A gene promoter is mediated by a variant E2F site. *Proc. Natl. Acad. Sci. U. S. A.* **92**, 11264–11268 (1995).
  95. Peters, J. M. The anaphase promoting complex/cyclosome: A machine designed to destroy. *Nat. Rev. Mol. Cell Biol.* **7**, 644–656 (2006).
  96. Sivaprasad, U., Machida, Y. J. & Dutta, A. APC/C - The master controller of origin licensing? *Cell Div.* **2**, 4–9 (2007).
  97. Li, M. & Zhang, P. The function of APC/CCdh1 in cell cycle and beyond. *Cell Div.* **4**, 2 (2009).
  98. Qiao, X., Zhang, L., Gamper, A. M., Fujita, T. & Wan, Y. APC/C-Cdh1: From cell cycle to cellular differentiation and genomic integrity. *Cell Cycle* **9**, 3904–3912 (2010).
  99. McGarry, T. J. & Kirschner, M. W. Geminin, an inhibitor of DNA replication, is degraded during mitosis. *Cell* **93**, 1043–1053 (1998).
  100. Lee, C. *et al.* Structural basis for inhibition of the replication licensing factor Cdt1 by geminin. *Nature* **430**, 913–917 (2004).
  101. De Marco, V. *et al.* Quaternary structure of the human Cdt1-Geminin complex regulates DNA replication licensing. *Proc. Natl. Acad. Sci.* **106**, 19807–19812 (2009).
  102. Petersen, B. O., Lukas, J., Sørensen, C. S., Bartek, J. & Helin, K. Phosphorylation of mammalian CDC6 by cyclin A/CDK2 regulates its subcellular localization. *EMBO J.* **18**, 396–410 (1999).
  103. Petersen, B. O. *et al.* Cell cycle- and cell growth-regulated proteolysis of mammalian CDC6 is dependent on APC-CDH1. *Genes Dev.* **14**, 2330–2343 (2000).
  104. Jiang, W., Wells, N. J. & Hunter, T. Multistep regulation of DNA replication by Cdk phosphorylation of hsCdc6. *Proc. Natl. Acad. Sci. U. S. A.* **96**, 6193–6198 (1999).
  105. Blow, J. J. & Dutta, A. Preventing re-replication of chromosomal DNA. *Nat. Rev. Mol. Cell Biol.* **6**, 476–486 (2005).
  106. Eguren, M., Machado, E. & Malumbres, M. Non-mitotic functions of the Anaphase-Promoting Complex. *Semin. Cell Dev. Biol.* **22**, 572–578 (2011).
  107. Zhang, J., Wan, L., Dai, X., Sun, Y. & Wei, W. Functional characterization of Anaphase Promoting Complex/Cyclosome (APC/C) E3 ubiquitin ligases in tumorigenesis. *Biochim. Biophys. Acta* **1845**, 277–93 (2014).
  108. Sudo, T. *et al.* Activation of Cdh1-dependent APC is required for G1 cell cycle arrest and DNA damage-induced G2 checkpoint in vertebrate cells. *EMBO J.* **20**, 6499–6508 (2001).
  109. Bassermann, F. *et al.* The Cdc14B-Cdh1-Plk1 Axis Controls the G2 DNA-Damage-Response

- Checkpoint. *Cell* **134**, 256–267 (2008).
110. Bassermann, F. & Pagano, M. Dissecting the role of ubiquitylation in the DNA damage response checkpoint in G2. *Cell Death Differ.* **17**, 78–85 (2010).
  111. Lee, J., Kim, J. A., Barbier, V., Fotedar, A. & Fotedar, R. DNA Damage Triggers p21(WAF1)-dependent Emi1 Down-Regulation That Maintains G2 Arrest. *Mol. Biol. Cell* **20**, 1891–1902 (2009).
  112. Wiebusch, L. & Hagemeyer, C. p53- and p21-dependent premature APC/C-Cdh1 activation in G2 is part of the long-term response to genotoxic stress. *Oncogene* **29**, 3477–89 (2010).
  113. Lafranchi, L. *et al.* APC / C Cdh 1 controls CtIP stability during the cell cycle and in response to DNA damage. *EMBO J.* **33**, 2860–2879 (2014).
  114. Lafranchi, L. & Sartori, A. a. The ubiquitin ligase APC/C Cdh1 puts the brakes on DNA-end resection. *Mol Cell Oncol.* **2**, e1000696 (2015).
  115. Gao, D. *et al.* Cdh1 Regulates Cell Cycle through Modulating the Claspin/Chk1 and the Rb/E2F1 Pathways. *Mol. Biol. Cell* **20**, 3305–3316 (2009).
  116. Cotto-Rios, X. M., Jones, M. J. K., Busino, L., Pagano, M. & Huang, T. T. APC/CCdh1-dependent proteolysis of USP1 regulates the response to UV-mediated DNA damage. *J. Cell Biol.* **194**, 177–186 (2011).
  117. Zhang, L. *et al.* Proteolysis of Rad17 by Cdh1/APC regulates checkpoint termination and recovery from genotoxic stress. *EMBO J.* **29**, 1726–1737 (2010).
  118. Takahashi, A. *et al.* DNA damage signaling triggers degradation of histone methyltransferases through APC/C Cdh1 in senescent cells. *Mol. Cell* **45**, 123–131 (2012).
  119. Watson, J. & Crick, F. Genetical implications of the structure of deoxyribonucleic acid. *Nature* **171**, 964–967 (1953).
  120. Meselson, M. & Stahl, F. W. The replication of DNA in Escherichia coli. *Proc Natl Acad Sci U S A* **44**, 671–682 (1958).
  121. Kornberg, A., Lehman, I. R., Bessman, M. J. & Simms, E. S. Enzymic synthesis of deoxyribonucleic acid. *Biochim. Biophys. Acta* **21**, 197–198 (1956).
  122. Masai, H. & Foiani, M. *DNA Replication: From Old Principles to New Discoveries. Advances in Experimental Medicine and Biology* **1042**, (2017).
  123. Pasero, P. & Vindigni, A. Nucleases Acting at Stalled Forks: How to Reboot the Replication Program with a Few Shortcuts. *Annu. Rev. Genet.* **51**, 477–499 (2017).
  124. Branzei, D. & Foiani, M. Interplay of replication checkpoints and repair proteins at stalled replication forks. *DNA Repair (Amst)*. **6**, 994–1003 (2007).
  125. Groth, A. *et al.* Regulation of replication fork progression through histone supply and demand. *Science* **318**, 1928–31 (2007).
  126. Alabert, C. & Groth, A. Chromatin replication and epigenome maintenance. *Nat. Rev. Mol. Cell Biol.* **13**, 153–167 (2012).
  127. Almouzni, G. & Cedar, H. Maintenance of epigenetic information. *Cold Spring Harb. Perspect. Biol.* **8**, a019372 (2016).
  128. Aranda, S., Rutishauser, D. & Ernfors, P. Identification of a large protein network involved in epigenetic transmission in replicating DNA of embryonic stem cells. *Nucleic Acids Res.* **42**, 6972–6986 (2014).
  129. Cea, V., Cipolla, L. & Sabbioneda, S. Replication of Structured DNA and its implication in epigenetic stability. *Front. Genet.* **6**, 209 (2015).
  130. Kurat, C. F., Yeeles, J. T. P., Patel, H., Early, A. & Diffley, J. F. X. Chromatin Controls DNA Replication Origin Selection, Lagging Strand Synthesis, and Replication Fork Rates. *Mol. Cell* **65**, 117–130 (2017).
  131. MacNeill, S. *The Eukaryotic Replisome: A Guide to Protein Structure and Function.* (2002).
  132. Yeeles, J. T. P., Deegan, T. D., Janska, A., Early, A. & Diffley, J. F. X. Regulated eukaryotic DNA replication origin firing with purified proteins. *Nature* **519**, 431–435 (2015).
  133. Arias, E. E. & Walter, J. C. Strength in numbers: Preventing rereplication via multiple mechanisms in eukaryotic cells. *Genes Dev.* **21**, 497–518 (2007).
  134. Alver, R. C., Chadha, G. S. & Blow, J. J. The contribution of dormant origins to genome stability: From cell biology to human genetics. *DNA Repair (Amst)*. **19**, 182–189 (2014).

135. Fragkos, M., Ganier, O., Coulombe, P. & Méchali, M. DNA replication origin activation in space and time. *Nat. Rev. Mol. Cell Biol.* **16**, 360–374 (2015).
136. Bell, S. P. & Stillman, B. ATP-dependent recognition of eukaryotic origins of DNA replication by a multiprotein complex. *Nature* **357**, 128–134 (1992).
137. Méchali, M. Eukaryotic DNA replication origins: Many choices for appropriate answers. *Nat. Rev. Mol. Cell Biol.* **11**, 728–738 (2010).
138. Vashee, S. *et al.* Sequence-independent DNA binding and replication initiation by the human origin recognition complex. *Genes Dev.* **17**, 1894–1908 (2003).
139. Lubelsky, Y. *et al.* Pre-replication complex proteins assemble at regions of low nucleosome occupancy within the Chinese hamster dihydrofolate reductase initiation zone. *Nucleic Acids Res.* **39**, 3141–3155 (2011).
140. Hoshina, S. *et al.* Human origin recognition complex binds preferentially to G-quadruplex-preferable RNA and single-stranded DNA. *J. Biol. Chem.* **288**, 30161–30171 (2013).
141. Harvey, K. J. & Newport, J. Metazoan origin selection: Origin recognition complex chromatin binding is regulated by CDC6 recruitment and ATP hydrolysis. *J. Biol. Chem.* **278**, 48524–48528 (2003).
142. Maiorano, D., Moreau, J. & Méchali, M. XCDT1 is required for the assembly of pre-replicative complexes in *Xenopus laevis*. *Nature* **404**, 622–625 (2000).
143. You, Z. & Masai, H. Cdt1 forms a complex with the minichromosome maintenance protein (MCM) and activates its helicase activity. *J. Biol. Chem.* **283**, 24469–24477 (2008).
144. Deegan, T. D. & Diffley, J. F. X. MCM: One ring to rule them all. *Curr. Opin. Struct. Biol.* **37**, 145–151 (2016).
145. Parker, M. W., Botchan, M. R. & Berger, J. M. Mechanisms and regulation of DNA replication initiation in eukaryotes. *Crit Rev Biochem Mol Biol.* **52**, 107–144 (2017).
146. Evrin, C. *et al.* A double-hexameric MCM2-7 complex is loaded onto origin DNA during licensing of eukaryotic DNA replication. *Proc. Natl. Acad. Sci.* **106**, 20240–20245 (2009).
147. Remus, D. *et al.* Concerted Loading of Mcm2-7 Double Hexamers around DNA during DNA Replication Origin Licensing. *Cell* **139**, 719–730 (2009).
148. Gambus, A., Khoudoli, G. A., Jones, R. C. & Blow, J. J. MCM2-7 form double hexamers at licensed origins in *Xenopus* egg extract. *J. Biol. Chem.* **286**, 11855–11864 (2011).
149. Ticau, S., Friedman, L. J., Ivica, N. A., Gelles, J. & Bell, S. P. Single-molecule studies of origin licensing reveal mechanisms ensuring bidirectional helicase loading. *Cell* **161**, 513–525 (2015).
150. McIntosh, D. & Blow, J. J. Dormant origins, the licensing checkpoint, and the response to replicative stresses. *Cold Spring Harb. Perspect. Biol.* **4**, 1–13 (2012).
151. Blow, J. J., Ge, X. Q. & Jackson, D. a. How dormant origins promote complete genome replication. *Trends Biochem. Sci.* **36**, 405–414 (2011).
152. Brambati, A. *et al.* Dormant origins and fork protection mechanisms rescue sister forks arrested by transcription. *Nucleic Acids Res.* **46**, 1227–1239 (2018).
153. Yekezare, M., Gomez-Gonzalez, B. & Diffley, J. F. X. Controlling DNA replication origins in response to DNA damage - inhibit globally, activate locally. *J. Cell Sci.* **126**, 1297–1306 (2013).
154. Moyer, S. E., Lewis, P. W. & Botchan, M. R. Isolation of the Cdc45/Mcm2–7/GINS (CMG) complex, a candidate for the eukaryotic DNA replication fork helicase. *Proc Natl Acad Sci U S A* **103**, 10236–10241 (2006).
155. Zou, L. & Stillman, B. Formation of a preinitiation complex by S-phase cyclin CDK-dependent loading of Cdc45p onto chromatin. *Science* **280**, 593–596 (1998).
156. Ilves, I., Petojevic, T., Pesavento, J. J. & Botchan, M. R. Activation of the MCM2-7 Helicase by Association with Cdc45 and GINS Proteins. *Mol. Cell* **37**, 247–258 (2010).
157. Tanaka, S. & Araki, H. Helicase activation and establishment of replication forks at chromosomal origins of replication. *Cold Spring Harb. Perspect. Biol.* **5**, a010371 (2013).
158. Heller, R. C. *et al.* Eukaryotic origin-dependent DNA replication in vitro reveals sequential action of DDK and S-CDK kinases. *Cell* **146**, 80–91 (2011).
159. Tanaka, S. & Araki, H. Regulation of the initiation step of DNA replication by cyclin-dependent kinases. *Chromosoma* **119**, 565–574 (2010).

160. Jares, P. & Blow, J. J. *Xenopus* Cdc7 function is dependent on licensing but not on XORC, XCdc6, or CDK activity and is required for XCdc45 loading. *Genes Dev.* **14**, 1528–1540 (2000).
161. Sheu, Y. J. & Stillman, B. Cdc7-Dbf4 Phosphorylates MCM Proteins via a Docking Site-Mediated Mechanism to Promote S Phase Progression. *Mol. Cell* **24**, 101–113 (2006).
162. Zegerman, P. & Diffley, J. F. X. Phosphorylation of Sld2 and Sld3 by cyclin-dependent kinases promotes DNA replication in budding yeast. *Nature* **445**, 281–285 (2007).
163. Masumoto, H., Muramatsu, S., Kamimura, Y. & Araki, H. S-Cdk-dependent phosphorylation of Sld2 essential for chromosomal DNA replication in budding yeast. *Nature* **415**, 651–655 (2002).
164. Tanaka, S. *et al.* CDK-dependent phosphorylation of Sld2 and Sld3 initiates DNA replication in budding yeast. *Nature* **445**, 328–332 (2007).
165. Hashimoto, Y. & Takisawa, H. *Xenopus* Cut5 is essential for a CDK-dependent process in the initiation of DNA replication. *EMBO J.* **22**, 2526–2535 (2003).
166. Van Hatten, R. A. *et al.* The *Xenopus* Xmus101 protein is required for the recruitment of Cdc45 to origins of DNA replication. *J. Cell Biol.* **159**, 541–547 (2002).
167. Schmidt, U. *et al.* Characterization of the interaction between the human DNA topoisomerase II $\beta$ -binding protein 1 (TopBP1) and the cell division cycle 45 (Cdc45) protein. *Biochem. J.* **409**, 169–177 (2008).
168. Matsuno, K., Kumano, M., Kubota, Y., Hashimoto, Y. & Takisawa, H. The N-Terminal Ncatalytic Region of *Xenopus* RecQ4 Is Required for Chromatin Binding of DNA Polymerase in the Initiation of DNA Replication. *Mol. Cell. Biol.* **26**, 4843–4852 (2006).
169. Sangrithi, M. N. *et al.* Initiation of DNA replication requires the RECQL4 protein mutated in Rothmund-Thomson syndrome. *Cell* **121**, 887–898 (2005).
170. Sanuki, Y. *et al.* RecQ4 promotes the conversion of the pre-initiation complex at a site-specific origin for DNA unwinding in *xenopus* egg extracts. *Cell Cycle* **14**, 1010–1023 (2015).
171. Xu, X., Rochette, P. J., Feyissa, E. A., Su, T. V. & Liu, Y. MCM10 mediates RECQ4 association with MCM2-7 helicase complex during DNA replication. *EMBO J.* **28**, 3005–3014 (2009).
172. Thangavel, S. *et al.* Human RECQ1 and RECQ4 Helicases Play Distinct Roles in DNA Replication Initiation. *Mol. Cell. Biol.* **30**, 1382–1396 (2010).
173. Kumagai, A., Shevchenko, A., Shevchenko, A. & Dunphy, W. G. Treslin collaborates with TopBP1 in triggering the initiation of DNA replication. *Cell* **140**, 349–59 (2010).
174. Kumagai, A., Shevchenko, A., Shevchenko, A. & Dunphy, W. G. Direct regulation of Treslin by cyclin-dependent kinase is essential for the onset of DNA replication. *J. Cell Biol.* **193**, 995–1007 (2011).
175. Balestrini, A., Cosentino, C., Errico, A., Garner, E. & Costanzo, V. GEMC1 is a TopBP1-interacting protein involved in chromosomal DNA replication. *Nat. Cell Biol.* **12**, 484–491 (2010).
176. Piergiovanni, G. & Costanzo, V. GEMC1 is a novel TopBP1-interacting protein involved in chromosomal DNA replication. *Cell Cycle* **9**, 3662–3666 (2010).
177. Chowdhury, A. *et al.* The DNA Unwinding Element Binding Protein DUE-B Interacts with Cdc45 in Preinitiation Complex Formation. *Mol. Cell. Biol.* **30**, 1495–1507 (2010).
178. Watase, G., Takisawa, H. & Kanemaki, M. T. Mcm10 plays a role in functioning of the eukaryotic replicative DNA helicase, Cdc45-Mcm-GINS. *Curr. Biol.* **22**, 343–349 (2012).
179. Van Deursen, F., Sengupta, S., De Piccoli, G., Sanchez-Diaz, A. & Labib, K. Mcm 10 associates with the loaded DNA helicase at replication origins and defines a novel step in its activation. *EMBO J.* **31**, 2195–2206 (2012).
180. Perez-Arnaiz, P., Bruck, I. & Kaplan, D. L. Mcm10 coordinates the timely assembly and activation of the replication fork helicase. *Nucleic Acids Res.* **44**, 315–329 (2015).
181. Perez-Arnaiz, P. & Kaplan, D. L. An Mcm10 Mutant Defective in ssDNA Binding Shows Defects in DNA Replication Initiation. *J. Mol. Biol.* **428**, 4608–4625 (2016).
182. Izumi, M. *et al.* The Mcm2–7-interacting domain of human mini-chromosome maintenance 10 (Mcm10) protein is important for stable chromatin association and origin firing. *J Biol Chem.* **292**, 13008–13021 (2017).
183. Douglas, M. E., Ali, F. A., Costa, A. & Diffley, J. F. X. The mechanism of eukaryotic CMG helicase activation. *Nat. Publ. Gr.* (2018).
184. Kliszczak, M. *et al.* Interaction of RECQ4 and MCM10 is important for efficient DNA replication

- origin firing in human cells. *Oncotarget* **6**, 40464–40479 (2015).
185. Baxley, R. & Bielinsky, A.-K. Mcm10: A Dynamic Scaffold at Eukaryotic Replication Forks. *Genes (Basel)*. **8**, E73 (2017).
  186. Masai, H., Yang, C. C. & Matsumoto, S. Mrc1/Claspin: a new role for regulation of origin firing. *Curr. Genet.* **63**, 813–818 (2017).
  187. Labib, K. How do Cdc7 and cyclin-dependent kinases trigger the initiation of chromosome replication in eukaryotic cells? *Genes Dev.* **24**, 1208–19 (2010).
  188. Bruck, I. & Kaplan, D. L. The replication initiation protein Sld3/Treslin orchestrates the assembly of the replication fork helicase during S phase. *J. Biol. Chem.* **290**, 27414–27424 (2015).
  189. Burgers, P. M. J. & Kunkel, T. A. Eukaryotic DNA Replication Fork. *Annu. Rev. Biochem.* **86**, 9.1-9.22 (2017).
  190. Oakley, G. G. & Patrick, S. M. Replication protein A: directing traffic at the intersection of replication and repair. *Front. Biosci.* **15**, 883–900 (2010).
  191. Liu, T. & Huang, J. Replication protein A and more: Single-stranded DNA-binding proteins in eukaryotic cells. *Acta Biochim. Biophys. Sin. (Shanghai)*. **48**, 665–670 (2016).
  192. Krasikova, Y. S., Rechkunova, N. I. & Lavrik, O. I. Replication protein A as a major eukaryotic single-stranded DNA-binding protein and its role in DNA repair. *Mol. Biol.* **50**, 649–662 (2016).
  193. Lujan, S. a., Williams, J. S. & Kunkel, T. a. DNA Polymerases Divide the Labor of Genome Replication. *Trends Cell Biol.* 1–15 (2016).
  194. Burgers, P. M. J. Polymerase dynamics at the eukaryotic DNA replication fork. *J. Biol. Chem.* **284**, 4041–4045 (2009).
  195. Stillman, B. DNA Polymerases at the Replication Fork in Eukaryotes. *Mol. Cell* **30**, 259–260 (2008).
  196. Johnson, R. E., Klassen, R., Prakash, L. & Prakash, S. A Major Role of DNA Polymerase delta in Replication of Both the Leading and Lagging DNA Strands. *Mol. Cell* **59**, 163–175 (2015).
  197. Stillman, B. Reconsidering DNA Polymerases at the Replication Fork in Eukaryotes. *Mol. Cell* **59**, 139–141 (2015).
  198. Aria, V. & Yeeles, J. T. P. Mechanism of Bidirectional Leading-Strand Synthesis Establishment at Eukaryotic DNA Replication Origins. *Mol. Cell* **73**, 1–13 (2019).
  199. Pandey, M. *et al.* Coordinating DNA replication by means of priming loop and differential synthesis rate. *Nature* **462**, 940–943 (2009).
  200. Graham, J. E., Marians, K. J. & Kowalczykowski, S. C. Independent and Stochastic Action of DNA Polymerases in the Replisome. *Cell* **169**, 1201–1213.e17 (2017).
  201. Boehm, E. M., Gildenberg, M. S. & Washington, M. T. The many roles of PCNA in eukaryotic DNA replication. *Enzymes* **39**, 231–254 (2016).
  202. Balakrishnan, L. & Bambara, R. A. Flap Endonuclease 1. *Annu. Rev. Biochem.* **82**, 119–138 (2013).
  203. Errico, A. *et al.* Tipin/Tim1/And1 protein complex promotes Pola chromatin binding and sister chromatid cohesion. *EMBO J.* **28**, 3681–3692 (2009).
  204. Errico, A. & Costanzo, V. Mechanisms of replication fork protection: a safeguard for genome stability. *Crit. Rev. Biochem. Mol. Biol.* **47**, 222–35 (2012).
  205. Gambus, A. *et al.* A key role for Ctf4 in coupling the MCM2-7 helicase to DNA polymerase  $\alpha$  within the eukaryotic replisome. *EMBO J.* **28**, 2992–3004 (2009).
  206. Simon, A. C. *et al.* A Ctf4 trimer couples the CMG helicase to DNA polymerase  $\alpha$  in the eukaryotic replisome. *Nature* **510**, 293–7 (2014).
  207. Kilkenny, M. L. *et al.* The human CTF4-orthologue AND-1 interacts with DNA polymerase  $\alpha$  / primase via its unique C-terminal HMG box. *Open Biol.* **7**, 170217 (2017).
  208. Gambus, A. *et al.* GINS maintains association of Cdc45 with MCM in replisome progression complexes at eukaryotic DNA replication forks. *Nat. Cell Biol.* **8**, 358–366 (2006).
  209. Sherwood, R., Takahashi, T. S. & Jallepalli, P. V. Sister acts: Coordinating DNA replication and cohesion establishment. *Genes Dev.* **24**, 2723–2731 (2010).
  210. Remeseiro, S. & Losada, A. Cohesin, a chromatin engagement ring. *Curr. Opin. Cell Biol.* **25**, 1–9 (2013).
  211. Moreno, S. P., Bailey, R., Campion, N., Herron, S. & Gambus, A. Polyubiquitylation drives replisome disassembly at the termination of DNA replication. *Science* **346**, 477–481 (2014).

212. Dewar, J. M. & Walter, J. C. Mechanisms of DNA replication termination. *Nat. Rev. Mol. Cell Biol.* **18**, 507–516 (2017).
213. Courbet, S. *et al.* Replication fork movement sets chromatin loop size and origin choice in mammalian cells. *Nature* **455**, 557–560 (2008).
214. Shima, N. & Pederson, K. D. Dormant origins as a built-in safeguard in eukaryotic DNA replication against genome instability and disease development. *DNA Repair* **56**, 166–173 (2017).
215. Courtot, L., Hoffmann, J.-S. & Bergoglio, V. The Protective Role of Dormant Origins in Response to Replicative Stress. *Int. J. Mol. Sci.* **19**, 3569 (2018).
216. Yost, B. K., Rosenberg, M. J. & Nishioka, D. J. Incorporation of tritiated uridine into DNA of Ehrlich ascites tumor cells. *J. Natl. Cancer Inst.* **57**, 289–293 (1976).
217. Osborn, A. J. *et al.* Checking on the fork : the DNA-replication stress-response pathway. *Trends Cell Biol.* **12**, 509–516 (2002).
218. Zou, L. & Elledge, S. J. Sensing DNA damage through ATRIP recognition of RPA-ssDNA complexes. *Science* **300**, 1542–8 (2003).
219. Zeman, M. K. & Cimprich, K. a. Causes and consequences of replication stress. *Nat. Cell Biol.* **16**, 2–9 (2014).
220. Berti, M. & Vindigni, A. Replication stress: getting back on track. *Nat. Struct. Mol. Biol.* **23**, 103–109 (2016).
221. Muñoz, S. & Méndez, J. DNA replication stress: from molecular mechanisms to human disease. *Chromosoma* 1–15 (2016).
222. Branzei, D. & Foiani, M. The checkpoint response to replication stress. *DNA Repair (Amst)*. **8**, 1038–1046 (2009).
223. Magdalou, I., Lopez, B. S., Pasero, P. & Lambert, S. a E. The causes of replication stress and their consequences on genome stability and cell fate. *Semin. Cell Dev. Biol.* **30**, 154–164 (2014).
224. Lecona, E. & Fernández-Capetillo, O. Replication stress and cancer: it takes two to tango. *Exp. Cell Res.* **329**, 26–34 (2014).
225. Gaillard, H., García-Muse, T. & Aguilera, A. Replication stress and cancer. *Nat. Rev. Cancer* **15**, 276–289 (2015).
226. Cortez, D. Preventing Replication Fork Collapse to Maintain Genome Integrity. *DNA Repair* **32**, 149–157 (2015).
227. Toledo, L., Neelsen, K. J. & Lukas, J. Replication Catastrophe : When a Checkpoint Fails because of Exhaustion. *Mol. Cell* **66**, 735–749 (2017).
228. Zlotorynski, E. *et al.* Molecular Basis for Expression of Common and Rare Fragile Sites. *Mol. Cell Biol.* **23**, 7143–7151 (2003).
229. Helmrich, A., Ballarino, M. & Tora, L. Collisions between Replication and Transcription Complexes Cause Common Fragile Site Instability at the Longest Human Genes. *Mol. Cell* **44**, 966–977 (2011).
230. Ozeri-Galai, E. *et al.* Failure of Origin Activation in Response to Fork Stalling Leads to Chromosomal Instability at Fragile Sites. *Mol. Cell* **43**, 122–131 (2011).
231. Forment, J. V. & O'Connor, M. J. Targeting the replication stress response in cancer. *Pharmacol. Ther.* **188**, 155–167 (2018).
232. Marians, K. J. Lesion Bypass and the Reactivation of Stalled Replication Forks. *Annu Rev Biochem.* **87**, 217–238 (2018).
233. Wei, X. *et al.* Segregation of transcription and replication sites into higher order domains. *Science* **281**, 1502–1505 (1998).
234. Bermejo, R., Lai, M. S. & Foiani, M. Preventing Replication Stress to Maintain Genome Stability: Resolving Conflicts between Replication and Transcription. *Mol. Cell* **45**, 710–718 (2012).
235. Huertas, P. & Aguilera, A. Cotranscriptionally formed DNA:RNA hybrids mediate transcription elongation impairment and transcription-associated recombination. *Mol. Cell* **12**, 711–721 (2003).
236. Aguilera, A. & García-Muse, T. Causes of Genome Instability. *Annu. Rev. Genet.* **47**, 1–32 (2013).
237. Gelot, C., Magdalou, I. & Lopez, B. S. Replication Stress in Mammalian Cells and Its Consequences for Mitosis. *Genes (Basel)*. **6**, 267–298 (2015).
238. Mejlvang, J. *et al.* New histone supply regulates replication fork speed and PCNA unloading. *J. Cell Biol.* **204**, 29–43 (2014).

239. Toledo, L. I. *et al.* ATR Prohibits Replication Catastrophe by Preventing Global Exhaustion of RPA. *Cell* **155**, 1088–1103 (2013).
240. Gay, S. *et al.* Nucleotide supply, not local histone acetylation, sets replication origin usage in transcribed regions. *EMBO Rep.* **11**, 698–704 (2010).
241. Chabosseau, P. *et al.* Pyrimidine pool imbalance induced by BLM helicase deficiency contributes to genetic instability in Bloom syndrome. *Nat. Commun.* **2**, 368 (2011).
242. Bester, A. C. *et al.* Nucleotide deficiency promotes genomic instability in early stages of cancer development. *Cell* **145**, 435–446 (2011).
243. Poli, J. *et al.* dNTP pools determine fork progression and origin usage under replication stress. *EMBO J.* **31**, 883–894 (2012).
244. Eklund, H., Uhlin, U., Färnegårdh, M., Logan, D. T. & Nordlund, P. Structure and function of the radical enzyme ribonucleotide reductase. *Prog. Biophys. Mol. Biol.* **77**, 177–268 (2001).
245. Singh, A. & Xu, Y.-J. The Cell Killing Mechanisms of Hydroxyurea. *Genes (Basel)*. **7**, E99 (2016).
246. WHO Model List of Essential Medicines.  
<http://www.who.int/medicines/publications/essentialmedicines/en/> (2017).
247. Hsieh, H. J. & Peng, G. Cellular responses to replication stress: Implications in cancer biology and therapy. *DNA Repair (Amst)*. **49**, 9–20 (2017).
248. Kotsantis, P. *et al.* Increased global transcription activity as a mechanism of replication stress in cancer. *Nat. Commun.* **7**, 13087 (2016).
249. Rohban, S. & Campaner, S. Myc induced replicative stress response: How to cope with it and exploit it. *Biochim. Biophys. Acta - Gene Regul. Mech.* **1849**, 517–524 (2015).
250. Jones, R. M. *et al.* Increased replication initiation and conflicts with transcription underlie Cyclin E-induced replication stress. *Oncogene* **32**, 3744–3753 (2013).
251. Macheret, M. & Halazonetis, T. D. Intragenic origins due to short G1 phases underlie oncogene-induced DNA replication stress. *Nature* **555**, 112–116 (2018).
252. Srinivasan, S. V., Dominguez-Sola, D., Wang, L. C., Hyrien, O. & Gautier, J. Cdc45 Is a Critical Effector of Myc-Dependent DNA Replication Stress. *Cell Rep.* **3**, 1629–1639 (2013).
253. Herlihy, A. E. & De Bruin, R. a M. The Role of the Transcriptional Response to DNA Replication Stress. *Genes (Basel)*. **4**, 1–15 (2017).
254. Nyberg, K. a, Michelson, R. J., Putnam, C. W. & Weinert, T. a. Toward maintaining the genome: DNA damage and replication checkpoints. *Annu. Rev. Genet.* **36**, 617–656 (2002).
255. Sancar, A., Lindsey-Boltz, L. a, Unsal-Kaçmaz, K. & Linn, S. Molecular mechanisms of mammalian DNA repair and the DNA damage checkpoints. *Annu. Rev. Biochem.* **73**, 39–85 (2004).
256. Abraham, R. T. Cell cycle checkpoint signaling through the ATM and ATR kinases. *Genes Dev.* **15**, 2177–2196 (2001).
257. Magdalou, I., Lopez, B. S., Pasero, P. & Lambert, S. A. E. The causes of replication stress and their consequences on genome stability and cell fate. *Semin. Cell Dev. Biol.* **30**, 154–164 (2014).
258. Warmerdam, D. O. & Kanaar, R. Dealing with DNA damage: Relationships between checkpoint and repair pathways. *Mutat. Res. - Rev. Mutat. Res.* **704**, 2–11 (2010).
259. Sirbu, B. M. & Cortez, D. DNA damage response: three levels of DNA repair regulation. *Cold Spring Harb. Perspect. Biol.* **5**, a012724 (2013).
260. Burma, S. & Chen, D. J. Role of DNA-PK in the cellular response to DNA double-strand breaks. *DNA Repair (Amst)*. **3**, 909–918 (2004).
261. Jette, N. & Lees-Miller, S. P. The DNA-dependent protein kinase: A multifunctional protein kinase with roles in DNA double strand break repair and mitosis. *Prog. Biophys. Mol. Biol.* **117**, 194–205 (2015).
262. De Klein, A. *et al.* Targeted disruption of the cell-cycle checkpoint gene ATR leads to early embryonic lethality in mice. *Curr. Biol.* **10**, 479–482 (2000).
263. Brown, E. J. & Baltimore, D. ATR disruption leads to chromosomal fragmentation and early embryonic lethality. *Genes Dev.* **14**, 397–402 (2000).
264. Xu, Y. *et al.* Targeted disruption of ATM leads to growth retardation, chromosomal fragmentation during meiosis, immune defects, and thymic lymphoma. *Genes Dev.* **10**, 2411–2422 (1996).
265. Barlow, C. *et al.* Atm-Deficient Mice: A Paradigm of Ataxia Telangiectasia. *Cell* **86**, 159–171 (1996).

266. Daniel, J. A. *et al.* Loss of ATM kinase activity leads to embryonic lethality in mice. *J. Cell Biol.* **198**, 295–304 (2012).
267. Cimprich, K. A. & Cortez, D. ATR: An essential regulator of genome integrity. *Nat. Rev. Mol. Cell Biol.* **9**, 616–627 (2008).
268. Durocher, D. & Jackson, S. P. DNA-PK, ATM and ATR as sensors of DNA damage: Variations on a theme? *Curr. Opin. Cell Biol.* **13**, 225–231 (2001).
269. Blackford, A. N. & Jackson, S. P. ATM, ATR, and DNA-PK: The Trinity at the Heart of the DNA Damage Response. *Mol. Cell* **66**, 801–817 (2017).
270. Rogakou, E. P., Pilch, D. R., Orr, A. H., Ivanova, V. S. & Bonner, W. M. Double-stranded Breaks Induce Histone H2AX phosphorylation on Serine 139. *J. Biol. Chem.* **273**, 5858–5868 (1998).
271. Harper, J. W. & Elledge, S. J. The DNA Damage Response: Ten Years After. *Mol. Cell* **28**, 739–745 (2007).
272. Feraudy, S. De, Revet, I., Bezrookove, V., Feeney, L. & Cleaver, J. E. A minority of foci or pan-nuclear apoptotic staining of  $\gamma$  H2AX in the S phase after UV damage contain DNA double-strand breaks. *Proc Natl Acad Sci* **107**, 6870–6875 (2010).
273. Shao, R. G. *et al.* Replication-mediated DNA damage by camptothecin induces phosphorylation of RPA by DNA-dependent protein kinase and dissociates RPA:DNA-PK complexes. *EMBO J.* **18**, 1397–1406 (1999).
274. Block, W. D., Yu, Y. & Lees-Miller, S. P. Phosphatidyl inositol 3-kinase-like serine/threonine protein kinases (PIKKs) are required for DNA damage-induced phosphorylation of the 32 kDA subunit of replication protein A at threonine 21. *Nucleic Acids Res.* **32**, 997–1005 (2004).
275. Wang, H. *et al.* Replication protein A2 phosphorylation after DNA damage by the coordinated action of ataxia telangiectasia-mutated and DNA-dependent protein kinase. *Cancer Res.* **61**, 8554–8563 (2001).
276. Liu, S. *et al.* Distinct roles for DNA-PK, ATM and ATR in RPA phosphorylation and checkpoint activation in response to replication stress. *Nucleic Acids Res.* **40**, 10780–94 (2012).
277. Cortez, D. Unwind and slow down: Checkpoint activation by helicase and polymerase uncoupling. *Genes Dev.* **19**, 1007–1012 (2005).
278. Yeeles, J. T. P., Poli, J., Marians, K. J. & Pasero, P. Rescuing Stalled or Damaged Replication Forks. *Cold Spring Harb Perspect Biol* **5**, 1–15 (2013).
279. Byun, T. S., Pacek, M., Yee, M. C., Walter, J. C. & Cimprich, K. A. Functional uncoupling of MCM helicase and DNA polymerase activities activates the ATR-dependent checkpoint. *Genes Dev.* **19**, 1040–1052 (2005).
280. Xu, X. *et al.* The Basic Cleft of RPA70N Binds Multiple Checkpoint Proteins, Including RAD9, To Regulate ATR Signaling. *Mol. Cell Biol.* **28**, 7345–7353 (2008).
281. Nam, E. a & Cortez, D. ATR signalling: more than meeting at the fork. *Biochem. J.* **436**, 527–536 (2011).
282. Saldivar, J. C., Cortez, D. & Cimprich, K. A. The essential kinase ATR: ensuring faithful duplication of a challenging genome. *Nat. Publ. Gr.* **18**, 622–636 (2017).
283. Cortez, D., Guntuku, S. & Qin, J. ATR and ATRIP : Partners in Checkpoint Signaling. *Science* **294**, 1713–1717 (2001).
284. Zhang, H. *et al.* ATRIP Deacetylation by SIRT2 Drives ATR Checkpoint Activation by Promoting Binding to RPA-ssDNA. *Cell Rep.* **14**, 1435–1447 (2016).
285. Kumagai, A., Lee, J., Yoo, H. Y. & Dunphy, W. G. TopBP1 activates the ATR-ATRIP complex. *Cell* **124**, 943–955 (2006).
286. Mordes, D. A., Glick, G. G., Zhao, R. & Cortez, D. TopBP1 activates ATR through ATRIP and a PIKK regulatory domain. *Genes Dev.* **22**, 1478–1489 (2008).
287. Bass, T. E. *et al.* ETAA1 acts at stalled replication forks to maintain genome integrity. *Nat. Cell Biol.* **18**, 1185–1195 (2016).
288. Haahr, P. *et al.* Activation of the ATR kinase by the RPA-binding protein ETAA1. *Nat. Cell Biol.* **18**, 1196–1207 (2016).
289. Lee, Y.-C., Zhou, Q., Chen, J. & Yuan, J. RPA-Binding Protein ETAA1 Is an ATR Activator Involved in DNA Replication Stress Response. *Curr. Biol.* **26**, 3257–3268 (2016).

290. Zou, L. DNA Replication Checkpoint: New ATR Activator Identified. *Curr. Biol.* **27**, R33–R35 (2017).
291. Lee, J., Kumagai, A. & Dunphy, W. G. The Rad9-Hus1-Rad1 checkpoint clamp regulates interaction of TopBP1 with ATR. *J. Biol. Chem.* **282**, 28036–28044 (2007).
292. Delacroix, S., Wagner, J. M., Kobayashi, M., Yamamoto, K. I. & Karnitz, L. M. The Rad9-Hus1-Rad1 (9-1-1) clamp activates checkpoint signaling via TopBP1. *Genes Dev.* **21**, 1472–1477 (2007).
293. Bermudez, V. P. *et al.* Loading of the human 9-1-1 checkpoint complex onto DNA by the checkpoint clamp loader hRad17-replication factor C complex in vitro. *Proc. Natl. Acad. Sci.* **100**, 1633–1638 (2003).
294. Zou, L., Liu, D. & Elledge, S. J. Replication protein A-mediated recruitment and activation of Rad17 complexes. *Proc. Natl. Acad. Sci.* **100**, 13827–13832 (2003).
295. Duursma, A. M., Driscoll, R., Elias, J. E. & Cimprich, K. A. A Role for the MRN Complex in ATR Activation via TOPBP1 Recruitment. *Mol. Cell* **50**, 116–122 (2013).
296. Lee, J. & Dunphy, W. G. The Mre11-Rad50-Nbs1 (MRN) complex has a specific role in the activation of Chk1 in response to stalled replication forks. *Mol. Biol. Cell* **24**, 1343–1353 (2013).
297. Cotta-ramusino, C. *et al.* A DNA Damage Response Screen Identifies RHINO, a 9-1-1 and TopBP1 interacting protein required for ATR signaling. *Science* **332**, 1313–1317 (2011).
298. Lindsey-Boltz, L. A., Kemp, M. G., Capp, C. & Sancar, A. RHINO forms a stoichiometric complex with the 9-1-1 checkpoint clamp and mediates ATR-Chk1 signaling. *Cell Cycle* **14**, 99–108 (2015).
299. Ohashi, E., Takeishi, Y., Ueda, S. & Tsurimoto, T. Interaction between Rad9-Hus1-Rad1 and TopBP1 activates ATR-ATRIP and promotes TopBP1 recruitment to sites of UV-damage. *DNA Repair (Amst)*. **21**, 1–11 (2014).
300. Liu, S. *et al.* ATR Autophosphorylation as a Molecular Switch for Checkpoint Activation. *Mol. Cell* **43**, 192–202 (2011).
301. Liu, Q. *et al.* Chk1 is an essential kinase that is regulated by Atr and required for the G2/M DNA damage checkpoint. *Genes Dev.* **14**, 1448–1459 (2000).
302. Zhao, H. & Piwnicka-Worms, H. ATR-Mediated Checkpoint Pathways Regulate Phosphorylation and Activation of Human Chk1. *Mol. Cell. Biol.* **21**, 4129–4139 (2001).
303. Kasahara, K. *et al.* 14-3-3 $\gamma$  3 mediates Cdc25A proteolysis to block premature mitotic entry after DNA damage. *EMBO J.* **29**, 2802–2812 (2010).
304. Kumagai, a & Dunphy, W. G. Claspin, a novel protein required for the activation of Chk1 during a DNA replication checkpoint response in *Xenopus* egg extracts. *Mol. Cell* **6**, 839–849 (2000).
305. Unsal-Kacmaz, K. *et al.* The Human Tim/Tipin Complex Coordinates an Intra-S Checkpoint Response to UV That Slows Replication Fork Displacement. *Mol. Cell. Biol.* **27**, 3131–3142 (2007).
306. Min, W. *et al.* Poly(ADP-ribose) binding to Chk1 at stalled replication forks is required for S-phase checkpoint activation. *Nat. Commun.* **4**, 2993 (2013).
307. Meng, Z., Capalbo, L., Glover, D. M. & Dunphy, W. G. Role for casein kinase 1 in the phosphorylation of Claspin on critical residues necessary for the activation of Chk1. *Mol. Biol. Cell* **22**, 2834–2847 (2011).
308. Chini, C. C. S. & Chen, J. Claspin, a regulator of Chk1 in DNA replication stress pathway. *DNA Repair (Amst)*. **3**, 1033–1037 (2004).
309. Chini, C. C. S., Wood, J. & Chen, J. Chk1 is required to maintain Claspin stability. *Oncogene* **25**, 4165–4171 (2006).
310. Kumagai, A. & Dunphy, W. G. Repeated phosphopeptide motifs in claspin mediate the regulated binding of Chk1. *Nat. Cell Biol.* **5**, 161–165 (2003).
311. Lindsey-Boltz, L. A., Serçin, Ö., Choi, J. H. & Sancar, A. Reconstitution of human claspin-mediated phosphorylation of Chk1 by the ATR (Ataxia Telangiectasia-mutated and Rad3-related) checkpoint kinase. *J. Biol. Chem.* **284**, 33107–33114 (2009).
312. Shechter, D., Costanzo, V. & Gautier, J. ATR and ATM regulate the timing of DNA replication origin firing. *Nat. Cell Biol.* **6**, 648–655 (2004).
313. Syljuåsen, R. G. *et al.* Inhibition of Human Chk1 Causes Increased Initiation of DNA Replication, Phosphorylation of ATR Targets, and DNA Breakage Inhibition of Human Chk1 Causes Increased Initiation of DNA Replication, Phosphorylation of ATR Targets, and DNA Breakage. *Mol. Cell. Biol.* **25**, 3553–3562 (2005).

314. Petermann, E., Woodcock, M. & Helleday, T. Chk1 promotes replication fork progression by controlling replication initiation. *Proc Natl Acad Sci* **107**, 16090–16095 (2010).
315. Marheineke, K. & Hyrien, O. Control of replication origin density and firing time in *Xenopus* egg extracts. Role of a caffeine-sensitive, ATR-dependent checkpoint. *J. Biol. Chem.* **279**, 28071–28081 (2004).
316. Santocanale, C. & Diffie, J. F. X. A Mec1- and Rad53-dependent checkpoint controls late-firing origins of DNA replication. *Nature* **395**, 615–618 (1998).
317. Costanzo, V. *et al.* An ATR- and Cdc7-dependent DNA damage checkpoint that inhibits initiation of DNA replication. *Mol. Cell* **11**, 203–213 (2003).
318. Karnani, N. & Dutta, A. The effect of the intra-S-phase checkpoint on origins of replication in human cells. *Genes Dev.* **25**, 621–633 (2011).
319. Liu, H. *et al.* Phosphorylation of MLL by ATR is required for execution of mammalian S-phase checkpoint. *Nature* **467**, 343–346 (2010).
320. Guo, C. *et al.* Interaction of Chk1 with Treslin Negatively Regulates the Initiation of Chromosomal DNA Replication. *Mol. Cell* **57**, 492–505 (2015).
321. Alver, R. C., Chadha, G. S., Gillespie, P. J. & Blow, J. J. Reversal of DDK-Mediated MCM Phosphorylation by Rif1-PP1 Regulates Replication Initiation and Replisome Stability Independently of ATR/Chk1. *Cell Rep.* **18**, 2508–2520 (2017).
322. Ge, X. Q. & Blow, J. J. Chk1 inhibits replication factory activation but allows dormant origin firing in existing factories. *J. Cell Biol.* **191**, 1285–1297 (2010).
323. Chen, Y.-H. *et al.* ATR-Mediated Phosphorylation of FANCI Regulates Dormant Origin Firing in Response to Replication Stress. *Mol. Cell* **58**, 323–338 (2015).
324. Chanoux, R. A. *et al.* ATR and H2AX Cooperate in Maintaining Genome Stability under Replication Stress. *J. Biol. Chem.* **284**, 5994–6003 (2009).
325. Cobb, J. A., Bjergbaek, L., Shimada, K., Frei, C. & Gasser, S. M. DNA polymerase stabilization at stalled replication forks requires Mec1 and the RecQ helicase Sgs1. *EMBO J.* **22**, 4325–36 (2003).
326. Lucca, C. *et al.* Checkpoint-mediated control of replisome-fork association and signalling in response to replication pausing. *Oncogene* **23**, 1206–13 (2004).
327. Cobb, J. A. *et al.* Replisome instability, fork collapse, and gross chromosomal rearrangements arise synergistically from Mec1 kinase and RecQ helicase mutations. *Genes Dev.* **19**, 3055–69 (2005).
328. Lossaint, G. *et al.* FANCD2 binds MCM proteins and controls replisome function upon activation of S phase checkpoint signaling. *Mol. Cell* **51**, 678–90 (2013).
329. Wu, N. & Yu, H. The SMC complexes in DNA damage response. *Cell Biosci.* **2**, 1–11 (2012).
330. Remeseiro, S. & Losada, A. Cohesin, a chromatin engagement ring. *Curr. Opin. Cell Biol.* **25**, 63–71 (2013).
331. Frattini, C. *et al.* Cohesin Ubiquitylation and Mobilization Facilitate Stalled Replication Fork Dynamics. *Mol. Cell* **68**, 758–772 (2017).
332. Quinet, A., Lemaçon, D. & Vindigni, A. Replication Fork Reversal: Players and Guardians. *Mol. Cell* **68**, 830–833 (2017).
333. Higgins, N. P., Kato, K. & Strauss, B. A model for replication repair in mammalian cells. *J. Mol. Biol.* **101**, 417–425 (1976).
334. Neelsen, K. J. & Lopes, M. Replication fork reversal in eukaryotes: from dead end to dynamic response. *Nat. Rev. Mol. Cell Biol.* **16**, 207–220 (2015).
335. Kolinjivadi, A. M. *et al.* Smarcal1-Mediated Fork Reversal Triggers Mre11-Dependent Degradation of Nascent DNA in the Absence of Brca2 and Stable Rad51 Nucleofilaments. *Mol. Cell* **67**, 867–881 (2017).
336. Tagliatela, A. *et al.* Restoration of Replication Fork Stability in BRCA1- and BRCA2-Deficient Cells by Inactivation of SNF2-Family Fork Remodelers. *Mol. Cell* **68**, 414–430.e8 (2017).
337. Couch, F. B., Bansbach, C. E., Driscoll, R., Luzwick, J. W. & Glick, G. G. ATR phosphorylates SMARCAL1 to prevent replication fork collapse. *Genes Dev.* **27**, 1610–1623 (2013).
338. Couch, F. B. & Cortez, D. Fork reversal, too much of a good thing. *Cell Cycle* **13**, 1049–1050 (2014).
339. Bétous, R. *et al.* SMARCAL1 catalyzes fork regression and holliday junction migration to maintain genome stability during DNA replication. *Genes Dev.* **26**, 151–162 (2012).

340. Técher, H. *et al.* Signaling from Mus81-Eme2-Dependent DNA Damage Elicited by Chk1 Deficiency Modulates Replication Fork Speed and Origin Usage. *Cell Rep.* **14**, 1–14 (2016).
341. Forment, J. V., Blasius, M., Guerini, I. & Jackson, S. P. Structure-specific DNA endonuclease Mus81/Eme1 generates DNA damage caused by Chk1 inactivation. *PLoS One* **6**, e23517 (2011).
342. Thompson, R., Montano, R. & Eastman, A. The Mre11 Nuclease Is Critical for the Sensitivity of Cells to Chk1 Inhibition. *PLoS One* **7**, e44021 (2012).
343. Wang, H., Wang, H., Powell, S. N., Iliakis, G. & Wang, Y. ATR affecting cell radiosensitivity is dependent on homologous recombination repair but independent of nonhomologous end joining. *Cancer Res.* **64**, 7139–7143 (2004).
344. Foray, N. *et al.* A subset of ATM- and ATR-dependent phosphorylation events requires the BRCA1 protein. *EMBO J.* **22**, 2860–2871 (2003).
345. Tibbetts, R. S. *et al.* Functional interactions between BRCA1 and the checkpoint kinase ATR during genotoxic stress. *Genes Dev.* **14**, 2989–3002 (2000).
346. Takaoka, M. & Miki, Y. BRCA1 gene: function and deficiency. *Int. J. Clin. Oncol.* **23**, 36–44 (2018).
347. Sørensen, C. S. *et al.* The cell-cycle checkpoint kinase Chk1 is required for mammalian homologous recombination repair. *Nat. Cell Biol.* **7**, 195–201 (2005).
348. Ishiai, M. *et al.* FANCI phosphorylation functions as a molecular switch to turn on the Fanconi anemia pathway. *Nat. Struct. Mol. Biol.* **15**, 1138–1146 (2008).
349. Andreassen, P. R., D'Andrea, A. D. & Taniguchi, T. ATR couples FANCD2 monoubiquitination to the DNA-damage response. *Genes Dev.* **18**, 1958–1963 (2004).
350. Ishiai, M. *et al.* Activation of the FA pathway mediated by phosphorylation and ubiquitination. *Mutat. Res. - Fundam. Mol. Mech. Mutagen.* **803–805**, 89–95 (2017).
351. Singh, T. R. *et al.* ATR-dependent phosphorylation of FANCM at serine 1045 is essential for FANCM functions. *Cancer Res.* **73**, 4300–4310 (2013).
352. Mourón, S. *et al.* Repriming of DNA synthesis at stalled replication forks by human PrimPol. *Nat. Struct. Mol. Biol.* **20**, 1383–1389 (2013).
353. Guillian, T. & Doherty, A. PrimPol—Prime Time to Reprime. *Genes (Basel)*. **8**, E20 (2017).
354. Guillian, T. A. *et al.* Molecular basis for PrimPol recruitment to replication forks by RPA. *Nat. Commun.* **8**, 15222 (2017).
355. Vaisman, A. & Woodgate, R. Translesion DNA polymerases in eukaryotes: what makes them tick? *Crit. Rev. Biochem. Mol. Biol.* **52**, 274–303 (2017).
356. Costes, A. & Lambert, S. A. E. Homologous Recombination as a Replication Fork Escort: Fork-Protection and Recovery. *Biomolecules* **3**, 39–71 (2013).
357. Kolinjivadi, A. M. *et al.* Moonlighting at replication forks: a new life for homologous recombination proteins BRCA1, BRCA2 and RAD51. *FEBS Lett.* **591**, 1083–1100 (2017).
358. Feng, W. & Jasin, M. Homologous Recombination and Replication Fork Protection: BRCA2 and More! *Cold Spring Harb. Symp. Quant. Biol.* **82**, 329–338 (2017).
359. Sabbioneda, S., Bortolomai, I., Giannattasio, M., Plevani, P. & Muzi-Falconi, M. Yeast Rev1 is cell cycle regulated, phosphorylated in response to DNA damage and its binding to chromosomes is dependent upon MEC1. *DNA Repair (Amst)*. **6**, 121–127 (2007).
360. Pagès, V., Santa Maria, S. R., Prakash, L. & Prakash, S. Role of DNA damage-induced replication checkpoint in promoting lesion bypass by translesion synthesis in yeast. *Genes Dev.* **23**, 1438–1449 (2009).
361. Göhler, T., Sabbioneda, S., Green, C. M. & Lehmann, A. R. ATR-mediated phosphorylation of DNA polymerase  $\eta$  is needed for efficient recovery from UV damage. *J. Cell Biol.* **192**, 219–227 (2011).
362. Sale, J. E. Translesion DNA Synthesis and Mutagenesis in Eukaryotes. *Cold Spring Harb. Perspect. Biol.* **5**, a012708 (2013).
363. Yamada, M. *et al.* ATR-Chk1-APC/CCdh1-dependent stabilization of Cdc7-ASK (Dbf4) kinase is required for DNA lesion bypass under replication stress. *Genes Dev.* **27**, 2459–2472 (2013).
364. Yang, K., Weinacht, C. P. & Zhuang, Z. Regulatory role of ubiquitin in eukaryotic DNA translesion synthesis. *Biochemistry* **52**, 3217–3228 (2013).
365. Vassin, V. M., Anantha, R. W., Sokolova, E., Kanner, S. & Borowiec, J. a. Human RPA phosphorylation by ATR stimulates DNA synthesis and prevents ssDNA accumulation during DNA-

- replication stress. *J. Cell Sci.* **122**, 4070–4080 (2009).
366. Murphy, A. K. *et al.* Phosphorylated RPA recruits PALB2 to stalled DNA replication forks to facilitate fork recovery. *J. Cell Biol.* **206**, 493–507 (2014).
367. Ahlskog, J. K., Larsen, B. D., Achanta, K. & Sørensen, C. S. ATM/ATR-mediated phosphorylation of PALB2 promotes RAD51 function. *EMBO Rep.* **17**, 1–11 (2016).
368. Somyajit, K., Basavaraju, S., Scully, R. & Nagaraju, G. ATM- and ATR-Mediated Phosphorylation of XRCC3 Regulates DNA Double-Strand Break-Induced Checkpoint Activation and Repair. *Mol. Cell Biol.* **33**, 1830–1844 (2013).
369. Bahassi, E. M. *et al.* The checkpoint kinases Chk1 and Chk2 regulate the functional associations between hBRCA2 and Rad51 in response to DNA damage. *Oncogene* **27**, 3977–3985 (2008).
370. Petermann, E., Orta, M. L., Issaeva, N., Schultz, N. & Helleday, T. Hydroxyurea-stalled replication forks become progressively inactivated and require two different RAD51-mediated pathways for restart and repair. *Mol. Cell* **37**, 492–502 (2010).
371. Davies, S. L., North, P. S., Dart, A., Lakin, N. D. & Hickson, I. D. Phosphorylation of the Bloom's Syndrome Helicase and Its Role in Recovery from S-Phase Arrest. *Mol. Cell Biol.* **24**, 1279–1291 (2004).
372. Ammazalorso, F., Pirzio, L. M., Bignami, M., Franchitto, A. & Pichierri, P. ATR and ATM differently regulate WRN to prevent DSBs at stalled replication forks and promote replication fork recovery. *EMBO J.* **29**, 3156–3169 (2010).
373. Jackson, S. P. & Bartek, J. The DNA-damage response in human biology and disease. *Nature* **461**, 1071–8 (2009).
374. Ciccia, A. & Elledge, S. J. The DNA Damage Response: Making It Safe to Play with Knives. *Mol. Cell* **40**, 179–204 (2010).
375. Uziel, T. *et al.* Requirement of the MRN complex for ATM activation by DNA damage. *EMBO J.* **22**, 5612–5621 (2003).
376. Shiloh, Y. & Ziv, Y. The ATM protein kinase: Regulating the cellular response to genotoxic stress, and more. *Nat. Rev. Mol. Cell Biol.* **14**, 197–210 (2013).
377. Stracker, T. H. & Petrini, J. H. J. The MRE11 complex: Starting from the ends. *Nat. Rev. Mol. Cell Biol.* **12**, 90–103 (2011).
378. Paull, T. T. Mechanisms of ATM Activation. *Annu. Rev. Biochem.* **84**, 711–738 (2015).
379. Lee, J. H. & Paull, T. T. ATM activation by DNA double-strand breaks through the Mre11-Rad50}{Nbs1} complex. *Science* **308**, 551–554 (2005).
380. Lee, J. H., Goodarzi, A. A., Jeggo, P. A. & Paull, T. T. 53BP1 promotes ATM activity through direct interactions with the MRN complex. *EMBO J.* **29**, 574–585 (2010).
381. So, S., Davis, A. J. & Chen, D. J. Autophosphorylation at serine 1981 stabilizes ATM at DNA damage sites. *J. Cell Biol.* **187**, 977–990 (2009).
382. Bensimon, A. *et al.* ATM-Dependent and -Independent Dynamics of the Nuclear Phosphoproteome After DNA Damage. *Sci. Signal.* **3**, rs3 (2010).
383. Kozlov, S. V. *et al.* Involvement of novel autophosphorylation sites in ATM activation. *EMBO J.* **25**, 3504–3514 (2006).
384. Kozlov, S. V. *et al.* Autophosphorylation and ATM activation: Additional sites add to the complexity. *J. Biol. Chem.* **286**, 9107–9119 (2011).
385. Sun, Y., Jiang, X., Chen, S., Fernandes, N. & Price, B. D. A role for the Tip60 histone acetyltransferase in the acetylation and activation of ATM. *Proc. Natl. Acad. Sci.* **102**, 13182–13187 (2005).
386. Sun, Y., Xu, Y., Roy, K. & Price, B. D. DNA Damage-Induced Acetylation of Lysine 3016 of ATM Activates ATM Kinase Activity. *Mol. Cell Biol.* **27**, 8502–8509 (2007).
387. Bakkenist, C. J. & Kastan, M. B. DNA damage activates ATM through intermolecular autophosphorylation and dimer dissociation. *Nature* **421**, 499–506 (2003).
388. Matsuoka, S. *et al.* Ataxia telangiectasia-mutated phosphorylates Chk2 *in vivo* and *in vitro*. *Proc. Natl. Acad. Sci.* **97**, 10389–10394 (2000).
389. Stiff, T. *et al.* ATM and DNA-PK Function Redundantly to Phosphorylate H2AX after Exposure to Ionizing Radiation. *Cancer Res.* **64**, 2390–2396 (2004).
390. Ward, I. M. & Chen, J. Histone H2AX Is Phosphorylated in an ATR-dependent Manner in Response

- to Replicational Stress. *J. Biol. Chem.* **276**, 47759–47762 (2001).
391. Reinhardt, H. C. & Yaffe, M. B. Kinases that control the cell cycle in response to DNA damage: Chk1, Chk2, and MK2. *Curr. Opin. Cell Biol.* **21**, 245–255 (2009).
  392. Mailand, N. *et al.* RNF8 Ubiquitylates Histones at DNA Double-Strand Breaks and Promotes Assembly of Repair Proteins. *Cell* **131**, 887–900 (2007).
  393. Huen, M. S. Y. *et al.* RNF8 Transduces the DNA-Damage Signal via Histone Ubiquitylation and Checkpoint Protein Assembly. *Cell* **131**, 901–914 (2007).
  394. Thorslund, T. *et al.* Histone H1 couples initiation and amplification of ubiquitin signalling after DNA damage. *Nature* **527**, 389–393 (2015).
  395. Bartek, J. & Lukas, J. DNA damage checkpoints: from initiation to recovery or adaptation. *Curr. Opin. Cell Biol.* **19**, 238–245 (2007).
  396. Mimitou, E. P. & Symington, L. S. DNA end resection: Many nucleases make light work. *DNA Repair (Amst)*. **8**, 983–995 (2008).
  397. Sartori, A. A. *et al.* Human CtIP promotes DNA end resection. *Nature* **450**, 509–514 (2007).
  398. Liao, S., Toczylowski, T. & Yan, H. Identification of the *Xenopus* DNA2 protein as a major nuclease for the 5' → 3' strand-specific processing of DNA ends. *Nucleic Acids Res.* **36**, 6091–6100 (2008).
  399. Nimonkar, A. V, Ozsoy, A. Z., Genschel, J., Modrich, P. & Kowalczykowski, S. C. Human exonuclease 1 and BLM helicase interact to resect DNA and initiate DNA repair. *Proc Natl Acad Sci U S A* **105**, 16906–16911 (2008).
  400. Huertas, P. DNA resection in eukaryotes: deciding how to fix the break. *Nat. Struct. Mol. Biol.* **17**, 11–16 (2010).
  401. Cejka, P. DNA end resection: nucleases team up with the right partners to initiate homologous recombination. *J Biol Chem.* **290**, 22931–22938 (2015).
  402. McVey, M., Khodaverdian, V. Y., Meyer, D., Cerqueira, P. G. & Heyer, W.-D. Eukaryotic DNA Polymerases in Homologous Recombination. *Annu. Rev. Genet.* **50**, 393–421 (2016).
  403. Li, J. & Xu, X. DNA double-strand break repair: A tale of pathway choices. *Acta Biochim. Biophys. Sin. (Shanghai)*. **48**, 641–646 (2016).
  404. Lieber, M. R. The Mechanism of Double-Strand DNA Break Repair by the Nonhomologous DNA End-Joining Pathway. *Annu. Rev. Biochem.* **79**, 181–211 (2010).
  405. Chiruvella, K. K. *et al.* Repair of Double-Strand Breaks by End Joining. *Cold Spring Harb. Perspect. Biol.* **5**, a012757 (2013).
  406. Chang, H. H. Y., Pannunzio, N. R., Adachi, N. & Lieber, M. R. Non-homologous DNA end joining and alternative pathways to double-strand break repair. *Nat. Rev. Mol. Cell Biol.* **18**, 495–506 (2017).
  407. Daley, J. M. & Sung, P. 53BP1, BRCA1, and the choice between recombination and end joining at DNA double-strand breaks. *Mol. Cell. Biol.* **34**, 1380–8 (2014).
  408. Zimmermann, M. & De Lange, T. 53BP1: Pro choice in DNA repair. *Trends Cell Biol.* **24**, 108–117 (2014).
  409. Shibata, A. Regulation of repair pathway choice at two-ended DNA double-strand breaks. *Mutat. Res. - Fundam. Mol. Mech. Mutagen.* **803–805**, 51–55 (2017).
  410. Ha, K. *et al.* The anaphase promoting complex impacts repair choice by protecting ubiquitin signalling at DNA damage sites. *Nat. Commun.* **8**, 1–15 (2017).
  411. Matt, S. *et al.* The DNA damage-induced cell death response : a roadmap to kill cancer cells. *Cell. Mol. Life Sci.* **73**, 2829–2850 (2016).
  412. Kastan, M. B. & Lim, D. The many substrates and functions of ATM. *Mol. Cell Biol.* **1**, 179–186 (2000).
  413. Shiloh, Y. ATM and related protein kinases: safeguarding genome integrity. *Nat. Rev. Cancer* **3**, 155–168 (2003).
  414. Bartek, J. & Lukas, J. Chk1 and Chk2 kinases in checkpoint control and cancer. *Cancer Cell* **3**, 421–429 (2003).
  415. Maya, R. *et al.* ATM-dependent phosphorylation of Mdm2 on serine 395: Role in p53 activation by DNA damage. *Genes Dev.* **15**, 1067–1077 (2001).
  416. El-Deiry, W. S. *et al.* WAF1, a Potential Mediator of p53 Tumor Suppression. *Cell* **75**, 817–825 (1993).

417. Gartel, A. L. & Tyner, A. L. Transcriptional Regulation of the p21 ( WAF1 / CIP1 ) Gene. *Exp. Cell Res.* **289**, 280–289 (1999).
418. Waga, S., Hannon, G. J., Beach, D. & Stillman, B. The p21 inhibitor of cyclin-dependent kinases controls DNA replication by interaction with PCNA. *Nature* **369**, 574–578 (1994).
419. Luo, Y., Hurwitz, J. & Massagué, J. Cell-cycle inhibition by independent CDK and PCNA binding domains in p21Cip1. *Nature* **375**, 159–161 (1995).
420. Oku, T. *et al.* Functional sites of human PCNA which interact with p21 (Cip1/Waf1), DNA polymerase  $\delta$  and replication factor C. *Genes to Cells* **3**, 357–369 (1998).
421. Soria, G., Speroni, J., Podhajcer, O. L., Prives, C. & Gottifredi, V. p21 differentially regulates DNA replication and DNA-repair-associated processes after UV irradiation. *J. Cell Sci.* **121**, 3271–3282 (2008).
422. Avkin, S. *et al.* p53 and p21 Regulate Error-Prone DNA Repair to Yield a Lower Mutation Load. *Mol. Cell* **22**, 407–413 (2006).
423. Soria, G., Podhajcer, O., Prives, C. & Gottifredi, V. P21Cip1/WAF1 downregulation is required for efficient PCNA ubiquitination after UV irradiation. *Oncogene* **25**, 2829–2838 (2006).
424. Cazzalini, O., Scovassi, A. I., Savio, M., Stivala, L. A. & Prosperi, E. Multiple roles of the cell cycle inhibitor p21CDKN1A in the DNA damage response. *Mutat. Res. - Rev. Mutat. Res.* **704**, 12–20 (2010).
425. Macheret, M. & Halazonetis, T. D. DNA Replication Stress as a Hallmark of Cancer. *Annu. Rev. Pathol. Mech. Dis.* **10**, 425–448 (2015).
426. Dungrawala, H. *et al.* The Replication Checkpoint Prevents Two Types of Fork Collapse without Regulating Replisome Stability. *Mol. Cell* **59**, 998–1010 (2015).
427. Renard-guillet, C., Kanoh, Y., Shirahige, K. & Masai, H. Temporal and spatial regulation of eukaryotic DNA replication : From regulated initiation to genome-scale timing program. *Semin. Cell Dev. Biol.* **30**, 110–120 (2014).
428. Méchali, M., Yoshida, K., Coulombe, P. & Pasero, P. Genetic and epigenetic determinants of DNA replication origins, position and activation. *Curr. Opin. Genet. Dev.* **23**, 124–131 (2013).
429. Heller, R. C. & Marians, K. J. Replication fork reactivation downstream of a blocked nascent leading strand. *Nature* **439**, 557–562 (2006).
430. Yeeles, J. T. P. & Marians, K. J. The Escherichia coli Replisome Is Inherently DNA Damage Tolerant. *Science* **334**, 235–239 (2011).
431. Lopes, M., Foiani, M. & Sogo, J. M. Multiple mechanisms control chromosome integrity after replication fork uncoupling and restart at irreparable UV lesions. *Mol. Cell* **21**, 15–27 (2006).
432. Evers, I., Johansson, F., Groth, P., Erixon, K. & Helleday, T. UV stalled replication forks restart by re-priming in human fibroblasts. *Nucleic Acids Res.* **39**, 7049–7057 (2011).
433. Iyer, L. M., Koonin, E. V., Leipe, D. D. & Aravind, L. Origin and evolution of the archaeo-eukaryotic primase superfamily and related palm-domain proteins: Structural insights and new members. *Nucleic Acids Res.* **33**, 3875–3896 (2005).
434. Bianchi, J. *et al.* PrimPol bypasses UV photoproducts during eukaryotic chromosomal DNA replication. *Mol. Cell* **52**, 566–573 (2013).
435. García-Gómez, S. *et al.* PrimPol, an Archaic Primase/Polymerase Operating in Human Cells. *Mol. Cell* **52**, 541–553 (2013).
436. Kobayashi, K. *et al.* Repriming by PrimPol is critical for DNA replication restart downstream of lesions and chain-terminating nucleosides. *Cell Cycle* **15**, 1997–2008 (2016).
437. Schauer, G. D. & O'Donnell, M. E. Quality control mechanisms exclude incorrect polymerases from the eukaryotic replication fork. *Proc. Natl. Acad. Sci.* **114**, 675–680 (2017).
438. Yang, W. & Woodgate, R. What a difference a decade makes: Insights into translesion DNA synthesis. *Proc Natl Acad Sci* **104**, 15591–15598 (2007).
439. McCulloch, S. D. & Kunkel, T. A. The fidelity of DNA synthesis by eukaryotic replicative and translesion synthesis polymerases. *Cell Res.* **18**, 148–161 (2008).
440. Goodman, M. F. Error-Prone Repair DNA Polymerases in Prokaryotes and Eukaryotes. *Annu. Rev. Biochem.* **71**, 17–50 (2002).
441. Shcherbakova, P. V., Bebenek, K. & Kunkel, T. A. Functions of Eukaryotic DNA Polymerases. *Sci.*

- Aging Knowl. Environ.* **2003**, RE3 (2003).
442. Gao, Y., Mutter-Rottmayer, E., Zlatanou, A., Vaziri, C. & Yang, Y. Mechanisms of Post-Replication DNA Repair. *Genes (Basel)*. **8**, E64 (2017).
  443. Zhao, L. & Washington, M. Translesion Synthesis: Insights into the Selection and Switching of DNA Polymerases. *Genes (Basel)*. **8**, e24 (2017).
  444. Kannouche, P. L., Wing, J. & Lehmann, A. R. Interaction of human DNA polymerase  $\eta$  with monoubiquitinated PCNA: A possible mechanism for the polymerase switch in response to DNA damage. *Mol. Cell* **14**, 491–500 (2004).
  445. Watanabe, K. *et al.* Rad18 guides pol $\eta$  to replication stalling sites through physical interaction and PCNA monoubiquitination. *EMBO J.* **23**, 3886–3896 (2004).
  446. Acharya, N. *et al.* Roles of PCNA-binding and ubiquitin-binding domains in human DNA polymerase  $\eta$  in translesion DNA synthesis. *Proc. Natl. Acad. Sci.* **105**, 17724–17729 (2008).
  447. Gueranger, Q. *et al.* Role of DNA polymerases  $\eta$ ,  $\iota$  and  $\zeta$  in UV resistance and UV-induced mutagenesis in a human cell line. *DNA Repair (Amst)*. **7**, 1551–1562 (2008).
  448. Acharya, N., Yoon, J.-H., Hurwitz, J., Prakash, L. & Prakash, S. DNA polymerase  $\eta$  lacking the ubiquitin-binding domain promotes replicative lesion bypass in human cells. *Proc. Natl. Acad. Sci.* **107**, 10401–10405 (2010).
  449. Hendel, A. *et al.* PCNA ubiquitination is important, but not essential for translesion DNA synthesis in mammalian cells. *PLoS Genet.* **7**, e1002262 (2011).
  450. Nevin, P., Gabbai, C. C. & Marians, K. J. Replisome-mediated Translesion Synthesis by a Cellular Replicase. *J Biol Chem.* **292**, 13833–13842 (2017).
  451. Taylor, M. R. G., Yeeles, J. T. P., Taylor, M. R. G. & Yeeles, J. T. P. The Initial Response of a Eukaryotic Replisome to DNA Damage. *Mol. Cell* **70**, 1–14 (2018).
  452. Hirota, K. *et al.* The POLD3 subunit of DNA polymerase  $\delta$  can promote translesion synthesis independently of DNA polymerase  $\epsilon$ . *Nucleic Acids Res.* **43**, 1671–1683 (2015).
  453. Hirota, K. *et al.* In vivo evidence for translesion synthesis by the replicative DNA polymerase  $\delta$ . *Nucleic Acids Res.* **44**, 7242–7250 (2016).
  454. Kanao, R. & Masutani, C. Regulation of DNA damage tolerance in mammalian cells by post-translational modifications of PCNA. *Mutat. Res.* **803–805**, 82–88 (2017).
  455. Hoegge, C., Pfander, B., Moldovan, G. L., Pyrowolakis, G. & Jentsch, S. RAD6-dependent DNA repair is linked to modification of PCNA by ubiquitin and SUMO. *Nature* **419**, 135–141 (2002).
  456. Branzei, D. & Szakal, B. DNA damage tolerance by recombination: Molecular pathways and DNA structures. *DNA Repair (Amst)*. **44**, 68–75 (2016).
  457. Branzei, D. & Szakal, B. Building up and breaking down: mechanisms controlling recombination during replication. *Crit. Rev. Biochem. Mol. Biol.* **52**, 381–394 (2017).
  458. Lovett, S. T. Template-switching during replication fork repair in bacteria. *DNA Repair (Amst)*. **56**, 118–128 (2017).
  459. Vanoli, F., Fumasoni, M., Szakal, B., Maloisel, L. & Branzei, D. Replication and recombination factors contributing to recombination-dependent bypass of DNA lesions by template switch. *PLoS Genet.* **6**, e1001205 (2010).
  460. Giannattasio, M. *et al.* Visualization of recombination-mediated damage bypass by template switching. *Nat. Struct. Mol. Biol.* **21**, 884–892 (2014).
  461. Liberi, G. *et al.* Rad51-dependent DNA structures accumulate at damaged replication forks in *sgs1* mutants defective in the yeast ortholog of BLM RecQ helicase. *Genes Dev.* **19**, 339–350 (2005).
  462. Zellweger, R. *et al.* Rad51-mediated replication fork reversal is a global response to genotoxic treatments in human cells. *J. Cell Biol.* **208**, 563–79 (2015).
  463. Bugreev, D. V., Rossi, M. J. & Mazin, A. V. Cooperation of RAD51 and RAD54 in regression of a model replication fork. *Nucleic Acids Res.* **39**, 2153–2164 (2011).
  464. Gari, K., Decaillet, C., Delannoy, M., Wu, L. & Constantinou, A. Remodeling of DNA replication structures by the branch point translocase FANCM. *Proc. Natl. Acad. Sci.* **105**, 16107–16112 (2008).
  465. Yuan, J., Ghosal, G. & Chen, J. The HARP-like Domain-Containing Protein AH2/ZRANB3 Binds to PCNA and Participates in Cellular Response to Replication Stress. *Mol. Cell* **47**, 410–421 (2012).
  466. Ciccio, A. *et al.* Polyubiquitinated PCNA Recruits the ZRANB3 Translocase to Maintain Genomic

- Integrity after Replication Stress. *Mol. Cell* **47**, 396–409 (2012).
467. Blastyak, A., Hajdu, I., Unk, I. & Haracska, L. Role of Double-Stranded DNA Translocase Activity of Human HLTf in Replication of Damaged DNA. *Mol. Cell. Biol.* **30**, 684–693 (2010).
  468. Achar, Y. J., Balogh, D. & Haracska, L. Coordinated protein and DNA remodeling by human HLTf on stalled replication fork. *Proc. Natl. Acad. Sci.* **108**, 14073–14078 (2011).
  469. Kile, A. C. *et al.* HLTf's Ancient HIRAN Domain Binds 3' DNA Ends to Drive Replication Fork Reversal. *Mol. Cell* **58**, 1090–1100 (2015).
  470. Fugger, K. *et al.* FBH1 Catalyzes Regression of Stalled Replication Forks. *Cell Rep.* **10**, 1749–1757 (2015).
  471. Kanagaraj, R., Saydam, N., Garcia, P. L., Zheng, L. & Janscak, P. Human RECQ5 $\beta$  helicase promotes strand exchange on synthetic DNA structures resembling a stalled replication fork. *Nucleic Acids Res.* **34**, 5217–5231 (2006).
  472. Machwe, A., Xiao, L., Groden, J. & Orren, D. K. The Werner and Bloom syndrome proteins catalyze regression of a model replication fork. *Biochemistry* **45**, 13939–13946 (2006).
  473. Vujanovic, M. *et al.* Replication Fork Slowing and Reversal upon DNA Damage Require PCNA Polyubiquitination and ZRANB3 DNA Translocase Activity. *Mol. Cell* **67**, 882–890.e5 (2017).
  474. Bhat, K. P. & Cortez, D. RPA and RAD51: fork reversal, fork protection, and genome stability. *Nat. Struct. Mol. Biol.* **25**, 446–453 (2018).
  475. Kowalczykowski, S. C. An Overview of the Molecular Mechanisms of Recombinational DNA Repair. *Cold Spring Harb. Perspect. Biol.* **7**, a016410 (2015).
  476. Hashimoto, Y., Ray Chaudhuri, A., Lopes, M. & Costanzo, V. Rad51 protects nascent DNA from Mre11-dependent degradation and promotes continuous DNA synthesis. *Nat. Struct. Mol. Biol.* **17**, 1305–11 (2010).
  477. Schlacher, K. *et al.* Double-Strand Break Repair Independent Role For BRCA2 In Blocking Stalled Replication Fork Degradation By MRE11. *Cell* **145**, 529–542 (2011).
  478. Mijic, S. *et al.* Replication fork reversal triggers fork degradation in BRCA2-defective cells. *Nat Commun* **8**, 859 (2017).
  479. Schlacher, K., Wu, H. & Jasin, M. A Distinct Replication Fork Protection Pathway Connects Fanconi Anemia Tumor Suppressors to RAD51-BRCA1/2. *Cancer Cell* **22**, 106–116 (2012).
  480. Higgs, M. R. *et al.* BOD1L Is Required to Suppress Deleterious Resection of Stressed Replication Forks. *Mol. Cell* **59**, 462–477 (2015).
  481. Berti, M. *et al.* Human RECQ1 promotes restart of replication forks reversed by DNA topoisomerase I inhibition. *Nat. Publ. Gr.* **20**, 347–354 (2013).
  482. Thangavel, S. *et al.* DNA2 drives processing and restart of reversed replication forks in human cells. *J. Cell Biol.* **208**, 545–62 (2015).
  483. Hanada, K. *et al.* The structure-specific endonuclease Mus81 contributes to replication restart by generating double-strand DNA breaks. *Nat. Struct. Mol. Biol.* **14**, 1096–1104 (2007).
  484. Regairaz, M. *et al.* Mus81-mediated DNA cleavage resolves replication forks stalled by topoisomerase I-DNA complexes. *J. Cell Biol.* **195**, 739–749 (2011).
  485. Llorente, B., Smith, C. E. & Symington, L. S. Break-induced replication: What is it and what is it for? *Cell Cycle* **7**, 859–864 (2008).
  486. Sakofsky, C. J. & Malkova, A. Break induced replication in eukaryotes: mechanisms, functions, and consequences. *Crit. Rev. Biochem. Mol. Biol.* **52**, 395–413 (2017).
  487. Kramara, J., Osia, B. & Malkova, A. Break-induced replication: An unhealthy choice for stress relief? *Nat. Struct. Mol. Biol.* **24**, 11–12 (2017).
  488. Costantino, L., Sotiriou, S. K., Rantala, J. K., Magin, S. & Halazonetis, T. D. Break-induced replication repair of damaged forks induces genomic duplications in human cells. *Science* **343**, 88–91 (2014).
  489. Malkova, A. & Ira, G. Break-induced replication: Functions and molecular mechanism. *Curr. Opin. Genet. Dev.* **23**, 271–279 (2013).
  490. Donnianni, R. A. & Symington, L. S. Break-induced replication occurs by conservative DNA synthesis. *Proc. Natl. Acad. Sci.* **110**, 13475–13480 (2013).
  491. Saini, N. *et al.* Migrating bubble during break-induced replication drives conservative DNA synthesis. *Nature* **502**, 389–392 (2013).

492. Wilson, M. A. *et al.* Pif1 helicase and Pol $\delta$  promote recombination-coupled DNA synthesis via bubble migration. *Nature* **502**, 393–396 (2013).
493. Sotiriou, S. K. *et al.* Mammalian RAD52 Functions in Break-Induced Replication Repair of Collapsed DNA Replication Forks. *Mol. Cell* **64**, 1127–1134 (2016).
494. Buzovetsky, O. *et al.* Role of the Pif1-PCNA Complex in Pol  $\delta$ -Dependent Strand Displacement DNA Synthesis and Break-Induced Replication. *Cell Rep.* **21**, 1707–1714 (2017).
495. Lemaçon, D., Jackson, J., Quinet, A., Brickner, J. R. & Li, S. MRE11 and EXO1 nucleases degrade reversed forks and elicit MUS81- dependent fork rescue in BRCA2-deficient cells . *Nat. Commun.* **8**, 860 (2017).
496. Couch, F. B. *et al.* ATR phosphorylates SMARCAL1 to prevent replication fork collapse. *Genes Dev.* **27**, 1610–1623 (2013).
497. Bicknell, L. S. *et al.* Mutations in the pre-replication complex cause Meier-Gorlin syndrome. *Nat. Genet.* **43**, 356–360 (2011).
498. Fenwick, A. L. *et al.* Mutations in CDC45, Encoding an Essential Component of the Pre-initiation Complex, Cause Meier-Gorlin Syndrome and Craniosynostosis. *Am. J. Hum. Genet.* **99**, 125–138 (2016).
499. Alderton, G. K. *et al.* Seckel syndrome exhibits cellular features demonstrating defects in the ATR-signalling pathway. *Hum. Mol. Genet.* **13**, 3127–3138 (2004).
500. O’Driscoll, M., Ruiz-Perez, V. L., Woods, C. G., Jeggo, P. A. & Goodship, J. A. A splicing mutation affecting expression of ataxia-telangiectasia and Rad3-related protein (ATR) results in Seckel syndrome. *Nat. Genet.* **33**, 497–501 (2003).
501. Ogi, T. *et al.* Identification of the First ATRIP-Deficient Patient and Novel Mutations in ATR Define a Clinical Spectrum for ATR-ATRIP Seckel Syndrome. *PLoS Genet.* **8**, e1002945 (2012).
502. Llorens-Agost, M. *et al.* Analysis of novel missense ATR mutations reveals new splicing defects underlying Seckel Syndrome. *Hum. Mutat.* **39**, 1847–1853 (2018).
503. Crow, Y. J. *et al.* Mutations in genes encoding ribonuclease H2 subunits cause Aicardi-Goutières syndrome and mimic congenital viral brain infection. *Nat. Genet.* **38**, 910–916 (2006).
504. Boerkoel, C. F. *et al.* Mutant chromatin remodeling protein SMARCAL1 causes Schimke immuno-osseous dysplasia. *Nat. Genet.* **30**, 215–220 (2002).
505. Elizonod, L. I. *et al.* Schimke immuno-osseous dysplasia: SMARCAL1 loss-of-function and phenotypic correlation. *J. Med. Genet.* **46**, 49–59 (2009).
506. Santangelo, L. *et al.* A novel SMARCAL1 mutation associated with a mild phenotype of Schimke immuno-osseous dysplasia (SIOD). *BMC Nephrol.* **15**, 1–5 (2014).
507. Bachrati, C. Z. & Hickson, I. D. RecQ helicases: Guardian angels of the DNA replication fork. *Chromosoma* **117**, 219–233 (2008).
508. Lobitz, S. & Velleuer, E. Guido Fanconi (1892-1979): A jack of all trades. *Nat. Rev. Cancer* **6**, 893–898 (2006).
509. Masutani, C. *et al.* The XPV (xeroderma pigmentosum variant) gene encodes human DNA polymerase  $\eta$ . *Nature* **399**, 700–704 (1999).
510. Hanahan, D. & Weinberg, R. a. The hallmarks of cancer. *Cell* **100**, 57–70 (2000).
511. Hanahan, D. & Weinberg, R. a. Hallmarks of cancer: The next generation. *Cell* **144**, 646–674 (2011).
512. Luo, J., Solimini, N. L. & Elledge, S. J. Principles of Cancer Therapy: Oncogene and Non-oncogene Addiction. *Cell* **136**, 823–837 (2009).
513. Gorgoulis, V. G. *et al.* Activation of the DNA damage checkpoint and genomic instability in human precancerous lesions. *Nature* **434**, 907–913 (2005).
514. Bartkova, J. *et al.* DNA damage response as a candidate anti-cancer barrier in early human tumorigenesis. *Nature* **434**, 864–70 (2005).
515. Bartkova, J. *et al.* Oncogene-induced senescence is part of the tumorigenesis barrier imposed by DNA damage checkpoints. *Nature* **444**, 633–7 (2006).
516. Halazonetis, T. D., Gorgoulis, V. G. & Bartek, J. An Oncogene-Induced DNA Damage Model for Cancer Development. *Science* **319**, 1352–1355 (2008).
517. Lawrence, M. S. *et al.* Discovery and saturation analysis of cancer genes across 21 tumour types. *Nature* **505**, 495–501 (2014).

518. <http://www.tumorportal.org/>.
519. Tomasetti, C. & Vogelstein, B. Variation in cancer risk among tissues can be explained by the number of stem cell divisions. *Science* **347**, 78–81 (2015).
520. Dobbstein, M. & Sørensen, C. S. Exploiting replicative stress to treat cancer. *Nat. Rev. Drug Discov.* **14**, 405–23 (2015).
521. Denisenko, T. V., Sorokina, I. V., Gogvadze, V. & Zhivotovsky, B. Mitotic catastrophe and cancer drug resistance: A link that must to be broken. *Drug Resist. Updat.* **24**, 1–12 (2016).
522. Jossé, R. *et al.* ATR Inhibitors VE-821 and VX-970 Sensitize Cancer Cells to Topoisomerase I Inhibitors by Disabling DNA Replication Initiation and Fork Elongation Responses. *Cancer Res.* **74**, 6968–6979 (2014).
523. Hosoya, N. & Miyagawa, K. Targeting DNA damage response in cancer therapy. *Cancer Sci.* **105**, 370–388 (2014).
524. Karp, J. E. *et al.* Phase I and pharmacologic trial of cytosine arabinoside with the selective checkpoint 1 inhibitor Sch 900776 in refractory acute leukemias. *Clin. Cancer Res.* **18**, 6723–6731 (2012).
525. Sausville, E. *et al.* Phase I dose-escalation study of AZD7762, a checkpoint kinase inhibitor, in combination with gemcitabine in US patients with advanced solid tumors. *Cancer Chemother. Pharmacol.* **73**, 539–549 (2014).
526. Seto, T. *et al.* Phase I, dose-escalation study of AZD7762 alone and in combination with gemcitabine in Japanese patients with advanced solid tumours. *Cancer Chemother. Pharmacol.* **72**, 619–627 (2013).
527. Li, T. *et al.* A phase II study of cell cycle inhibitor UCN-01 in patients with metastatic melanoma: A California Cancer Consortium trial. *Invest. New Drugs* **30**, 741–748 (2012).
528. Ma, C. X. *et al.* A phase II study of UCN-01 in combination with irinotecan in patients with metastatic triple negative breast cancer. *Breast Cancer Res. Treat.* **137**, 483–492 (2013).
529. Dupré, A. *et al.* A forward chemical genetic screen reveals an inhibitor of the Mre11-Rad50-Nbs1 complex. *Nat. Chem. Biol.* **4**, 119–125 (2008).
530. Allen, C., Ashley, A. K., Hromas, R. & Nickoloff, J. A. More forks on the road to replication stress recovery. *J. Mol. Cell Biol.* **3**, 4–12 (2011).
531. Huang, F. *et al.* Identification of specific inhibitors of human RAD51 recombinase using high-throughput screening. *ACS Chem. Biol.* **6**, 628–635 (2011).
532. Huang, F., Mazina, O. M., Zentner, I. J., Cocklin, S. & Mazin, A. V. Inhibition of homologous recombination in human cells by targeting RAD51 recombinase. *J. Med. Chem.* **55**, 3011–3020 (2012).
533. Huang, F. & Mazin, A. V. A small molecule inhibitor of human RAD51 potentiates breast cancer cell killing by therapeutic agents in mouse xenografts. *PLoS One* **9**, e100993 (2014).
534. Alagpulinsa, D. A., Ayyadevara, S. & Shmookler Reis, R. J. A Small-Molecule Inhibitor of RAD51 Reduces Homologous Recombination and Sensitizes Multiple Myeloma Cells to Doxorubicin. *Front. Oncol.* **4**, 1–11 (2014).
535. Gavande, N. S. *et al.* DNA repair targeted therapy: The past or future of cancer treatment? *Pharmacol. Ther.* **160**, 65–83 (2016).
536. Ercilla, A. *et al.* New origin firing is inhibited by APC / C Cdh1 activation in S-phase after severe replication stress. *Nucleic Acids Res.* **44**, 4745–4762 (2016).
537. Di Micco, R. *et al.* Oncogene-induced senescence is a DNA damage response triggered by DNA hyper-replication. *Nature* **444**, 638–642 (2006).
538. Liu, X., Ding, J. & Meng, L. Oncogene-induced senescence: a double edged sword in cancer. *Acta Pharmacol. Sin.* **39**, 1553–1558 (2018).
539. Reimann, J. D. R., Gardner, B. E., Margottin-goguet, F. & Jackson, P. K. Emi1 regulates the anaphase-promoting complex by a different mechanism than Mad2 proteins. *Genes Dev.* **15**, 3278–3285 (2001).
540. Fiore, B. Di & Pines, J. Emi1 is needed to couple DNA replication with mitosis but does not regulate activation of the mitotic APC/C. *J. Cell Biol.* **117**, 425–437 (2007).
541. Llopis, A. *et al.* The stress-activated protein kinases p38 $\alpha$ / $\beta$  and JNK1/2 cooperate with Chk1 to

- inhibit mitotic entry upon DNA replication arrest. *Cell Cycle* **11**, 3627–3637 (2012).
542. Rodríguez-Bravo, V., Guaita-Esteruelas, S., Salvador, N., Bachs, O. & Agell, N. Different S/M checkpoint responses of tumor and non-tumor cell lines to DNA replication inhibition. *Cancer Res.* **67**, 11648–11656 (2007).
  543. Quinet, A., Carvajal-Maldonado, D., Lemacon, D. & Vindigni, A. *DNA Fiber Analysis: Mind the Gap! Methods in Enzymology* **591**, (Elsevier Inc., 2017).
  544. Harrigan, J. A. *et al.* Replication stress induces 53BP1-containing OPT domains in G1 cells. *J. Cell Biol.* **193**, 97–108 (2011).
  545. Lukas, C. *et al.* 53BP1 nuclear bodies form around DNA lesions generated by mitotic transmission of chromosomes under replication stress. *Nat. Cell Biol.* **13**, 243–253 (2011).
  546. Moreno, A. *et al.* Unreplicated DNA remaining from unperturbed S phases passes through mitosis for resolution in daughter cells. *Proc. Natl. Acad. Sci. U. S. A.* **113**, E5757–64 (2016).
  547. Ren, L. *et al.* Potential biomarkers of DNA replication stress in cancer. *Oncotarget* **8**, 36996–37008 (2017).
  548. Machida, Y. J. & Dutta, A. The APC/C inhibitor, Emi1, is essential for prevention of rereplication. *Genes Dev.* **21**, 184–194 (2007).
  549. Verschuren, E. W., Ban, K. H., Masek, M. a, Lehman, N. L. & Jackson, P. K. Loss of Emi1-dependent anaphase-promoting complex/cyclosome inhibition deregulates E2F target expression and elicits DNA damage-induced senescence. *Mol. Cell. Biol.* **27**, 7955–65 (2007).
  550. Sirbu, B. M. *et al.* Analysis of protein dynamics at active, stalled, and collapsed replication forks. *Genes Dev.* **25**, 1320–7 (2011).
  551. Sirbu, B. M., Couch, F. B. & Cortez, D. Monitoring the spatiotemporal dynamics of proteins at replication forks and in assembled chromatin using isolation of proteins on nascent DNA. *Nat. Protoc.* **7**, 594–605 (2012).
  552. Sirbu, B. M. *et al.* Identification of proteins at active, stalled, and collapsed replication forks using isolation of proteins on nascent DNA (iPOND) coupled with mass spectrometry. *J. Biol. Chem.* **288**, 31458–67 (2013).
  553. Petermann, E. & Helleday, T. Pathways of mammalian replication fork restart. *Nat. Rev. Mol. Cell Biol.* **11**, 683–7 (2010).
  554. Raderschall, E., Golub, E. I. & Haaf, T. Nuclear foci of mammalian recombination proteins are located at single-stranded DNA regions formed after DNA damage. *Proc. Natl. Acad. Sci. U. S. A.* **96**, 1921–1926 (1999).
  555. Meijer, L. *et al.* Biochemical and cellular effects of roscovitine, a potent and selective inhibitor of the cyclin-dependent kinases cdc2, cdk2 and cdk5. *Eur. J. Biochem.* **243**, 527–36 (1997).
  556. Labib, K. How do Cdc7 and cyclin-dependent kinases trigger the initiation of chromosomes in eukaryotic cells? *Genes Dev.* **24**, 1208–1219 (2010).
  557. Araki, H. Cyclin-dependent kinase-dependent initiation of chromosomal DNA replication. *Curr. Opin. Cell Biol.* **22**, 766–71 (2010).
  558. Peng, C.-Y. *et al.* Mitotic and G2 Checkpoint Control: Regulation of 14-3-3 Protein Binding by Phosphorylation of Cdc25C on Serine-216. *Science* **277**, 1501–1505 (1997).
  559. Sanchez, Y. *et al.* Conservation of the Chk1 checkpoint pathway in mammals: Linkage of DNA damage to Cdk regulation through Cdc25. *Science* **277**, 1497–1501 (1997).
  560. Mailand, N. *et al.* Rapid destruction of human Cdc25A in response to DNA damage. *Science* **288**, 1425–1429 (2000).
  561. Lee, J., Kumagai, A. & Dunphy, W. G. Positive Regulation of Wee1 by Chk1 and 14-3-3 Proteins. *Mol. Biol. Cell* **12**, 551–563 (2001).
  562. Sogo, J. M., Lopes, M. & Foiani, M. Fork Reversal and ssDNA Accumulation at Stalled Replication Forks Owing to Checkpoint Defects. *Science* **297**, 599–602 (2002).
  563. Ray Chaudhuri, A. *et al.* Topoisomerase I poisoning results in PARP-mediated replication fork reversal. *Nat. Struct. Mol. Biol.* **19**, 417–423 (2012).
  564. Chavez, D. A. & Greer, B. H. The HIRAN domain of helicase-like transcription factor positions the DNA translocase motor to drive efficient DNA. *J Biol Chem.* **293**, 8484–8494 (2018).
  565. Cotta-ramusino, C. *et al.* Exo1 Processes Stalled Replication Forks and Counteracts Fork Reversal in

- Checkpoint-Defective Cells. *Mol Cell*. **17**, 153–159 (2005).
566. Hu, J. *et al.* The Intra-S Phase Checkpoint Targets Dna2 to Prevent Stalled Replication Forks from Reversing. *Cell* **149**, 1221–1232 (2012).
567. Manosas, M., Perumal, S. K., Croquette, V. & Benkovic, S. J. Direct Observation of Stalled Fork Restart via Fork Regression in the T4 Replication System. *Science* **338**, 1217–1220 (2012).
568. Vallerga, M. B., Mansilla, S. F., Federico, M. B., Bertolin, a. P. & Gottifredi, V. Rad51 recombinase prevents Mre11 nuclease-dependent degradation and excessive PrimPol-mediated elongation of nascent DNA after UV irradiation. *Proc. Natl. Acad. Sci.* **112**, E6624–33 (2015).
569. Iannascoli, C. *et al.* The WRN exonuclease domain protects nascent strands from pathological MRE11 / EXO1-dependent degradation. *Nucleic Acids Res.* **43**, 9788–9803 (2015).
570. Coquel, F. *et al.* SAMHD1 acts at stalled replication forks to prevent interferon induction. *Nature* **557**, 57–61 (2018).
571. Su, X., Bernal, J. A. & Venkitaraman, A. R. Cell-cycle coordination between DNA replication and recombination revealed by a vertebrate N-end rule degron-Rad51. *Nat. Struct. Mol. Biol.* **15**, 1049–1058 (2008).
572. Huyen, Y. *et al.* Methylated lysine 79 of histone H3 targets 53BP1 to DNA double-strand breaks. *Nature* **432**, 406–411 (2004).
573. Liu, S. *et al.* Claspin operates downstream of TopBP1 to direct ATR signaling towards Chk1 activation. *Mol. Cell Biol.* **26**, 6056–6064 (2006).
574. Chini, C. C. S. & Chen, J. Human claspin is required for replication checkpoint control. *J. Biol. Chem.* **278**, 30057–30062 (2003).
575. Bellefroid, E. J. *et al.* The evolutionarily conserved Kruppel-associated box domain defines a subfamily of eukaryotic multifingered proteins (DNA-binding proteins/sequence conservation/ceil differentiation). *Biochemistry* **88**, 3608–3612 (1991).
576. Le Chalony, C. *et al.* The OZF Gene Encodes a Protein Consisting Essentially of Zinc Finger Motifs. *J. Mol. Biol.* **236**, 399–404 (1994).
577. Ferbus, D. *et al.* Identification, nuclear localization, and binding activities of OZF, a human protein solely composed of zinc-finger motifs. *Eur. J. Biochem.* **236**, 991–5 (1996).
578. Antoine, K., Ferbus, D., Kolahgar, G., Prospéri, M. T. & Goubin, G. Zinc finger protein overexpressed in colon carcinoma interacts with the telomeric protein hRap1. *J. Cell. Biochem.* **95**, 763–768 (2005).
579. Antoine, K., Prospéri, M. T., Ferbus, D., Boule, C. & Goubin, G. A Kruppel zinc finger of ZNF 146 interacts with the SUMO-1 conjugating enzyme UBC9 and is sumoylated in vivo. *Mol. Cell. Biochem.* **271**, 215–223 (2005).
580. Katou, Y. *et al.* S-phase checkpoint proteins Tof1 and Mrc1 form a stable replication-pausing complex. *Nature* **424**, 1078–1083 (2003).
581. Lou, H. *et al.* Mrc1 and DNA Polymerase  $\epsilon$  Function Together in Linking DNA Replication and the S Phase Checkpoint. *Mol. Cell* **32**, 106–117 (2008).
582. Bando, M. *et al.* Csm3, Tof1, and Mrc1 form a heterotrimeric mediator complex that associates with DNA replication forks. *J. Biol. Chem.* **284**, 34355–34365 (2009).
583. Szyjka, S. J., Viggiani, C. J. & Aparicio, O. M. Mrc1 is required for normal progression of replication forks throughout chromatin in *S. cerevisiae*. *Mol. Cell* **19**, 691–697 (2005).
584. Osborn, A. J. & Elledge, S. J. Mrc1 is a replication fork component whose phosphorylation in response to DNA replication stress activates Rad53. *Genes Dev.* 1755–1767 (2003).
585. Yang, C.-C. *et al.* Claspin recruits Cdc7 kinase for initiation of DNA replication in human cells. *Nat. Commun.* **7**, 1–14 (2016).
586. Smits, V. a. J. & Gillespie, D. a. DNA damage control: regulation and functions of checkpoint kinase 1. *FEBS J.* **282**, 3681–3692 (2015).
587. Ferbus, D. *et al.* Amplification and over-expression of OZF, a gene encoding a zinc finger protein, in human pancreatic carcinomas. *Int. J. Cancer* **80**, 369–372 (1999).
588. Ferbus, D., Bovin, C., Validire, P. & Goubin, G. The zinc finger protein OZF (ZNF146) in overexpressed in colorectal cancer. *J. Pathol.* **200**, 177–182 (2003).
589. Fernandez, P. C. *et al.* Genomic targets of the human c-Myc protein. *Genes Dev.* **17**, 1115–1129

- (2003).
590. Hills, S. A. & Diffley, J. F. X. DNA replication and oncogene-induced replicative stress. *Curr. Biol.* **24**, R435–R444 (2014).
  591. Wang, Q. *et al.* Alterations of anaphase-promoting complex genes in human colon cancer cells. *Oncogene* **22**, 1486–1490 (2003).
  592. Utani, K. *et al.* Phosphorylated SIRT1 associates with replication origins to prevent excess replication initiation and preserve genomic stability. *Nucleic Acids Res.* **45**, 7807–7824 (2017).
  593. Neelsen, K. J. *et al.* Deregulated origin licensing leads to chromosomal breaks by rereplication of a gapped DNA template. *Genes Dev.* **27**, 2537–2542 (2013).
  594. Lehman, N. L. *et al.* Oncogenic regulators and substrates of the anaphase promoting complex/cyclosome are frequently overexpressed in malignant tumors. *Am. J. Pathol.* **170**, 1793–1805 (2007).
  595. Vaidyanathan, S. *et al.* In vivo overexpression of Emi1 promotes chromosome instability and tumorigenesis. *Oncogene* **35**, 5446–5455 (2016).
  596. Burkhart, D. L. & Sage, J. Cellular mechanisms of tumour suppression by the retinoblastoma gene. *Nat. Rev. Cancer* **8**, 671–682 (2008).
  597. Zhang, D., Zaugg, K., Mak, T. W. & Elledge, S. J. A Role for the Deubiquitinating Enzyme USP28 in Control of the DNA-Damage Response. *Cell* **126**, 529–542 (2006).
  598. Popov, N. *et al.* The ubiquitin-specific protease USP28 is required for MYC stability. *Nat. Cell Biol.* **9**, 765–774 (2007).
  599. Diefenbacher, M. E. *et al.* The deubiquitinase USP28 controls intestinal homeostasis and promotes colorectal cancer. *J. Clin. Invest.* **124**, 3407–3418 (2014).
  600. Zhang, L. *et al.* Overexpression of deubiquitinating enzyme USP28 promoted non-small cell lung cancer growth. *J. Cell. Mol. Med.* **19**, 799–805 (2015).
  601. Lopez-Contreras, A. J. *et al.* A proteomic characterization of factors enriched at nascent DNA molecules. *Cell Rep.* **3**, 1105–16 (2013).
  602. Byrum, A. K. *et al.* Mitotic regulators TPX2 and Aurora A protect DNA forks during replication stress by counteracting 53BP1 function. *J Cell Biol.* **218**, 422–432 (2019).
  603. Sullivan, M. R. & Bernstein, K. A. RAD-ical new insights into RAD51 regulation. *Genes (Basel)*. **9**, E629 (2018).
  604. Sato, K. *et al.* FANCI-FANCD2 stabilizes the RAD51-DNA complex by binding RAD51 and protects the 5'-DNA end. *Nucleic Acids Res.* **44**, 10758–10771 (2016).
  605. Zadorozhny, K. *et al.* Fanconi-Anemia-Associated Mutations Destabilize RAD51 Filaments and Impair Replication Fork Protection. *Cell Rep.* **21**, 333–340 (2017).
  606. Abeyta, A., Castella, M., Jacquemont, C. & Taniguchi, T. NEK8 regulates DNA damage-induced RAD51 foci formation and replication fork protection. *Cell Cycle* **16**, 335–347 (2017).
  607. Yoon, S.-W., Kim, D.-K., Kim, K. P. & Park, K.-S. Rad51 Regulates Cell Cycle Progression by Preserving G2/M Transition in Mouse Embryonic Stem Cells. *Stem Cells Dev.* **23**, 2700–2711 (2014).
  608. Banáth, J. P. *et al.* Explanation for excessive DNA single-strand breaks and endogenous repair foci in pluripotent mouse embryonic stem cells. *Exp. Cell Res.* **315**, 1505–1520 (2008).
  609. Ahuja, A. K. *et al.* A short G1 phase imposes constitutive replication stress and fork remodelling in mouse embryonic stem cells. *Nat. Commun.* **7**, 1–11 (2016).
  610. Zhao, B. *et al.* Mouse embryonic stem cells have increased capacity for replication fork restart driven by the specific FliA-Floped protein complex. *Cell Res.* **28**, 69–89 (2018).
  611. Kim, T. M. *et al.* RAD51 Mutants Cause Replication Defects and Chromosomal Instability. *Mol. Cell. Biol.* **32**, 3663–3680 (2012).
  612. Slupianek, A. *et al.* BCR/ABL regulates mammalian RecA homologs , resulting in drug resistance. *Mol. Cell* **8**, 795–806 (2001).
  613. Hansen, L. T., Lundin, C., Spang-Thomsen, M., Petersen, L. N. & Helleday, T. THE ROLE OF RAD51 IN ETOPOSIDE ( VP16 ) RESISTANCE IN SMALL CELL. *Int. J. Cancer* **105**, 472–479 (2003).
  614. Klein, H. L. The consequences of Rad51 overexpression for normal and tumor cells. *DNA Repair (Amst)*. **7**, 686–693 (2008).
  615. Ruíz, G. *et al.* Inhibition of RAD51 by siRNA and Resveratrol Sensitizes Cancer Stem Cells Derived

- from HeLa Cell Cultures to Apoptosis. *Stem Cells Int.* **2018**, 2493869 (2018).
616. Ko, J. *et al.* Involvement of Rad51 in cytotoxicity induced by epidermal growth factor receptor inhibitor ( gefitinib , Iressa R ) and chemotherapeutic agents in human lung cancer cells. *Carcinogenesis* **29**, 1448–1458 (2008).
617. Lee, J., Kumagai, A. & Dunphy, W. G. Claspin, a Chk1-regulatory protein, monitors DNA replication on chromatin independently of RPA, ATR, and Rad17. *Mol. Cell* **11**, 329–340 (2003).
618. Petermann, E., Helleday, T. & Caldecott, K. W. Claspin Promotes Normal Replication Fork Rates in Human Cells. *Mol. Biol. Cell* **19**, 2373–2378 (2008).
619. Scora, J. & McGowan, C. H. Claspin and Chk1 regulate replication fork stability by different mechanisms. *Cell Cycle* **8**, 1036–1043 (2009).
620. Maya-Mendoza, A. *et al.* Myc and Ras oncogenes engage different energy metabolism programs and evoke distinct patterns of oxidative and DNA replication stress. *Mol. Oncol.* **9**, 601–616 (2015).
621. Méndez, J. & Stillman, B. Chromatin Association of Human Origin Recognition Complex , Cdc6 , and Minichromosome Maintenance Proteins during the Cell Cycle : Assembly of Prereplication Complexes in Late Mitosis. *Mol. Cell. Biol.* **20**, 8602–8612 (2000).
622. Bradford, M. M. A rapid and sensitive method for the quantitation of microgram quantities of protein utilizing the principle of protein-dye binding. *Anal. Biochem.* **72**, 248–254 (1976).
623. Lowry, O. H., Rosebrough, N. J., Farr, L. & Randall, R. J. Protein measurement with the folin phenol reagent. *J Biol Chem.* **193**, 265–275 (1951).
624. Zor, T. & Selinger, Z. Linearization of the Bradford protein assay increases its sensitivity: theoretical and experimental studies. *Anal. Biochem.* **236**, 302–308 (1996).
625. Laemmli, U. K. Cleavage of structural proteins during the assembly of the head of bacteriophage T4. *Nature* **227**, 680–685 (1970).
626. Schwab, R. a. V. & Niedzwiedz, W. Visualization of DNA Replication in the Vertebrate Model System DT40 using the DNA Fiber Technique. *J. Vis. Exp.* 3–7 (2011).